

SYNTHESIS, REACTIVITY, AND CATALYTIC
STUDIES OF TRANSITION METAL COMPLEXES
OF CHELATING CYCLIC AND ACYCLIC
DIAMINOCARBENE LIGANDS

By

YOSHITHA ANJU WANNIARACHCHI

Bachelor of Science in Chemistry
University of Kelaniya
Sri Lanka
2003

Submitted to the Faculty of the
Graduate College of the
Oklahoma State University
in partial fulfillment of
the requirements for
the Degree of
DOCTOR OF PHILOSOPHY
December, 2008

SYNTHESIS, REACTIVITY, AND CATALYTIC
STUDIES OF TRANSITION METAL COMPLEXES
OF CHELATING CYCLIC AND ACYCLIC
DIAMINOCARBENE LIGANDS

Dissertation Approved:

Dr. LeGrande M. Slaughter

Dissertation Adviser

Dr. Warren T. Ford

Dr. Nicholas F. Materer

Dr. Charles S. Weinert

Dr. John Mintmire

Dr. A. Gordon Emslie

Dean of the Graduate College

Dedication

I dedicate this thesis to my loving parents Sarath Gunasena and Geethanganee Padmalatha. Thank you for all your love and unconditional support.

Acknowledgements

The time I spent at Oklahoma State University has been the biggest learning experience for me as a person and as a professional. I consider it a privilege to acknowledge many people who have encouraged, inspired, and guided me throughout my stay at the Oklahoma State University.

First, I would like to extend my sincere thanks to my adviser Dr. LeGrande M. Slaughter for been an inspiration to me and have always been there to guide and encourage me on all my endeavours. Thank you for all the advice, guidance and encouragement. I would also like to thank my thesis committee members, Dr. Warren T. Ford, Dr. Nicholas F. Materer, Dr. Charles S. Weinert, and Dr. John Mintmire for all the guidance, advice, and motivation given to me.

I am thankful to Dr. Joe M. Tanski and Dr. Masood A. Khan for their help in X-ray crystallography. Also I would like to thank all the former and current members of Dr. Slaughter's research group; Adriana, Manne, Millicent, Anthea, Sri, Dr. Dipesh, Yuri, Lindy, Tahereh, Ilya, Chase and Ahamad for their friendship and help given to me when needed. I must specially thank Anthea J. Miranda for synthesizing complexes **9a**, **9b**, **9c**, and **9d** that I used in my research. Also, Yuri Kogiso and Lindy Dewlen for synthesizing complex **20** and **4**. I also wish to thank the Faculty and Staff of the Department of Chemistry for giving me the opportunity to follow my dreams.

Finally, I wish to thank the people who are most responsible for my achievements, my parents, Geethangani Padmalatha and Sarath Gunasena for their love, encouragement and for guiding me throughout my life. I extend my sincere thanks and love to you both. I also thank my sister Sasanka and her husband, Sunjeewa for all the help and support given to me. Thanks guys.

Now, I thank the most precious person in my life, my husband Charaka. Thank you for all the love, support and encouragement; you have been the biggest strength to me and without you I won't be able to see my dreams come true. Also my thanks go to my three month old son, Supun, for his patients and for keep me going. Love you very much.

TABLE OF CONTENTS

Chapter	Page
I. LITRATURE REVIEW AND INTRODUCTION	1
Carbene Electronic Structure	2
Types of Carbene Ligands	5
Silver (NHC) Complexes as efficient Carbene Transferring Agents	14
Acyclic Diamino Carbenes (ADCs).....	20
Referances.....	27
II. SYNTHESIS, CHARACTERIZATION AND CARBENE TRANSFER REACTIVITY OF A SILVER BIS(N-HETEROCYCLIC CARBENE) COMPLEX.....	34
Introduction	35
Results and Discussion.....	38
Summary and Conclusions	60
Experimental	61
References.....	68
III. FACILE SYNTHESIS OF CHIRAL PALLADIUM BIS(ACYCLICDIAMINOCARBENE) COMPLEXES	72
Introduction	73
Results and Discussion.....	74
Summary and Conclusions	116
Experimental	117
References.....	126
IV. SYNTHESIS OF A TETRASUBSTITUTED CHUGAEV-TYPE BIS(CARBENE) PALLADIUM COMPLEX AND ITS REVERSIBLE CHELATE RING OPENING	131
Introduction	132
Results and Discussion.....	136
Summary and Conclusions	155

Experimental.....	156
References.....	161

V. CATALYTIC AZA-CLAISEN REARRANGEMENT WITH CHIRAL PALLADIUM BIS(ACYCLIC DIAMINOCARBENE) COMPLEXES	163
--	-----

Introduction	164
Results and Discussion.....	167
Summary and Conclusions	213
Experimental	216
References.....	230

LIST OF TABLES

Table	Page
2.1. Yields of free bis(NHC) ligands containing different R groups	36
2.2. Selected bond lengths (Å) and bond angles (°) of complex 3	42
2.3. Crystal data and structure refinement details for complex 3	43
2.4. Selected bond lengths (Å) and bond angles (°) of complex 5	52
2.5. Crystal data and structure refinement details for complex 5	53
2.6. Selected bond lengths (Å) and bond angles (°) of complex 7	58
2.7. Crystal data and structure refinement details for complex 7	59
3.1. Selected bond lengths (Å) and bond angles (°) of complex 8	79
3.2. Crystal data and structure refinement details for complex 8	80
3.3. Selected bond lengths (Å) and bond angles (°) of complex 9	86
3.4. Crystal data and structure refinement details for complex 9	87
3.5. Selected bond lengths (Å) and bond angles (°) of complex 10	92
3.6. Crystal data and structure refinement details for complex 10	93
3.7. Selected bond lengths (Å) and bond angles (°) of compound 11	98
3.8. Crystal data and structure refinement details for 11	99
3.9. Selected bond lengths (Å) and bond angles (°) of compound 13	105
3.10. Crystal data and structure refinement details for complex 13	106

3.11. Selected bond lengths (Å) and bond angles (°) of compound 15	114
3.12. Crystal data and structure refinement details for complex 15	115
4.1. Selected bond lengths (Å) and bond angles (°) of complex 16	140
4.2. Crystal data and structure refinement details for complex 16	141
4.3. Selected bond lengths (Å) and bond angles (°) of complex 17	147
4.4. Crystal data and structure refinement details for complex 17	148
4.5. Data for the van't Hoff Plot.....	152
4.2. Crystal data and structure refinement details for complex 16	141
4.3. Selected bond lengths (Å) and bond angles (°) of complex 17	147
4.4. Crystal data and structure refinement details for complex 17	148
4.5. Data for the van't Hoff Plot.....	152
5.1. Selected bond lengths (Å) and bond angles (°) of complex 21	179
5.2. Crystal data and structure refinement details for complex 21	180
5.3. Palladium catalyzed aza-Claisen rearrangement of γ -methylallyl N-phenylformimidate S1	187
5.4. Palladium catalyzed aza-Claisen rearrangement of allyl N-phenylformimidate S2	189
5.5. Aza-Claisen rearrangement of (<i>E</i>)-2-Hexenyl <i>N</i> -[4-(trifluoromethyl) phenyl]benzimidate S3 catalyzed by palladium complexes containing bis(ADC) and Bis(NHC) ligands	192
5.6. Aza-Claisen rearrangement of (<i>E</i>)-2-hexenyl- <i>N</i> -[4-(trifluoromethyl) phenyl]benzimidate S3 by palladium bis(ADC) complexes with different electronic properties	196
5.7. Aza-Claisen rearrangement with bis(phosphine) palladium complexes	198

5.8. Enantioselective catalytic results for (<i>E</i>)-2-hexenyl- <i>N</i> -[4-(trifluoromethyl)phenyl]benzimidate.....	200
5.9. Selected bond lengths (Å) and bond angles (°) of complex 23	204
5.10. Crystal data and structure refinement details for complex 23	205
5.11. Aza-Claisen rearrangement with different <i>N</i> -substituted phenyl benzimidates	207
5.12. Aza-Claisen rearrangement [3,3] product of (<i>E</i>)/(<i>Z</i>)-2-hexenyl trichloroacetimidate S6 and (<i>E</i>)/(<i>Z</i>)-2-Hexenyl- <i>N</i> -(4-methoxyphenyl) trifluoroacetimidate S7 using precatalyst ±9	212

LIST OF FIGURES

Figure	Page
1.1. Orbital distribution of a bent carbene	3
1.2. Orbital diagram of singlet carbene containing σ -electron withdrawing substituents	4
1.3. First stable Fischer carbene transition metal complex	5
1.4. Electron donation and possible resonance structures of Fischer carbenes	6
1.5. Schrock carbene complex formed by two covalent bonds with the metal	8
1.6. First NHC metal complexes synthesized	10
1.7. An acyclic diaminocarbene and an N-heterocyclic carbene	21
1.8. Early synthesis methods of metal ADC complexes	22
1.9. The synthesis of Chugaev carbene complex; correct structure and the originally proposed structure	25
2.1. Molecular structure of complex 3 with six different aryl-CH ₃ groups	41
2.2. Molecular structure of complex 3 displaying the exposed Ag ₂ core on one side of the complex	45
2.3. ¹ H NMR of complex 3 at 25 °C and at -90 °C	47
2.4. Molecular structure of complex 5	50
2.5. Molecular structure of complex 7	57
3.1. Molecular structure of complex 8	78
3.2. Molecular structure of complex 9	85

3.3. Molecular structure of complex 10	91
3.4. Molecular structure of complex 11	97
3.5. Molecular structure of complex 13	104
3.6. X-ray crystal structure of complex 15	113
4.1. Molecular structure of complex 16	138
4.2. Molecular structure of complex 17	146
4.3. ¹⁹ F NMR spectrum showing the equilibrium between complexes 16 and 17 at 25 °C in CD ₃ CN	150
4.4. The possible zwitterionic intermediate in the interconversion of complex 16 and 17	151
4.5. Van't Hoff plot for the equilibrium between monocarbene complex 16 and bis(ADC) complex 17	152
5.1. X-ray crystal structure of [(1,2-Bis(diphenylphosphino)ethane) Pd(CNCH ₃) ₂][BPh ₄] ₂ 21	178
5.2. Comparison of σ-donor ability of bis(ADC) ligands compared with bis(NHC) and bis(phosphine) ligands	182
5.3. Molecular structure of complex 23	203
5.4. N-substituted phenyl benzimidates used in palladium-catalyzed aza-Claisen rearrangements	208
5.5. Aza-Claisen rearrangements of (<i>E</i>)/(<i>Z</i>)-2-hexenyltrichloroacetimidate S6 and (<i>E</i>)/(<i>Z</i>)-2-Hexenyl- <i>N</i> -(4-methoxyphenyl) trifluoroacetimidate S7	211

CHAPTER I

LITERATURE REVIEW AND INTRODUCTION

Introduction

Carbenes are a widely used class of ligands in organometallic chemistry. Because of their unique properties, carbenes have attracted great interest in recent years. For example, they can be reactive or inert depending on their substitution pattern, and they are typically very strong donor ligands. The latter property has led to large advances in homogeneous catalysts containing carbene ligands in recent years. This chapter will provide an introduction to the ligand properties of carbenes and their attachment to catalytically useful transition metals. Chapter Two will describe the use of silver bis(N-heterocyclic carbene) complexes to transfer bulky bis(carbene) ligand onto catalytically important transition metals. Chapter Three concentrates on an efficient method to synthesize chiral bis(acyclic diaminecarbene) palladium complexes in one pot. Chapter Four describes the synthesis and reversible chelate ring opening of a tetrasubstituted Chugaev- type bis(carbene) palladium complex. Finally, Chapter Five focuses on the activity of chiral palladium bis(acyclic diaminecarbene) complexes on catalytic aza-Claisen rearrangement.

1.1 Carbene electronic structure

Carbenes are divalent, neutral carbon compounds which possess two non-bonding electrons on the central carbon.¹ Up until recent times, carbenes were considered to be highly reactive intermediates, which could only be generated in a reaction mixture at low temperatures,² but not isolated. Most carbenes are believed to adopt a bent geometry with three sp^2 hybridized σ -type orbitals and an unhybridized P_y (P_π) orbital on the carbene carbon (Figure 1.1).³

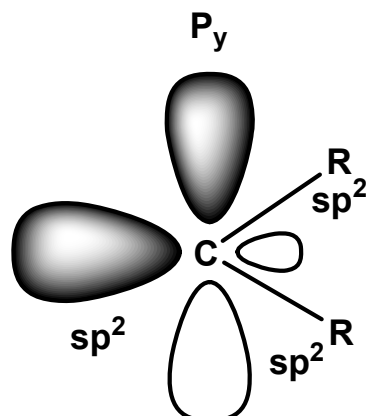


Figure 1.1. Orbital depiction of a bent carbene. Adapted from Reference 4.

The carbene ground state spin multiplicity can be one of two different states depending on the orbital location of the two nonbonding electrons. The singlet electronic state occurs when the two nonbonding electrons are located in one of the sp^2 hybridized (σ -type) orbitals with anti-parallel spins. The triplet electronic state occurs when the two nonbonding electrons are located separately on the sp^2 hybridized orbital and the empty P_π orbital with parallel spins. The triplet state is considered as a diradical state.¹ The energy gap between the sp^2 hybridized (σ -type) orbital and the P_π orbital is a critical consideration for understanding the ground state spin multiplicity and reactivity of carbenes.¹ An energy gap of less than 1.5 eV leads to a triplet ground state, while an energy gap higher than 2.0 eV results in a stable singlet ground state.⁴ The energy gap between the σ -type orbital and P_π orbital is determined by electronic effects (inductive effect and mesomeric effect) and the steric effect of the neighboring groups around the carbene. For example,

neighboring groups with σ -electron withdrawing properties, such as electronegative - F groups, reduce the energy of the non-bonding σ -orbital (HOMO) of the carbene due to the inductive effect. The reduction in energy of the nonbonding σ -orbital increases the $\sigma - P_\pi$ energy gap, allowing the singlet state of the carbene to be more stable (Figure 1.2).¹

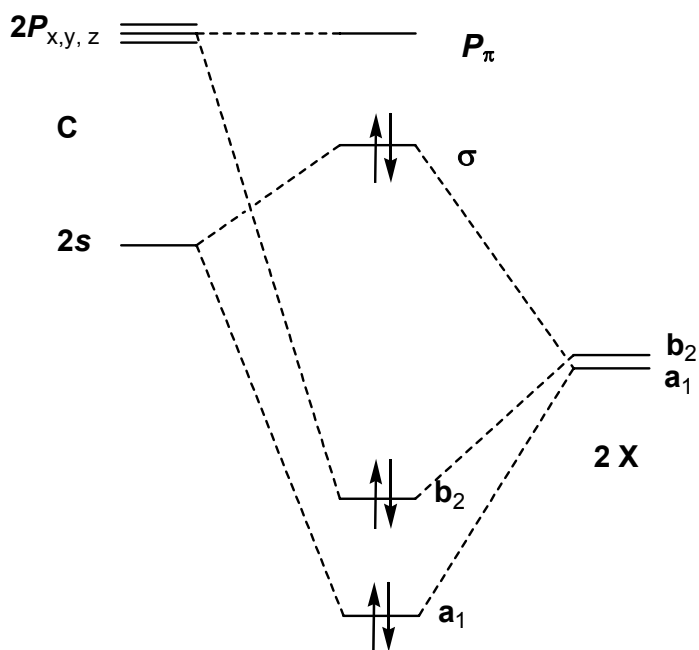


Figure 1.2. Orbital diagram of singlet carbene containing σ -electron withdrawing substituents. Adapted from Reference 1.

Steric effects also influence the ground state spin multiplicities of carbenes, especially when electronic effects are negligible. An increase in steric bulk on carbene neighboring groups favors a linear geometry by increasing the carbene bond angle and therefore promotes the triplet ground state.³ For example, carbenes

having bulky neighboring tert-butyl groups⁵ and adamantyl groups⁶ have displayed triplet ground state spin multiplicity while comparatively less bulky methyl groups substituted carbenes displayed singlet spin multiplicity.^{7,8}

1.2 Types of carbene Ligands

Fischer carbenes

Historically, carbene ligands bound to metals have been grouped into two categories: Fischer carbenes, which behave as singlet carbenes, and Schrock carbenes, which are regarded as triplet carbenes. Fischer carbenes were first introduced by Fischer and Maasböl in 1964 by synthesizing a stable tungsten carbene complex (Figure 1.3).⁹

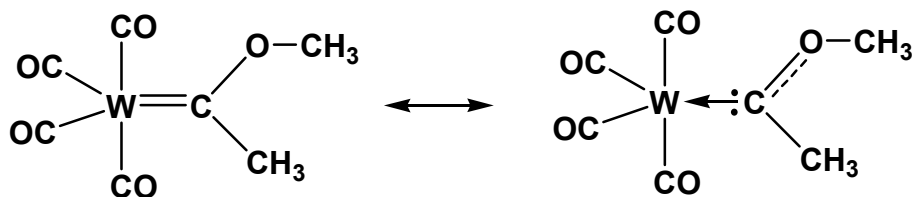


Figure 1.3. First stable Fischer carbene transition metal complex.

Fischer carbenes easily complex with late transition metals and early transition metals in low oxidation states. Also, the carbene complex formation is facilitated by having π -acceptor ligands (L) bound to the metal as well as by having π -donor substituents (R) such as -OMe and -NMe₂ groups adjacent to the carbene carbon (Figure 1.4 (a)).¹ Fischer carbenes are $2e^-$ donor singlet carbene ligands with

no formal charge. The carbene σ -donation to the metal occurs through a lone pair of electrons located in the filled sp^2 orbital. The presence of an empty $P\pi$ orbital which can accept electrons makes Fischer carbenes electrophilic.¹ The electrons in a metal filled $d\pi$ orbital and the lone pair of electrons on the carbene π -donor neighboring substituents can compete in donating to the empty $P\pi$ orbital of Fischer carbenes, leading to two possible resonance structures of the metal-carbene bond (Figure 1.4 (b)).¹ The zwitterionic resonance structure in Figure 1.4 (b) is more appropriate in describing a singlet carbene, because it indicates a longer $M-C_{\text{carbene}}$ bond and a comparatively shorter $C_{\text{carbene}}-O$ bond reflecting the low metal to carbon π -back donation in a singlet carbene.¹

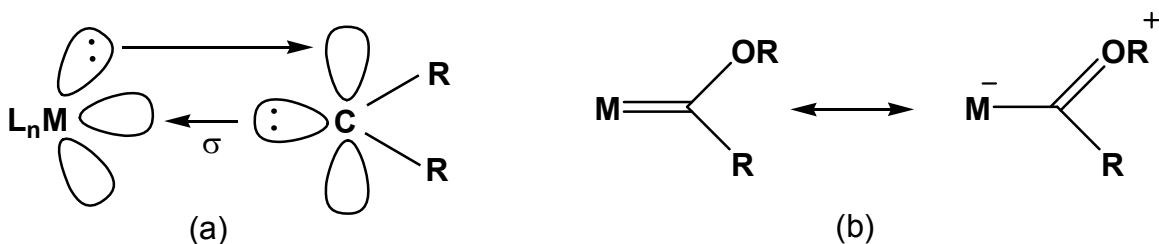
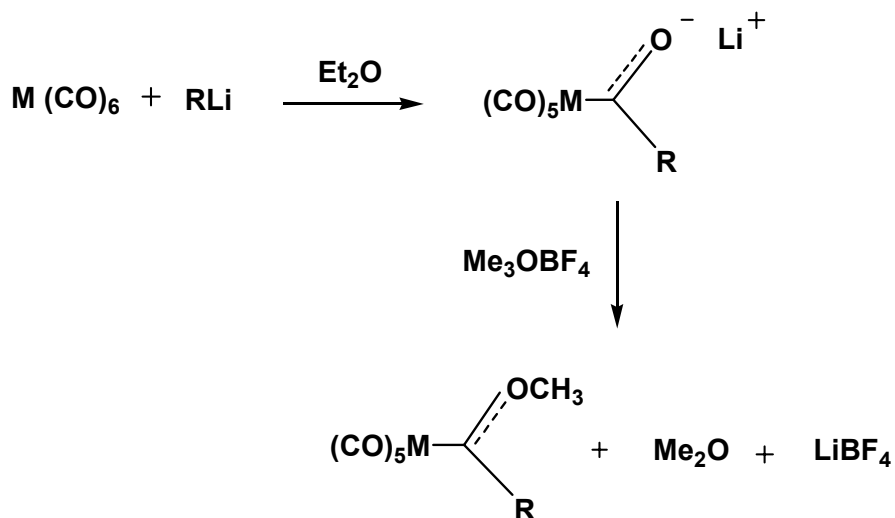


Figure 1.4. (a) Electron donation in Fischer carbene. (b) Possible resonance structures of Fischer carbenes.

Transition metal complexes containing Fischer carbenes are typically synthesized via nucleophilic attack of MeLi or PhLi on various metal carbonyl complexes followed by alkylation with Me_3OBF_4 (Scheme 1.1).^{10,9}



Scheme 1.1. Formation of Fischer carbene metal complex.

Schrock carbenes

Schrock carbenes are nucleophilic carbenes that are formally in the triplet ground state electron multiplicity. Schrock carbenes are known as “alkylidenes” and are assigned a -2 formal charge when bound to a metal. These carbenes readily form complexes with early transition metals in higher oxidation states which lack π -acceptor ligands.¹ Schrock carbenes do not require π -donor neighboring groups to form stable carbene complexes. These carbenes bind with metals by forming two covalent bonds using the two unpaired electrons on the carbene carbon and two unpaired metal electrons (Figure 1.5). Since carbon is more electronegative than the metal, the covalent bonds are polarized toward the carbene creating a nucleophilic carbene center.¹

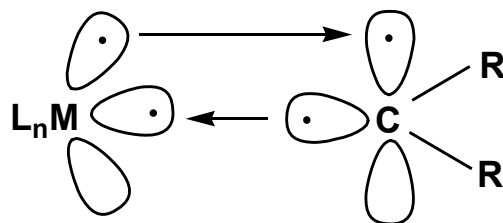
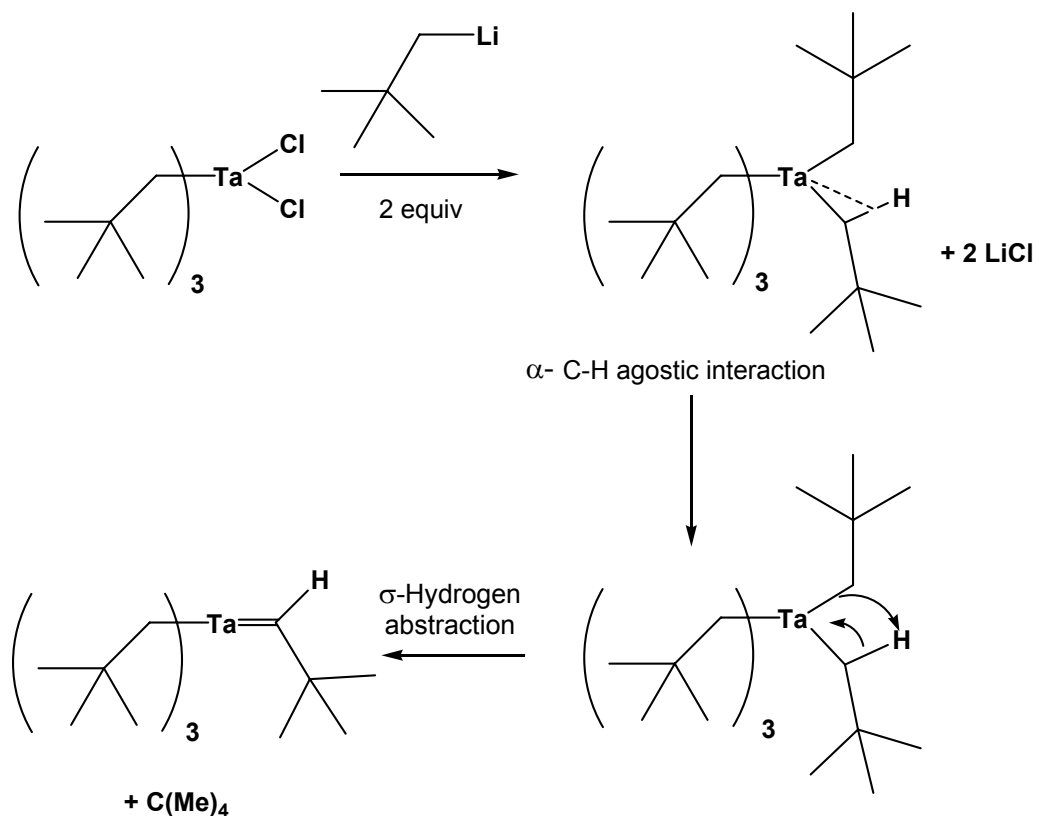


Figure 1.5. Schrock carbene complex formed by two covalent bonds with the metal.

Adapted from Reference 1.

Synthesis of Schrock carbenes was discovered by Schrock¹¹ in an attempt to synthesize the $Ta(CH_2CMe_3)_5$ complex. The synthesis involved substitution of chloride ligands of $Ta(CH_2CMe_3)_3Cl_2$ with 2 equiv of $LiCH_2CMe_3$ to obtain the first stable alkylidene metal complex $(Me_3CCH_2)_3Ta(ChCMe_3)$ (Scheme 1.2).¹² It is assumed that $Ta(CH_2CMe_3)_5$ formed during the reaction, but underwent α -agostic interaction with one of the neighboring C-H groups followed by α -hydrogen abstraction leading to the alkylidene formation at the metal.^{1,12}



Scheme 1.2. Synthesis of the first stable Schrock carbene complex. Adapted from Reference 13.

N-Heterocyclic Carbenes (NHCs)

N-heterocyclic carbenes can be considered as an extreme type of Fischer carbenes¹ which have two electronegative nitrogen atoms neighboring to the carbene carbon. NHCs are singlet carbenes with zero formal charge on the carbene carbon. NHC ligands act as very strong σ -donor ligands when binding to a metal complex.¹³ The metal coordination chemistry of N-heterocyclic carbenes began with the introduction of NHC metal complexes of Cr(0) and Hg(II) by Öfele¹⁴ and Wanzlick¹⁵ in 1968 (Figure 1.6).¹³

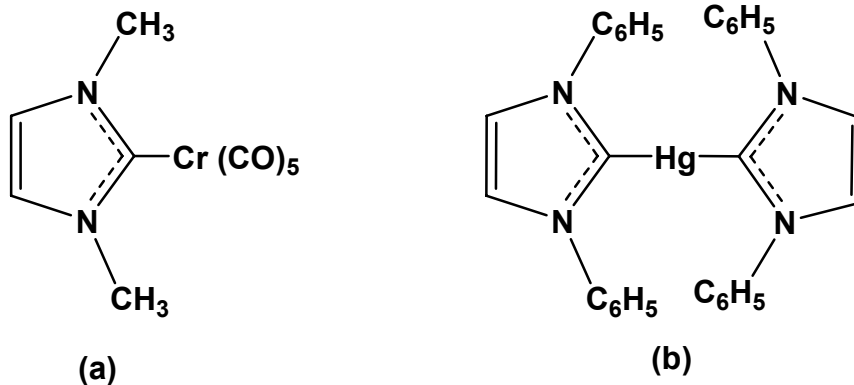
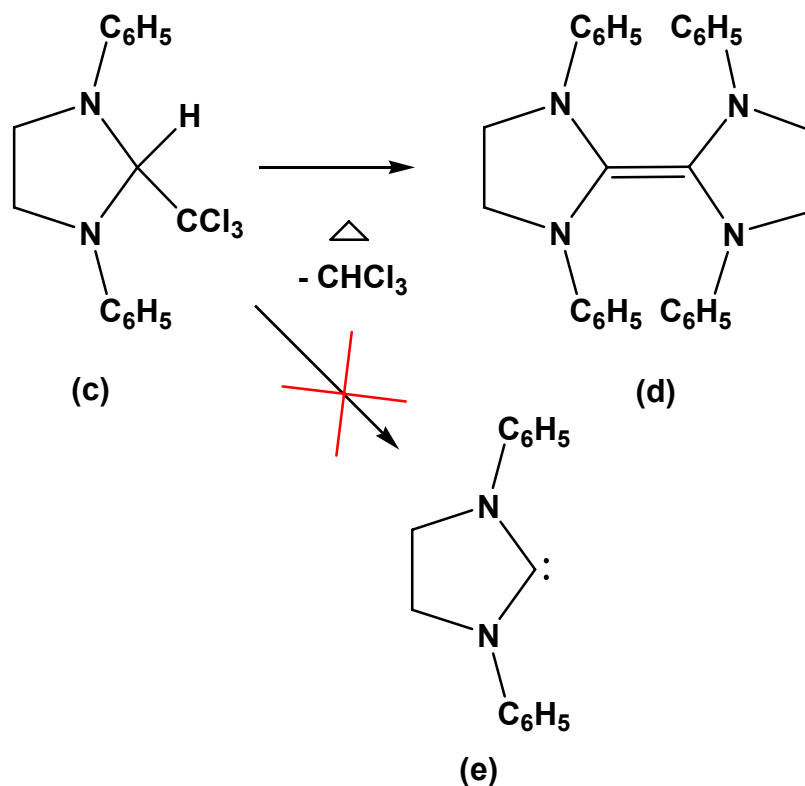


Figure 1.6. First NHC metal complexes synthesized by Öfele (a) and Wanzlick (b).

Adapted from Reference 14.

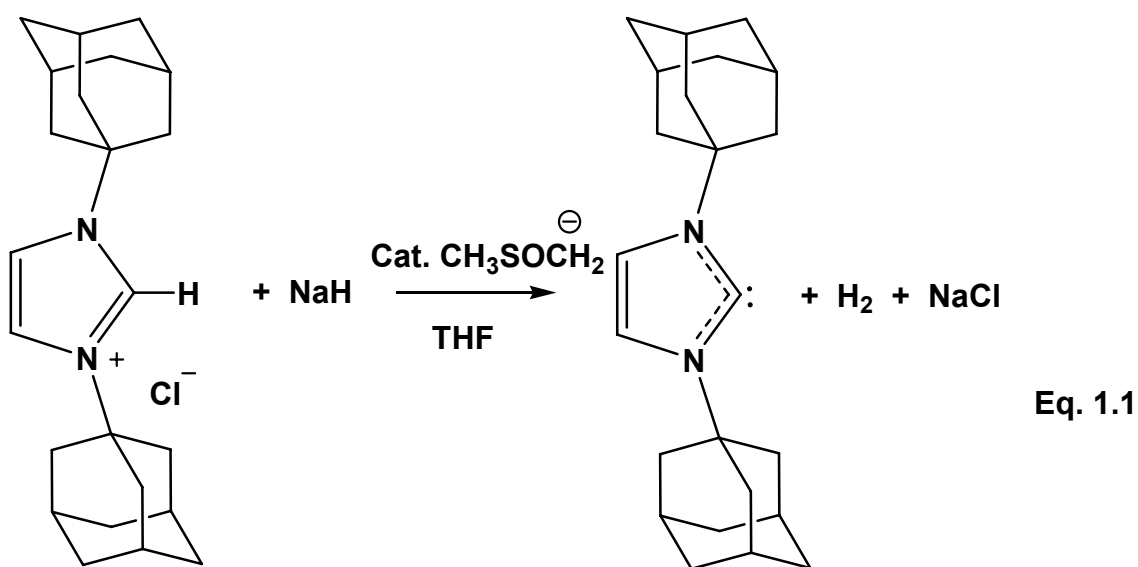
Vast application of NHC complexes in organometallic chemistry started with the discovery of a stable free NHC by Arduengo et al. in 1991,¹⁶ which spurred a new approach to synthesize various NHC metal complexes.¹⁷ Early in the 1960s Wanzlick et al.¹⁸ had worked on isolating free N-heterocyclic carbenes.¹³ This reaction was done using a saturated imidazole precursor (c), to generate the free carbene. However his initial attempt was unsuccessful, yielding a dimerized olefinic product (d) instead of the free carbene (e) (Scheme 1.3).^{13,17}



Scheme 1.3. Attempted free carbene synthesis by Wanzlick et al.¹⁸

Arduengo et al. substituted the saturated imidazole precursor (c) that Wanzlick used with an unsaturated imidazolium precursor containing bulky adamantyl groups to generate the stable free N-heterocyclic carbene. The synthesis involved deprotonation of 1,3-di-1-adamantylimidazolium bromide using catalytic amounts of dimsyl anion ($\text{CH}_3\text{SOCH}_2^-$) in the presence of 1 equiv of NaH in dry THF as the solvent (Eq. 1.1).¹⁶ The imidazole based free N-heterocyclic carbene was stable up to 241 °C in the absence of moisture and air.¹⁶ The high stabilities of imidazole-based NHCs are governed by favorable electronic effects and steric effects embedded in the molecular structure of the free carbene.^{19,20} Favorable electronic effects are due to the presence of neighboring π -donor nitrogen atoms,

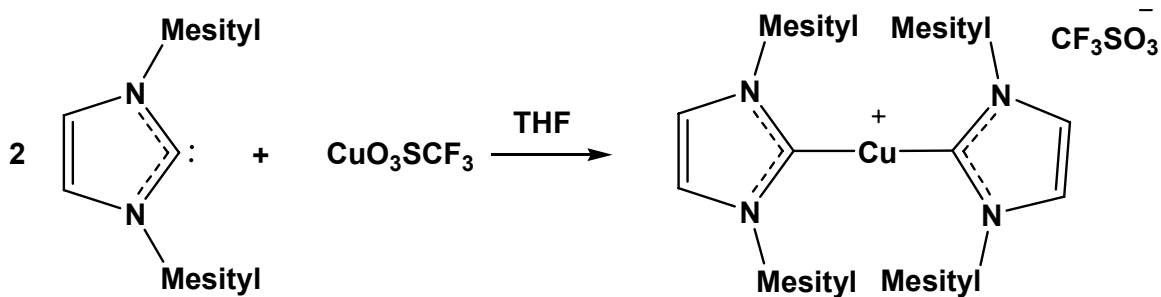
which donate electrons into the empty $P\pi$ orbital on the carbene carbon, as well as to the σ -electronegativity effect of having electron-withdrawing nitrogen atoms neighboring to the carbene carbon, which lowers the energy of the filled sp^2 orbital of the carbene (HOMO).^{20,13} This lowering of energy of the HOMO in the free carbene favors NHCs in the singlet state rather than the higher energy triplet state by creating an energy gap of ~ 79 kcal/mol between the two spin states.^{20, 13} The steric effect also plays a role in providing kinetic stability to the free carbene by having bulky substituents that impose difficulties for reactive species to contact the carbene center.¹⁶



Following Arduengo's discovery of free NHC ligands, various NHC metal complexes have been synthesized simply by complexation of free carbenes with metal precursors.¹⁷ Efficient catalytic systems containing NHC ligands have been discovered for a wide range of metal-catalyzed transformations. Some of the

important catalytic reactions which were carried out using NHC metal complexes are; Olefin metathesis,²¹ Heck²² and Suzuki coupling,²³ aryl amination,²⁴ hydrosilylation²⁵ and C-H activation.^{26,27} The rapid development of NHC chemistry is attributed to the advantages of carbene ligands in catalysis. Carbenes are isolobal to phosphine ligands, which are very common in transition metal chemistry. Carbene ligands can be easily functionalized, modified to include a chiral center, customized to be used in water soluble reactions, and immobilized on solid supports.¹³ Additionally, carbenes have several advantages over phosphine ligands as efficient ligands in catalysis. Advantages of carbene ligands over phosphine ligands include, high air and thermal stability when bound to a metal, and high binding energy to metals. Metal-carbene bond energies are up to ~ 10 kcal/ mol high than phosphine ligands, which indicates a significantly better σ - donor ability than phosphine ligands.²⁸

Metal NHC complexes can be easily synthesized by treating free carbenes with the respective metal salts (Eq.1.2).²⁹ This method has been widely used for monodentate NHC metal complexes, but not for chelating bis(NHC) complexes due to difficulty in generation of free bis(NHC). However, chelating NHC ligands have possible advantages over monodentate carbenes due to the additional stabilization provided to the carbene metal complex through the chelate effect. In chelated bis(NHC) metal complexes, the susceptibility of bis-imidazolium salts to be reductively eliminated is very low.³⁰ This also helps in stabilizing highly reactive metal intermediates in catalytic reactions.²⁷ To date syntheses of bis(NHC) containing metal complexes have been rarely reported.^{30,31,32,33,34}



Mesityl = 2,4,6- trimethylphenyl

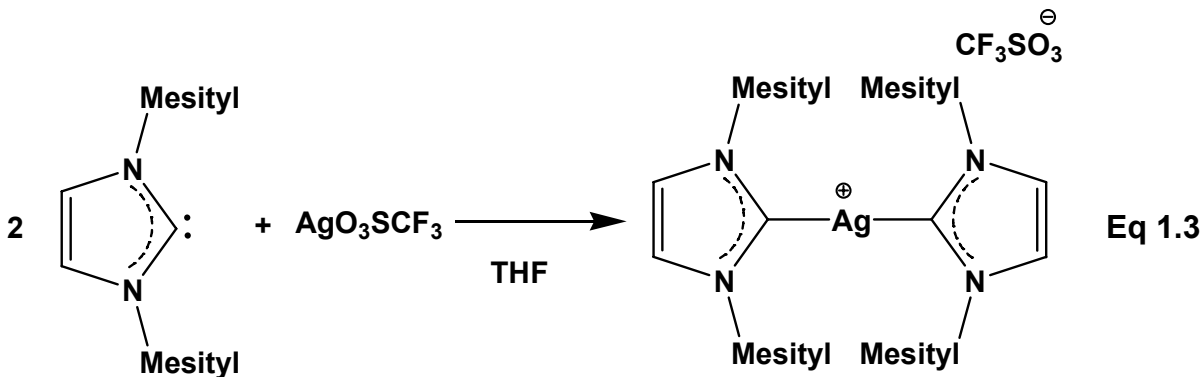
Eq. 1.2

1.3 Silver (NHC) complexes as efficient carbene transferring agents

One possible approach to overcome the difficulty of synthesizing bis(NHC) complexes is the use of a silver bis(carbene) complex as a carbene transferring agent to transfer the ligand onto various catalytically important transition metals.³⁵ This method was first discovered by Wang and Lin in 1998 for monodentate carbenes.³⁶ Silver carbene chemistry has gained attention due to growing interest in discovering efficient catalysts. Silver carbene complexes were first revealed in 1993 by Arduengo, with his discovery of a silver-NHC complex from the reaction between free carbene and a silver salt.²⁹ Currently, Ag-NHC complexes are synthesized by four different methods as described by Garrison et al.³⁵ (1) reactions between silver salts and free carbenes; (2) treatment of basic silver reagents with imidazolium salts; (3) in-situ generation of free carbenes from imidazolium salts using a base in the presence of silver salts, (4) transmetalation between tungsten-NHC complexes and silver complexes.

Synthesis of Ag-NHC using free carbenes and silver salts

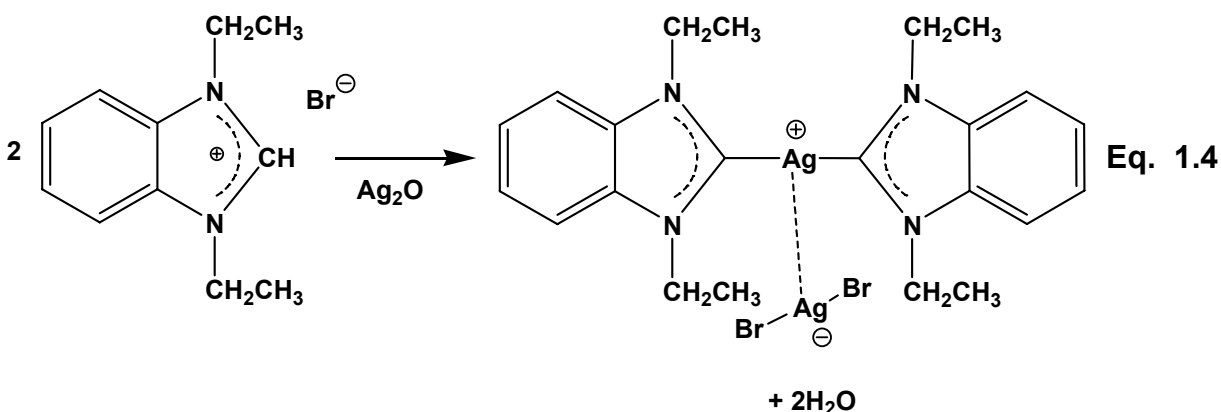
The first silver N-heterocyclic carbene complex was synthesized using free carbenes and silver salts as described by Arduengo et al.²⁹ This synthesis involved the reaction between free N,N'-dimesityl imidazolyldene and silver triflate in THF to generate a silver bis(N,N'-dimesityl imidazolyldene) adduct (Eq. 1.3). The efficiency of this method relies on the stability of the free carbene, which is usually generated via deprotonation of the respective imidazolium salt using a base such as KO^tBu or KH. This use of a strong base sometimes results in decomposition of the free carbene (especially those containing acidic groups, such as methylene groups α to the imidazole nitrogen).³⁵



Synthesis of Ag-NHC using basic silver reagents and imidazolium salts

Silver N-heterocyclic carbene complexes are widely synthesized using this method, where mild silver bases such as Ag₂O, AgOAc and Ag₂CO₃ are used to deprotonate imidazolium salts. The first example of this method was reported in 1998 by Lin and coworkers.³⁶ The reaction involved treatment of 1,3-diethylbenzimidazolium bromide with 0.5 equivalents of Ag₂O to generate a bis(1,3-

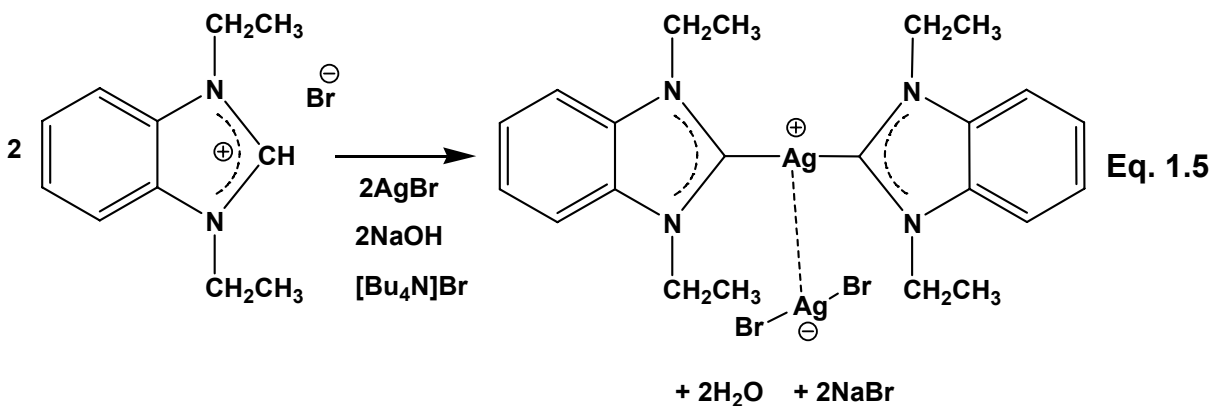
diethylbenzimidazolylidene) silver complex containing $[\text{AgBr}_2]^-$ as a linear anion (Eq. 1.4). This method gives high yields and is accompanied by several advantages, such as stability in atmospheric conditions, no requirement for pretreated solvents, no use of strong bases, and controlled deprotonation at the imidazolium carbon.³⁷



In-situ generation of free carbenes from imidazolium salts using a base and silver salts

In this method, the deprotonation of the imidazolium salt is achieved by adding a base. A silver salt is also present in the reaction mixture to couple with the free carbene generated in situ during the reaction. Example of this type of reaction was reported by Lin and coworkers in which they used NaOH as the base to deprotonate a benzimidazolium salt.³⁶ The free carbene generated was then coupled with AgBr in the presence of $[\text{Bu}_4\text{N}]\text{Br}$, which act as a phase transfer catalyst to synthesize the silver-NHC complex (Eq. 1.5).³⁶ However, this method has not gained much attention, as it has been difficult to use this technique efficiently with other

silver N-heterocyclic carbenes besides the examples reported by Lin and coworkers.³⁵



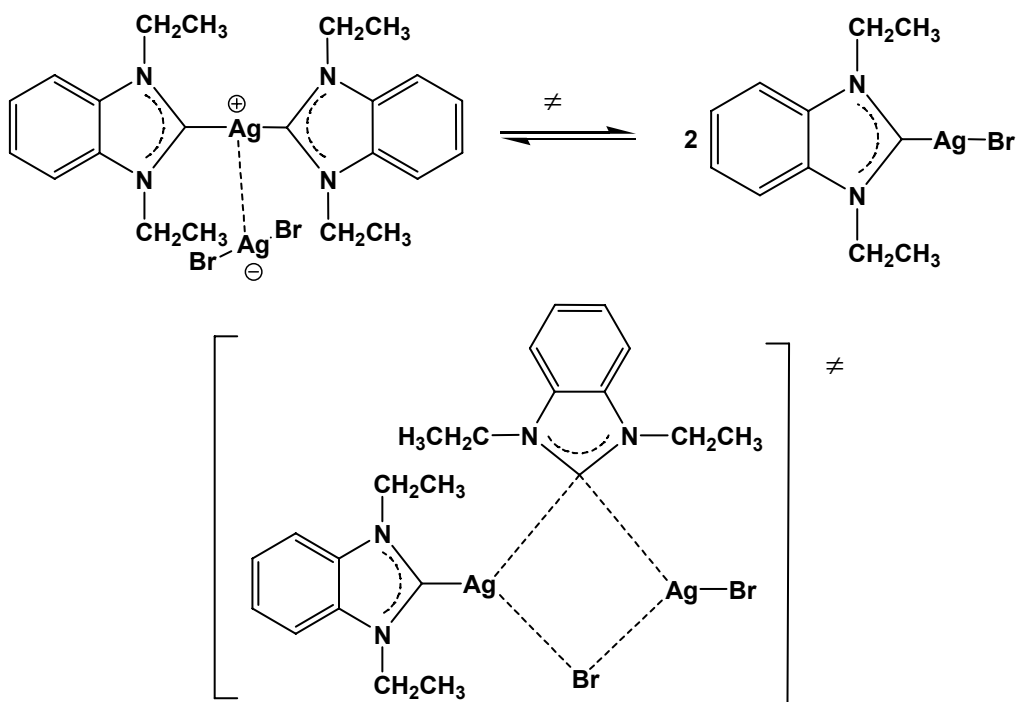
Transmetalation between tungsten-NHC complexes and silver complexes

In 1999 Liu et al. reported formation of silver-NHC complexes via transmetalation using the (1,3-ethylimidazolidin-2-ylidene)W(CO)₅ complex.³⁸ However, these silver(NHC) complexes were very reactive with H₂O. A trace of moisture present in the reaction medium could decompose the silver(NHC) to the imidazolinium cation. Therefore, currently this method is not recognized as an efficient method to synthesize of silver-NHC complexes.

Detection of Ag-NHC complexes

One of the most definitive techniques for the detection of Ag-C_{Carbene} bond formation in silver-NHC complex synthesis is the spectroscopic detection of Ag-C_{Carbene} coupling using ¹³C NMR. The carbene carbon resonance of silver-NHC complexes generally comes in the range of 213.7 – 163.2 ppm, and the Ag-C_{Carbene}

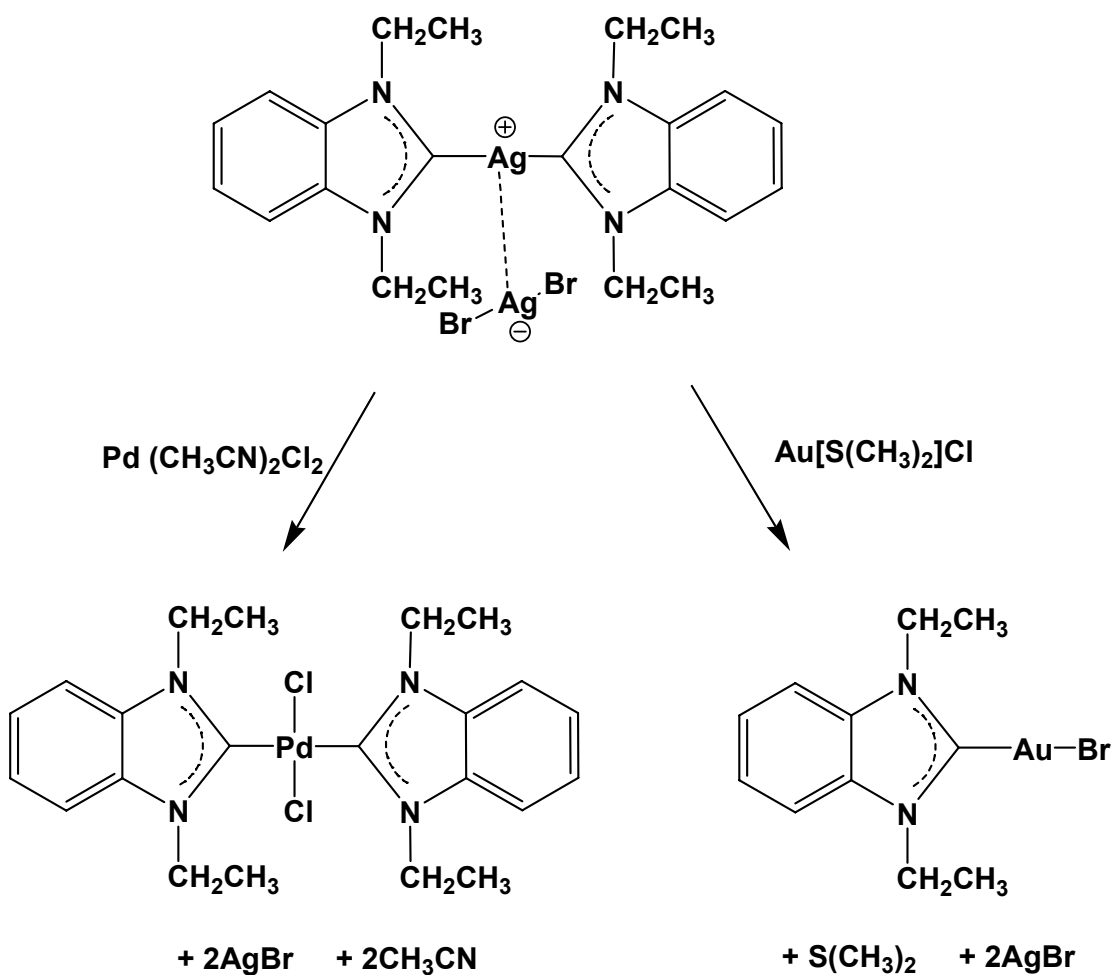
coupling constant falls between 180 – 234 Hz for ^{107}Ag and 204 – 270 Hz for ^{109}Ag isotopes, which have natural abundances of 51.839(7)% and 48.161(7)% respectively.³⁵ However, some silver-NHC complexes have been reported to have no detectable Ag-C_{Carbene} coupling or C_{Carbene} resonances. This observation was explained by Lin and coworkers as a result of fluxional behavior of silver-NHC complexes in solution (Scheme 1.4).³⁶



Scheme 1.4. Fluxional behavior of silver-NHC complexes in solution. Adapted from Reference 37.

The concept of using silver-NHC complexes to transfer the carbene ligand to another metal complex was first established by Lin and coworkers.³⁶ They were able to transfer an N,N'-diethylbenzimidazol-2-ylidene ligand from silver to Pd(II) and Au(I) complexes successfully (Eq. 1.6) and have mentioned that the fluxional

behavior of silver-NHC complexes (Scheme 1.4) is important in carbene transmetalation reactions .



Eq. 1.6

Among the various silver-NHC complexes reported to date, the number of bis(NHC) complexes is comparatively low. Among these few reported bis(NHC) silver complexes are dimeric silver(NHC) complexes derived from bis(1,1'-methylimidazolium)-3,3'-methylenediiodide as well as bis(1,1'-*n*-butylimidazolium)-3,3'-methylenediiodide³⁹ and bidentate silver-NHC complexes derived from

imidazolium linked cyclophanes.^{40,41} However, synthesis of silver bis(NHC) complexes bearing bulky N-substituents and their carbene transfer reactions have not investigated thoroughly.^{35,42} Access to bulky bis(NHC) complexes is important since they can be easily used to synthesize various other metal complexes containing bulky bis(NHC) ligands. These bulky bis(NHC) metal complexes are predicted to be more stable during catalysis and useful in inhibiting catalyst decomposition since the steric bulk protects reactive metal centers. Therefore, further investigation on the synthesis and reactivity of sterically bulky bis(NHC) complexes is needed and will be discussed in Chapter 2.

1.4 Acyclic Diamino Carbenes (ADCs)

N-heterocyclic carbenes (NHCs) or cyclic diaminocarbenes, are the most widely known type of carbenes, and they have been extensively used in transition metal chemistry to date. After the first discovery of NHCs and subsequent isolation of “bottle-able” free carbenes by Arduengo et al.,¹⁶ the application of NHCs in transition metal chemistry was triggered due to their strong σ -donating abilities exceeding those of phosphine ligands,²⁸ high thermal stabilities and unique steric properties.⁴³ However, tuning of steric properties and σ -donor abilities of NHC ligands by introducing different N-substituents have not yet been as readily achieved as compared with phosphine ligands.⁴⁴ In addition, the number of chiral NHC ligands reported is also much smaller than the large number of chiral phosphine ligands available for enantioselective catalysis.^{45,46} Therefore, developing new approaches

to obtain new carbene ligands with tunable steric properties, novel electron donor properties, and improved chirality are important goals.

Acyclic diamino carbenes (ADCs) are singlet carbenes which have no formal charge on the carbene carbon (Figure 1.7). ADCs are electronically similar to NHCs because they have two strong σ -withdrawing and π -donating nitrogen groups neighboring the carbene carbon. In addition, ADCs are proposed to be potentially stronger σ -donors than NHCs,⁴⁷ but they have not been substantially investigated as coordinating ligands in contrast with NHCs.^{48,49}

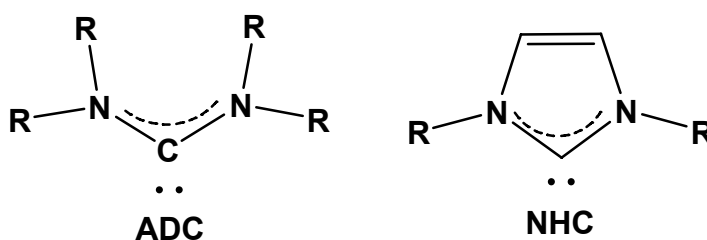


Figure 1.7. An acyclic diaminocarbene and an N-heterocyclic carbene.

ADC ligands have unique properties that could potentially make them effective ligands. These properties include the high basicity of ADCs, which allows them to act as strong σ -donor ligands,^{50,51,48} increased NCN bond angles compared to NHC ligands which allows N-substituents to be closer to the metal center,^{49,52,47} and the easy introduction of chirality to the ligand.

Early methods of synthesizing ADC-containing metal complexes involved nucleophilic attack of secondary amines on metal bound isocyanide groups to generate a diaminocarbene complex (Figure 1.8A),⁵³ deprotonation of a tetrazolium ion with carbonyl ferrate to generate an iron-ADC complex as a by product (Figure

1.8B),⁵⁴ and reaction of chloroformamidinium chloride with $\text{Fe}_2(\text{CO})_9$ to generate a bis(dimethylamino)carbene iron carbonyl complex⁵⁵ (Figure 1.8C).⁵² Unfortunately, method (B) and (C) are highly specific reactions for their respective starting compounds. Method (A) has been investigated for synthesizing a number of monodentate ADC containing metal complexes.

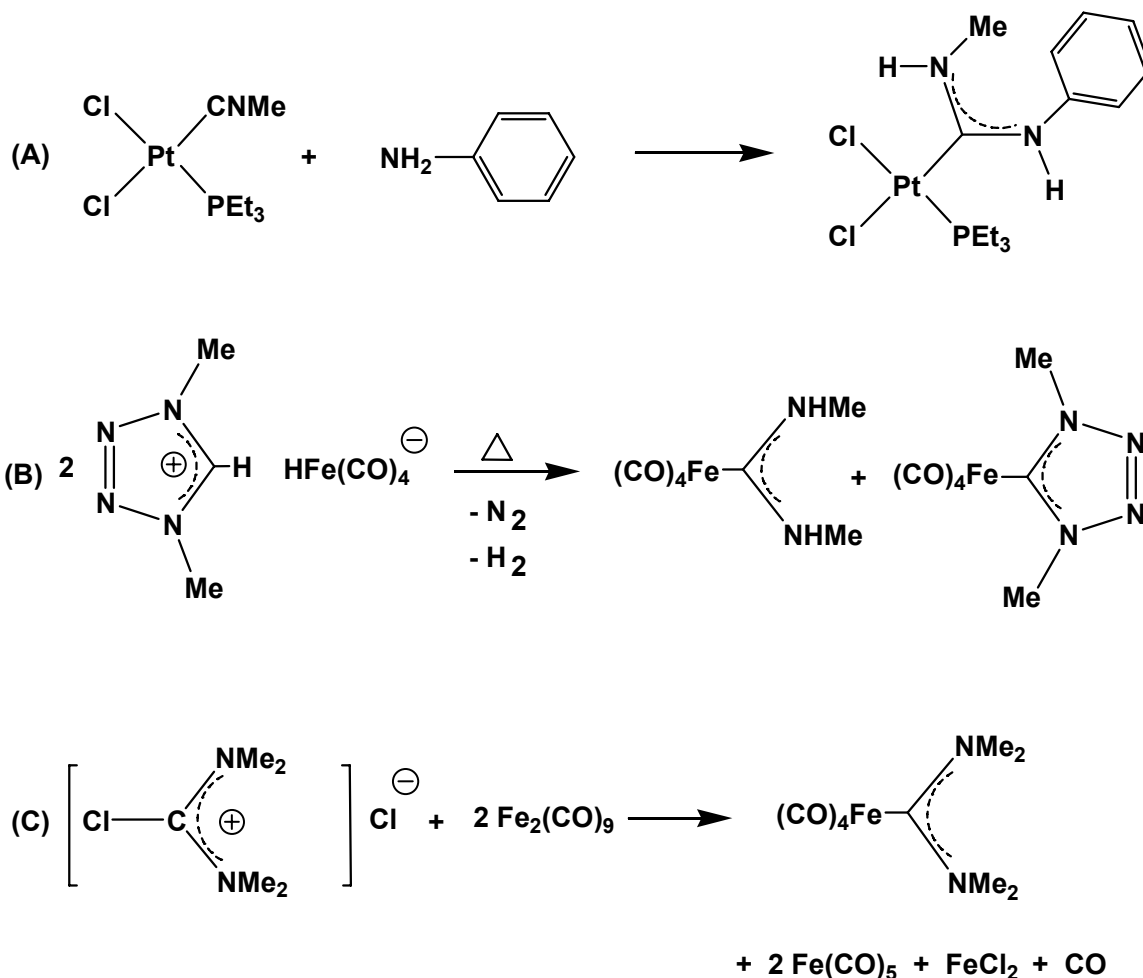
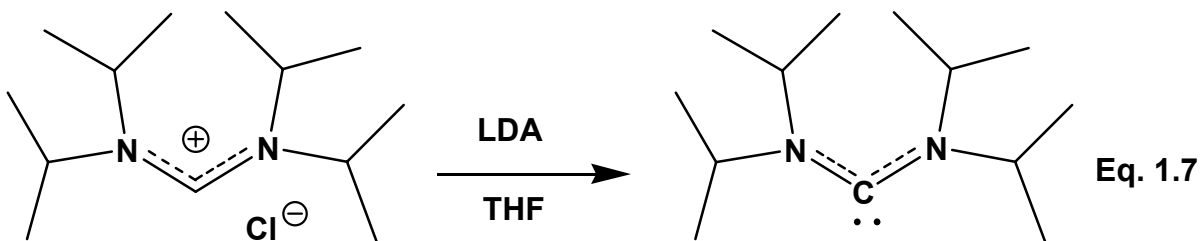


Figure 1.8. Early synthesis methods of metal ADC complexes.

Recent interest in acyclic diamino carbenes as ancillary ligands in metal complexes was initiated by Alder et al. in 1996 by the synthesis and isolation of the first stable free acyclic diaminocarbene via deprotonation of N,N,N',N'- tetraisopropyl

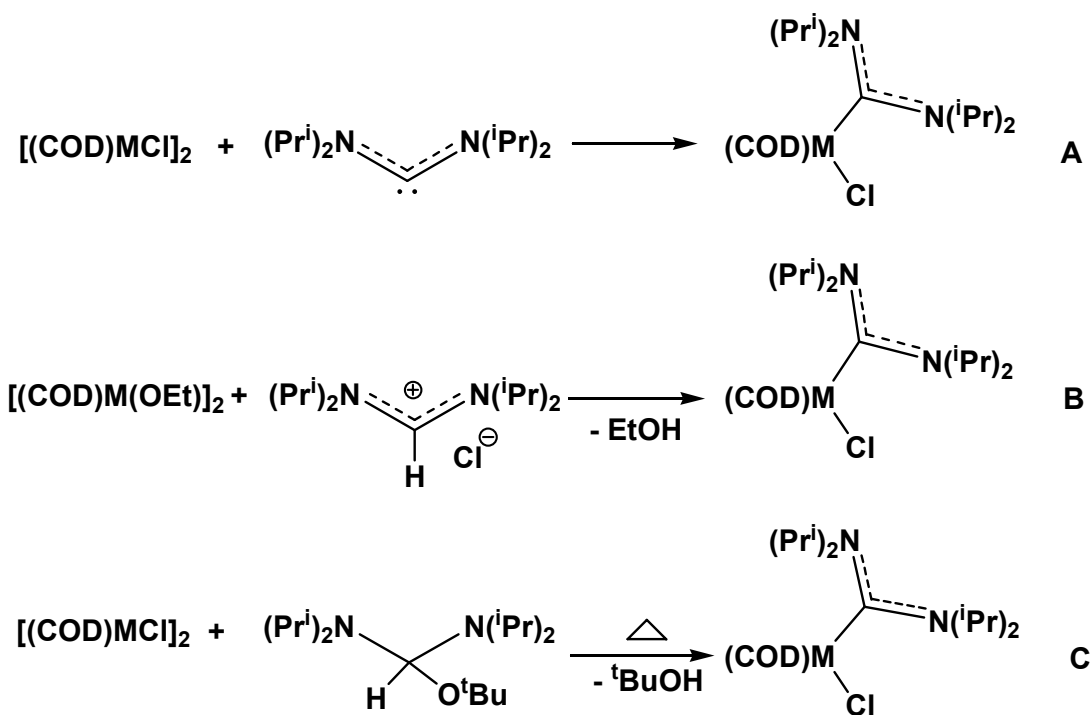
formamidinium chloride with lithium diisopropylamide (LDA) (Eq. 1.7).⁵⁶ The free bis(diisopropylamino)carbene generated was stable and could be sublimed under nitrogen, although it displayed higher sensitivity for oxygen and moisture than other types of free carbenes.⁵⁶



Less hindered ADCs such as bis(dimethylamino)carbenes have been reported to be only slightly stable tending to decompose at 0 °C after few hours in solution.⁵⁷ However, comparatively less sterically hindered ADC ligands such as bis(N-piperidyl)carbene⁵⁸ and bis(diethylamino)carbene⁵⁹ were kinetically stable, displaying solution-phase dimerisation only upon complexation with alkali metals. These alkali metals which induce carbene dimerisation are counterions from the strong base used in the generation of free carbenes. However, the relative instability of free acyclic diamino carbenes displayed by decomposition and dimerisation indicates the difficulty of using them in subsequent metalation reactions.⁴⁹

Relatively stable free acyclic diamino carbenes have been coupled with metal precursors to synthesize new metal-ADC complexes.⁴⁹ Rhodium and iridium complexes containing bis(diisopropylamino)carbene have been synthesized by Herrmann et al. following three different methods.⁶⁰ These methods involve; reaction of free ADC with metal precursors containing bridging chlorides (Scheme1.5A), *in*

situ deprotonation of formamidine chloride and coupling with a metal precursor containing an ethoxy bridge which acts as an internal base for deprotonation of the formamidine salt (Scheme 1.5B), and the reaction of metal precursors with an alcoholate adduct of the formamidine salt to generate the free carbene *in situ* by eliminating the corresponding alcohol (Scheme 1.5C).⁴⁷



Scheme 1.5. Methods of synthesizing metal(ADC) complexes using free bis(diisopropylamino)carbene and different metal precursors.

However, attempts by Herrmann et al. to synthesize chelating bis(ADC) metal complexes by the free carbene method were unsuccessful due to the high reactivity of the free bis(ADC) generated.⁶¹ However, there is precedent in the early literature

for bis(ADC) complex formation by other methods. In 1915 Chugaev synthesized a bis(ADC) complex via metal-templated nucleophilic attack of hydrazine on platinum bound isocyanide ligands (Figure 1.9a).^{62,63} Unfortunately, the correct structure of this first metal carbene complex was not recognized until 1970, since the structure was originally assigned incorrectly based on analytical and conductivity data (Figure 1.9b).^{64,65} The correct structure of this complex was determined by Shaw et al.^{65,66} using spectroscopic studies and Burke et al.⁶⁴ using X-ray crystallography in 1970.

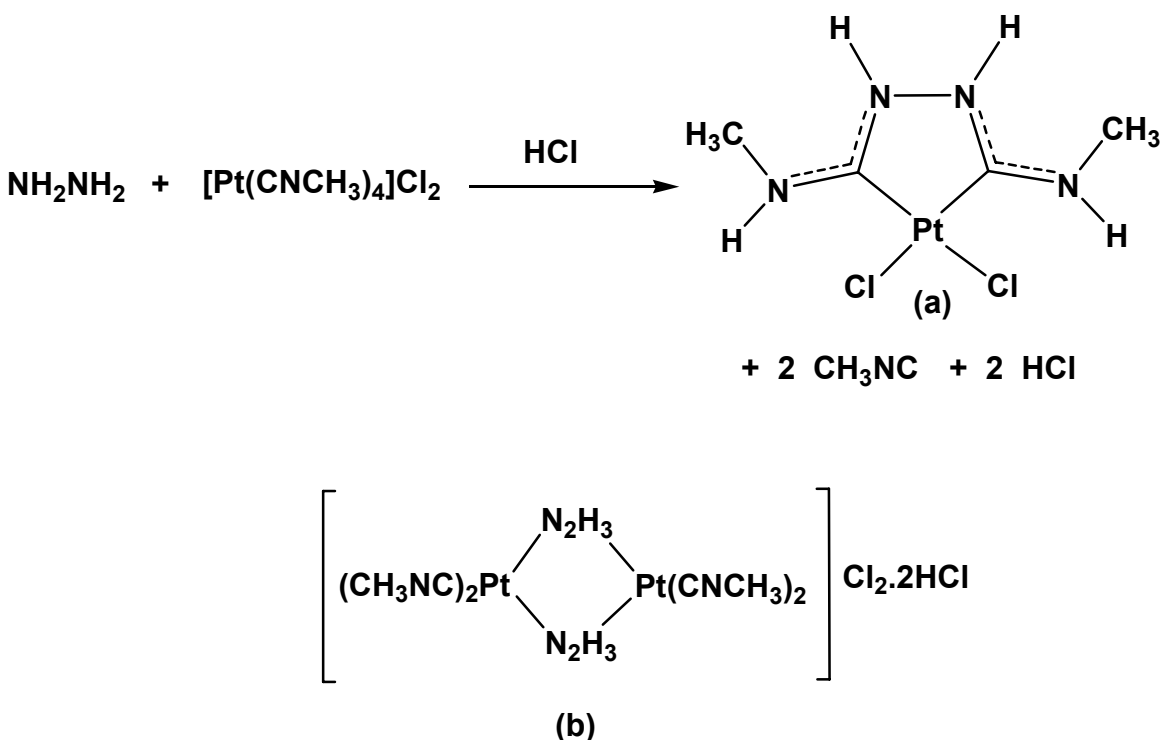


Figure 1.9. The synthesis of Chugaev carbene complex; correct structure (a) and the originally proposed structure (b). Adapted from References 65 and 50.

Following Chugaev's basic method of synthesizing metal bis(ADC) complexes, a general preparative procedure was reported for an array of palladium

bis(ADC) complexes which contained various N-substituents derived from different alkyl isocyanides (Me, ⁱPr, Cy, ^tBu), different halides (Cl, Br), and different hydrazine back bones.^{67,68,69} In early reports, Chugaev's method has been followed in synthesizing iron(ADC),⁷⁰ ruthenium (ADC)⁷¹ and gold(ADC)⁷² complexes. Most of the chelating bis(ADC) metal complexes reported in these studies were comparatively less sterically hindered. Attempts to make bulky chelating bis(ADC) metal complexes were unsuccessful, producing a metal complex with two mono(ADC) ligands.⁶⁸ Therefore further exploration of chelating bis(ADC) metal complexes including bulky ligand structures and chiral examples, are warranted and could be critical for the development of new catalytically important metal carbene complexes. Development of a new synthetic method based on nucleophilic attack of secondary amines on metal-bound isocyanide groups for the synthesis of bulky and chiral chelating bis(ADC) palladium complexes is the main focus of this dissertation.

References

1. Crabtree, R. H. *The Organometallic Chemistry of the Transition Metals*; Wiley International: New York, 2001.
2. Smith, M. B.; March, J. *MARCH'S Advanced Organic Chemistry: Reactions, Mechanisms, and Structure*; John Wiley & Sons: New York, 2001.
3. Bourissou, D.; Guerret, O.; Gabbai, F. P.; Bertrand, G. *Chem.Rev.* **2000**, *100*, 39.
4. Gleiter, R.; Hoffmann, R. *J. Am. Chem. Soc.* **1968**, *90*, 5457.
5. Myers, D. R.; Senthilnathan, V. P.; Platz, M. S.; Jones, J.; Jr. *J. Am. Chem. Soc.* **1986**, *108*, 4232.
6. Gano, J. E.; Wettach, R. H.; Platz, M. S.; Senthilnathan, V. P. *J. Am. Chem. Soc.* **1982**, *104*, 2326.
7. Moradelli, D. A.; Morgan, S.; Platz, M. S. *J. Am. Chem. Soc.* **1992**, *114*, 7034.
8. Richards, C. A.; Jr.; Kim, S. J.; Yamaguchi, Y.; Schaefer, H. F.; III. *J. Am. Chem. Soc.* **1995**, *117*, 10104.
9. Fischer, E. O.; Maasbol, A. *Angew.Chem., Int.Ed.Engl.* **1964**, *3*, 580.
10. Darensböurg, M. Y.; Darensböurg, D. J. *Inorg.Chem.* **1970**, *9*, 32.

11. Schrock, R. R. *J. Am. Chem. Soc.* **1974**, *96*, 6796.
12. Schrock, R. R. *J. Chem. Soc. Dalton Trans.* **2001**, 2541.
13. Herrmann, W. A.; Kocher, C. *Angew. Chemie., Int. Ed. Engl.* **1997**, *36*, 2163.
14. Öfele, K. *J. Organomet. Chem.* **1968**, *12*, 42.
15. Wanzlick, H. W.; Schönher, H. J. *Angew. Chemie., Int. Ed. Engl.* **1968**, *7*, 141.
16. Arduengo, A. J.; Harlow, R. L.; Kline, M. J. *Am. Chem. Soc.* **1991**, *113*, 361.
17. Diez-Gonzalez, S.; Nolan, S. P. *Coord. Chem. Rev.* **2007**, *251*, 874.
18. Wanzlick, H. W. *Angew. Chem., Int. Ed. Engl.* **1962**, *1*, 75.
19. Arduengo, A. J.; Dias, H. V. R.; Harlow, R. L.; Kline, M. J. *Am. Chem. Soc.* **1992**, *114*, 5530.
20. Dixon, D. A.; Arduengo, A. J. *J. Phys. Chem.* **1991**, *95*, 4180.
21. Trnka, T. M.; Grubbs, R. H. *Acc. Chem. Res.* **2001**, *34*, 18.
22. Herrmann, W. A.; Elison, M.; Fischer, J.; Kocher, C.; Artus, G. R. J. *Angew. Chemie., Int. Ed. Engl.* **1995**, *34*, 2371.

23. Gstottmayr, C. W. K.; Bohm, V. P. W.; Herdtweck, E.; Grosche, M.; Herrmann, W. A. *Angew. Chemie., Int. Ed. Engl.* **2002**, *41*, 1363.
24. Stauffer, S. R.; Lee, S. W.; Stambuli, J. P.; Hauck, S. I.; Hartwig, J. F. *Org. Lett.* **2000**, *2*, 1423.
25. Herrmann, W. A.; Goossen, L. J.; Kocher, C.; Artus, G. R. J. *Angew. Chemie., Int. Ed. Engl.* **1996**, *35*, 2805.
26. Prinz, M.; Grosche, M.; Herdtweck, E.; Herrmann, W. A. *Organometallics* **2000**, *19*, 1692.
27. Herrmann, W. A. *Angew. Chemie., Int. Ed. Engl.* **2002**, *41*, 1290.
28. Huang, J. K.; Schanz, H. J.; Stevens, E. D.; Nolan, S. P. *Organometallics* **1999**, *18*, 2370.
29. Arduengo, A. J.; Dias, H. V. R.; Calabrese, J. C.; Davidson, F. *Organometallics* **1993**, *12*, 3405.
30. Albrecht, M.; Miecznikowski, J. R.; Samuel, A.; Faller, J. W.; Crabtree, R. H. *Organometallics* **2002**, *21*, 3596.
31. Wanniarachchi, Y. A.; Khan, M. A.; Slaughter, L. M. *Organometallics* **2004**, *23*, 5881.

32. Bonnet, L. G.; Douthwaite, R. E.; Hodgson, R. *Organometallics* **2003**, *22*, 4384.
33. Mata, J. A.; Chianese, A. R.; Miecznikowski, J. R.; Poyatos, M.; Peris, E.; Faller, J. W.; Crabtree, R. H. *Organometallics* **2004**, *23*, 1253.
34. Muehlhofer, M.; Strassner, T.; Herdtweck, E.; Herrmann, W. A. *J. Organomet. Chem.* **2002**, *660*, 121.
35. Garrison, J. C.; Youngs, W. J. *Chem. Rev.* **2005**, *105*, 3978.
36. Wang, H. M. J.; Lin, I. J. B. *Organometallics* **1998**, *17*, 972.
37. Lin, I. J. B.; Vasam, C. S. *Comments on Inorganic Chemistry* **2004**, *25*, 75.
38. Ku, R. Z.; Huang, J. C.; Cho, J. Y.; Kiang, F. M.; Reddy, K. R.; Chen, Y. C.; Lee, K. J.; Lee, J. H.; Lee, G. H.; Peng, S. M.; Liu, S. T. *Organometallics* **1999**, *18*, 2145.
39. Quezada, C. A.; Garrison, J. C.; Panzner, M. J.; Tessier, C. A.; Youngs, W. J. *Organometallics* **2004**, *23*, 4846.
40. Baker, M. V.; Brown, D. H.; Haque, R. A.; Skelton, B. W.; White, A. H. *Dalton Trans.* **2004**, 3756.
41. Garrison, J. C.; Simons, R. S.; Kofron, W. G.; Tessier, C. A.; Youngs, W. J. *Chem. Commun.* **2001**, 1780.

42. Lin, I. J. B.; Vasam, C. S. *Coord. Chem. Rev.* **2007**, *251*, 642.
43. Scott, N. M.; Nolan, S. P. *Eur. J. Inorg. Chem.* **2005**, 1815-1828.
44. Cavallo, L.; Correa, A.; Costabile, C.; Jacobsen, H. J. *J. Organomet. Chem.* **2005**, *690*, 5407.
45. Douthwaite, R. E. *Coord. Chem. Rev.* **2007**, *251*, 702.
46. Tang, W. J.; Zhang, X. M. *Chem. Rev.* **2003**, *103*, 3029.
47. Denk, K.; Sirsch, P.; Herrmann, W. A. *J. Organomet. Chem.* **2002**, *649*, 219.
48. Dhudshia, B.; Thadani, A. N. *Chem. Commun.* **2006**, 668.
49. Slaughter, L. M. *Comments on Inorganic Chemistry* **2008**, *29*, 46.
50. Magill, A. M.; Cavell, K. J.; Yates, B. F. *J. Am. Chem. Soc.* **2004**, *126*, 8717.
51. Lee, M. T.; Hu, C. H. *Organometallics* **2004**, *23*, 976.
52. Herrmann, W. A.; Ofele, K.; von Preysing, D.; Herdtweck, E. *J. Organomet. Chem.* **2003**, *684*, 235.
53. Badley, E. M.; Chatt, J.; Richards, R. L.; Sim, G. A. *Chem. Commun.* **1969**, 1322.
54. Ofele, K.; Kreiter, C. G. *Chem. Ber.* **1972**, *105*, 529.

55. Petz, W. *Angew. Chem.* **1975**, *87*, 288.
56. Alder, R. W.; Allen, P. R.; Murray, M.; Orpen, A. G. *Angew. Chemie., Int. Ed. Engl.* **1996**, *35*, 1121.
57. Otto, M.; Conejero, S.; Canac, Y.; Romanenko, V. D.; Rudzevitch, V.; Bertrand, G. *J. Am. Chem. Soc.* **2004**, *126*, 1016.
58. Alder, R. W.; Blake, M. E. *Chem. Commun.* **1997**, 1513.
59. Alder, R. W.; Chaker, L.; Paolini, F. P. V. *Chem. Commun.* **2004**, 2172.
60. Frey, G. D.; Herdtweck, E.; Herrmann, W. A. *J. Organomet. Chem.* **2006**, *691*, 2465.
61. Herrmann, W. A.; Schutz, J.; Frey, G. D.; Herdtweck, E. *Organometallics* **2006**, *25*, 2437.
62. Tschugajeff(Chugaev), L.; Skanawy-Grigorjewa, M. *J. Russ. Chem. Soc.* **1915**, *47*, 776.
63. Tschugajeff, L.; Grigorjewa, M.; Posnjak, A. Z. *Anorg. Allg. Chem.* **1925**, *148*, 37.
64. Burke, A.; Balch, A. L.; Enemark, J. H. *J. Am. Chem. Soc.* **1970**, *92*, 2555
65. Rouschias, G.; Shaw, B. L. *Chem. Commun.* **1970**, 183.

66. Rouschias, G.; Shaw, B. L. *J. Chem. Soc. (A)*. **1971**, 2097.
67. Moncada, A. I.; Manne, S.; Tanski, J. M.; Slaughter, L. M. *Organometallics* **2006**, 25, 491.
68. Moncada, A. I.; Tanski, J. M.; Slaughter, L. G. M. *J. Organomet. Chem.* **2005**, 690, 6247.
69. Moncada, A. I. Master's Oklahoma State University, 2005.
70. Balch, A. L.; Miller, J. *J. Am. Chem. Soc.* **1972**, 94, 417.
71. Doonan, D. J.; Balch, A. L. *Inorg. Chem.* **1974**, 13, 921.
72. Uson, R.; Laguna, A.; Villacampa, M. D.; Jones, P. G.; Sheldrick, G. M. *J. Chem. Soc., Dalton Trans.*, **1984**, 2035.

CHAPTER II

SYNTHESIS, CHARACTERIZATION AND CARBENE TRANSFER REACTIVITY OF A SILVER BIS(N-HETEROCYCLIC CARBENE) COMPLEX

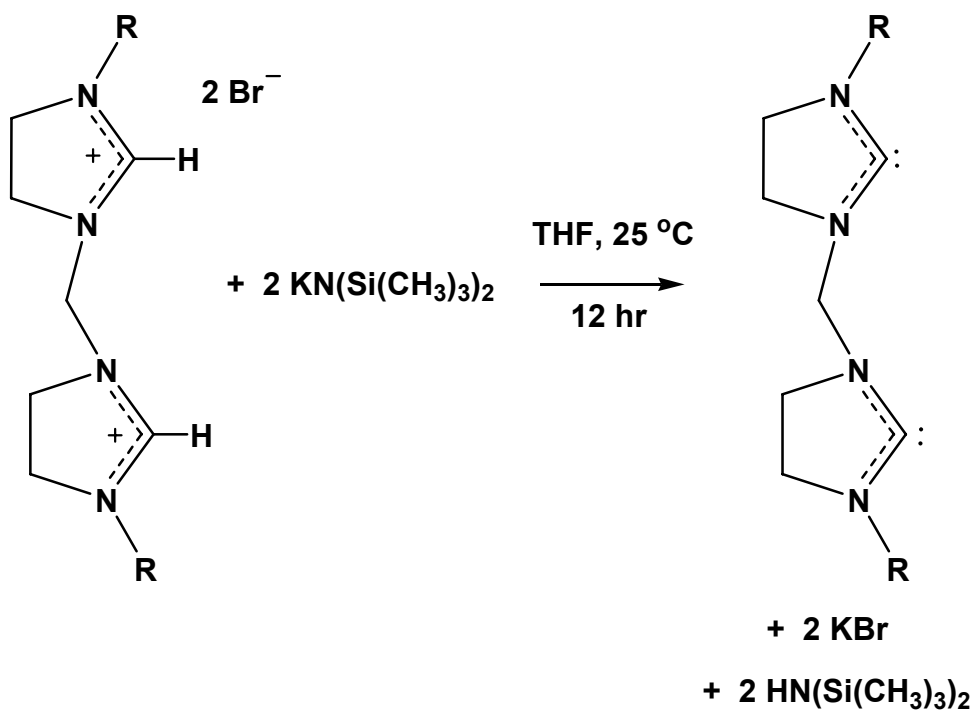
“Portions reproduced with permission from [Wanniarachchi, Y. A., Khan, M. A., Slaughter, L. M. *Organometallics*, **2004**, 5881-5884. Copyright [2004] American Chemical Society.”

Introduction

N-Heterocyclic carbenes (NHCs) are one of the most useful ligand types used in transition metal catalysis in recent years. This is mainly due to the strong σ -donacity and thermal stability of NHCs compared to analogous phosphine ligands.¹ The synthesis of silver NHC complexes was first reported by Arduengo and coworkers in 1993.² Since then, many reports have been appeared on the synthesis of silver NHC complexes. These include a polymeric 1,2,4-triazole-3,5-diylidene silver (I) complex reported in 1997 by Bertrand and coworkers using silver acetate as a mild base to deprotonate the triazodinium precursor³ and a bis(diethylbenzimidazole-2-ylidene) silver(I) complexes reported by Lin et al. in 1998 using silver oxide as the base.⁴

Currently, one of the most widely used methods for synthesizing metal NHC complexes involves the use of silver NHC complexes as carbene transferring agents. This method of synthesizing novel metal NHC complexes was first discovered by Wang and Lin in 1998. Their synthesis involved the use of silver diethylbenzimidazol-2-ylidene complexes to transfer the diethylbenzimidazol-2-ylidene ligand to palladium(II) and gold(I) complexes.⁴ The use of silver NHC complexes as carbene transferring agents is important as free bis(NHC) ligands used in metalation reactions are difficult to generate. It has been observed that when

the bulkiness of the R- groups increases, the yield obtained for free bis(NHC) decreases (Table 1.1). The following free bis(NHCs) were synthesized according to the method reported by Douthwaite et al.⁵ for comparison. (Scheme 2.1).



Scheme 2.1. Free bis(NHC) formation.

Table 2.1. Yields of free bis(NHC) ligands containing different R groups.

	Yield
R = CH ₃	74 %
R = ^t Bu	63 % *
R = Mesityl	14 %

* The yield of 63 % was reported by Douthwaite et al.⁵

The use of silver NHC complexes for the synthesis of other NHC metal complexes has several advantages over the free carbene method. The silver NHC complexes contain high air stability and have less decomposition due to the use of mild base such as Ag_2O rather than strong bases. Among reports of silver NHC complexes, only a few have investigated the synthesis and reactivity of silver bis(NHC) complexes.⁶ Few of the reported bis(NHC) silver complexes are dimeric silver(NHC) complexes derived from bis(1,1'-methylimidazolium)-3,3'-methylenediiodide, bis(1,1'-*n*-butylimidazolium)-3,3'-methylenediiodide⁷ and bidentate silver NHC complexes derived from imidazolium linked cyclophanes.^{8,9} However, the synthesis of silver bis(NHC) complexes bearing bulky N-substituents and their carbene transfer reactions have not been extensively investigated.^{6,10}

Sterically bulky transition metal complexes with bis(carbene) ligands are expected to be stable during catalysis since the bulky groups on the ligand can protect reactive metal intermediates from unwanted side reactions.¹¹ Some silver NHC complexes display a fluxional behavior of the carbene ligand and the metal in solution that can be used as an indication for the ability of silver NHC complexes to transfer the carbene ligand onto other metals.⁴

As an approach to synthesize stable, catalytically important transition metal complexes containing bulky bis(carbene) ligands, the synthesis of a silver complex which contains a sterically crowded bis(carbene) ligand has been targeted. This study describes the synthesis and characterization of a silver complex of the bulky 1,1'-dimesityl-3,3'-methylenediimidazol-2,2'-diylidene ligand, which was first reported by Herrmann and coworkers in a palladium catalyst used in

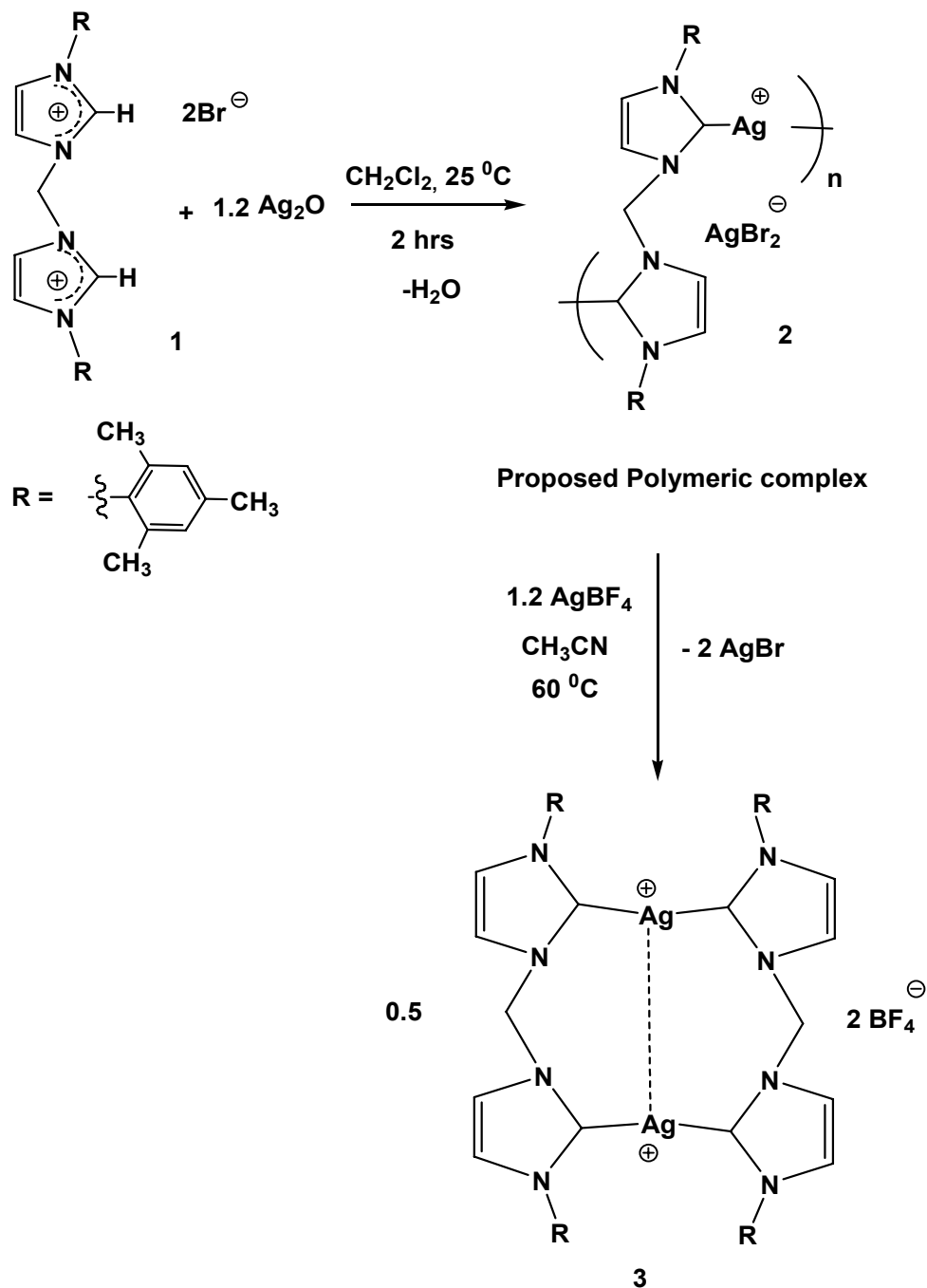
copolymerization of ethylene and CO.¹² In addition, the bulky 1,1'-dimesityl-3,3'-methylenediimidazol-2,2'-diylidene silver complex does not display a fluxional behavior in solution although it displays a higher reactivity towards carbene transfer reactions and will be discussed in Chapter 2.

Results and Discussion

Synthesis and Characterization of a Silver Bis(1,1'-dimesityl-3,3'-methylenediimidazol-2,2'-diylidene) Complex [(κ^2 , μ_2 -DIMes^{Me})Ag]

Mesityl imidazole and 1,1'-dimesityl-3,3'-methylenediimidazolium dibromide were synthesized according to procedures published by Herrmann et al., 1999.¹² A sample of 1,1'-dimesityl-3,3'-methylenediimidazolium dibromide **1** was treated with silver oxide (1.2 equiv) in methylene chloride for 2 h at room temperature. Aluminum foil was used to cover the flask to protect from light. After 2 h, the reaction mixture was filtered through celite to obtain a brown filtrate, and the solvent was evaporated using rotovap to obtain a brown oily product. This product appeared amorphous, and all attempts to grow crystals suitable for X-ray crystallographic analysis failed. However, conversion to a carbene complex was evident in the disappearance of imidazolium proton in the ¹H NMR spectrum obtained in DMSO-*d*₆. Based on literature precedent¹³ and reaction stoichiometry, this intermediary product can be formulated as [(κ^2 , μ_2 -DIMes^{Me})Ag]_n[AgBr₂]_n **2** (Scheme 2.2). Compound **2** was further treated with 1.2 equiv of AgBF₄ in acetonitrile to displace the AgBr₂⁻ anion with the BF₄⁻ anion, generating compound **3**. The isolation of compound **3** from the reaction mixture was difficult, because the silver bromide byproduct was finely

dispersed in acetonitrile. Therefore, the product was isolated by re-dissolving the dry crude product in distilled methylene chloride and filtering through celite. The filtrate was layered with distilled diethyl ether to precipitate the product as a white microcrystalline solid.



Scheme 2.2. Formation of silver bis(carbene) complexes **2** and **3**.

X-ray quality crystals of **3** were grown by slow diffusion of distilled diethyl ether into a concentrated CH₂Cl₂ solution. According to the crystallographic analysis, compound **3** is a doubly bridged silver bis(NHC) complex with the formulation [(κ²,μ₂-DIMes^{Me})₂Ag₂] [BF₄]₂ (Figure 2.1). In complex **3**, the Ag-C_{carbene} bond lengths were in the range 2.081(2) - 2.095(2) Å, and the C_{carbene} - Ag - C_{carbene} bond angles were in the range 173.50(9) - 171.93(10)° (Table 2.2). These values were very close to the reported bond angles of similar silver bis(NHC) complexes.¹³ The average imidazole C-C back bone bond length of 1.344(4) Å is close to the reported value of 1.32 Å for C(sp²)- C(sp²) bonds.¹⁴ This suggests a localized carbon-carbon double bond in the imidazole ring. The average N(1)-C_{carbene} and N(2)-C_{carbene} bond lengths of 1.355(3) Å is between the expected value of 1.28 Å for C(sp²)- N(sp²) double bond and 1.38 Å for C(sp²)- N(sp³) single bond,¹⁴ which is consistent with a delocalized double bond system in the NCN unit of the imidazole rings.

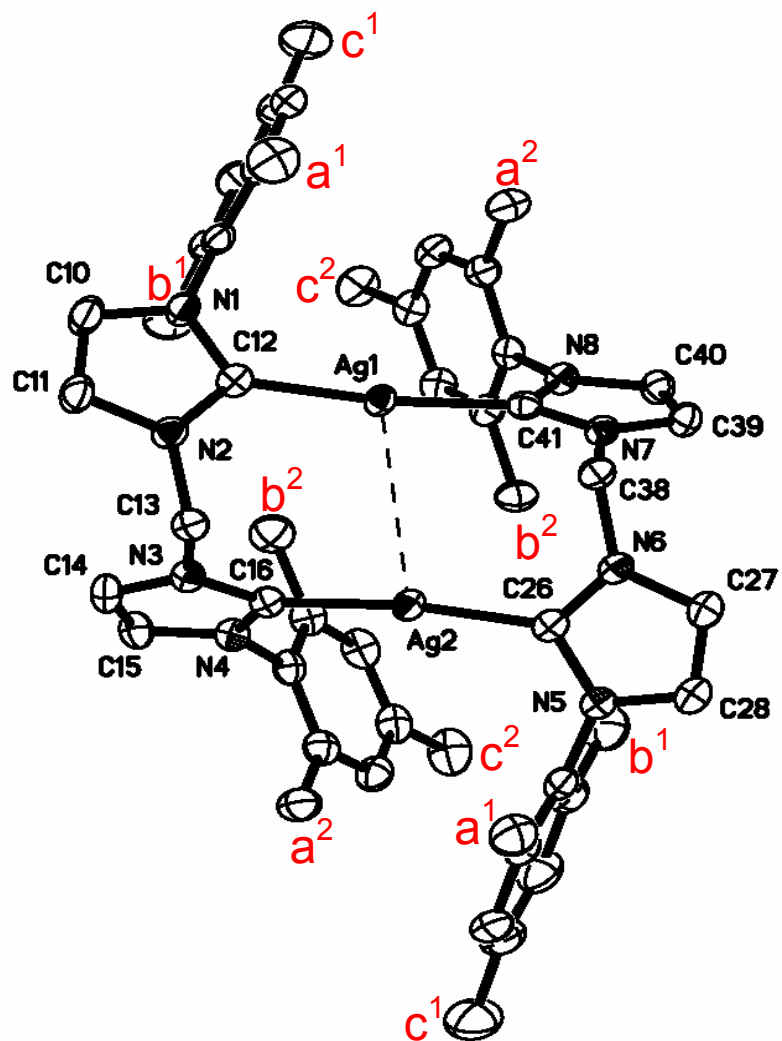


Figure 2.1. Molecular structure of complex **3** with six different aryl-CH₃ groups.

Tetrafluoroborate counter ions are omitted for clarity. Thermal ellipsoids are shown at the 50% probability level.

Table 2.2. Selected bond lengths (Å) and bond angles (°) of complex **3**.

	Bond Lengths (Å)
Ag(1)-C(12)	2.095(2)
Ag(1)-C(41)	2.093(2)
Ag(2)-C(26)	2.086(3)
Ag(2)-C(16)	2.081(2)
Ag(1)-Ag(2)	3.2039(3)
N(1)-C(12)	1.353(5)
N(1)-C(10)	1.394(3)
N(2)-C(12)	1.357(3)
N(2)-C(11)	1.389(3)
C(10)-C(11)	1.343(4)

	Bond angles (°)
C(12)-Ag(1)-C(41)	173.50(9)
C(16)-Ag(2)-C(26)	171.93(10)
N(1)-C(12)-N(2)	103.7(2)
N(4)-C(16)-N(3)	103.7(2)
N(6)-C(26)-N(5)	104.1(2)
N(8)-C(41)-N(7)	103.87(19)

Table 2.3. Crystal data and structure refinement details for complex **3**.

Empirical formula	C ₅₃ H ₆₂ Ag ₂ B ₂ Cl ₆ N ₈ F ₈
Formula weight	1413.17
Crystal system	Triclinic
Space group	<i>P</i> -1
Unit cell dimensions	<i>a</i> = 13.7737(13) Å <i>α</i> = 86.8310(10) ° <i>b</i> = 14.1295(14) Å <i>β</i> = 71.7930(10) ° <i>c</i> = 18.4534(18) Å <i>γ</i> = 68.0620(10) °
Volume	3156.8(5) Å ³
<i>Z</i>	2
Density (calculated)	1.487 Mg/m ³
Absorption coefficient	0.939 mm ⁻¹
Crystal size	0.22x0.18x0.12 mm ³
<i>θ</i> range for data collection	1.56 to 26.83°
Index ranges	-17 ≤ <i>h</i> ≤ 17 -17 ≤ <i>k</i> ≤ 17 -23 ≤ <i>l</i> ≤ 23
Temperature	103(2) K
Wavelength	0.71073 Å
Reflections collected	33693
Independent reflections	13348 (<i>R</i> _{int} = 0.0277)
Final <i>R</i> indices [<i>I</i> > 2σ(<i>I</i>)]	<i>R</i> 1 = 0.0355 <i>wR</i> 2 = 0.0886
<i>R</i> indices (all data)	<i>R</i> 1 = 0.0529 <i>wR</i> 2 = 0.0986
Goodness-of-fit on <i>F</i> ²	1.058

Complex **3** displays an argentophilic interaction as evidenced by an Ag^I-Ag^I contact distance (3.20 Å), that is less than the sum of two van der Waals radii (3.40 Å) for silver.¹⁵ The strength of this interaction is likely relatively low as judged by the values reported for “ligand-unsupported” Ag^I-Ag^I distances (2.80 to 3.30 Å).¹⁵ This type of closed-shell, d¹⁰ - d¹⁰ metallophilic interaction is common for Group 11 elements (Cu, Ag and Au). They are proposed to be stronger than a typical hydrogen bond but weaker than a covalent bond or an ionic bond.¹⁶ Structurally similar silver bis(NHC) complexes, which contain methyl or n-butyl imidazole substituents, have not been reported to display Ag^I-Ag^I interactions.⁷ However, there are some examples of silver(NHC) complexes with argentophilic interactions.^{17,18} Complex **3** is a C₂-symmetric dimer in a twisted-boat conformation. Both methylene linkers are facing one side of the Ag₂ core in the dimer, creating a non-polar cavity with bulky mesityl groups facing the other direction. The X-ray structure shows that the two silver atoms are not sterically protected on one side of the dimer, allowing an interaction with one of the BF₄⁻ anions with close Ag – F interactions of 3.510, 3.461 Å (Figure 2.2).

Most reported silver bis(N-heterocyclic carbene) based complexes are monomeric, containing terminal halides,¹⁹ or polymeric, containing bridging halides or [AgX₂]⁻ anions.¹³ Silver (I) complexes of NHC linked cyclophanes also show similar dimeric structures.²⁰

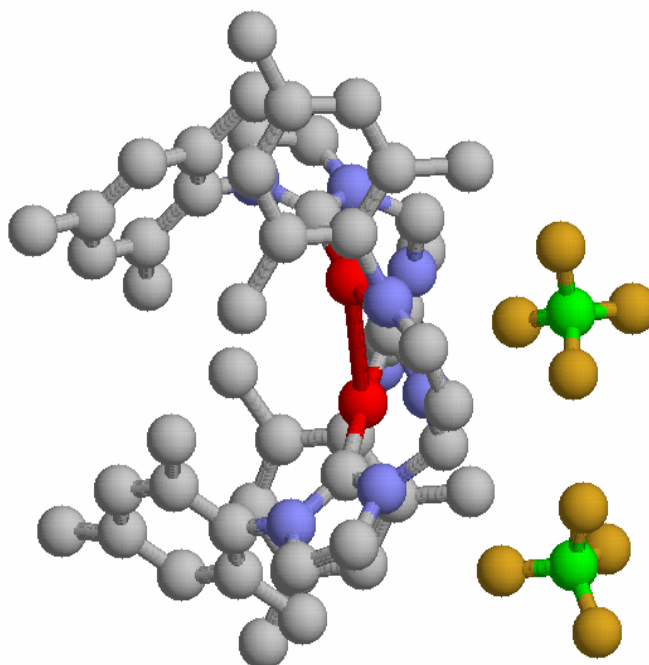


Figure 2.2. Molecular structure of complex **3** displaying the exposed Ag₂ core on one side of the complex. Red (Ag atoms), blue (N atoms), green (B atoms), yellow (F atoms) and gray (C atoms).

A similar type of dimeric bis(N- heterocyclic) carbene silver complexes have been reported by Quezada et al. in 2004 which contain methyl and *n*-butyl substituted bis(imidazole-2-ylidene) ligands.⁷ In comparison to these complexes, complex **3** shows a static nature in solution. This may be due to the ligand bulkiness caused by the mesityl groups in the bis(imidazole-2-ylidene) ligand. The ¹³CNMR of complex **3** indicates two sharp doublets centered at δ 180.9 for carbene carbons in the ligand with coupling constants $^1J^{107}_{\text{Ag-C}} = 182$ Hz and $^1J^{109}_{\text{Ag-C}} = 210$ Hz indicating the static nature of the complex in solution. The values obtained for silver-carbene coupling constants are similar to another reported chelating silver bis(NHC) dimer which contains bridging pyridine groups between the carbene units.²¹ Interestingly, a

structurally similar silver bis(NHC) dimer, which contains methyl groups instead mesityl groups as in complex **3**, did not show silver-carbene coupling in the ^{13}C NMR.⁷ This observation of silver-carbene carbon bond couplings in the ^{13}C NMR supports the existence of nonlabile silver-carbene carbon bonds in the complex. Formation of bulky bis(NHC) silver complex was studied using 1,1'-di(^tbutyl)-3,3'-methylene-bisimidazolium dibromide following the same procedure described for complex **3**. An intermediary oily product obtained similar to the previous complex **2** which could be assigned based on the disappeared imidazolium proton in the ^1H NMR. Attempts to re-crystallize the product from the crude reaction mixture by slow cooling of a CH_2Cl_2 solution using an ice bath and by adding diethyl ether drop wise was unsuccessful giving an oily product instead of a crystalline solid. Therefore, this intermediary product was treated with silver triflate (AgOTf) to obtain a crystalline complex **4**. According to the ^1H NMR and ^{13}C NMR spectrums, this product may exist as a dimer similar to complex **3**. However, the carbene carbon signal and $\text{Ag-C}_{\text{carbene}}$ coupling were missing in the ^{13}C NMR which is different from complex **3**. This may be due to the fluxional behavior of silver-NHC complex in solution, facilitated by the presence of bulky N-^tbutyl substituents in the imidazole ring.

^1H NMR experiments were performed for complex **3** at low temperatures to examine whether the X-ray geometry of complex **3** is present in solution. According to the X-ray structure of complex **3**, six different aryl- CH_3 resonances are expected for the mesityl groups in the molecule (Figure 2.1), However, ^1H NMR at room temperature revealed only three different aryl- CH_3 resonances at δ 2.42, 1.58 and 1.25 (Figure 2.3) indicating a rotational barrier for the mesityl groups but a fluxional

structure in solution in which all mesityl substituents are identical. ^1H NMR at -90°C shows five different aryl- CH_3 resonances at δ 2.39, 1.86, 1.38, 1.14 and 1.05 (Figure 2.3) due to splitting of each *o*- CH_3 resonance in mesityl into two different peaks. This is consistent with the C_2 -symmetric boat conformation seen in the X-ray structure also being present in solution at low temperature. However, at room temperature the molecule possesses enough thermal energy to undergo rapid interconversion between the two enantiomeric conformers, which leads to a ^1H NMR spectrum displaying higher effective symmetry at room temperature.

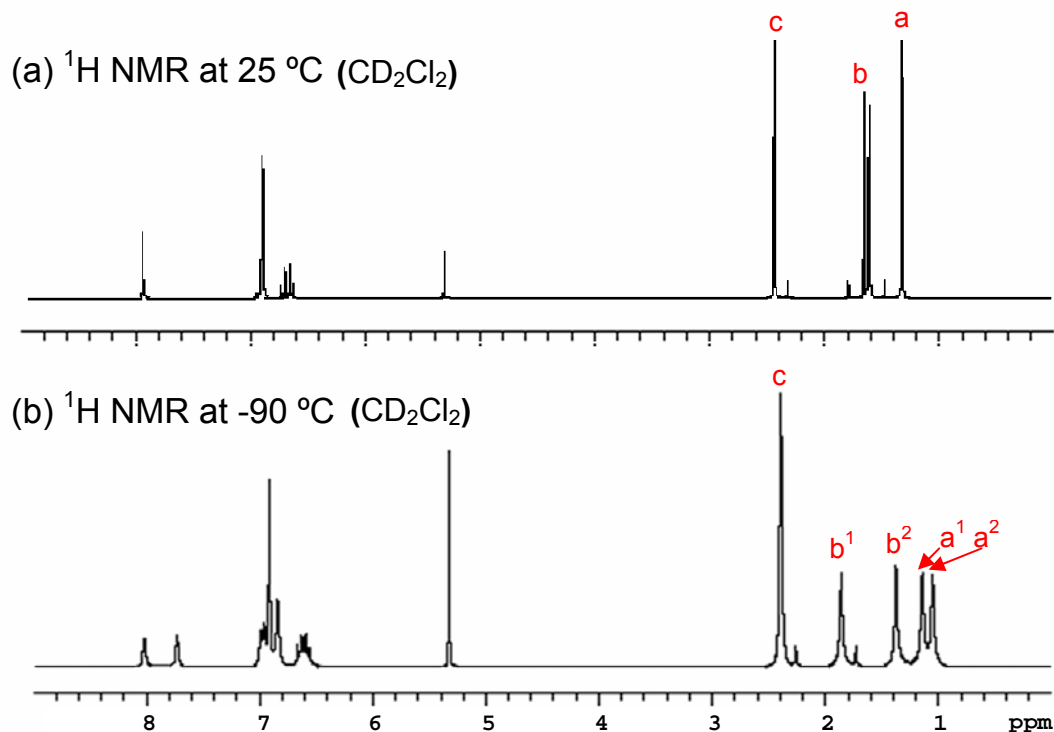


Figure 2.3. ^1H NMR of complex **3** at 25°C (a) and at -90°C (b).

The absence of labile Ag-C bonds in the solution state is also confirmed by higher thermal stability that complex **3** has in solution. Complex **3** displayed a very

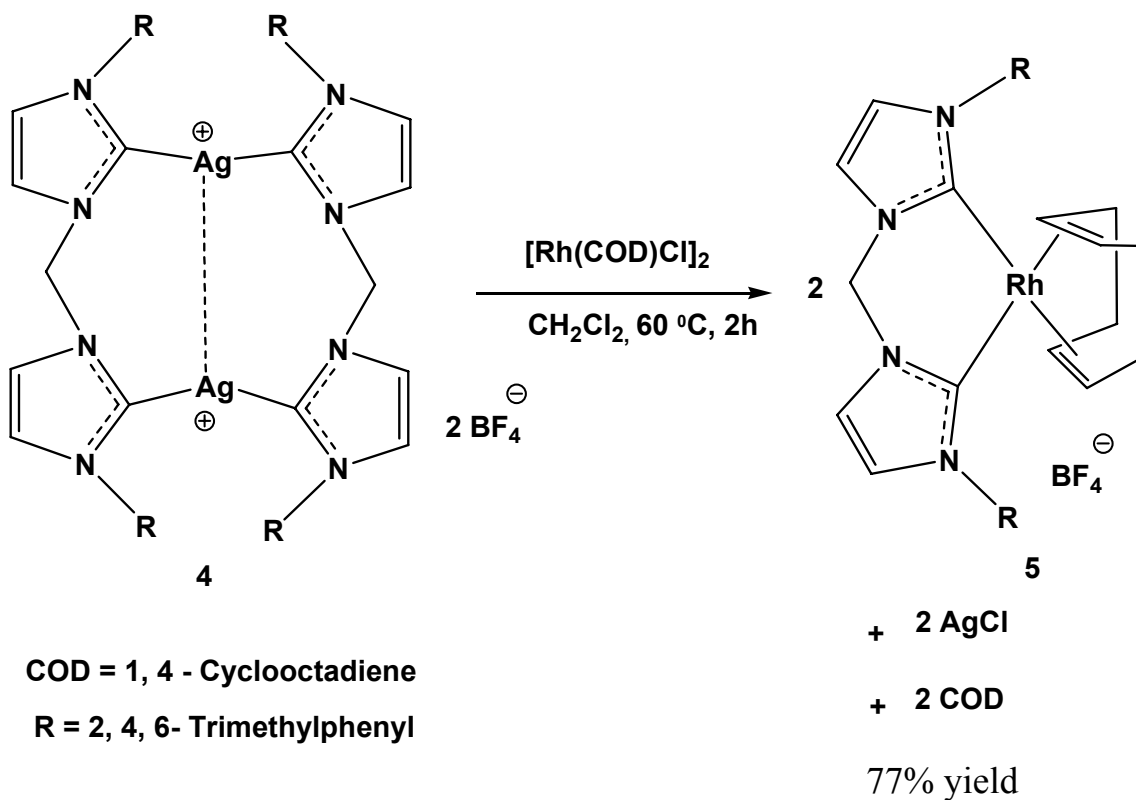
slow decomposition, with only 16% degradation in DMSO- d_6 even after heating at 100°C for five days. Most of the silver NHC complexes reported display rapid ligand exchange behavior in solution as evident by the absence which is evident by the presence of carbene carbon signals, or in some cases broad singlets in the ^{13}C NMR.⁴ The existence of non-labile silver-carbene bonds in complex **3** raised the question of whether this complex could perform as an efficient carbene transferring agent.

Synthesis of Rhodium and Palladium bis(NHC) complexes by carbene transfer from silver

Although complex **3** displays apparently non-labile Ag-C bonds at room temperature, complex **3** acts as an efficient carbene ligand transfer agent to form new biscarbene rhodium and palladium complexes. Upon treatment of 1 equivalent of complex **3** with $[\text{Rh}(\text{COD})\text{Cl}]_2$ (COD = 1,5-cyclooctadiene), a complex formulated as $[(\kappa^2\text{-DIMes}^{\text{Me}})\text{Rh}(\eta^2\text{-COD})][\text{BF}_4]$ **5** was obtained (Scheme 2.3). The reaction was performed in distilled CH_2Cl_2 in a glass bomb heated at 60 °C for 2 h. The AgCl that precipitated during the reaction was removed by filtering through celite. Distilled hexanes were added to the filtrate to precipitate complex **3** as an orange crystalline solid.

X-ray crystallographic data and ^{13}C NMR spectrum obtained for complex **5** revealed the presence of a bis(N-heterocyclic carbene) bound to the rhodium atom in a boat-shape conformation to form a six membered chelating ring (Figure 2.4). In the ^{13}C NMR, a doublet was observed at δ 178.8 for the carbene carbon atoms

bound to rhodium, with a coupling constant of $^1J_{\text{RhC}} = 54$ Hz which was comparable to similar bis(carbene) Rh complexes.²²



Scheme 2.3. Formation of Rhodium carbene complex **5**.

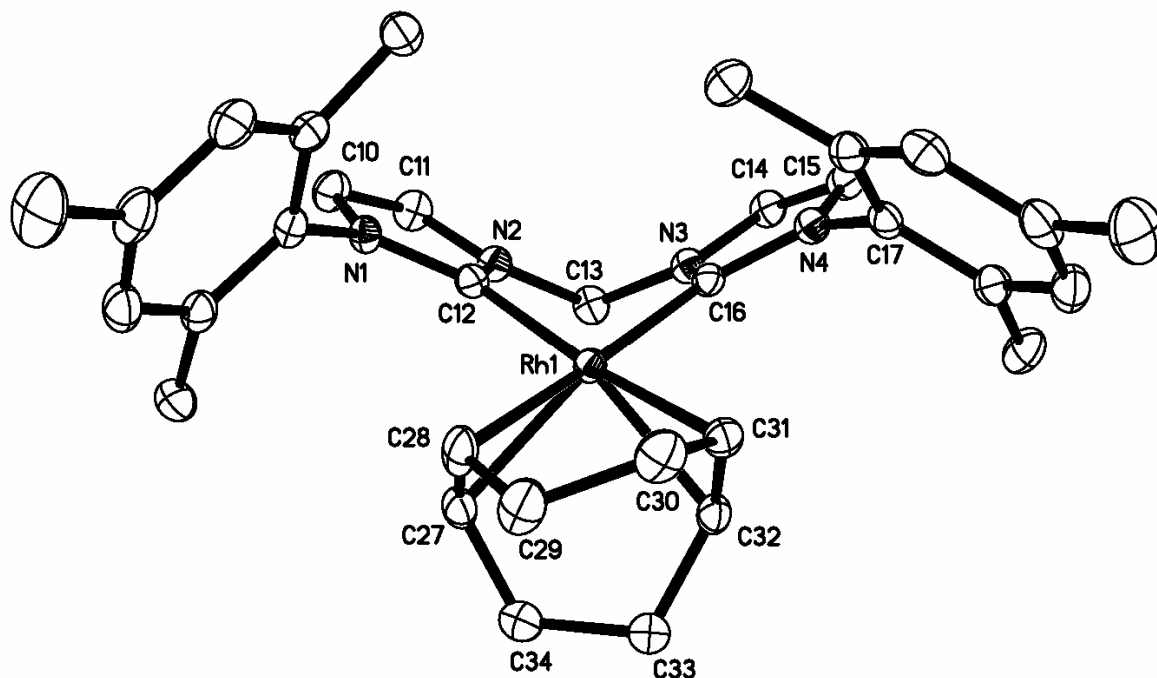


Figure 2.4. Molecular structure of complex **5**. Tetrafluoroborate ion was omitted for clarity. Thermal ellipsoids are shown at the 50% probability level.

Single crystals suitable for X-ray crystallography analysis were grown by slow diffusion of n-hexane to a saturated CH_2Cl_2 solution. The X-ray crystal structure of complex **5** displays Rh- $\text{C}_{\text{carbene}}$ bond lengths of 2.054(3) and 2.058(3) (Table 2.4) which are slightly longer than the Rh- $\text{C}_{\text{carbene}}$ bond lengths of 2.038(3) and 2.029(3) reported for a similar bis(NHC) rhodium complex with propylene linkage ($-\text{CH}_2-\text{CH}_2-\text{CH}_2-$) by Crabtree et al.²³ This may be due the steric hindrance imposed by the methylene ($-\text{CH}_2-$) linkage with bulky mesityl imidazole ligand in complex **5**. The $\text{C}_{\text{carbene}}-\text{Rh}-\text{C}_{\text{carbene}}$ bond angle of 85.29(12) is slightly smaller than the bond angle of 87.60(12) reported for a similar bis(NHC) complex. This may be due to the difference in chelate ring size.²³ Interestingly, Crabtree et al. reported that, when bulky

n-butyl groups are attached to the bis(imidazole) rings with a methylene linkage, it results in a dinuclear rhodium complex where the bis(NHC) ligand forms a bridge between the two rhodium atoms.²³ However, with N-bound mesityl rings, chelating bis(NHC) rhodium complex formation is possible due to the presence of planar mesityl rings, which can rotate and enable co-planar spatial arrangement of the ligand with the metal center.

As a new bulky bis(NHC) complex of Rh, complex **5** has potential utility in several catalytic applications. Complex **5** may act as a good catalyst for hydrosilylation reactions of terminal alkynes since structurally similar biscarbene Rh complexes have been reported as efficient catalysts for hydrosilylation reactions with $\text{HSi}(\text{OEt})_3$ and HSiMe_2Ph using several alkynes²² and for hydroformylation reactions with olefins.²⁴

Table 2.4. Selected bond lengths (Å) and bond angles (°) of complex **5**.

	Bond Lengths (Å)
Rh(1)-C(12)	2.054(3)
Rh(1)-C(16)	2.058(3)
Rh(1)-C(27)	2.185(3)
Rh(1)-C(28)	2.223(3)
Rh(1)-C(31)	2.216(3)
Rh(1)-C(32)	2.204(3)
N(1)-C(12)	1.367(4)
N(2)-C(12)	1.358(4)
N(3)-C(16)	1.358(4)
N(4)-C(16)	1.375(4)

	Bond angles (°)
C(12)-Rh(1)-C(16)	85.29(12)
C(12)-Rh(1)-C(27)	88.15(12)
C(16)-Rh(1)-C(31)	95.85(12)
C(16)-Rh(1)-C(32)	93.15(12)
C(12)-Rh(1)-C(28)	97.76(12)
N(2)-C(12)-N(1)	102.8(3)
N(3)-C(16)-N(4)	102.7(3)

Table 2.5. Crystal data and structure refinement details for complex **5**.

Empirical formula	C ₃₄ H ₄₂ BCl ₂ N ₄ F ₄ Rh
Formula weight	767.34
Crystal system	Monoclinic
Space group	P2(1)/c
Unit cell dimensions	a = 17.605(3) Å b = 13.365(2) Å c = 16.052(2) Å α = 90° β = 115.776(2)° γ = 90°
Volume	3401.1(9) Å ³
Z	4
Density (calculated)	1.499 Mg/m ³
Absorption coefficient	0.712 mm ⁻¹
Crystal size	0.44 x 0.22 x 0.06 mm ³
θ range for data collection	1.99 to 28.43°
Index ranges	-23 ≤ h ≤ 23 -17 ≤ k ≤ 17 -21 ≤ l ≤ 21
Temperature	103(2) K
Wavelength	0.71073 Å
Reflections collected	28463
Independent reflections	8057 (R _{int} = 0.0274)
Final R indices [I > 2σ(I)]	R1 = 0.0469 wR2 = 0.1257
R indices (all data)	R1 = 0.0497 wR2 = 0.1271
Goodness-of-fit on F ²	1.031

Complex **3** could also be used to transfer the bis(NHC) ligand onto palladium by treating with bis(acetonitrile)palladium dichloride precursor. One equiv of complex **3** was treated with two equiv of palladium precursor in distilled dichloromethane and was heated at 80 °C for 12 hours in a sealed glass vessel for 12 h. The mixture was then, filtered through celite to remove the precipitated AgCl from the reaction mixture. The solvent present in the clear filtrate was evaporated under reduced pressure. The product obtained was crystallized by layering diethyl ether onto a concentrated dichloromethane solution to obtain complex **6** [κ^2 -DIMes^{Me})Pd(NCCH₃)₂][BF₄]₂ as a white precipitate. This complex was first reported by Gardiner et al.¹² with the hexfluorophosphate anion and the ¹H NMR data agreed with the reported values.

Synthesis of a Cationic *Bis(1,1'-dimesityl-3,3'-methylenediimidazol-2,2'-diylidene) Palladium Complex* [κ^2 -DIMes^{Me})₂Pd₂Br₂][$(BAR^F_4)_2$] (7)

Further investigation of the bis(*1,1'-dimesityl-3,3'-methylenediimidazol-2,2'-diylidene*) ligand was carried out to synthesize cationic bis(NHC)palladium complexes which can be used as pre-catalysts for palladium catalyzed electrophilic reactions. Bis(*1,1'-dimesityl-3,3'-methylenediimidazol-2,2'-diylidene*)palladium dibromide¹² was used as the starting palladium complex and was treated with one equiv of silver acetate (AgOAc) and one equiv of silver tetrafluoroborate (AgBF₄) with the hope to generate a cationic bis(NHC)palladium complex containing η^2 acetate ligand. Unfortunately, the resulting product could not be re-crystallized from the reaction mixture. However, the ¹H NMR spectrum obtained for the crude product

was consistent with the expected structure. Therefore, silver tetrafluoroborate was replaced with silver tetrakis[3,5-bis(trifluoromethyl)phenyl]borate ($\text{AgBAR}^{\text{F}}_4$) in order to obtain the $\text{BAR}^{\text{F}}_4^-$ anion of the complex for easy recrystallization of the final product. Unexpectedly, addition of $\text{AgBAR}^{\text{F}}_4$ to the reaction mixture led to the formation of a cationic bis(1,1'-dimesityl-3,3'-methylenediimidazol-2,2'-diylidene) palladium dibromide dimer $[(\kappa^2\text{-DIMes}^{\text{Me}})_2\text{Pd}_2\text{Br}_2][(\text{BAR}^{\text{F}}_4)_2]$ **7**.

The synthesis begins by treating one molar equiv of palladium(II)dibromide¹² with one molar equiv of silver acetate and one molar equiv of $\text{AgBAR}^{\text{F}}_4$ in a thick walled glass vessel under nitrogen in dry acetonitrile. The reaction mixture was stirred at 60 °C for 12 hrs using a constant temperature oil bath. After the completion of the reaction, the solution was filtered through celite to remove the precipitated AgBr and AgOAc . The remaining solvent was evaporated using the rotovap, and distilled methylene chloride was added to the reaction mixture. Distilled diethyl ether and hexanes were added to recrystallize complex **7** as a white crystalline solid.

According to the ^1H NMR spectrum, aryl protons coming from the $\text{BAR}^{\text{F}}_4^-$ anion appeared most downfield at 7.72 ppm and 7.56 ppm with a 2:1 integration ratio. Imidazole hydrogens and mesityl meta-hydrogens appeared at 7.40-7.35 ppm and 6.99-6.85 ppm. The methylene protons were split into two and were visible at 6.54-6.46 ppm and 5.93-5.80 ppm. Signals from the mesityl *o*- CH_3 groups in the complex were split into two at 2.39, 2.27 ppm and 1.90, 1.94 ppm. Mesityl *p*- CH_3 groups were also split into two peaks at 2.09 and 1.76 ppm.

The ^{13}C NMR spectrum of complex **7** displayed BAR^{F}_4 *ipso* C at 162.2 ppm with B-C coupling of $^1J_{10\text{BC}}=16.8$ and $^1J_{11\text{BC}}=50.2\text{Hz}$. Carbene carbons appeared at

152.4 ppm and 151.3 ppm. Imidazole carbons were at 135.6, 135.4, 130.1 and 129.8 ppm. BAr^{F}_4 *meta* C appeared at 129.3 ppm with C-F coupling constant of 32 Hz. BAr^{F}_4 CF_3 appeared at 125.0 ppm with the characteristic C-F coupling of $^1J_{\text{CF}}=272$ Hz. Quartet at 117.9 ppm corresponded to the BAr^{F}_4 *para* protons with $^3J_{\text{CF}}=3.8$ Hz.

Single crystals suitable for X-ray crystallography were developed by slow diffusion of distilled hexanes into a concentrated solution of complex **7** in methylene chloride and diethyl ether. X-ray crystal structure of complex **7** confirmed the presence of a bromide bridge and the dimeric nature of complex **7** (Figure 2.5). Complex **7** Pd-C_{carbene} bond distances, 1.991(3) and 1.994(3) Å were slightly higher than the values 1.966(2) and 1.972(3) Å reported for dicationic bis(NHC)palladium complex by Gardiner et al.¹² This may be due to the increased charge on palladium in the dicataionic complex. The sum of bond angles around the palladium center is close to 360 ° indicating square planer geometry in complex **7**. The imidazole N-C-N bond angles of 105.0(2)° and 104.8(2)° were close to the values 104.5 (7) and 105.3 (6) reported by Herrmann et al. for bis(NHC) ligand(Table 2.6).²⁵

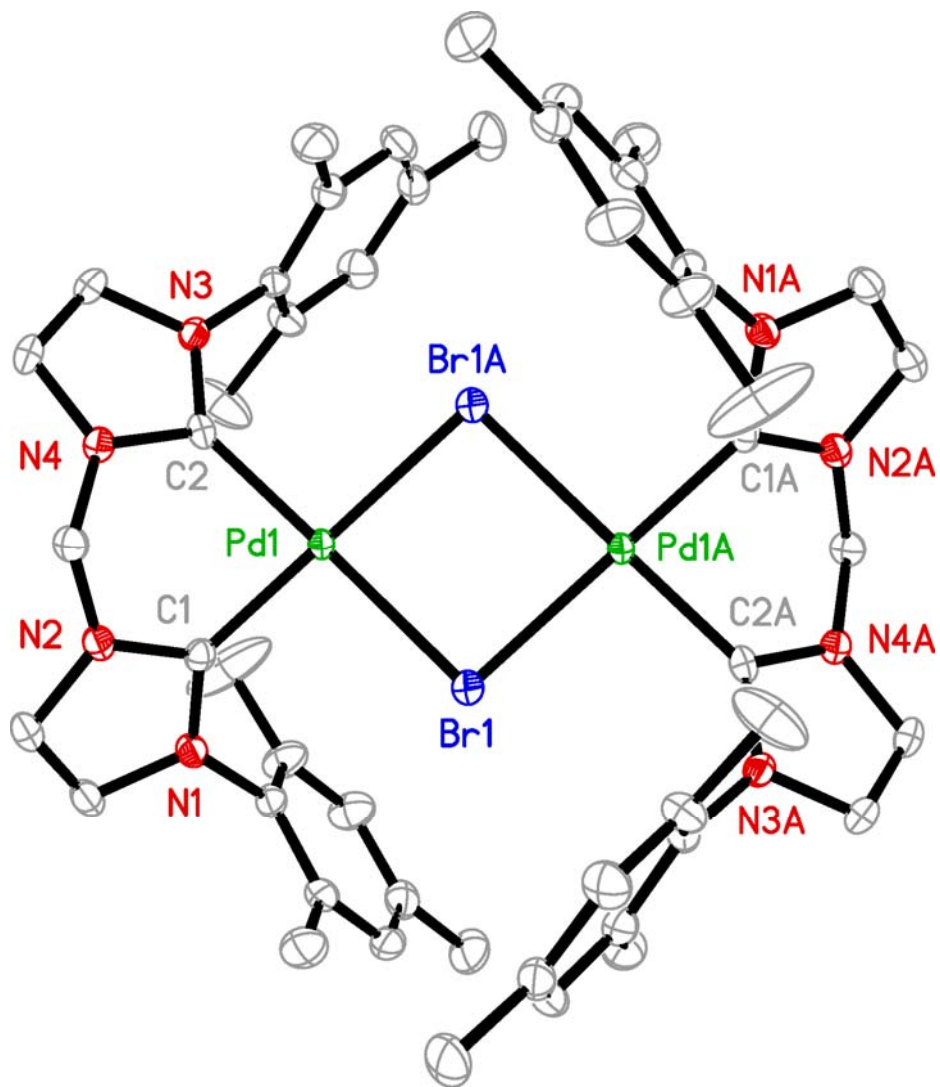


Figure 2.5. Molecular structure of complex 7. Thermal ellipsoids are shown at the 50% probability level.

Table 2.6. Selected bond lengths (Å) and bond angles (°) of complex **7**.

	Bond Lengths (Å)
Pd(1)-C(1)	1.991(3)
Pd(1)-C(2)	1.994(3)
Pd(1)-Br(1A)	2.4813(3)
Pd(1)-Br(1)	2.4805(3)
C(1)-N(2)	1.354(3)
C(2)-N(4)	1.359(3)
C(1)-N(1)	1.348(3)
C(2)-N(3)	1.348(3)

	Bond angles (°)
C(1)-Pd(1)-C(2)	86.01(10)
C(1)-Pd(1)-Br(1)	93.49(7)
C(2)-Pd(1)-Br(1A)	94.14(7)
Br(1)-Pd(1)-Br(1A)	93.15(12)
N(1)-C(1)-N(2)	105.0(2)
N(3)-C(2)-N(4)	104.8(2)

Table 2.7. Crystal data and structure refinement details for complex **7**.

Empirical formula	C ₁₂₂ H ₁₀₀ B ₂ Br ₂ N ₈ F ₄₈ O ₂ Pd ₂
Formula weight	3016.34
Crystal system	Triclinic
Space group	P $\bar{1}$
Unit cell dimensions	a = 14.4303(4) Å b = 15.4764(4) Å c = 15.5652(5) Å α = 94.1150(10) $^\circ$ β = 114.5660(10) $^\circ$ γ = 93.3760(10) $^\circ$
Volume	3138.24(16) Å ³
Z	1
Density (calculated)	1.596 Mg/m ³
Absorption coefficient	1.048 mm ⁻¹
Crystal size	0.19 x 0.15 x 0.12 mm ³
θ range for data collection	2.06 to 29.06 $^\circ$
Index ranges	-19 \leq h \leq 18 -21 \leq k \leq 21 -21 \leq l \leq 20
Temperature	102(2) K
Wavelength	0.71073 Å
Reflections collected	30653
Independent reflections	16459 (R _{int} = 0.0302)
Final R indices [$I > 2\sigma(I)$]	R1 = 0.0427 wR2 = 0.0992
R indices (all data)	R1 = 0.0607 wR2 = 0.1082
Goodness-of-fit on F ²	1.026

Summary and Conclusions

Dimeric, silver bis(N-heterocyclic carbene) complex **3** has been synthesized by treatment of the respective bis(imidazolium) salt with Ag_2O and AgBF_4 . This sterically hindered silver bisimidazole carbene complex shows an unusual static structure and high thermal stability in solution. Appearance of $\text{Ag-C}_{\text{Carbene}}$ coupling in the ^{13}C NMR shows evidence for the presence of non-labile carbene ligands at $25\text{ }^\circ\text{C}$ in solution. Despite its static nature in solution, silver biscarbene complex **3** acts as a good carbene transferring agent to transfer the bulky bis(carbene) ligand onto rhodium and palladium complexes. This may be due to labile metal-carbene bonds at elevated temperatures. Interestingly, complex **5** displayed a chelating bis(NHC) ligand bound to one rhodium atom, although Crabtree and coworkers suggests that bis(NHC) ligands with short linkers such as methylene, do not form chelating rhodium complexes which instead forms dinuclear metal complexes where the bis(NHC) ligand acts as a bridge between the two rhodium atoms.²³

Experimental

General Comments

Diethyl ether and hexanes were purified by distillation from sodium benzophenone ketyl. Dichloromethane was washed with concentrated H₂SO₄, water, and 5% Na₂CO₃, followed by pre-drying over anhydrous CaCl₂ and distillation from P₂O₅. DMSO-*d*₆ was dried over molecular sieves (4 Å) and distilled under vacuum. All other reagents were used as supplied (Aldrich or Acros). 1,1'-di(mesityl)-3,3'-methylenediimidazolium dibromide, palladium(II)dibromide¹², [Rh(COD)Cl]₂²⁶ and silver tetrakis[3,5-bis(trifluoromethyl)phenyl]borate (AgBAr^F₄)²⁷ were synthesized according to published procedures. NMR spectra were acquired on Varian Unity INOVA 400 MHz and Gemini-2000 300 MHz spectrometers and low temperature NMR experiment was performed in a J Young tube using dry CD₂Cl₂ as the NMR solvent. Reported chemical shifts are referenced to residual solvent peaks (¹H, ¹³C)²⁸ or to an external standard (¹⁹F, 1-fluoro-4-nitrobenzene, -103.0 ppm). Combustions analyses were performed by Desert Analytics, Tucson, Arizona.

[(κ²,μ₂-DIMes^{Me})₂Ag₂][BF₄]₂ (3)

A mixture of 1,1'-dimesityl-3,3'-methylenediimidazolium dibromide (300 mg, 0.549 mmol) and Ag₂O (153 mg, 0.659 mmol) was stirred in dichloromethane (10 mL) for 2 h at 25 °C. The reaction flask was protected from light by covering with foil. The mixture was filtered through celite, and the solvent was removed under vacuum

to obtain an intermediate product **2** which can be formulated as $[(\kappa^2, \mu_2\text{-DIMes}^{\text{Me}})\text{Ag}]_n[\text{AgBr}_2]_n$. ^1H NMR (300 MHz, DMSO- d_6): δ 8.2-7.9 (m, 2H), 7.6-7.2 (m, 2H), 7.1-6.2 (m, 6H), 2.6-2.2 (m, 6H), 2.1-1.0 (m, 12 H). Intermediate **2** was dissolved in hot acetonitrile in a bomb and AgBF_4 (128 mg, 0.659 mmol) was added. The mixture was stirred for 30 min at 60 °C in a constant temperature oil bath. The precipitated AgBr was removed by filtering through celite. The colorless filtrate was stirred under vacuum to evaporate the solvent. The resulting solid was triturated 3 times with dichloromethane to remove traces of acetonitrile, dichloromethane 10 mL was added, and the mixture was filtered through a fine frit. The solution was concentrated to approximately 1 mL under reduced pressure, and Et_2O was added dropwise to precipitate a white, microcrystalline solid. The product was washed with Et_2O and dried in vacuum overnight. Yield: 260 mg, 81%. ^1H NMR (300 MHz, DMSO- d_6 , 25 °C): δ 8.06 (s, 4H, *CH* imidazole), 7.48 (s, 4H, *CH* imidazole), 7.26 (d, 2H, $^2J_{\text{HH}} = 13.6$ Hz, CH_2), 7.07 (s, 4H, *m*-H), 6.95 (s, 4H, *m*-H), 6.53 (d, 2H, $^2J_{\text{HH}} = 13.6$ Hz, CH_2), 2.42 (s, 12H, *p*- CH_3), 1.58 (s, 12H, *o*- CH_3), 1.25 (s, 12H, *o*- CH_3). ^1H NMR (400 MHz, CD_2Cl_2 , -90 °C): δ 8.02 (s, 2H, *CH* imidazole), 7.73 (s, 2H, *CH* imidazole), 6.99 (s, 2H, *CH* imidazole), 6.95 (s, 2H, *CH* imidazole), 6.91 (s, 4H, *m*-H), 6.84 (s, 4H, *m*-H), 6.61 (AB, 4H, $J = 13.4$, $C = 14.1$ Hz, CH_2), 2.39 (s, 12H, *p*- CH_3), 1.86 (s, 6H, *o*- CH_3), 1.38 (s, 6H, *o*- CH_3), 1.14 (s, 6H, *o*- CH_3), 1.05 (s, 6H, *o*- CH_3). ^{13}C NMR (101 MHz, DMSO- d_6): δ 180.9 (2 d, $^1J_{107\text{AgC}}=182$, $^1J_{109\text{AgC}}=210$ Hz, AgC), 138.8 (Mes), 135.0 (Mes), 134.0 (Mes), 133.8 (Mes), 129.2 (imidazole), 129.0 (imidazole), 124.6 (Mes), 122.3 (Mes), 63.5 (CH_2), 20.7 (*p*- CH_3), 16.7 (*o*- CH_3), 16.4 (*o*- CH_3). ^{19}F NMR (376 MHz, DMSO- d_6): δ -148.5. Anal. Calcd for

C₅₀H₅₆B₂F₈N₈Ag₂·0.16CH₂Cl₂: C, 51.38; H, 4.84; N, 9.55. Found: C, 51.05; H, 4.99; N, 9.48.

[(κ²,μ₂-DIMes^{Me})₂Ag₂][OTf]₂ (4)

The synthesis begins with 1,1'-di(^tbutyl)-3,3'-methylene-bisimidazolium dibromide which was synthesized using a procedure similar to the one described by Gardiner et al.¹² with mesityl imidazolium dibromide. 1,1'-di(^tbutyl)-3,3'-methylene-bisimidazolium dibromide (0.20 g, 0.474 mmol) was treated with silver oxide (0.11 g, 0.474 mmol) in 15 mL of distilled methylene chloride in a flask and was stirred for 2 hours at room temperature. During the reaction, the flask was covered with foil paper to protect the reaction from light. After the reaction was completed, the solution was filtered through celite and the solvent was evaporated under vacuum using the rotatory evaporator. The crude product was scraped out of the flask. The yield was 55%, 0.166 g. ¹H NMR (300 MHz, DMSO-*d*₆): δ 7.8 (s, 4H, imidazole), 6.7 (s, 2H, -CH₂-), 1.64 (s, 18H, -CH₃). The crude product (0.20 g, 0.314 mmol) was treated with AgOTf (0.105 g, 0.409 mmol) in dry acetonitrile (10 mL). The reaction was setup in a thick wall glass vessel under inert atmospheric conditions and was stirred at 60 °C for 2 hours. After cooling the reaction mixture to room temperature, the solution was filtered through celite under N₂. The solvent was removed under vacuum and was triturated with dry CH₂Cl₂. The solution was again filtered through celite to remove traces of AgBr from the crude product. The Methylene chloride solution was reduced using vacuum to create a super saturated solution of complex **4**, from which a crystalline solid was generated. ¹H NMR (300 MHz, dry DMSO-*d*₆): δ 7.8 (d, *J*= 7.5

Hz, 4H, imidazole), 7.0 (br s, 1H, -CH₂-), 6.4 (br s, 1H, -CH₂-), 1.62 (s, 18H, -CH₃).
¹³C NMR (101 MHz, dry DMSO-*d*₆): δ 121.6 (imidazole), 121.2 (imidazole), 66.0 (-CH₂-), 58.1(C(CH₃)₃), 31.1(-CH₃).

[(κ²-DIMEs^{Me})Rh(η²,η²-COD)][BF₄] (5)

Complex **3** (100 mg, 0.086 mmol) and [Rh(COD)Cl]₂ (43 mg, 0.086 mmol) were added to in dichloromethane (10 mL), and the mixture was stirred at 60 °C in a sealed ampoule for 2 h. The mixture was filtered through celite to give a clear orange solution, and the solvent was evaporated under reduced pressure. The product was crystallized by layering hexanes onto a concentrated dichloromethane solution of the crude material, and the resulting orange crystals were dried in vacuum. Yield: 90 mg, 77%. ¹H NMR (300 MHz, C₆D₆): δ 8.30 (d, 2H, ³J_{HH}=2.0 Hz, CH im), 7.39 (d, ²J_{HH}=12.8 Hz, 1H, CH₂), 6.66 (s, 2H, *m*-H), 6.51 (s, 2H, *m*-H), 6.15 (d, ³J_{HH} =12.8 Hz, 1H, CH₂), 5.92 (d, 2H, ³J_{HH} =2.0 Hz, CH im), 4.44 (s, 2H, COD CH), 3.42 (2, 2H, COD CH), 2.01 (s, 6H, *p*-CH₃), 1.91 (m, 2H, COD CH₂), 1.87 (s, 6H, *o*-CH₃), 1.70 (s, 6H, *o*-CH₃), 1.50 (m, 2H, COD CH₂), 1.41 (m, 4H, COD CH₂). ¹³C NMR (101 MHz, CD₂Cl₂): δ 178.7 (d, ¹J_{RhC}=54 Hz, RhC), 139.9 (Mes), 135.7 (Mes), 135.5 (Mes), 135.4 (Mes), 129.5 (im), 129.3 (im), 123.6 (Mes), 121.7 (Mes), 90.6 (d, ¹J_{RhC}=8.7 Hz, COD CH), 88.1 (d, ¹J_{RhC}=7.3 Hz, COD CH), 63.4 (CH₂), 30.9 (COD CH₂), 30.7 (COD CH₂), 21.1 (*p*-CH₃), 19.4 (*o*-CH₃), 18.0 (*o*-CH₃). ¹⁹F NMR (376 MHz, DMSO-*d*₆): δ -148.5 (s, BF₄⁻). Anal Calc. for C₃₃H₄₀BF₄N₄Rh·0.3CH₂Cl₂: C, 56.50; H, 5.78; N, 7.91%. Found: C, 55.94; H, 5.96; N, 8.19%.

[(κ²-DIMesMe)Pd(NCCH₃)₂][BF₄] (6)

Complex **4** (20 mg, 0.017 mmol) and bis(acetonitrile)palladium dichloride (9 mg, 0.034 mmol) were added into dichloromethane (10 mL), and the mixture was stirred at 80 °C in a sealed vessel for 12 h. The mixture was filtered through celite to obtain a clear solution, and the solvent was evaporated under reduced pressure. The product was crystallized by layering diethyl ether onto a concentrated dichloromethane solution to obtain the product as a white precipitate and was dried under vacuum. The yield was 13 mg, 49%. This complex was first reported by Gardiner et al.¹² for the hexfluorophosphate anion. The ¹H NMR spectrum in DMSO-d₆ was similar to the reported data.

[(κ²-DIMes^{Me})₂Pd₂Br₂][(BAR^F₄)₂] (7)

[1,1'-di(mesityl)-3,3'-methylenediimidazolin-2,2'-diylidene}palladium(II)dibromide]¹² (0.030 g, 0.046 mmol), silver acetate (0.0076 g, 0.046 mmol) and AgBAR^F₄ (0.0447 g, 0.046 mmol) were added into a thick walled glass vessel under nitrogen. Dry acetonitrile (5 mL) was added to the vessel as the solvent for the reaction. The reaction mixture was stirred at 60 °C for 12 hrs using a constant temperature oil bath. After the completion of the reaction, the solution was filtered through celite to remove precipitated AgBr. The solution was evaporated using the rotovap and distilled methylene chloride was added to the reaction mixture. Distilled diethyl ether and hexanes were added to the reaction mixture to recrystallize the product as a white crystalline solid. Drying under vacuum was used to remove traces of solvent from the product. (0.0661 g, 71% yield). ¹H NMR (400 MHz,

CD₂Cl₂): δ 7.72 (s, 16H, BAr^F₄), 7.56 (s, 8H, BAr^F₄), 7.40-7.35 (m, 4H, imidazole), 6.99-6.85 (m, 12H, imidazole and *m*-H), 6.54-6.46 (m, 2H, CH₂), 5.93-5.80 (m, 2H, CH₂), 2.39 (s, 6H, *o*-CH₃), 2.27 (s, 6H, *o*-CH₃), 2.09 (s, 6H, *p*-CH₃), 1.94 (s, 6H, *o*-CH₃), 1.90 (s, 6H, *o*-CH₃), 1.76 (s, 6H, *p*-CH₃). ¹³C NMR (151 MHz, CD₂Cl₂): δ 162.2 (4 s, ¹J_{10BC}=16.8, ¹J_{11BC}=50.2 Hz, BAr^F₄ *ipso*), 152.4 (carbene C), 151.3 (carbene C), 135.6 (imidazole), 135.4 (imidazole), 133.9 (dd, *J* = 59.3 Hz, 8.4 Hz, BAr^F₄ *ortho*), 130.1 (imidazole), 129.8 (imidazole), 129.7 (Mes), 129.3 (q, *J* = 32 Hz, BAr^F₄ *meta*), 126.5 (Mes), 126.4 (Mes), 125.0 (q, *J* = 272 Hz, BAr^F₄ -CF₃), 121.7 (Mes), 117.9 (q, *J* = 3.8 Hz, BAr^F₄ *para*), 63.6 (CH₂), 63.5 (CH₂), 21.4 (Mes, *o*-CH₃), 21.1 (Mes, *o*-CH₃), 19.3 (Mes, *p*-CH₃). Anal. Calcd for C₁₁₄H₈₀B₂Br₂F₄₈N₈Pd₂: C, 47.78; H, 2.84; N, 3.89 %. Found: C, 47.61; H, 2.84; N, 3.92 %.

Single Crystal X-ray Diffraction Analysis of $[(\kappa^2, \mu^2\text{-DIMes}^{\text{Me}})_2\text{Ag}_2][\text{BF}_4]_2$ (3)

Colorless prisms of complex **3** were obtained by slow diffusion of Et₂O over 3 d into a concentrated dichloromethane solution of **3**, with careful exclusion of light achieved by covering the vial with foil. A 0.22 x 0.18 x 0.12 mm crystal was selected, and data were collected at 103(2) K on a Bruker Apex diffractometer. The structure was solved and refined using the SHELXTL system.²⁹

Single Crystal X-ray Diffraction Analysis of $[(\kappa^2\text{-DIMes}^{\text{Me}})\text{Rh}(\eta^2, \eta^2\text{-COD})][\text{BF}_4]$ (5)

Orange plate-like crystals were obtained by slow evaporation of a solution of complex **4** in 70:30 dichloromethane/hexanes. A 0.44 x 0.22 x 0.06 mm crystal was

chosen, and data were collected at 103(2) K on a Bruker Apex diffractometer. The structure was solved and refined using the SHELXTL system.²⁹

References

1. Huang, J. K.; Schanz, H. J.; Stevens, E. D.; Nolan, S. P. *Organometallics* **1999**, *18*, 2370.
2. Arduengo, A. J.; Dias, H. V. R.; Calabrese, J. C.; Davidson, F. *Organometallics* **1993**, *12*, 3405.
3. Guerret, O.; Sole, S.; Gornitzka, H.; Teichert, M.; Trinquier, G.; Bertrand, G. *J. Am. Chem. Soc.* **1997**, *119*, 6668.
4. Wang, H. M. J.; Lin, I. J. B. *Organometallics* **1998**, *17*, 972.
5. Douthwaite, R. E.; Haussinger, D.; Green, M. L. H.; Silcock, P. J.; Gomes, P. T.; Martins, A. M.; Danopoulos, A. A. *Organometallics* **1999**, *18*, 4584.
6. Garrison, J. C.; Youngs, W. J. *Chem. Rev.* **2005**, *105*, 3978.
7. Quezada, C. A.; Garrison, J. C.; Panzner, M. J.; Tessier, C. A.; Youngs, W. J. *Organometallics* **2004**, *23*, 4846.
8. Baker, M. V.; Brown, D. H.; Haque, R. A.; Skelton, B. W.; White, A. H. *Dalton Trans.* **2004**, 3756.
9. Garrison, J. C.; Simons, R. S.; Kofron, W. G.; Tessier, C. A.; Youngs, W. J. *Chem. Comm.* **2001**, 1780.

10. Lin, I. J. B.; Vasam, C. S. *Coord. Chem. Rev.* **2007**, *251*, 642.
11. Wanniarachchi, Y. A.; Khan, M. A.; Slaughter, L. M. *Organometallics* **2004**, *23*, 5881.
12. Gardiner, M. G.; Herrmann, W. A.; Reisinger, C. P.; Schwarz, J.; Spiegler, M. *J. Organomet. Chem.* **1999**, *572*, 239.
13. Lee, K. M.; Wang, H. M. J.; Lin, I. J. B. *Journal of the Chemical Society-Dalton Trans.* **2002**, 2852.
14. Smith, M. B.; March, J. *MARCH'S Advanced Organic Chemistry: Reactions, Mechanisms, and Structure*; John Wiley & Sons: New York, 2001; pp.20.
15. Omary, M. A.; Webb, T. R.; Assefa, Z.; Shankle, G. E.; Patterson, H. H. *Inorg. Chem.* **1998**, *37*, 1380.
16. Pyykko, P. *Chem. Rev.* **1997**, *97*, 597.
17. Catalano, V. J.; Malwitz, M. A. *Inorg. Chem.* **2003**, *42*, 5483.
18. Zhou, Y. B.; Zhang, X. M.; Chen, W. Z.; Qiu, H. Y. *J. Organomet. Chem.* **2008**, *693*, 205.

19. Tulloch, A. A. D.; Danopoulos, A. A.; Winston, S.; Kleinhenz, S.; Eastham, G.
J. Chem. Soc.-Dalton Trans. **2000**, 4499.
20. Garrison, J. C.; Simons, R. S.; Talley, J. M.; Wesdemiotis, C.; Tessier, C. A.;
Youngs, W. J. *Organometallics* **2001**, *20*, 1276-1278.
21. Caballero, A.; ez-Barra, E.; Jalon, F. A.; Merino, S.; Tejada, J. *J. Organomet.
Chem.* **2001**, *617*, 395.
22. Poyatos, M.; Mas-Marza, E.; Mata, J. A.; Sanau, M.; Peris, E. *European J.
Inorg. Chem.* **2003**, 1215.
23. Mata, J. A.; Chianese, A. R.; Miecznikowski, J. R.; Poyatos, M.; Peris, E.;
Faller, J. W.; Crabtree, R. H. *Organometallics* **2004**, *23*, 1253.
24. Poyatos, M.; Uriz, P.; Mata, J. A.; Claver, C.; Fernandez, E.; Peris, E.
Organometallics **2003**, *22*, 440.
25. Herrmann, W. A.; Reisinger, C. P.; Spiegler, M. *J. Organomet. Chem.* **1998**,
557, 93.
26. Giordano, G.; Crabtree, R. H. *Inorg. Synth.* **1990**, *28*, 88.
27. Miller, K. J.; Kitagawa, T. T.; bu-Omar, M. M. *Organometallics* **2001**, *20*,
4403.

28. Gottlieb, H. E.; Kotlyar, V.; Nudelman, A. *J. Org. Chem.* **1997**, *62*, 7512.

29. Bruker (1997) SHELXTL (version 6.12), Bruker ACS Inc., Madison, Wisconsin. 1997.

CHAPTER III

Facile Synthesis of Chiral Palladium Bis(Acyclic Diaminocarbene) Complexes

“Portions were adapted from [Y. A. Wanniarachchi, Slaughter L. M. *Chem. Commun.*, **2007**, 3294-3296] with permission of The Royal Society of Chemistry and [Y. A. Wanniarachchi, Kogiso, Y., Slaughter L. M. *Organometallics*, **2008**, 27, 21-24]. Copyright [2004] American Chemical Society.”

Introduction

Acyclic diaminocarbenes (ADCs) are proposed to have strong σ -donor abilities possibly exceeding those of N-heterocyclic carbenes.¹ However, ADC ligands have not been as widely investigated as N-heterocyclic carbene ligands.² Only a few methods have been reported for the synthesis of ADC metal complexes. Among these methods, some are highly specific to the starting compounds³ while others are specific to the metal.¹ In addition, only a few ADC ligand containing catalytic systems have been reported. These have displayed favorable properties similar to those of NHCs, such as high air stability⁴ and high activity in Suzuki-Miyaura cross-coupling reactions using a variety of aryl chlorides and boronic acids,⁵ and high activity in Buchwald-Hartwig amination reactions.⁶ Therefore, further exploration of new ADC ligand containing metal complexes with potential catalytic applications is important. In particular, chiral examples of ADC ligands have not been reported, in contrast with the large number of chiral NHC ligands reported.^{7,8}

To date, the most common method for synthesis of free acyclic diamino carbenes involves deprotonation of amidinium salts using strong bases such as lithium diisopropylamide (LDA)⁹ or NaH.³ Subsequent metalation of these free ADCs with transition metal precursors such as $[(\text{COD})\text{MCl}]_2$ (M=Rh or Ir), $\text{M}(\text{CO})_6$ (M=Cr,

W, Mo)³ and Pd(PPh₃)₄⁶ have resulted in transition metal complexes containing monodentate ADC ligands. However, an attempt to make a chelating bis(ADC) complex by Herrmann and coworkers via in situ generation of the free acyclic diaminocarbene was unsuccessful because of the higher reactivity of free bis acyclic diaminocarbenes.¹⁰

A special type of bis(ADC) ligands known as Chugaev-type carbenes were synthesized unexpectedly by Chugaev et al. in 1915 via nucleophilic attack of hydrazine on platinum-bound methylisocyanide ligands.^{11,12} However, the correct structures of Chugaev carbene ligands were not identified until 1970 in a study by Burkr et al. using X-ray crystallography.¹³ Following Chugaev's chemistry, a series of palladium Chugaev-type bis(ADC) complexes was prepared by Moncada et al. utilizing various hydrazines and palladium alkyl isocyanide derivatives.¹⁴ These palladium bis(ADC) complexes have been studied to identify air-stable Suzuki-Miyaura coupling catalysts.⁴ Except for Chugaev-type complexes and a few related examples^{15,16} the synthesis of bis(ADC) complexes, especially chiral bis(ADC) complexes has not been reported. Chapter 3 discusses a facile, one-step method to synthesize the first chiral bis(acyclic diaminocarbene) palladium complexes without impurities or complicated chiral separations.

Results and Discussion

Isonitrile ligands coordinated to transition metals tend to undergo rapid nucleophilic attack with amines to generate metal carbene complexes.¹⁷ The use of this fundamental metal templated reaction is discussed here in synthesizing structurally diverse chiral versions of bis(acyclic diaminocarbene) (ADC) ligand at palladium metal centers. This method differs from most of the NHC and ADC complex syntheses by not having free carbene formation during the reaction.

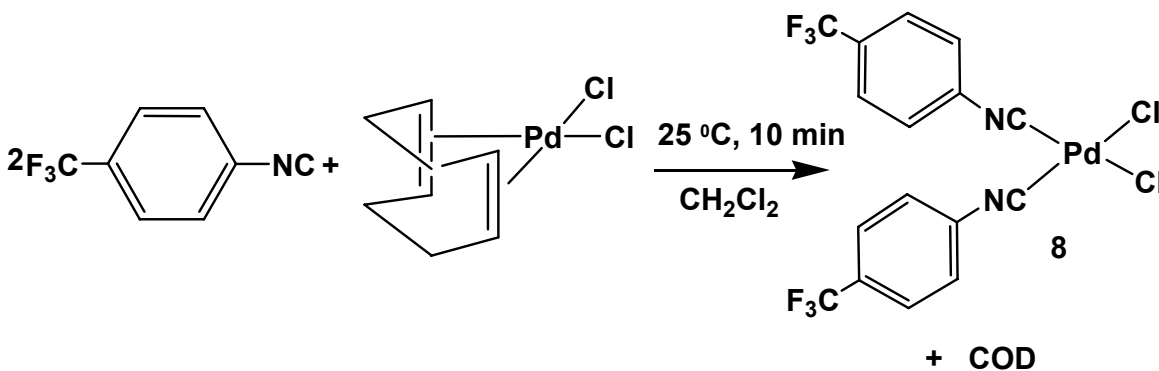
The synthesis of neutral palladium(II) complexes containing Chugaev-type ADCs involves two steps. First, the formation of a mono-deprotonated version of the dicarbene ligand from the reaction between hydrazine and palladium bound isocyanides followed by H⁺ abstraction. Secondly, the reaction with excess acid to form the neutral dicarbene palladium(II) complex.⁴ In contrast, the method described here generates neutral chiral palladium(II) ADC complexes in a one-step assembly process. In principle, this method can be extended followed to generate a library of structurally diverse chiral palladium(II) ADC complexes simply by varying the substitution pattern on the isocyanide and the backbone of the chiral diamines.

Carbene Precursor:

3.1 Bis(*p*-trifluoromethylphenyl isocyanide) palladium dichloride (**8**)

The synthesis of chiral bis(ADC) complexes begins with the formation of *cis*-bis(*p*-trifluoromethylphenyl isocyanide) palladium dichloride complex **8** via ligand substitution of (COD)PdCl₂ with the free arylisocyanide (Scheme 3.1). The advantage of using an aryl isocyanide containing electron withdrawing group such

as trifluoromethyl instead of an alkyl isocyanide is to make the palladium-bound isocyanide carbon more electrophilic, thereby promoting rapid nucleophilic attack by amines. (COD)PdCl₂ was treated with 2.2 equivalents of *p*-trifluoromethyl isocyanide in methylene chloride (Scheme 3.1). The reaction mixture was stirred for only 10 min since the reaction is rapid. This was confirmed by performing the reaction in an NMR tube using CD₂Cl₂ as the solvent. Complex **8** was stored under nitrogen (glove box) since prolonged storage under atmospheric conditions leads to changes in color from white to yellow. In addition, samples of complex **8** which were open to air for a long time showed a decrease in solubility in CH₂Cl₂. This may be due to air oxidation of the isocyanide to form relatively less soluble isocyanate complexes.¹⁸



Scheme 3.1. Formation of *cis*-bis(*p*-trifluoromethylphenyl isocyanide) palladium dichloride complex **8**.

Two IR stretching frequencies were visible at 2241 and 2221 cm⁻¹ for complex **8**, indicating *cis* geometry of the palladium-bound isocyanides due to IR-active

symmetric and asymmetric vibrations of the C≡N triple bonds. The IR stretching frequencies observed for the palladium bound isocyanide ligands were higher than the IR frequencies of free *p*-trifluoromethylphenyl isocyanide (2120 cm⁻¹) due to strong σ -donation from the isocyanide carbon-based “lone pair” with little or no π -back bonding from filled metal orbitals.

The NMR spectrum of complex **8** showed evidence for the presence of a symmetric molecule in solution with only one set of peaks in the ¹H NMR spectrum at 7.79 ppm showing an AB pattern for the *ortho*- and *meta*- protons on the aryl isocyanides. In the ¹³C NMR spectrum, aryl carbon atoms were easily identified because of the C-F couplings. Aryl *para* and *meta* carbons appeared at 133.4 ppm and 128.1 ppm as quartets with their characteristic coupling constants¹⁹ of ²J_{CF}=33.5 Hz and ³J_{CF} = 3.8 Hz respectively. The CF₃ carbons appears as a quartet at 124.3 ppm with a large coupling constant of 272 Hz, which is in the range (¹J_{CF}~ 270 Hz) expected for CF₃ groups bound to sp² carbons.¹⁹ However, the isocyanide NC carbon was not visible in the ¹³C NMR spectrum. Complex **8** displayed one fluorine signal at -63.8 ppm in the ¹⁹F NMR spectrum, giving further evidence for the presence of symmetry in the molecule.

Crystals suitable for X-ray crystallographic analysis were grown by slow diffusion of cyclohexane into a concentrated solution of complex **8** in chlorobenzene under nitrogen atmosphere. The x-ray crystal structure revealed C₁ symmetry in complex **8** (Figure 3.1) although complex **8** displays a C₂-like twofold symmetry in solution. This is due to the slight bend in one of the isocyanide groups attached to the palladium in solid state.

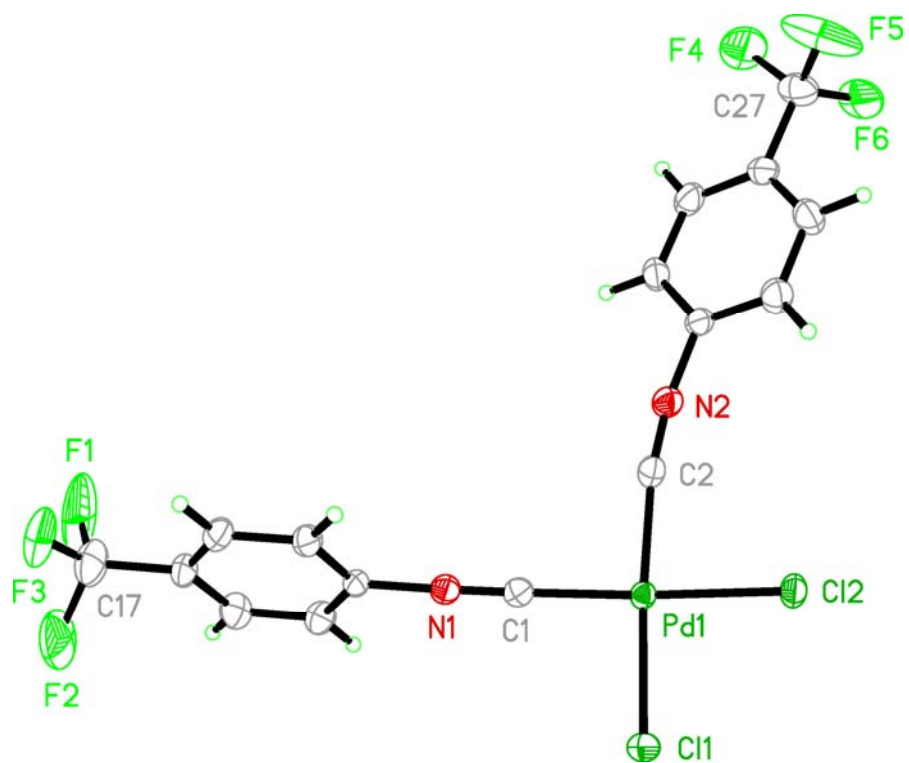


Figure 3.1. Molecular structure of complex **8** with 50% probability ellipsoids.

Table 3.1. Selected bond lengths (Å) and bond angles (°) of complex **8**.

	Bond lengths (Å)
N(1)-C(1)	1.146(3)
N(2)-C(2)	1.147(3)
Pd(1)-C(1)	1.939(2)
Pd(1)-C(2)	1.933(3)

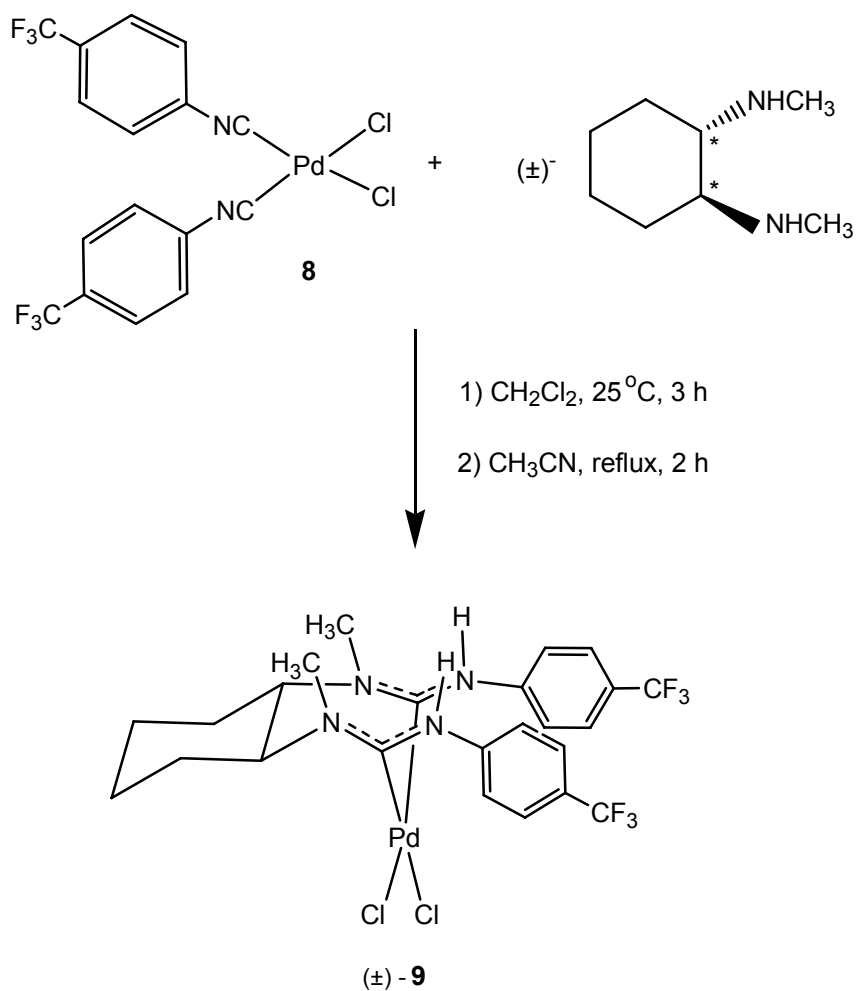
	Bond Angles (°)
Pd(1)-C(2)-N(2)	171.0(2)
Pd(1)-C(1)-N(1)	178.6(2)
C(2)-Pd(1)-C(1)	92.92(10)
C(1)-Pd(1)-Cl(1)	91.15(7)
C(2)-Pd(1)-Cl(2)	84.13(7)
Cl(2)-Pd(1)-Cl(1)	91.81(2)

Table 3.2. Crystal data and structure refinement details for complex **8**.

Empirical formula	C ₁₆ H ₈ Cl ₂ N ₂ F ₆ Pd
Formula weight	519.54
Crystal system	Monoclinic
Space group	<i>P</i> 2 ₁ / <i>c</i>
Unit cell dimensions	$a = 14.7788(10) \text{ \AA}$ $\alpha = 90^\circ$ $b = 17.9280(11) \text{ \AA}$ $\beta = 91.74(4)^\circ$ $c = 14.0492(10) \text{ \AA}$ $\gamma = 90^\circ$
Volume, <i>z</i>	3720.7(4) \AA^3 , 8
Density (calculated)	1.855 Mg/m ³
Absorption coefficient	1.345 mm ⁻¹
Crystal size	0.20x0.18x0.06 mm ³
θ range for data collection	1.79 to 29.32 $^\circ$
Index ranges	$-20 \leq h \leq 20$ $-24 \leq k \leq 20$ $-19 \leq l \leq 17$
Temperature	100(2) K
Wavelength	0.71073 \AA
Reflections collected	41955
Independent reflections	10152 ($R_{\text{int}} = 0.0390$)
Final <i>R</i> indices [$I > 2\sigma(I)$]	$R_1 = 0.0301$ $wR_2 = 0.0629$
<i>R</i> indices (all data)	$R_1 = 0.0430$ $wR_2 = 0.0679$

3.2. A chiral bis(carbene) palladium complex derived from N,N'-dimethyl-1,2-diaminocyclohexane (9)

The next goal was to use palladium isocyanide precursor **8** to synthesize chiral bis(ADC) palladium complexes. One molar equiv of complex **8** was dissolved in distilled CH₂Cl₂ and then treated with one equiv of (*rac*)-N,N'-dimethyl-1,2-diaminocyclohexane dissolved in distilled CH₂Cl₂ (Scheme 3.2). For the amine addition, a syringe pump was used at a regulated rate (4 mL/h) under argon atmosphere. The amine was dissolved in 4 mL of CH₂Cl₂. Slow addition of diamine via a syringe pump is essential for completion of the reaction between the diamine and the palladium bis(isocyanide) precursor and to avoid by-product formation. Polymeric carbene compounds with bridging amino groups are possible by-products in this reaction. The reaction was further stirred for two hours at room temperature, during which time a pale yellow precipitate started forming. The ¹H NMR spectrum of this precipitate revealed the expected bis(carbene) palladium dichloride complex **9**, but the yield was very low. To maximize the yield, CH₂Cl₂ was removed from the reaction using a rotovap followed by high vacuum. Acetonitrile solvent was then added to the reaction, and the mixture was refluxed using a heating mantle. The acetonitrile reflux was done under nitrogen or argon for two hours to maximize precipitate formation. During the reflux, the expected palladium bis(carbene) complex **9** started forming from the solution as a thick white paste. The reaction mixture was cooled and then filtered and dried under vacuum to isolate the product as a shiny white powder (Scheme 3.2).



Scheme 3.2. Formation of chiral bis(carbene) palladium complex **9** via one-step reaction of the palladium isocyanide precursor **8** with the chiral diamine.

Initial reaction scales used 70 mg of bis(isocyanide) palladium precursor **8** with 19.2 μL of *N,N'*-dimethyl diamino cyclohexane dissolved in acetonitrile. The reaction mixture was stirred for three hours at room temperature followed by refluxing at 80°C for two hours, yielding 55% of the product without any impurities. Reaction scales of >100 mg of palladium precursor **8** yielded impure samples of the

bis(carbene) palladium complex **9** following this method. However, when the syringe pump was used to add amine slowly to the reaction mixture, we could synthesize complex **9** with out impurities, at scales greater than 600 mg of palladium precursor **8**.

Complex **9** was only soluble in polar solvents; therefore NMR studies were done in DMSO-*d*₆. The ¹H NMR spectrum revealed two different NH peaks at 9.62, 9.05 ppm and two different NCH₃ peaks at 3.20, 3.10 ppm indicating that the two halves of the molecule were not symmetrically equivalent. The aryl protons appeared as four different resonances at 8.25 ppm, 7.71 ppm, 7.55 ppm and 7.19 ppm which were split into doublets due to coupling between neighboring protons. The ¹³C NMR spectrum provided evidence for the formation of the palladium bound bis(carbene) ligand by displaying carbene carbon peaks at 190.3 and 184.4 ppm. The appearance of two different carbene carbons in the ¹³C NMR support the absence of C₂ symmetry in complex **9**. Two different signals each for aryl *meta* carbons and *para* carbons were observed as quartets at 125.4 ppm, 124.4 ppm, 125.6 ppm, and 124.8 ppm respectively with their signature C-F coupling constants (³J_{CF} = ~ 4 Hz and ²J_{CF} = ~ 32 Hz respectively).¹⁹ In addition, two different CF₃ carbons were visible in the ¹³C NMR at 124.3 ppm (¹J_{CF}=272 Hz) and 124.2 ppm (¹J_{CF} =272 Hz) as quartets with large coupling constants.

Crystals of complex **9** suitable for X-ray crystallographic analysis were obtained by slow evaporation of a concentrated methanol solution open to air. According to the X-ray crystal structure, complex **9** has a seven membered chelating ring and C₁ symmetry in the molecule (Figure 3.2). Pd-C_{carbene} bond lengths of 1.982

Å and 1.992 Å (Table 3.3) were in the range expected for palladium bis(carbene) complexes.²⁰ Bond distances between C(1)-N(1), C(1)-N(3), C(2)-N(4) and C(2)-N(2) were relatively similar due to delocalized π electrons between these atoms. The bond distances of 1.341 Å, 1.326 Å, 1.338 Å and 1.338 Å obtained respectively for the above atoms were longer than the double bond distance reported for Csp^2-N (1.28 Å)²¹ due to this bond delocalization. The N-C_{carbene}-N angles of 116.6° and 117.3° were also comparable with known ADC ligands.^{22, 23} The average dihedral angles between N-substituents were -6.8(6) and 179.7(4)° for NC_{carbene}NC_{Me} and NC_{carbene}NC_{cyclohex}. Therefore, the N-substituents were in a near coplanar arrangement with the NCN carbene units in the molecule. The sum of bond angles around the palladium center was close to 360°, indicating distorted square planar geometry around the palladium center (Table 3.3).

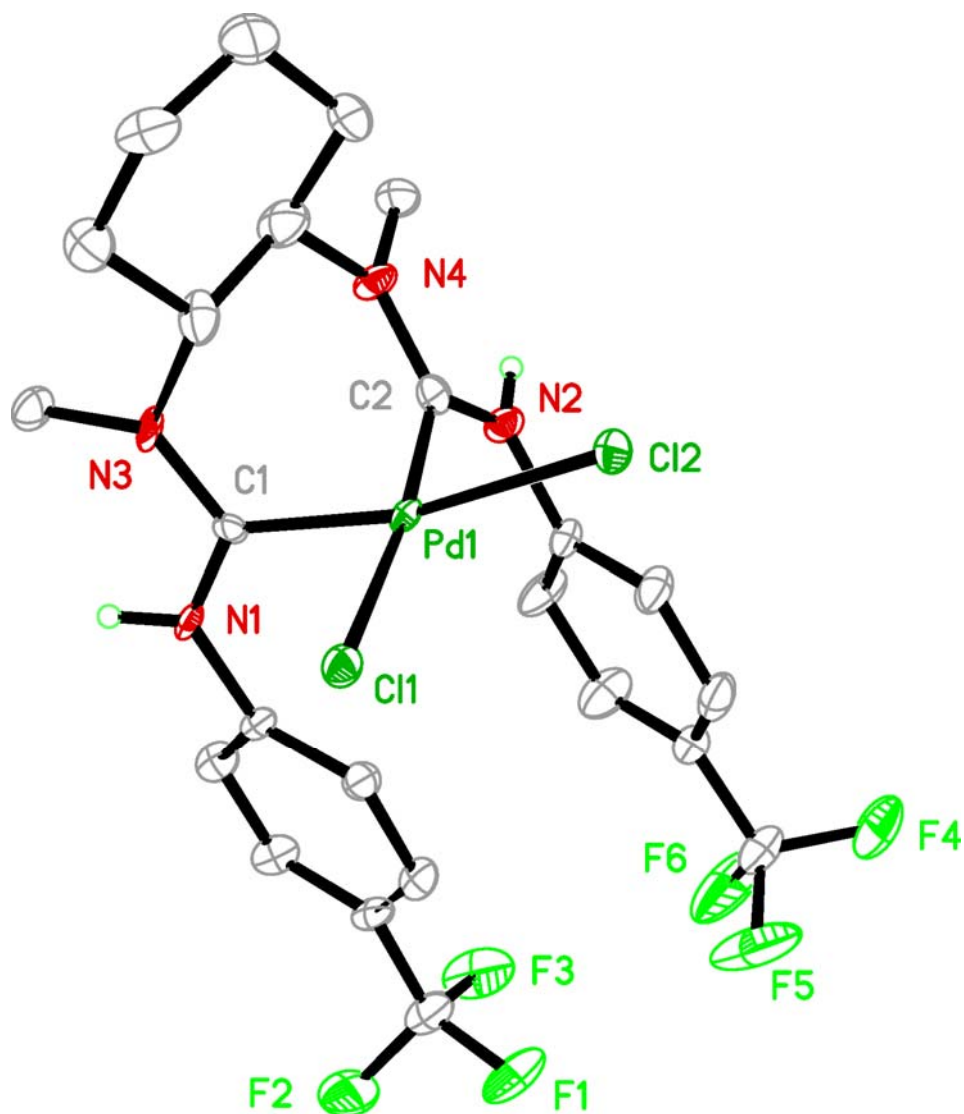


Figure 3.2. Molecular structure of complex **9** displaying 50% probability ellipsoids. Hydrogen atoms, except those are bound to nitrogens, have been omitted for clarity.

Table 3.3. Selected bond lengths (Å) and bond angles (°) of complex **9**.

	Bond Lengths (Å)
N(1)-C(1)	1.341(6)
N(2)-C(2)	1.338(6)
N(4)-C(2)	1.338(6)
N(3)-C(1)	1.326(6)
C(1)-Pd(1)	1.982(5)
C(2)-Pd(1)	1.992(5)
Pd(1)-Cl(1)	2.3930(13)
Pd(1)-Cl(2)	2.3898(13)

	Bond Angles (°)
N(4)-C(2)-N(2)	116.6(5)
N(3)-C(1)-N(1)	117.3(4)
C(1)-Pd(1)-Cl(1)	91.75(14)
C(2)-Pd(1)-Cl(2)	93.41(4)
Cl(1)-Pd(1)-Cl(2)	91.35(4)
C(1)-Pd(1)-C(2)	82.76(19)

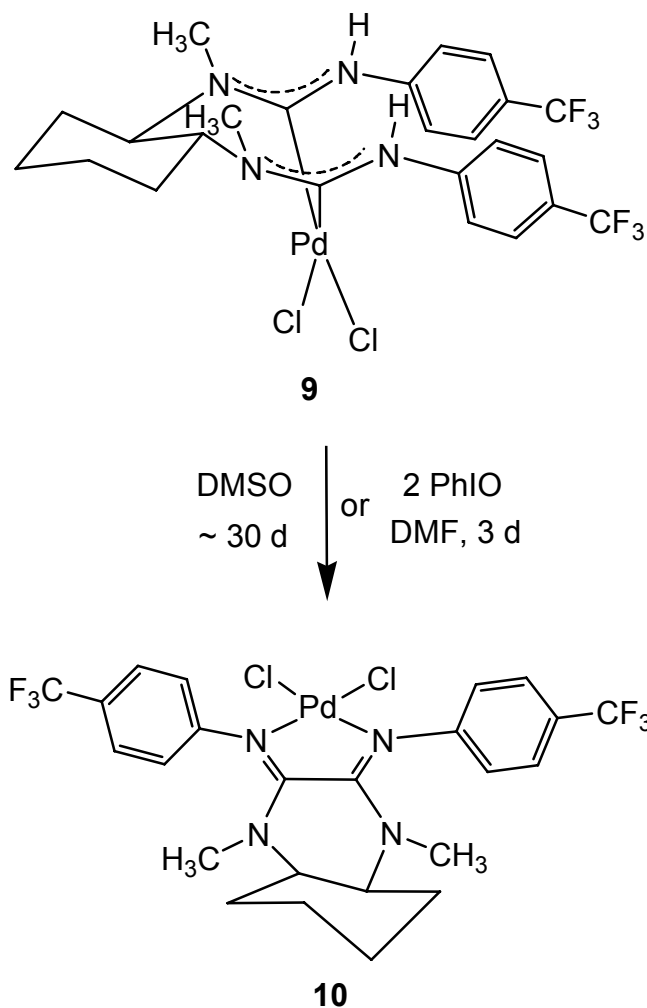
Table 3.4. Crystal data and structure refinement details for complex **9**.

Empirical formula	$C_{26}H_{34}Cl_2N_4F_6Pd$
Formula weight	725.87
Crystal system	Triclinic
Space group	$P\bar{1}$
Unit cell dimensions	$a = 8.0588(4) \text{ \AA}$ $\alpha = 84.861(4)^\circ$ $b = 14.0376(8) \text{ \AA}$ $\beta = 85.869(4)^\circ$ $c = 14.1642(8) \text{ \AA}$ $\gamma = 74.662(4)^\circ$
Volume, z	$1537.11(15) \text{ \AA}^3$, 2
Density (calculated)	1.568 Mg/m^3
Absorption coefficient	0.844 mm^{-1}
Crystal size	$0.55 \times 0.05 \times 0.02 \text{ mm}^3$
θ range for data collection	1.45 to 23.25°
Index ranges	$-8 \leq h \leq 8$, $-15 \leq k \leq 15$, $0 \leq l \leq 15$
Temperature	$100(2) \text{ K}$
Wavelength	0.71073 \AA
Reflections collected	9760
Independent reflections	4285 ($R_{\text{int}} = 0.057$)
Final R indices [$I > 2\sigma(I)$]	$R1 = 0.051$ $wR2 = 0.1073$
R indices (all data)	$R1 = 0.0758$ $wR2 = 0.1141$

3.3. Oxidation of bis(carbene) complex (9) to a bis(amidine) complex (10)

Complex **9** was an air and moisture stable molecule under most conditions. The thermal stability was moderate in solution, where only 26% decomposition occurred when heating complex **9** in degassed DMSO-*d*₆ for 5 days at 80°C. However, it was slowly oxidized to a palladium bis(amidine) complex **10** (Scheme 3.3) when it was dissolved in DMSO under air. This was discovered accidentally from one of the crystal growing samples of complex **9**, when attempting to grow x-ray quality crystals. The oxidized form of complex **9** precipitated from the solution as orange crystals over a long period of time (~ one month), while the original compound (complex **9**) was white in color as a solid. X-ray analysis of the crystal confirmed a bis(amidine) complex (Scheme 3.3).

Complex **10** was prepared in large scale using iodosobenzene as a mild oxidizing agent. In this reaction, 1 equiv of complex **9** and 2 equiv of iodosobenzene were mixed in dry N,N-dimethyl formamide (DMF) solvent, and the mixture was stirred for three days at room temperature (Scheme 3.3). The reaction was performed in a sealed NMR tube (J Young tube) since the yield improved significantly when using the NMR tube rather than a round bottom flask. The product precipitated from the reaction mixture as orange crystals. This reaction gave a 69 % yield.



Scheme 3.3. Oxidation of the bis(carbene) complex **9** to bis(amidine) complex **10** in the presence of oxygen or iodosobenzene as oxidizing agents.

When 1 equiv of iodosobenzene was used, a significant lowering of the yield of complex **10** was observed in 21 % yield. This may be due to the poor solubility of iodosobenzene in N,N-dimethyl formamide. The produced palladium bis(amidine) complex **10** also displayed poor solubility properties in all common solvents which made it impossible to characterize by NMR spectroscopy. However, elemental

analysis, crystallographic indexing of several crystals, and thermal decomposition points were similar to the sample prepared by air oxidation in DMSO for ~ 30 days. The decomposition temperature range of the crystals of complex **10** obtained by iodosobenzene oxidation (230-235 °C) was comparable with that of crystals prepared by air oxidation of **9** (235-248 °C). The higher range in decomposition temperatures for the latter sample is attributed to the fact that crystals developed from air oxidation of complex **9** were bigger in size than the crystals developed by the iodosobenzene method. In both samples, decomposition during melting point analysis produced a black char along with a trace of colorless crystalline material which deposited at the top part of the capillary tube indicated a similar behavior to the free bis(amidine) **11**.

An X-ray crystal structure showed that the complex **10** contained a palladium (II) bound bis(amidine) ligand (Figure 3.3). This resulted from a two electron oxidation of the original bis(carbene) ligand with overall loss of two hydrogen atoms attached in the NH groups accompanied by coupling between the two carbene carbon atoms in the molecule to form a new σ -bond. The C(1)-N(1) distance of 1.316(3) Å agrees with the presence of C=N ($C_{sp^2}=N$ 1.28 Å) double bonds in the bis(amidine) ligand (Table 3.5).²¹ This type of an oxidative decomposition pathway was previously unknown for bis(ADC) complexes. However a related reaction reported by Herrmann and coworkers resulted in conversion of a monodentate ADC ligand into an amidine.²⁴

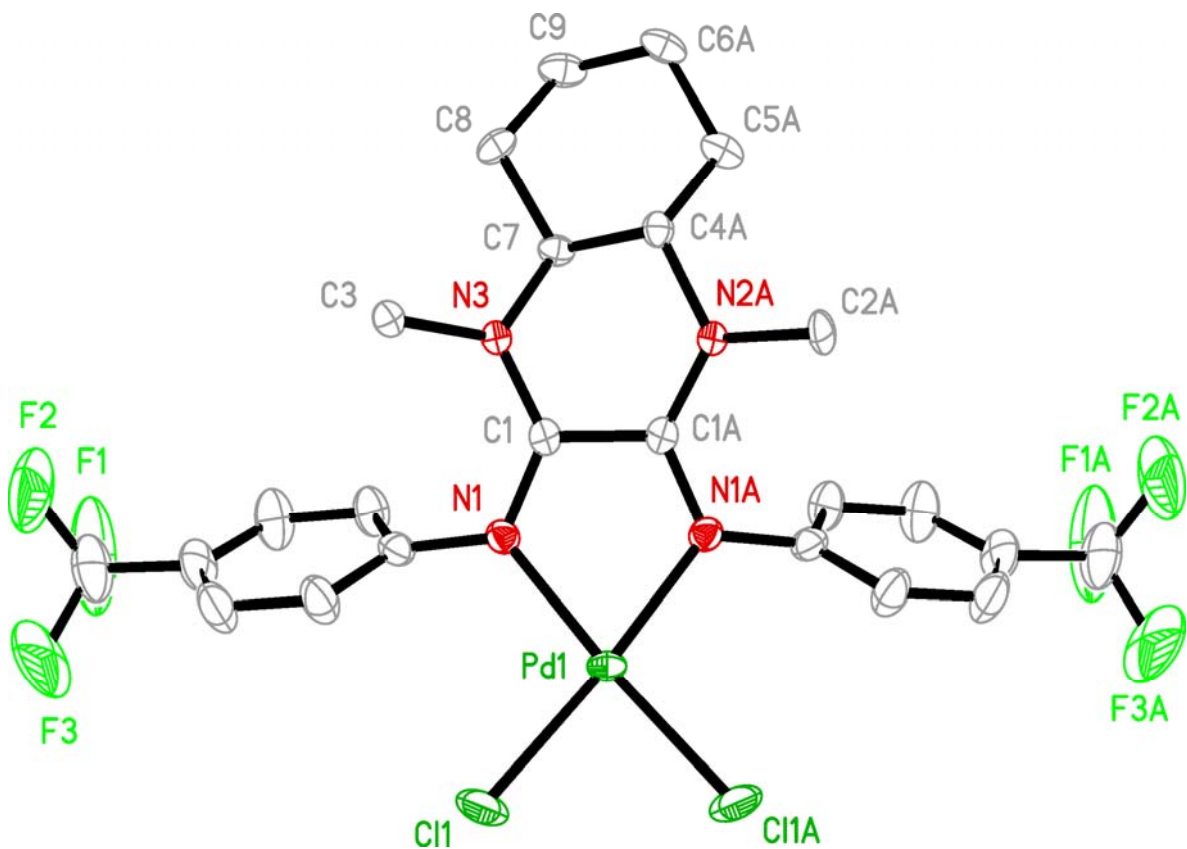


Figure 3.3. Molecular structure of complex **10** with 50% probability ellipsoids. Atoms labeled “A” are located at the symmetry equivalent position $(x, \frac{1}{2} - y, z)$.

Table 3.5. Selected bond lengths (Å) and bond angles (°) of complex **10**.

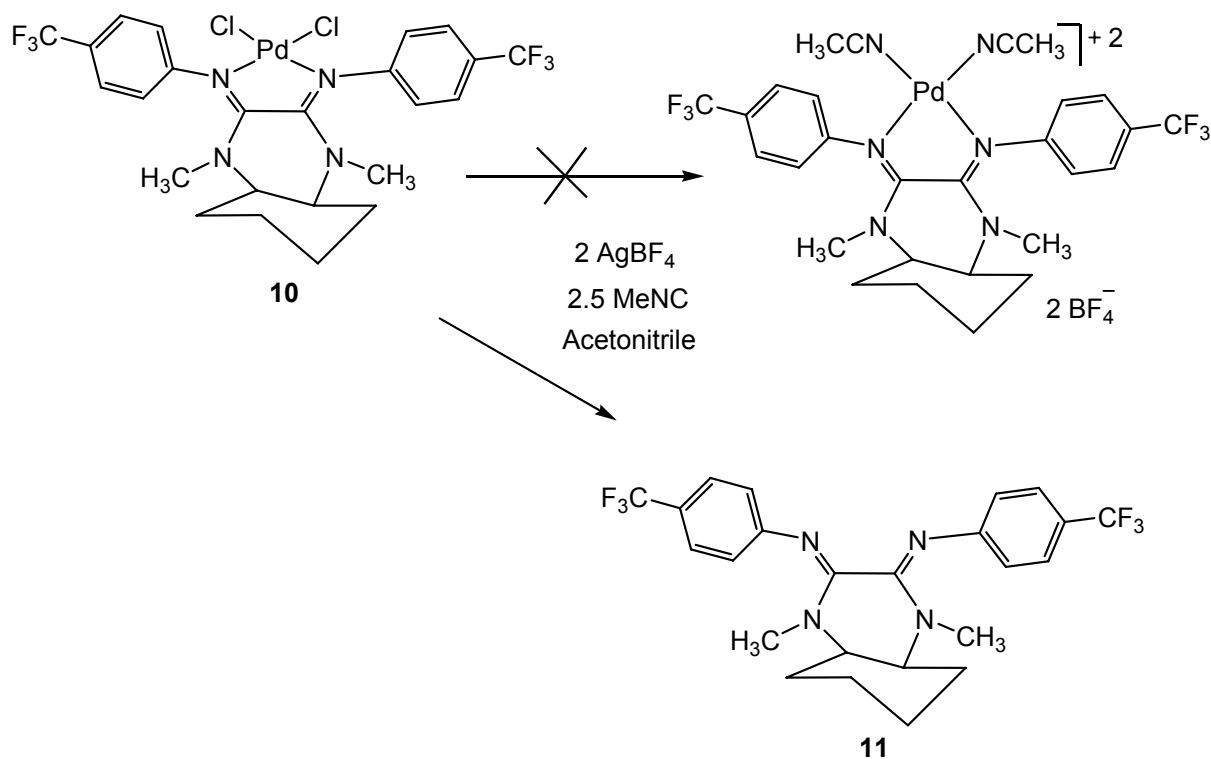
	Bond Lengths (Å)
N(1)-C(1)	1.316(3)
N(3)-C(1)	1.340(11)
C(1)-C(1A)	1.502(5)
N(1)-Pd(1)	2.036(2)
N(1A)-Pd(1)	2.036(2)
Pd(1)-Cl(1)	2.2848(7)
Pd(1)-Cl(1A)	2.2848(7)

	Bond Angles (°)
N(1)-C(1)-N(3)	125.5(4)
N(3)-C(1)-C(1A)	118.4(4)
N(1)-C(1)-C(1A)	114.8(14)
N(1)-Pd(1)-N(1A)	79.60(12)
N(1)-Pd(1)-Cl(1)	96.08(6)
N(1A)-Pd(1)-Cl(1A)	96.09(6)
Cl(1)-Pd(1)-Cl(1A)	88.21(4)

Table 3.6. Crystal data and structure refinement details for complex **10**.

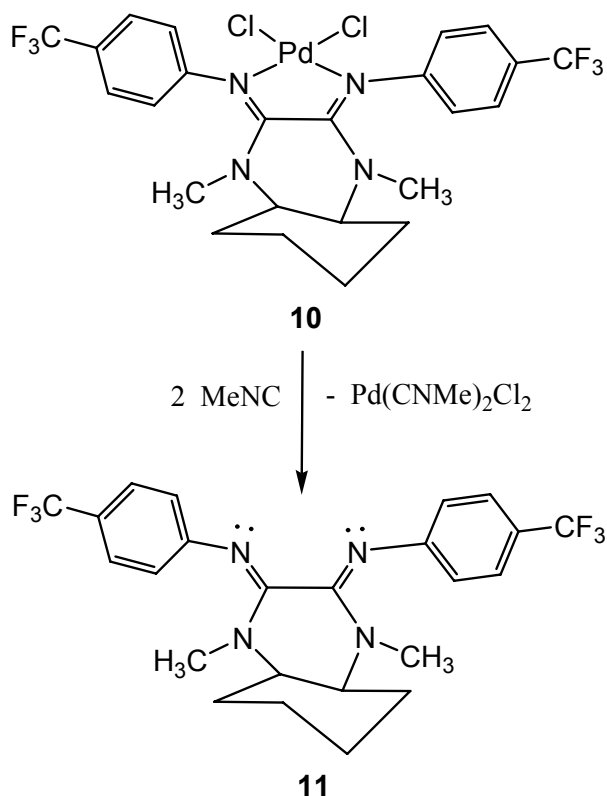
Empirical formula	C ₂₄ H ₂₄ Cl ₂ N ₄ F ₆ Pd
Formula weight	659.77
Crystal system	Orthorhombic
Space group	<i>Pnma</i>
Unit cell dimensions	$a = 12.8242(6) \text{ \AA}$ $\alpha = 90^\circ$ $b = 24.6468(11) \text{ \AA}$ $\beta = 90^\circ$ $c = 8.0601(14) \text{ \AA}$ $\gamma = 90^\circ$
Volume, <i>z</i>	2547.6 (2) \AA^3 , 4
Density (calculated)	1.720 Mg/m ³
Absorption coefficient	1.004 mm ⁻¹
Crystal size	0.27 x 0.15 x 0.04 mm ³
θ range for data collection	2.66 to 28.28 °
Index ranges	$-17 \leq h \leq 10$, $-32 \leq k \leq 27$, $-10 \leq l \leq 5$
Temperature	100(2) K
Wavelength	0.71073 \AA
Reflections collected	16960
Independent reflections	3226 ($R_{\text{int}} = 0.0488$)
Final <i>R</i> indices [$I > 2\sigma(I)$]	$R1 = 0.0342$ $wR2 = 0.0782$
<i>R</i> indices (all data)	$R1 = 0.0431$ $wR2 = 0.0825$

All attempts to make a more soluble form of complex **10** such as a bis(methylisocyanide) adduct (Scheme 3.4) by treatment with 2 equiv AgBF_4 followed by free methylisocyanide were unsuccessful as the bis(amidine) ligand was detaching from the palladium center. The reason for this facile ligand dissociation may be the high ligand strain that exists in the molecule. The free bis(amidine) ligand **11**, which was released upon treating with methylisocyanide, was isolated and characterized by ^1H NMR, ^{13}C NMR, elemental analysis, melting point determination, and x-ray crystallography.



Scheme 3.4. Attempted derivatization of bis(amidine) palladium dichloride complex **10** yielding the free bis(amidine).

Stoichiometric amounts of free bis(amidine) **11** was synthesized by treating bis(amidine) palladium complex **10** with methylisocyanide in DMF for 12 hours at room temperature. During the reaction, the bis(amidine) ligand in the palladium complex **10** gets substituted by methyl isocyanide ligands. The solvent was evaporated under vacuum, and the product was recrystallized from ether and hexanes at 0 °C to obtain the product as a pale yellow crystalline solid (Scheme 3.5).



Scheme 3.5. The synthesis of the free bis(amidine) **11** via ligand replacement in complex **10** upon treatment with methylisocyanide.

Free bis(amidine) **11** displayed high solubility in a range of solvents, varying from non-polar solvents such as diethyl ether to polar solvents such as DMSO. Therefore, the NMR spectroscopic studies of free bis(amidine) **11** could be done in C₆D₆. In the ¹H NMR spectrum, aryl *meta* and *ortho* protons could be seen at 7.26 ppm and 6.35 ppm as doublets with coupling constants of 8.1 Hz, which is in the range expected for ³J_{ortho} H-H coupling (³J_{ortho} ≈ 7-10 Hz).²⁵ The resonance due to NCH₃ groups in the molecule appeared as one peak at 2.68 ppm, consistent with C₂ symmetry in the molecule. The C₂ symmetry of the molecule could also be seen in the ¹³C NMR, with the N-C=N carbon atoms were appearing as a single peak at 152.8 ppm due to the symmetry in the molecule. Aryl *meta* and *para* carbon atoms and CF₃ carbons appeared as quartets at 125.7 ppm, 123.7 ppm and 125.7 ppm respectively, with characteristic coupling constants of ³J_{CF}=3.8 Hz, ²J_{CF}=32.1 Hz, and ¹J_{CF}=271 Hz.¹⁹

Single crystals of compound **11** were grown from slow evaporation of cyclohexane. The X-ray structure of compound **11** (Figure 3.4) displayed approximate C₂ symmetry and confirmed that the ligand is free from the metal. Bond lengths between C(2)-N(2) and C(1)-N(1) were 1.288 Å and 1.289 Å (Table 3.7), indicating localized C=N bonds between the atoms.²¹ The distance between C(2)-N(4) and C(1)-N(3) were 1.347 Å, and 1.359 Å, respectively, and these values were close to the average value reported for single bonds between C_{sp}²-N atoms (1.38 Å).²¹ The C(2)-C(1) distance was slightly larger than the average expected values for C_{sp}²-C_{sp}² single bonds (1.48 Å).²¹ This may be due to the steric strain imposed by

the large *p*-trifluoromethylphenyl groups or it could be a result of the twisted bis amidine geometry, imposed by the cyclohexyl ring, which permits ideal overlap.

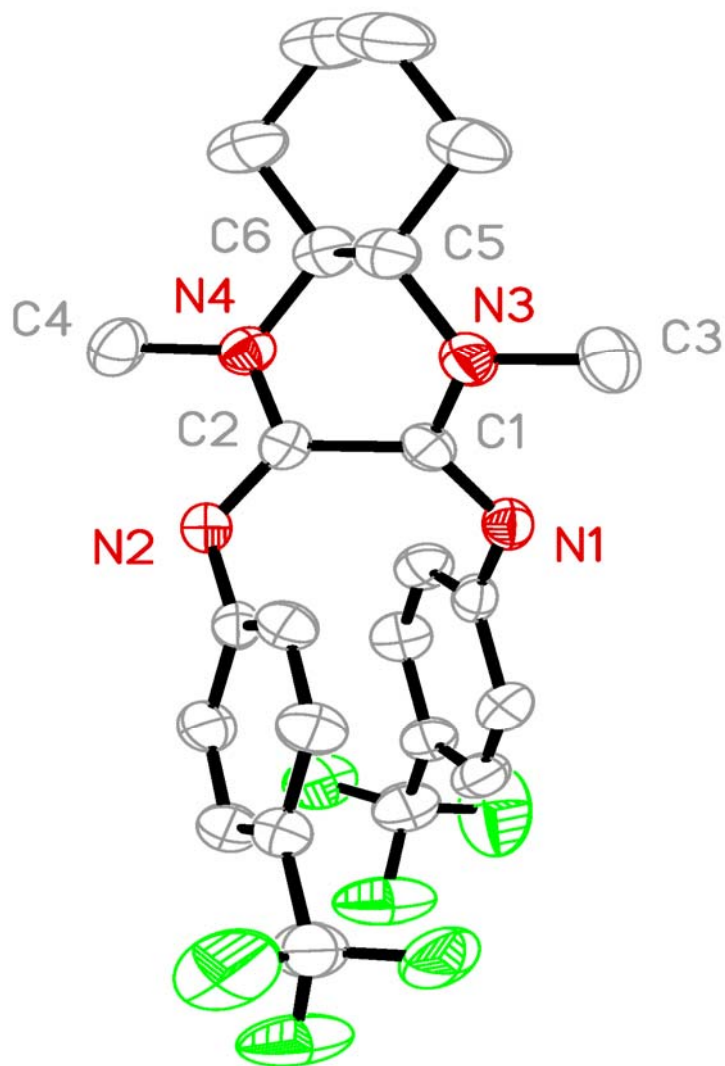


Figure 3.4. Molecular structure of **11** with 30% probability ellipsoids.

Table 3.7. Selected bond lengths (Å) and bond angles (°) of compound **11**.

	Bond Lengths (Å)
N(1)-C(1)	1.288(4)
N(3)-C(1)	1.359(4)
N(2)-C(2)	1.289(4)
N(4)-C(2)	1.347(5)
C(1)-C(2)	1.512(5)

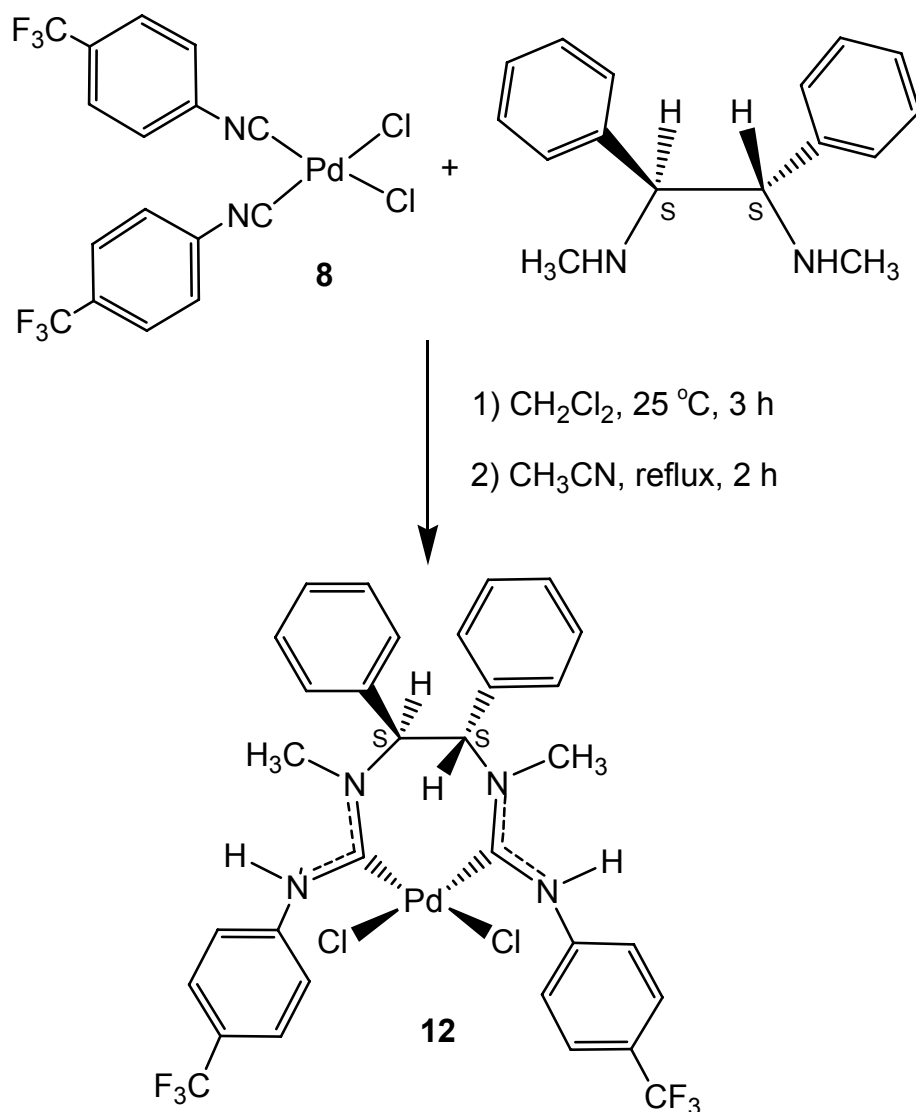
	Bond Angles (°)
N(4)-C(2)-N(2)	121.4(4)
N(3)-C(1)-N(1)	121.2(4)

Table 3.8. Crystal data and structure refinement details for **11**.

Empirical formula	$C_{24}H_{24}N_4F_6$
Formula weight	482.47
Crystal system	Monoclinic
Space group	$P2_1/n$
Unit cell dimensions	$a = 7.1121(3) \text{ \AA}$ $\alpha = 90^\circ$ $b = 11.9950(5) \text{ \AA}$ $\beta = 90.481(3)^\circ$ $c = 26.9486(11) \text{ \AA}$ $\gamma = 90^\circ$
Volume, z	$2298.89(17) \text{ \AA}^3$, 4
Density (calculated)	1.394 Mg/m^3
Absorption coefficient	0.118 mm^{-1}
Crystal size	$0.17 \times 0.17 \times 0.11 \text{ mm}^3$
θ range for data collection	1.51 to 21.96°
Index ranges	$-7 \leq h \leq 7$, $-11 \leq k \leq 12$, $-28 \leq l \leq 28$
Temperature	$297(2) \text{ K}$
Wavelength	0.71073 \AA
Reflections collected	11851
Independent reflections	2813 ($R_{\text{int}} = 0.0409$)
Final R indices [$I > 2\sigma(I)$]	$R1 = 0.048$ $wR2 = 0.1175$
R indices (all data)	$R1 = 0.0769$ $wR2 = 0.1363$

3.5. A bis(carbene) palladium complex with more pronounced chirality, derived from (1*S*,2*S*)-(-)-*N,N'*-dimethyl-1,2-diphenyl-1,2-ethanediamine (**12**)

In order to achieve a more pronounced asymmetric environment around the palladium center in chiral palladium bis(ADC) complex, enantiomerically pure bis(ADC) complex **12** (Scheme 3.6) was synthesized following the same procedure as complex **9**. For the synthesis, (1*S*,2*S*)-(-)-*N,N'*-dimethyl-1,2-diphenyl-1,2-ethanediamine (91 mg, 0.38 mmol) was used together with palladium precursor **8** (216 mg, 0.415 mmol) to obtain the enantiomerically pure palladium bis(carbene) dichloride **12** in 71% yield with out any impurities or by products. According to the X-ray crystal structure of complex **9** (Figure 3.2), complex **12** was designed to obtain an improved asymmetric environment around the palladium center as, of the phenyl rings on the amine back bone could orient towards the palladium center while the other phenyl group could orient away from the palladium center.



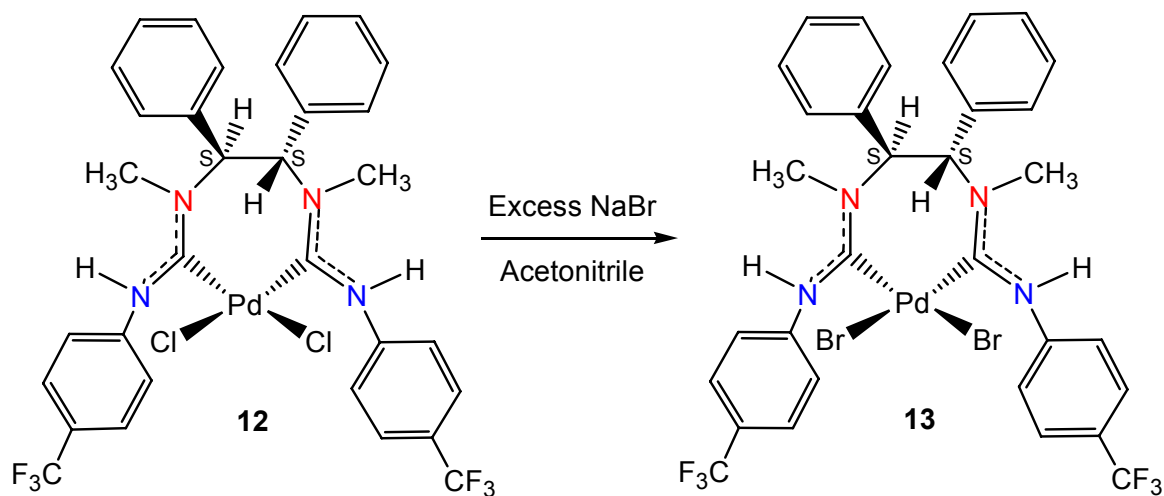
Scheme 3.6. Formation of palladium bis(carbene) complex **12** using palladium isocyanide precursor **8** and enantiomerically pure (1*S*,2*S*)-(-)-*N,N'*-dimethyl-1,2-diphenyl-1,2-ethanediamine.

Like the similar carbene complex **9**, complex **12** also displayed limited solubility properties in solvents such as methanol. However, the solubility of complex **12** in DMSO was sufficient to perform NMR experiments in DMSO-*d*₆. In the ¹H

NMR, two different *NH* peaks appeared at δ 9.87, and 9.29 and two different NCH_3 peaks appeared at δ 3.19, 2.93, providing evidence for that the two halves of the molecule are symmetrically inequivalent. The ^{13}C NMR spectrum displayed two different carbene carbon resonances at δ 190.7 ppm and 184.3 ppm, providing further evidence for the asymmetry in the molecule. Two different peaks each were observed for *p*-(trifluoromethylphenyl) isocyanide *meta* carbons at δ 125.9 and 124.4 and *para* carbons at δ 126.2 and 124.8 ppm respectively, in the ^{13}C NMR spectrum. C-F coupling constants for the *meta* carbons were 3.3 Hz and 3.1 Hz. For the *para* carbons, coupling constants observed were 34.2 Hz and 31.4 Hz. The two CF_3 carbons appeared as quartets at δ 124.3 and 124.2 with their characteristic large coupling constant of 272 Hz. These C-F coupling constants obtained for aryl *meta*, *para* and CF_3 carbons were within the ranges expected.¹⁹ In addition, ^{19}F NMR showed two different fluorine signals at δ -61.28 and -61.33 for the CF_3 groups in the molecule. These observations provided evidence for the presence of C_7 symmetry in the molecule.

Attempts to grow single crystals suitable for X-ray crystallographic analysis were unsuccessful because of the poor solubility of complex **12** in many solvents. The use of polar solvents such as methanol, DMF and DMSO for crystal growing by slow evaporation produced very thin crystals, not suitable for X-ray crystallographic analysis. In order to improve the solubility properties of complex **12**, a different strategy was used, which was to replace the chloride ligands with bromides. Bromides are larger and less electronegative than chlorides, resulting in smaller dipole moments for the complex and increased solubility in relatively non-polar

solvents such as acetonitrile. The halide exchange was performed in acetonitrile using excess NaBr as the bromide source (Scheme 3.7). The product, complex **13**, was sensitive to heat and displayed evidence for existence of a mixture of products by ^1H NMR. This may be due to the presence of both *cis* and *trans* isomers of **13** in solution.



Scheme 3.7. The conversion of dichloride complex **12** to dibromide complex **13**.

Single crystals suitable for X-ray crystallographic analysis were developed by slow evaporation of a concentrated methanol solution of complex **13**. The X-ray structure of complex **13** contained a seven-membered bis(ADC) chelating ring with an increased asymmetric environment around the palladium center relative to cyclohexanediamine-derived complex **9**. This asymmetric environment in complex **13** is created by having one of the phenyl groups in the backbone pointing towards the palladium center while the other phenyl group on the back-bone points away

from the metal center (Figure 3.5). Respective bond distances of 1.356 Å, 1.335 Å, 1.351 Å and 1.327 Å (Table 3.9) between C(1)-N(1), C(1)-N(3), C(2)-N(2), and C(2)-N(4) were larger than the expected average for Csp^2-N double bond distance (1.28 Å)²¹ due to the delocalized π bond system between these atoms. The Pd- C_{carbene} bond lengths of 1.987 Å and 2.011 Å (Table 3.9) were within the range reported for similar complexes.²⁰ The N- C_{carbene} -N bond angles were 114.5 ° and 116.5° which were comparable with bond angles reported for known ADC ligands.^{22, 23} The sum of bond angles around the palladium center was close to 360° indicating distorted square planer geometry around the palladium center (Table 3.9).

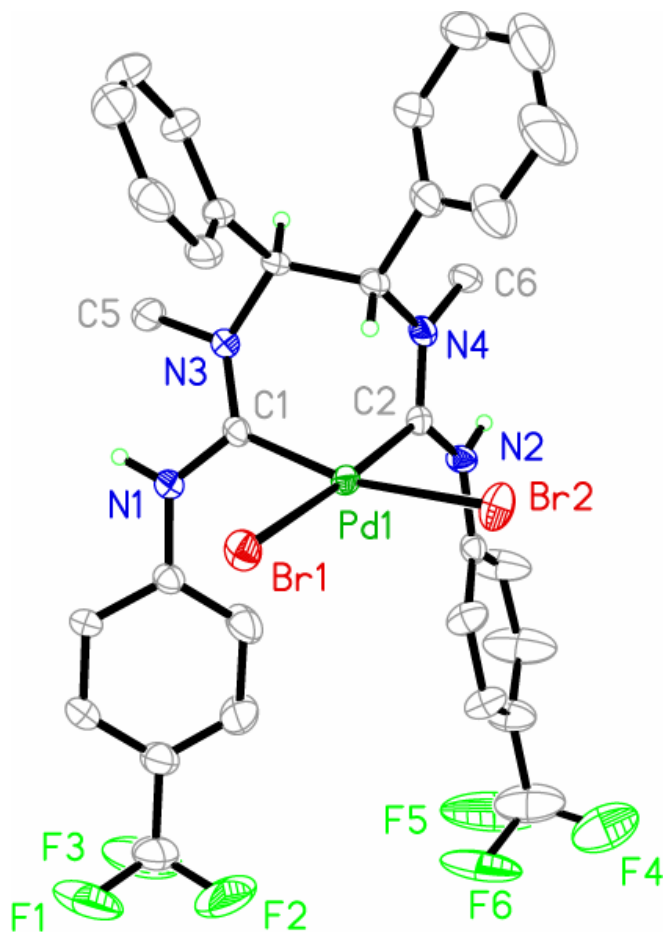


Figure 3.5. Molecular structure of **13** with 50% probability ellipsoids.

Table 3.9. Selected bond lengths (Å) and bond angles (°) of compound **13**.

	Bond Lengths (Å)
N(1)-C(1)	1.356(3)
N(3)-C(1)	1.335(4)
N(2)-C(2)	1.351(4)
N(4)-C(2)	1.327(4)
Pd(1)-C(1)	2.011(3)
Pd(1)-C(2)	1.987(3)
Pd(1)-Br(1)	2.4929(5)
Pd(1)-Br(2)	2.5238(5)

	Bond Angles (°)
N(1)-C(1)-N(3)	114.5(2)
N(2)-C(2)-N(4)	116.6(3)
C(1)-Pd(1)-C(2)	86.55(10)
C(1)-Pd(1)-Br(1)	92.15(8)
C(2)-Pd(1)-Br(2)	88.35(7)
Br(1)-Pd(1)-Br(2)	92.213(13)

Table 3.10. Crystal data and structure refinement details for complex **13** (contained 2 molecules of methanol in the structure).

Empirical formula	$C_{34}H_{36}Br_2N_4F_6O_2Pd$
Formula weight	912.89
Crystal system	Orthorhombic
Space group	$P2_12_12_1$
Unit cell dimensions	$a = 8.8307(11) \text{ \AA}$ $\alpha = 90^\circ$ $b = 13.1779(15) \text{ \AA}$ $\beta = 90^\circ$ $c = 30.571(4) \text{ \AA}$ $\gamma = 90^\circ$
Volume, z	$3557.6(8) \text{ \AA}^3$, 4
Density (calculated)	1.704 Mg/m^3
Absorption coefficient	2.836 mm^{-1}
Crystal size	$0.50 \times 0.35 \times 0.08 \text{ mm}^3$
θ range for data collection	1.68 to 30.51°
Index ranges	$-12 \leq h \leq 12$, $-18 \leq k \leq 18$, $-43 \leq l \leq 43$
Temperature	$115(2) \text{ K}$
Wavelength	0.71073 \AA
Reflections collected	85137
Independent reflections	10870 ($R_{\text{int}} = 0.0531$)
Final R indices [$I > 2\sigma(I)$]	$R1 = 0.0324$ $wR2 = 0.0743$
R indices (all data)	$R1 = 0.0382$ $wR2 = 0.0766$

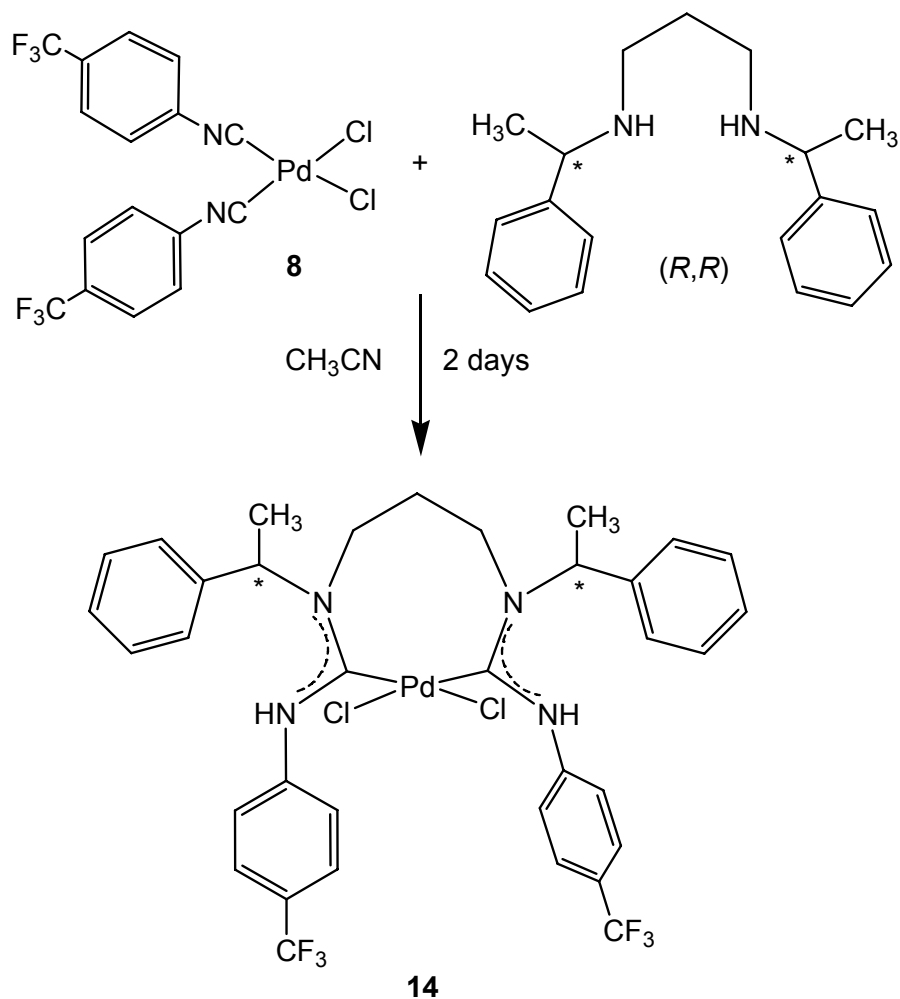
Bis(carbene) palladium complexes with larger chelate rings derived from N-alkylated 1,3-diamino propanes

Most efficient chiral catalysts are known to contain C_2 symmetry in the molecule.²⁶ Unfortunately, the transferring of C_2 symmetry present in chiral diamines onto bis(acyclic diaminocarbene) palladium complexes to produce C_2 symmetric bis(ADC) ligand does not occur during the synthesis of complexes **9** and **13**. The disappearance of C_2 symmetry in the bis(ADC) complex most likely arises due to strain present in the seven-membered chelate ring that forces a C_1 geometry in order to keep planar carbene units. An increase in the chelate ring size would provide more flexibility in the complex to preserve the C_2 symmetry of the amine back bone. In order to study the effect of having larger chelate ring sizes on the geometry of the palladium bis(ADC) complex, chiral N-alkylated 1,3-diaminopropanes, which are capable of producing eight membered chelating rings, were used as the diamine precursors for this study. N, N'-bis(1-naphthylethyl)-1,3-propanediamine and N, N'-bis(benzylmethyl)-1,3-propanediamine were used as bis(ADC) ligand precursors. These amines were prepared according to the method published by Alexakis et al.²⁷ with modifications.

3.6.1 bis(carbene) palladium complex 14 derived from (R,R)-N, N'-bis(benzylmethyl)-1,3-diaminopropane

Bis(*p*-trifluoromethyl phenylisocyanide) palladium dichloride precursor **8** (1.1 molar equiv) was treated with 1 molar equiv of (R,R)-N, N'-bis(benzylmethyl)-1,3-propanediamine in distilled acetonitrile. During this reaction, the bis(carbene)

palladium complex **14** started precipitating as an off-white crystalline solid from the reaction mixture. A yield of 40% was obtained by stirring the reaction mixture for two days at room temperature (Scheme 3.8).



Scheme 3.8. Formation of an eight membered chelate bis(ADC)PdCl₂ complex **14** from (*R,R*)-*N,N'*-bis(benzylmethyl)-1,3-propanediamine and palladium precursor **8**.

The ¹H NMR spectrum of complex **14** displayed two peaks at δ 9.63 and 9.56 indicating two different NH hydrogens in the complex. In addition, all of the propylene backbone hydrogen peaks were split into two peaks in the ¹H NMR

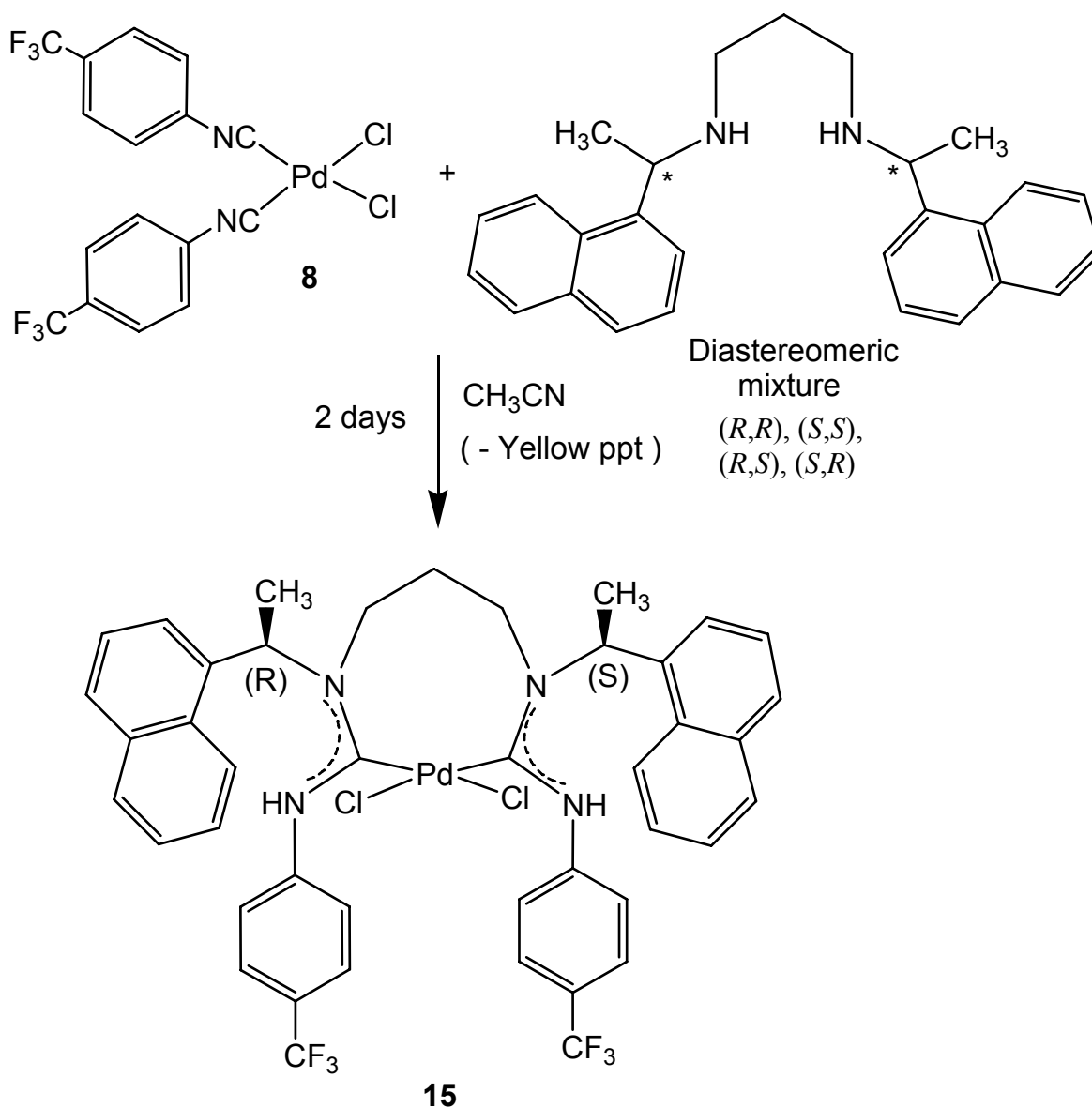
spectrum. This splitting of ^1H NMR signals suggests that complex **14** does not contain C_2 symmetry in the molecule. Unfortunately, the ^{13}C NMR spectrum of complex **14** displayed poor resolution between peaks due to high baseline noise. This is mainly because of the poor solubility of complex **14** in DMSO. However, two different carbene carbon peaks could be seen at δ 193 and 191 further indicating a lack of two fold symmetry. Some of the peaks on the ^{13}C NMR spectrum was not assigned as these peaks were not resolved well in the spectrum.

All the attempts to grow x-ray quality crystals of complex **14** from polar solvents such as DMSO, methanol and DMF were unsuccessful, producing very thin and fiber-like crystals which were not suitable for single crystal X-ray diffraction study.

3.6.2 N, N'-bis(1-naphthylethyl)-1,3-propanediamine derived bis(carbene) palladium complex (15)

A similar reaction to that described in the previous section was done using N,N'-bis(1-naphthylethyl)-1,3-propanediamine as the diamine and palladium precursor **8**. This reaction was performed to obtain an eight membered chelating palladium bis(ADC) complex with significant steric bulk assuming that the increased steric bulk would force formation of a C_2 symmetric complex. During the reaction 1.1 molar equiv of bis(*p*-trifluoromethyl phenylisocyanide) palladium dichloride precursor **8** was treated with 1 molar equiv of N,N'-bis(1-naphthylethyl)-1,3-propanediamine, consisting of a diastereomeric mixture of (*R,R*), (*S,S*), (*R,S*) and (*S,R*) isomers, in distilled acetonitrile. The reason behind the use of a diastereomeric mixture of the

amine was to see which diastereomer gives a stable chelating carbene complex. Within 15 min of the reaction, a yellow precipitate started forming rapidly from the reaction mixture. This yellow precipitate was isolated by filtration and was identified using ^1H NMR spectroscopy as the bis(ammonium) salt of the starting diamine. To remove all of the yellow bis(ammonium) salt, the reaction was stirred for three hours at room temperature and filtered to obtain a colorless solution. This clear filtrate was stirred further for two additional days at room temperature to isolate bis(ADC) complex **15** as a white precipitate in 19% yield (Scheme 3.9). Attempts to repeat this procedure with the enantiomerically pure (*R,R*) isomer of *N,N'*-bis(1-naphthylethyl)-1,3-propanediamine were unsuccessful, yielding only the yellow bis(ammonium) salt instead of the expected bis(ADC) palladium complex. This may be due to chelate ring opening and subsequent decomposition which may be due to unfavorable steric crowding of the (*R,R*) or (*S,S*) enantiomers of the bis(ADC) palladium complexes, producing the bis(ammonium) salt as a by-product.



Scheme 3.8. Formation of bis(ADC) palladium complex **15** derived from (*R,S*)-*N,N'*-bis(1-naphthylethyl)-1,3-propanediamine.

The ¹H NMR spectrum of complex **15** displayed a single peak at 9.72 ppm indicating one type of NH group in the molecule. However, ¹H NMR peaks due to hydrogens present in the amine backbone were split into two, indicating twofold symmetry (*C*₂ or *C*_s) in the molecule. The appearance of one carbene carbon signal

at 191 ppm in the ^{13}C NMR indicates that both carbene carbon atoms in the ligand have identical chemical environments. Aryl *para* carbon atoms on isocyanide groups appeared at 124.5 ppm as a quartet with a coupling constant ($^2J_{\text{CF}}$) of 32.6 Hz. The CF_3 carbons were displayed at 124.2 ppm as a quartet with a large coupling constant ($^1J_{\text{CF}}=272$ Hz). The coupling constants observed above were within the expected range.¹⁹

To determine the symmetry of complex **15**, crystals suitable for X-ray crystallography were developed by slow evaporation of a concentrated DMSO solution. The X-ray crystal structure displayed C_s symmetry in the complex, confirming the (*R,S*) configuration of the amine N-substituents (Figure 3.6). That only the C_s symmetry was obtained may be due to the steric crowding created by the naphthyl groups on the amine backbone. Bond lengths from carbene carbon atoms C(1) and C(2) to adjacent nitrogen atoms N(1), N(3), N(2), and N(4) were close in value due to the delocalized double bond system in the carbene unit (Table 3.11). The average bond distance of 1.34 Å obtained for $\text{C}_{\text{carbene}}\text{-N}$ was comparable with the values reported for similar bis(acyclic diaminocarbene) complexes¹⁴ and bis(N-heterocyclic carbene) complexes.^{28, 29} The $\text{N-C}_{\text{carbene}}\text{-N}$ bond angles of 117.6 ° and 118.3 ° and $\text{Pd-C}_{\text{carbene}}$ distances of 1.99 Å and 2.00 Å were in the range reported for other bis(acyclic diaminocarbene) complexes.¹⁴ The summation of bond angles around the palladium center was 360 °, indicating a distorted square planar geometry around the palladium center. The $\text{C}_{\text{carbene}}\text{-Pd-C}_{\text{carbene}}$ angle was 84 °, which is less than the ideal bond angle of 90 ° in square planar complexes.

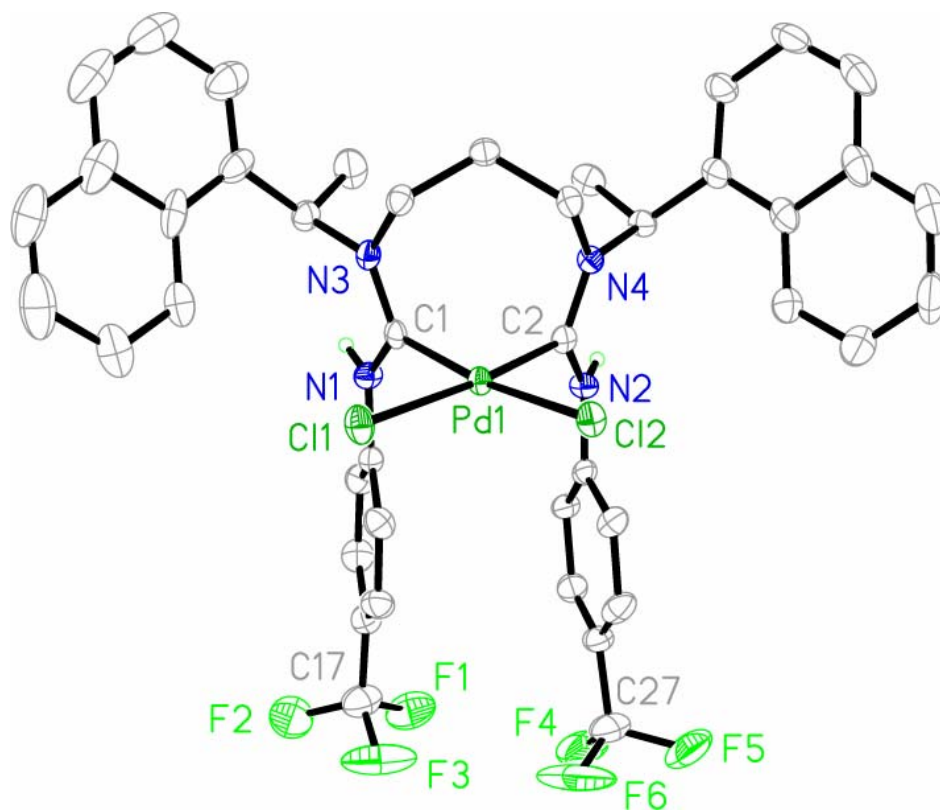


Figure 3.6. X-ray crystal structure of **15** displaying eight membered chelating bis(carbene) ring with 50% probability ellipsoids.

Table 3.11. Selected bond lengths (Å) and bond angles (°) of compound **15**.

	Bond Lengths (Å)
N(1)-C(1)	1.350(4)
N(3)-C(1)	1.331(4)
N(2)-C(2)	1.348(4)
N(4)-C(2)	1.330(4)
Pd(1)-C(1)	1.993(3)
Pd(1)-C(2)	2.000(3)
Pd(1)-Cl(1)	2.3804(7)
Pd(1)-Cl(2)	2.3721(7)

	Bond Angles (°)
N(1)-C(1)-N(3)	117.6(3)
N(2)-C(2)-N(4)	118.3(3)
C(1)-Pd(1)-C(2)	84.41(11)
C(1)-Pd(1)-Cl(1)	88.99(8)
C(2)-Pd(1)-Cl(2)	94.05(8)
Cl(1)-Pd(1)-Cl(2)	92.32(3)

Table 3.15. Crystal data and structure refinement details for complex **15**.

Empirical formula	C ₄₅ H ₄₄ Cl ₂ N ₄ F ₆ OPdS
Formula weight	980.20
Crystal system	Monoclinic
Space group	P _{21/c}
Unit cell dimensions	$a = 13.6755(6) \text{ \AA}$ $\alpha = 90^\circ$ $b = 24.5368(11) \text{ \AA}$ $\beta = 114.9970(10)^\circ$ $c = 14.0915(10) \text{ \AA}$ $\gamma = 90^\circ$
Volume, z	4285.5(3) \AA^3 , 4
Density (calculated)	1.519 Mg/m ³
Absorption coefficient	0.673 mm ⁻¹
Crystal size	0.19 x 0.17 x 0.02 mm ³
θ range for data collection	1.64 to 28.28 $^\circ$
Index ranges	$-18 \leq h \leq 18$, $-32 \leq k \leq 32$, $-18 \leq l \leq 18$
Temperature	125(2) K
Wavelength	0.71073 \AA
Reflections collected	41955
Independent reflections	10627 ($R_{\text{int}} = 0.0672$)
Final R indices [$I > 2\sigma(I)$]	$R1 = 0.0432$ $wR2 = 0.0925$
R indices (all data)	$R1 = 0.0720$ $wR2 = 0.1048$

Summary and Conclusions

The synthesis of the first chiral bis(acyclic diaminocarbene) palladium complexes via nucleophilic attack of chiral amines on a bis(*p*-trifluoromethylphenyl isocyanide) palladium dichloride precursor **8** has been accomplished. This method is a convenient, one-step procedure that can be scaled up to synthesize more than 600 mg of chiral palladium bis(ADC) complexes, in some cases without impurities and in one-pot. This procedure was followed to synthesize several examples of chiral palladium bis(ADC) complexes, containing seven and eight membered chelate bis(carbene) ligands. These chiral bis(ADC) complexes showed a tendency to adopt C_1 symmetry, likely to accommodate near-planar carbene moieties in the strained chelate rings. However, an eight membered chelate palladium bis(ADC) complex derived from , N, N'-bis(1-naphthylethyl)-1,3-propanediamine displayed C_s symmetry. Therefore, twofold symmetry is attachable in these complexes, although no C_2 symmetric ligands have yet been obtained. The poor solubility properties of chiral palladium bis(ADC) complexes was an obstacle when characterizing these complexes by NMR and developing crystals for X-ray crystallography, but this could be overcome by substituting chloride ligands with bromides. These complexes appeared to be generally stable. However, in the case of diaminocyclohexane derived complex **9**, slow $2e^-$ oxidation of the bis(carbene) ligand to form a bis(amidine)palladium complex was observed. This unfavorable oxidation in the carbene ligand can probably be minimized by substituting -NH groups in the carbene unit with N-alkyl or N-aryl groups.

Experimental

General Considerations. All manipulations were performed under air unless otherwise noted. Anhydrous DMF and acetonitrile were purchased in septum-sealed bottles from Acros and were used as received. Dichloromethane (Pharmco), diethyl ether (Acros) and hexanes (Pharmco) were dried according to the methods described previously in Chapter Two. NMR solvents were purchased from Cambridge Isotopes Laboratories. CD₃CN and DMSO-*d*₆ were dried by stirring over activated 4Å molecular sieves followed by distillation under vacuum and stored in an air free glove box under nitrogen atmosphere. CD₂Cl₂ was dried similarly and then stored over and distilled from P₂O₅ before use. All other reagents were purchased from Aldrich or Acros and used as received. *p*-Trifluoromethylphenyl isocyanide was synthesized via a phase-transfer Hofmann reaction.³⁰ (COD)PdCl₂,³¹ iodosobenzene,³² and methylisocyanide³³ were prepared by literature procedures. NMR spectra were recorded on Varian GEMINI 2000 (300 MHz) and Unity INOVA (400 MHz) spectrometers. Reported NMR chemical shifts are referenced to residual solvent peaks (¹³C, ¹H) or to calibrated external standards (¹⁹F, ³¹P). IR spectra were acquired from Nujol mulls on a Nicolet Protégé 460 FT-IR spectrometer. Elemental analyses were performed by Desert Analytics, Tucson, Arizona and Midwest Microlab, LLC, Indianapolis.

***cis*-Bis(*p*-trifluoromethylphenyl isocyanide)palladium dichloride (8)**

To a solution of *p*-trifluoromethylphenylisocyanide (133 mg, 0.78 mmol) in 10 mL of dichloromethane was added (COD)PdCl₂ (100 mg, 0.35 mmol). The reaction

mixture was stirred under air at 25 °C for 10 min. Layering of hexanes onto the solution resulted in precipitation of **8** as white crystalline precipitate. The product was collected by filtration and dried under vacuum. Yield: 130 mg, 72%. ¹H NMR (300 MHz, CD₂Cl₂): δ 7.79 (AB, *J*=8.6, *C*=8.9 Hz, *ortho*, *meta*-H). ¹³C NMR (101 MHz, CD₃CN): δ 133.4 (q, ²*J*_{CF} =33.5 Hz, Ar *para*), 129.4 (s, Ar *ipso*), 129.1 (s, Ar *ortho*), 128.1 (q, ³*J*_{CF} =3.8 Hz, Ar *meta*), 124.3 (q, ¹*J*_{CF} =272 Hz, CF₃), ArNC not detected. ¹⁹F NMR (282 MHz, CD₂Cl₂): δ -63.8 (s). IR (Nujo, cm⁻¹): ν 2241, 2221. Anal. Calc. for C₁₆H₈Cl₂F₆N₂Pd: C, 36.99; H, 1.55; N, 5.39 %. Found: C, 36.70; H, 1.33; N, 5.31 %.

(Racemic) bis(N,N'-dimethyldiaminocyclohexane biscarbene)palladium dichloride (9)

To a stirred solution of **8** (885 mg, 1.7 mmol) under argon in 70 mL of dichloromethane at 25 °C was slowly added N,N'-dimethyl-1,2-diaminocyclohexane (244 μL, 220 mg, 1.55 mmol) as a solution in 12 mL of dichloromethane, using a syringe pump set at an addition rate of 12 mL h⁻¹. The solution was stirred for further 2 hours at room temperature, during which time a light yellow precipitate formed. ¹H NMR analysis of the solid at this point showed it to be analytically pure **9**, but the following procedure was followed to maximize the yield. The solvent was removed under vacuum, anhydrous acetonitrile (30 mL) was added to the solid residue, and the mixture was heated at reflux under Ar for 2 hours. The pale yellow precipitate was collected by filtration, washed with acetonitrile, and dried under vacuum. Yield: 661 mg, 65 %. ¹H NMR (300 MHz, DMSO-*d*₆): δ 9.62 (1H, s, *NH*), 9.05 (1H, s, *NH*),

8.25 (2H, d, $J=8.3$ Hz, Ar), 7.71 (2H, d, $J=7.7$ Hz, Ar), 7.55 (2H, d, $J=8.3$ Hz, Ar), 7.42 (1H, m, $^{\circ}\text{Hex}$ ipso CH), 7.19 (2H, d, $J=7.7$ Hz, Ar), 3.68 (1H, m, $^{\circ}\text{Hex}$ ipso CH), 3.20 (3H, s, NCH₃), 3.10 (3H, s, NCH₃), 2.36-2.22 (1H, m, $^{\circ}\text{Hex}$), 2.22-2.08 (1H, m, $^{\circ}\text{Hex}$), 2.04-1.78 (4H, m, $^{\circ}\text{Hex}$), 1.63-1.38 (2H, m, $^{\circ}\text{Hex}$). ^{13}C NMR (101 MHz, DMSO- d_6): δ 190.3 (carbene), 184.4 (carbene), 144.4 (Ar ipso), 143.6 (Ar ipso), 125.6 (q, $^2J_{\text{CF}}=31.2$ Hz, Ar *para*), 125.4 (q, $^3J_{\text{CF}}=4.1$ Hz, Ar *meta*), 124.8 (q, $^2J_{\text{CF}}=32.5$ Hz, Ar *para*), 124.4 (q, $^3J_{\text{CF}}=3.8$ Hz, Ar *meta*), 124.3 (q, $^1J_{\text{CF}}=272$ Hz, CF₃), 124.2 (q, $^1J_{\text{CF}}=272$ Hz, CF₃), 123.8 (Ar *ortho*), 123.5 (Ar *ortho*), 67.9 (NCH₃), 66.9 (NCH₃), 40.7 ($^{\circ}\text{Hex}$), 31.7 ($^{\circ}\text{Hex}$), 31.4 ($^{\circ}\text{Hex}$), 29.9 ($^{\circ}\text{Hex}$), 25.3 ($^{\circ}\text{Hex}$), 24.6 ($^{\circ}\text{Hex}$). ^{19}F NMR (282 MHz, DMSO- d_6): δ -61.28 (s), -61.32 (s). Anal. Calc for C₂₄H₂₆Cl₂F₆N₄Pd: C, 43.56; H, 3.96; N, 8.47 %. Found: C, 43.41; H, 3.93; N, 8.63 %.

Bis(amidine)palladium dichloride (10)

Bis(carbene) palladium complex **9** (100 mg, 0.151 mmol) and iodosobenzene (66 mg, 0.30 mmol) were measured into a sealable J Young NMR tube. Anhydrous DMF (1.2 mL) was added to the NMR tube under nitrogen, and the tube was sealed with the teflon stopcock. The mixture was shaken under nitrogen for 3 days to obtain an orange, crystalline product. The solid was filtered off under air, washed with 5 mL of DMF and 5 mL of dichloromethane, and dried in vacuum. Yield: 69 mg, 69%.

Decomposition points were 230 °C to 235 °C for complex **7** derived from iodosobenzene method and 235 °C to 248 °C for complex **7** obtained by air oxidation in DMSO solution. Anal. Calc for C₂₄H₂₄Cl₂N₄F₆Pd: C, 43.68; H, 3.67; N, 8.49 %. Found: C, 43.59; H, 3.56; N, 8.61 %.

Free Bis(amidine) (11)

To a solution of bis(amidine) palladium complex **10** (100 mg, 0.151 mmol) in 10 mL of DMF was added methylisocyanide (21 μ L, 0.38 mmol), and the mixture was stirred for 12 hours at room temperature. The solvent was then evaporated under vacuum, and the residue was dried under vacuum for 12 hours. The residue was taken up in 10 mL of a 20:80 mixture of hexane and diethyl ether and filtered through celite. The volume of the filtrate was reduced under vacuum, the solution was cooled to 0 °C, and hexane was added to maximize crystal formation. Filtration afforded pale yellow crystals of **11**, which were dried in vacuum for 3 hours. Yield: 49 mg, 67%. ^1H NMR (300 MHz, C_6D_6): δ 7.26 (4H, d, $J=8.1$ Hz, Ar), 6.35 (4H, d, $J=8.1$ Hz, Ar), 2.68 (6H, s, NCH_3), 2.63-2.46 (2H, m, $^{\circ}\text{Hex}$), 1.58-1.38 (2H, m, $^{\circ}\text{Hex}$), 1.38-1.18 (2H, m, $^{\circ}\text{Hex}$), 0.79-0.54 (4H, m, $^{\circ}\text{Hex}$). ^{13}C NMR (101 MHz, C_6D_6): δ 152.8 (NC=N), 148.0 (s, Ar *ipso*), 125.7 (q, $^3J_{\text{CF}}=3.8$ Hz, Ar *meta*), 125.7 (q, $^1J_{\text{CF}}=271$ Hz, CF_3), 123.7 (q, $^2J_{\text{CF}}=32.1$ Hz, Ar *para*), 121.6 (s, Ar *ortho*), 59.9 (NCH_3), 29.9 ($^{\circ}\text{Hex}$), 28.4 ($^{\circ}\text{Hex}$), 23.8 ($^{\circ}\text{Hex}$). Anal. Calc. for $\text{C}_{24}\text{H}_{24}\text{N}_4\text{F}_6$: C, 59.75; H, 5.01; N, 11.61 %. Found: C, 59.46; H, 4.73; N, 11.42 %. Melting point range 179-182 °C.

(1S, 2S)-N,N'-dimethyl-1,2-diphenylethanediaminobiscarbenepalladium dichloride (12)

The synthesis was performed similarly to the procedure reported for complex **9**. Compound **8** (216 mg, 0.415 mmol) was treated with (1S, 2S)-N,N'-dimethyl-1,2-diphenylethanediamine (90.8 mg, 0.377 mmol) to obtain compound **12** in 75% yield,

238 mg. ^1H NMR (300 MHz, $\text{DMSO-}d_6$): δ 9.87 (1H, s, *NH*), 9.46 (1H, d, $J=12.9$ Hz, *CH*), 9.29 (1H, s, *NH*), 8.44 (2H, d, $J=8.7$ Hz, *Ar*), 8.19 (2H, d, $J=6.6$ Hz, *Ar*), 7.79 (2H, d, $J=8.7$ Hz, *Ar*), 7.71 (2H, d, $J=7.2$ Hz, *Ar*), 7.52 (2H, d, $J=8.4$ Hz, *Ar*), 7.40-7.23 (6H, m, *Ar*), 7.12 (2H, d, $J=8.4$ Hz, *Ar*), 5.86 (1H, d, $J=12.9$, *CH*), 3.19 (3H, s, NCH_3), 2.93 (3H, s, NCH_3). ^{13}C NMR (101 MHz, $\text{DMSO-}d_6$): δ 190.7 (carbene), 184.3 (carbene), 144.7 (*Ar ipso*), 143.7 (*Ar ipso*), 136.8 (s, Ph), 133.4 (s, Ph), 130.7 (s, Ph), 129.3 (s, Ph), 129.0 (s, Ph), 128.6 (s, Ph), 128.5 (s, Ph), 126.2 (q, $^2J_{\text{CF}}=34.2$ Hz, *Ar para*), 125.9 (q, $^3J_{\text{CF}}=3.3$ Hz, *Ar meta*), 124.9 (s, *Ar ortho*), 124.8 (q, $^2J_{\text{CF}}=31.4$ Hz, *Ar para*), 124.4 (q, $^3J_{\text{CF}}=3.1$ Hz, *Ar meta*), 124.3 (q, $^1J_{\text{CF}}=271.6$ Hz, CF_3), 124.2 (q, $^1J_{\text{CF}}=271.6$ Hz, CF_3), 123.2 (s, *Ar ortho*), 70.7 (NCH_3), 68.0 (NCH_3), 41.5 (*CH*), 32.0 (*CH*). ^{19}F NMR (376 MHz, $\text{DMSO-}d_6$): δ -61.28 (s), -61.33 (s). Anal. Calc. for $\text{C}_{32}\text{H}_{28}\text{Cl}_2\text{F}_6\text{N}_4\text{Pd}$: C, 50.58%; H, 3.71%; N, 7.37% Found: C, 50.49%; H, 3.76%; N, 7.34%.

(1S, 2S)-N,N'-dimethyl-1,2-diphenylethanediaminobiscarbenepalladium dibromide (13)

Complex **12** (30 mg, 0.039 mmol) was suspended in 10 mL of distilled acetonitrile in a round bottom flask. Sodium bromide (169 mg, 1.64 mmol) and 0.5 mL of deionized water were added to the reaction mixture. The flask was secured using a plastic cap and stirred overnight (~10 hrs) at room temperature. During the reaction, the solution turned clear, and the color changed to pale yellow. The volume of the solution was reduced to ~2 mL under reduced pressure without applying heat. Deionized water (10 mL) was added to the flask and the product, which was floating

on the solution as a gray crystalline precipitate was isolated by filtering through a 2 mL frit. The product was washed with deionized water (10 mL) and distilled diethyl ether (5 mL). The product was then dried in the vacuum overnight. Yield: 23.6 mg, 70.4%. ^1H NMR (300 MHz, $\text{DMSO-}d_6$): δ 9.88 (1H, s, NH), 9.38 (1H, d, $J=12.4$ Hz, CH), C 8.44 (2H, d, $J=8.0$ Hz, Ar), 8.21 (2H, d, $J=7.6$ Hz, Ar), 7.86-7.75 (4H, m, Ar), 7.52 (2H, d, $J=8.4$ Hz, Ar), 7.43-7.23 (6H, m, Ar), 7.12 (2H, d, $J=7.6$ Hz, Ar), 5.88 (1H, d, $J=12.4$, CH), 3.23 (3H, s, NCH_3), 2.94 (3H, s, NCH_3). Anal. Calc. for $\text{C}_{32}\text{H}_{28}\text{Br}_2\text{F}_6\text{N}_4\text{Pd}$: C, 45.28%; H, 3.33%; N, 6.60% Found: C, 44.94%; H, 3.48%; N, 6.33%.

(*R,R*)-*N,N'*-bis(benzylmethyl)-1,3-propanediamine

The synthesis used a modification of an already published procedure by Alexakis et al.²⁷ 2 equiv of (*R*)-methylbenzyl amine (0.1 mL, 0.784 mmol) and 1 equiv of 1,3-dibromo propane (40 μL , 0.392 mmol) were dissolved in distilled toluene (5 mL) and heated at 150 $^\circ\text{C}$ for 12 hours. Upon cooling the reaction mixture to room temperature, white needle-shaped crystals started precipitating from the solution. The precipitate was filtered and washed with pure toluene then with diethyl ether, and the product was dried under vacuum overnight. The ^1H NMR spectrum revealed the product to be the bis(ammonium) salt of the starting diamine. Yield 59%. ^1H NMR (400 MHz, $\text{DMSO-}d_6$): δ 9.18 (2H, br s, NH_2), 9.02 (2H, br s, NH_2), 7.53-7.38 (10H, m, Ar), 4.36 (2H, s, CH), 2.90 (2H, s, CH_2), 2.63 (2H, s, CH_2), 1.99 (2H, s, CH_2), 1.55 (6H, d, $J=6.4$ Hz, CH_3). The bis(ammonium) salt was deprotonated by treating with 20 mL of NaOH 20% (w/v) solution in 20 mL of

methylene chloride. The solution was poured into an extraction funnel and extracted twice with fresh methylene chloride (20 mL). The separated methylene chloride layers were collected, dried over anhydrous Na_2SO_4 , and rotovaped to remove the solvent. The diamine was obtained in 86% yield as an oil after drying under vacuum. ^1H NMR (400 MHz, C_6D_6): δ 7.31-7.10 (10H, m, Ar), 3.55 (2H, s, CH), 2.40 (4H, s, CH_2), 1.44 (2H, s, CH_2), 1.20 (6H, d, $J=6.4$ Hz, CH_3).

N, N'-bis(1-naphthylethyl)-1,3-propanediamine (diastereomeric mixture)

The same method as above was followed starting with 2 equiv of (*rac*) (1-naphthylethyl) amine (0.1 mL, 0.62 mmol) and 1 equiv of 1,3-dibromopropane (32 μL , 0.32 mmol) to obtain the bis(ammonium) dibromide salt in 70% yield (0.119 g) ^1H NMR (400 MHz, $\text{DMSO}-d_6$): δ 9.41 (2H, br s, NH_2), 9.13 (2H, br s, NH_2), 8.22 (2H, d, $J=8.4$ Hz, Naphthyl), 7.99 (4H, m, Naphthyl), 7.86 (2H, s, Naphthyl), 7.60 (6H, m, Naphthyl), 5.27 (2H, s, CH), 3.06 (2H, s, CH_2), 2.82 (2H, s, CH_2), 2.07 (2H, s, CH_2), 1.63 (6H, d, CH_3). The diamine was isolated in 65% yield (0.078 g) ^1H NMR (400 MHz, C_6D_6): δ 8.21 (2H, t, $J=7.6$ Hz, Naphthyl), 7.74-7.69 (4H, m, Naphthyl), 7.59 (2H, d, $J=8.0$ Hz, Naphthyl), 7.36-7.28 (6H, m, Naphthyl), 4.40 (2H, q, $J=5.2$ Hz, CH), 2.48 (4H, m, CH_2), 1.49 (2H, m, CH_2), 1.33 (6H, dd, $J=6.6$ Hz and $J=1.6$ Hz, CH_3). Similarly, the enantiomerically pure (*R,R*)-N,N'-bis(1-naphthylethyl)-1,3-propanediamine was synthesized using 1 equiv of 1,3-dibromopropane (0.158 mL, 1.547 mmol) and 2 equiv of (*R*)-(+)- α -(1-naphthylethyl) amine (0.5 mL, 3.095 mmol) to obtain the bis(ammonium) bromide salt in 89% yield (0.753 g) and then the amine

in 77% yield (0.4543 g). The ^1H NMR spectra of these compounds were similar to the above values reported for the diastereomeric mixture of the amine.

(R,R) N, N'-bis(benzylmethyl)-1,3-diaminopropane-biscarbene palladium dichloride (14)

One equiv of (*R,R*)-N,N'-bis(benzylmethyl)-1,3-propanediamine (0.0295 g, 0.1044 mmol) dissolved in 4 mL of distilled acetonitrile was added drop by drop into a solution of 1.1 equiv of complex **8** (0.0596 g, 0.1149 mmol) dissolved in 22 mL of distilled acetonitrile. The reaction mixture was stirred for two days at room temperature to obtain the bis(carbene) palladium complex as a white crystalline precipitate. The precipitated product was filtered through a frit, washed with fresh acetonitrile and then with methylene chloride, and dried in vacuum overnight.

(0.0336 g, 40% yield). ^1H NMR (400 MHz, DMSO- d_6): δ 9.63 (1H, s, NH), 9.56 (1H, s, NH), 8.15 (2H, d, $J=8.4$ Hz, Ar), 8.02 (2H, d, $J=8.4$ Hz, Ar), 7.54-7.44 (6H, m, Ar), 7.26-7.20 (8H, m, Ar), 5.88 (1H, m, CH), 5.71 (1H, m, CH), 5.66-5.51 (2H, m, CH), 3.85 (1H, m, CH), 3.29 (1H, m, CH), 1.56 (1H, m, CH₂), 1.43 (6H, m, CH₃), 0.72 (1H, m, CH₂). Anal. Calc. for C₃₅H₃₄Cl₂F₆N₄Pd: C, 52.42%; H, 4.27%; N, 6.99% Found: C, 52.13%; H, 4.12%; N, 6.91%.

N, N'-bis(1-naphthylethyl)-1,3-diaminopropane-biscarbene palladium dichloride (15)

Mixture of N,N'-bis(1-naphthylethyl)-1,3-propanediamine (0.67 g, 0.175 mmol) was dissolved in 4 mL of distilled acetonitrile and added dropwise into a

solution of complex **8** in 30 mL of distilled acetonitrile followed by stirring at room temperature. Within 15 min, a yellow precipitate started forming from the reaction mixture. To ensure that all of the yellow precipitate had formed, the reaction was stirred for an additional 3 hours. The solution was filtered through a fine frit to remove the yellow byproduct, giving a clear filtrate. The filtrate was stirred for an additional 2 days at room temperature to obtain the bis(carbene) palladium dichloride complex as a white precipitate. The filtered product was washed with fresh acetonitrile and methylene chloride and dried in vacuum overnight. (0.0325 g, yield 19%). ^1H NMR (400 MHz, $\text{DMSO-}d_6$): δ 9.73 (2H, s, NH), 8.17 (4H, d, $J=8.4$ Hz, Ar), 7.94-7.92 (4H, m, Naphthyl), 7.79 (2H, d, Naphthyl), 7.59-7.54 (4H, m, Naphthyl), 7.49 (2H, t, $J=6.8$ Hz, Naphthyl), 7.37 (2H, t, $J=7.2$ Hz, Naphthyl), 7.28 (4H, d, $J=8.8$ Hz, Ar), 6.28 (2H, m, $J=6.0$ Hz, CH), 5.48 (2H, t, $J=14.4$ Hz, CH_2), 3.45-3.42 (2H, m, CH_2), 2.19 (1H, m, CH_2), 1.92 (7H, m, CH_2 and CH_3). ^{13}C NMR (151 MHz, $\text{DMSO-}d_6$): δ 191.3 (carbene), 144.0 (Ar *ipso*), 133.5 (Naphthyl), 133.4 (Naphthyl), 130.7 (Naphthyl), 129.2 (Naphthyl), 128.7 (Naphthyl), 127.0 (Naphthyl), 126.2 (Naphthyl), 125.4 (Naphthyl), 125.2 (Naphthyl), 125.0 (Ar *meta*), 124.5 (q, $^2J_{\text{CF}}=32.6$ Hz, Ar *para*), 124.2 (q, $^1J_{\text{CF}}=272$ Hz, CF_3), 123.2 (Naphthyl), 122.5 (Ar *ortho*), 54.3 (NCH₃), 53.8 (CH), 30.3 (NCH₂), 19.2 (CH₂). Anal. Calc. for $\text{C}_{43}\text{H}_{38}\text{Cl}_2\text{F}_6\text{N}_4\text{Pd}$: C, 57.25%; H, 4.25%; N, 6.21% Found: C, 57.49%; H, 4.36%; N, 6.49%.

General Considerations of X-ray Crystallographic Analyses

X-ray diffraction data were collected on a Bruker SMART APEX II diffractometer with a CCD detector using a combination of φ and ω scans. A Bruker Kryoflex liquid nitrogen cooling device was used for low-temperature data

collections. Data integration employed the Bruker SAINT software package.³⁴ All X-ray diffraction experiments employed graphite-monochromated Mo K α radiation ($\lambda=0.71073$ Å). Structures were solved by direct methods and refined by full-matrix least-squares on F^2 using the SHELXTL software suite.³⁵ Non-hydrogen atoms were assigned anisotropic temperature factors, with hydrogen atoms included in calculated positions (riding model).

References

1. Denk, K.; Sirsch, P.; Herrmann, W. A. *J. Organomet. Chem.* **2002**, *649*, 219.
2. Slaughter, L. M. *Comments on Inorganic Chemistry* **2008**, *29*, 46.
3. Herrmann, W. A.; Ofele, K.; von Preysing, D.; Herdtweck, E. *J. Organomet. Chem.* **2003**, *684*, 235.
4. Moncada, A. I.; Khan, M. A.; Slaughter, L. M. *Tetrahedron Lett.* **2005**, *46*, 1399.
5. Dhudshia, B.; Thadani, A. N. *Chem. Commun.* **2006**, 668.
6. Kremzow, D.; Seidel, G.; Lehmann, C. W.; Furstner, A. *Chemistry-A European Journal* **2005**, *11*, 1833.
7. Cesar, V.; Bellemin-Lapponnaz, S.; Gade, L. H. *Chem. Soc. Rev.* **2004**, *33*, 619.
8. Gade, L. H.; Bellemin-Lapponnaz, S. *Coord. Chem. Rev.* **2007**, *251*, 718.
9. Alder, R. W.; Allen, P. R.; Murray, M.; Orpen, A. G. *Angew. Chem. Int. Ed.* **1996**, *35*, 1121.

10. Herrmann, W. A.; Schutz, J.; Frey, G. D.; Herdtweck, E. *Organometallics* **2006**, *25*, 2437.
11. Tschugajeff(Chugaev), L.; Skanawy-Grigorjewa, M. *J. Russ. Chem. Soc.* **1915**, *47*, 776.
12. Tschugajeff, L.; Grigorjewa, M.; Posnjak, A. *Zeitschrift fur Anorganische und Allgemeine Chemie* **1925**, *148*, 37.
13. Burke, A.; Balch, A. L.; Enemark, J. H. *J. Am. Chem. Soc.* **1970**, *92*, 2555.
14. Moncada, A. I.; Manne, S.; Tanski, J. M.; Slaughter, L. M. *Organometallics* **2006**, *25*, 491.
15. Doonan, D. J.; Balch, A. L. *Inorg. Chem.* **1974**, *13*, 921.
16. Uson, R.; Laguna, A.; Villacampa, M. D.; Jones, P. G.; Sheldrick, G. M. *Journal of the Chemical Society-Dalton Trans.* **1984**, 2035.
17. Collman, J. P.; Hegedus, L. S.; Norton, J. R.; Finke, R. G. *Principles and Applications of Organotransition Metal Chemistry*; University Science Books: Sausalito California, 1987.
18. Braunstein, P.; Nobel, D. *Chem. Rev.* **1989**, *89*, 1927.

19. Wehrli, F. W.; Marchand, A. P.; Wehrli, S. *Interpretation of Carbon-13 NMR Spectra*; John Wiley & Sons: New York, 1988; pp.92.
20. Ahrens, S.; Zeller, A.; Taige, M.; Strassner, T. *Organometallics* **2006**, *25*, 5409.
21. Smith, M. B.; March, J. *MARCH'S Advanced Organic Chemistry: Reactions, Mechanisms, and Structure*; John Wiley & Sons: New York, 2001; pp.20.
22. Moncada, A. I. Master's Thesis, Oklahoma State University, 2005.
23. Fehlhammer, W. P.; Bliss, T.; Sperber, W.; Fuchs, J. *Zeitschrift fur Naturforschung Section B-A Journal of Chemical Sciences* **1994**, *49*, 494.
24. Frey, G. D.; Herdtweck, E.; Herrmann, W. A. *J. Organomet. Chem.* **2006**, *691*, 2465.
25. Pavia, D. L.; Lampman, G. M.; Kriz, G. S. *Introduction to Spectroscopy*; Brooks/Cole Thomson Learning, Wadsworth Group: Hartford, Connecticut, 2001.
26. Yoon, T. P.; Jacobsen, E. N. *Science* **2003**, *299*, 1691.
27. Equey, O.; Alexakis, A. *Tetrahedron-Asymmetry* **2004**, *15*, 1069.

28. Herrmann, W. A.; Elison, M.; Fischer, J.; Köcher, C.; Artus, G. R. J. *Angew. Chem. Int. Ed.* **1995**, *34*, 2371-2374.
29. Gardiner, M. G.; Herrmann, W. A.; Reisinger, C. P.; Schwarz, J.; Spiegler, M. *J. Organomet. Chem.* **1999**, *572*, 239.
30. Gokel, G. W.; Widera, R. P.; Weber, W. P. *Org. Synth.* **1976**, *55*, 96.
31. Drew, D.; Doyle, J. R.; Shaver, A. G. *Inorg. Synth.* **1972**, *13*, 52.
32. Saltzman, H.; Sharefkin, J. G. *Org. Synth.* **1963**, *43*, 60.
33. Schuster, R. E.; Scott, J. E.; Casanova, J. *Org. Synth.* **1966**, *46*, 75.
34. Bruker, *SAINT-plus*, Version 6.29, Bruker AXS, Madison, WI, USA. 2001.
35. Sheldrick, G. M. *SHELXTL*, Version 6.14; Bruker AXS: Madison, WI, USA, 2000.

CHAPTER IV

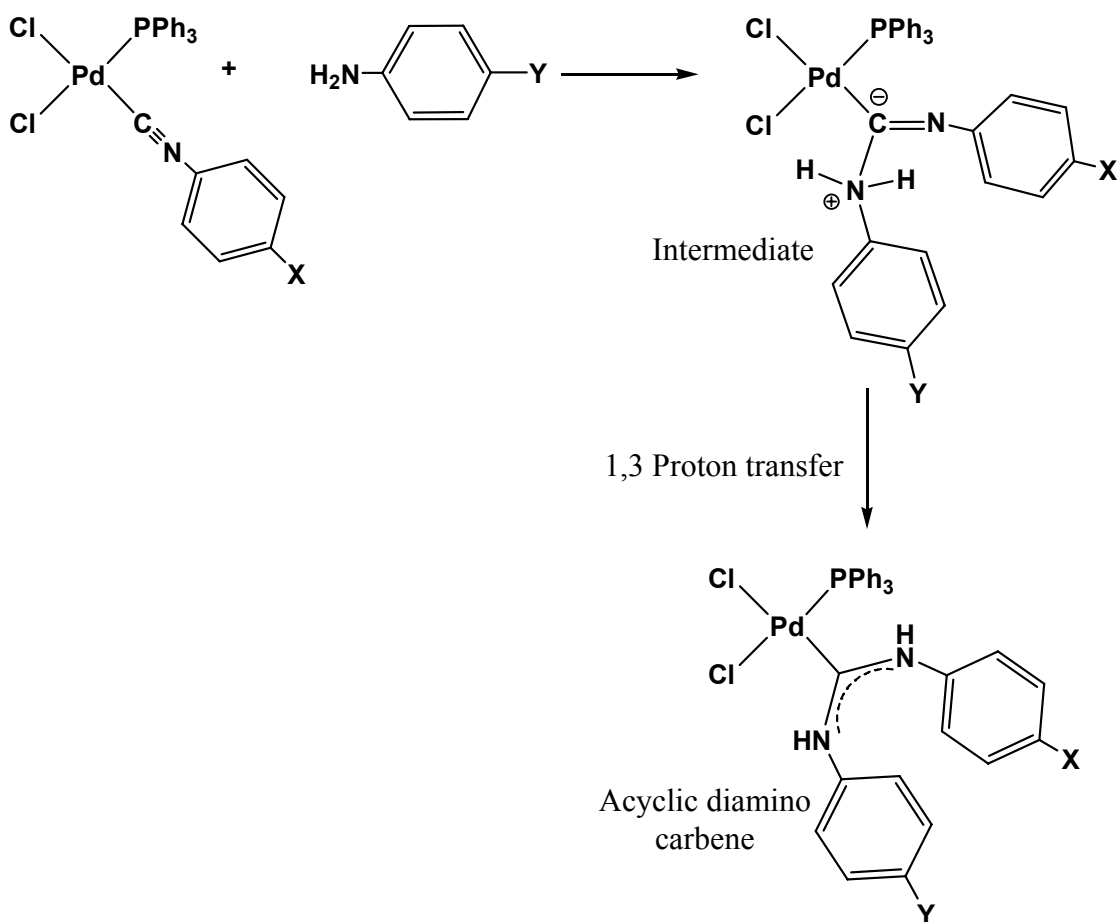
Synthesis of a Tetrasubstituted Chugaev-type Bis(Carbene) Palladium

Complex and its Reversible Chelate Ring Opening

“Portions reproduced with permission from [Wanniarachchi, Y. A.; Slaughter, L. M. *Organometallics*, **2008**, 27, 1055-1062.] Copyright [2008] American Chemical Society.”

Introduction

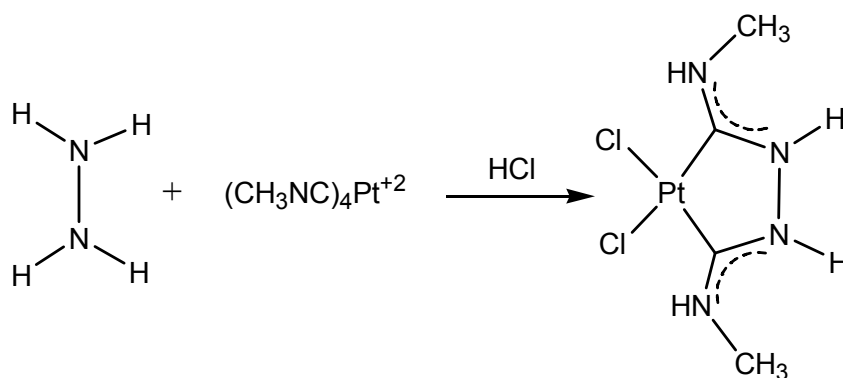
Nucleophilic addition of amines to metal-coordinated isocyanides has long been known as an efficient method for the synthesis of amino-substituted carbene ligands (Scheme 4.1).^{1,2} In the case of chelating diaminocarbenes formed from reaction of diamines with two isocyanides, the thermodynamic favorability of the reaction depends on a delicate balance between the favorable enthalpy change associated with new C-N bond formation and the unfavorable entropy factor due to the loss of degrees of freedom. A few early reports show that nucleophilic addition of amines to metal bound isocyanides can be reversible in some cases. For example, the monocarbene complex $(\eta^5\text{-C}_5\text{H}_5)\text{Fe}(\text{CO})(\text{CN})[\text{C}(\text{NHMe})(\text{NMe}_2)]$ underwent the reverse reaction of diaminocarbene formation by converting to its starting isocyanide complex $\eta^5\text{-C}_5\text{H}_5\text{Fe}(\text{CO})(\text{CN})(\text{CNMe})$ in solution may be due to the steric crowding created by the bulky C_5H_5 ligand.³ Similarly, Steinmetz et al. reported an equilibrium between the trisubstituted monocarbene complex $(\eta^5\text{-C}_5\text{H}_5)\text{Ru}(\text{CO})(\text{CN})[\text{C}(\text{NHMe})(\text{NMe}_2)]$ and the starting isocyanide complex $(\eta^5\text{-C}_5\text{H}_5)\text{Ru}(\text{CO})(\text{CN})(\text{CNMe})$ in solution in the presence and the absence of excess Me_2NH in solution.⁴



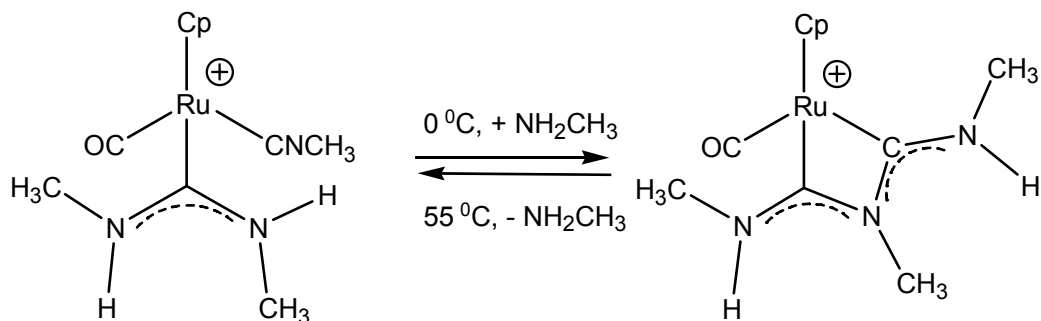
Scheme 4.1. Mechanism for the formation of acyclic diamino carbene palladium complexes via nucleophilic attack of the amine on an aryl isocyanide palladium complex. Adapted from Reference 2.

However, bis(acyclicdiamino carbene) ligand formation via nucleophilic attack of diamines on *cis*-isocyanide metal complexes have generally been reported to be rapid, with no observation of an equilibrium between the bis(carbene) metal complex and the starting isocyanide complex or the intermediate monocarbene isocyanide complex.⁵

Chugaev-type carbene complexes containing five membered chelate rings can also be synthesized from hydrazines and Pd(II) or Pt(II) isocyanide complexes. These reactions are rapid and do not show any indication of an intermediate monocarbene metal complex (Scheme 4.2).^{6,7} Chelating Chugaev-type bis(ADC) palladium complexes were readily formed from phenylhydrazine and comparatively less bulky methyl isocyanide ligands. However, a more bulky isopropyl isocyanide ligand led to the formation of a non-chelating monocarbene isocyanide ligand upon reaction with phenylhydrazine.⁸ Bis(acyclic diaminocarbene) metal complexes containing strained four membered chelate rings have displayed chelate ring opening at higher temperatures (Scheme 4.3)⁴ and when passing through a silica gel column.⁹ This suggests that steric and/or the steric strain in the molecule can disfavor the otherwise thermodynamically favorable chelate ring formation in these bis(acyclic diaminocarbene) metal complexes.



Scheme 4.2. Formation of a Chugaev-type chelating carbene complex from hydrazine and a platinum(II) isocyanide complex.



Scheme 4.3. Formation and reversible chelate ring opening of a four membered bis(acyclic diaminocarbene) ruthenium(II) complex. (Adapted from ⁴)

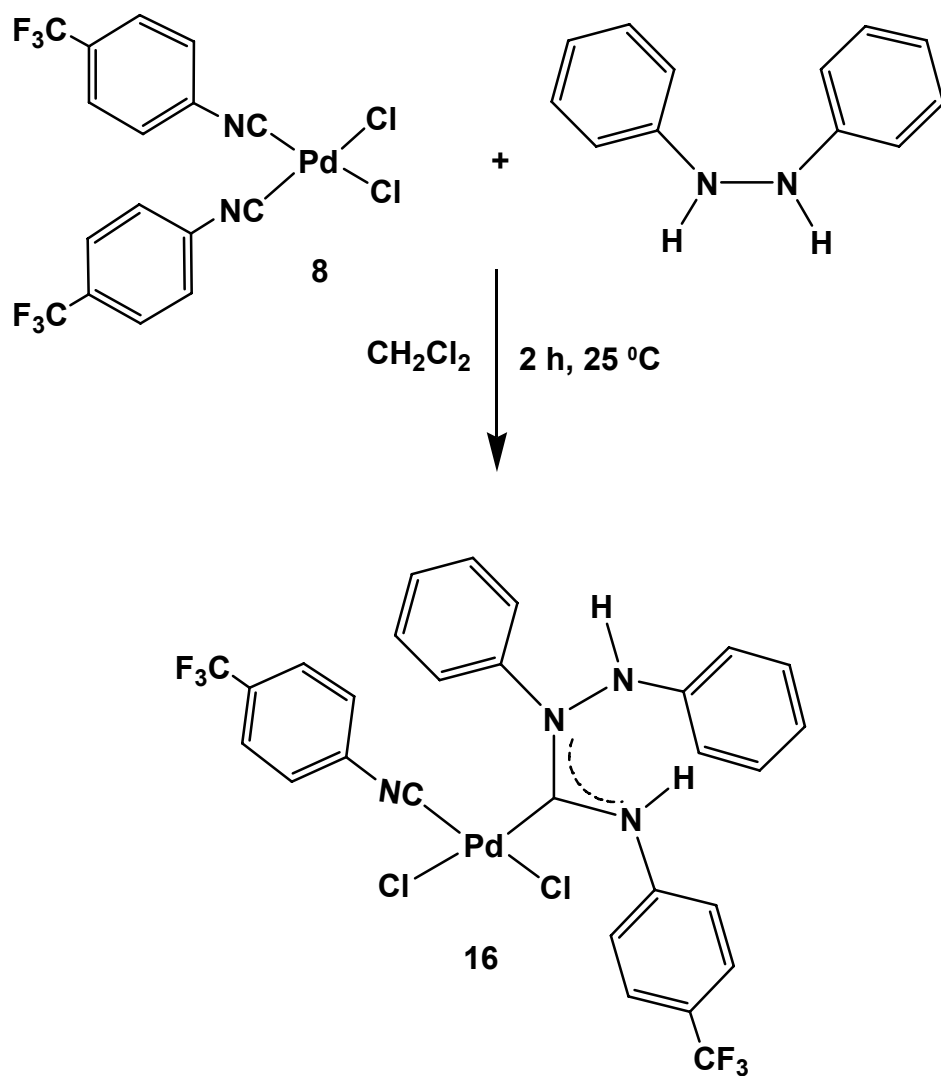
The current chapter focuses on the synthesis of a tetrasubstituted Chugaev-type bis(acyclic diaminocarbene) palladium complex via nucleophilic attack of hydrazobenzene on a palladium bis(arylisocyanide) complex. The highly strained hydrazobenzene derived bis(acyclic diaminocarbene) complex displayed a reversible chelate ring opening to give an equilibrium with the intermediate monocarbene isocyanide palladium complex in solution. This equilibrium provided an opportunity to study thermodynamic parameters governing bis(acyclic diaminocarbene) chelate ring formation. The monocarbene and bis(carbene) complexes were stable enough to be isolated and fully characterized by NMR and IR spectroscopies and X-ray crystallography.

Results and Discussion

Synthesis of Hydrazobenzene-derived Bis(carbene) and Monocarbene

Palladium Complexes

Bis(*p*-trifluoromethylphenyl isocyanide) palladium dichloride **8** was used in this study as a precursor in the stepwise formation of a tetra-substituted Chugaev-type carbene complex. Our goal was to examine carbene-forming reactions of 1,2-disubstituted hydrazines, which were not capable of forming stable Chugaev-type bis(ADC) complexes when treated with palladium alkylisocyanide complexes, with the relatively more electrophilic palladium arylisocyanide precursor **8**. Bis(*p*-trifluoromethylphenyl isocyanide) palladium dichloride was dissolved in distilled methylene chloride in a sealable, thick walled glass vessel, and one molar equivalent of hydrazobenzene (1,2-diphenylhydrazine) was added under nitrogen atmosphere (Scheme 4.4). The reaction mixture was stirred for two hours at room temperature. During this time a white precipitate started forming from the reaction. After two hours, the white precipitate was isolated by filtering through a fine frit open to air. This white precipitate was analyzed by ¹H NMR and IR spectroscopies and X-ray crystallography and was identified as a hydrazobenzene-derived monocarbene palladium complex **16** which has an unreacted *p*-trifluoromethylphenyl isocyanide ligand (Figure 4.1).



Scheme 4.4. Formation of the hydrazobenzene-derived monocarbene palladium dichloride complex **16**.

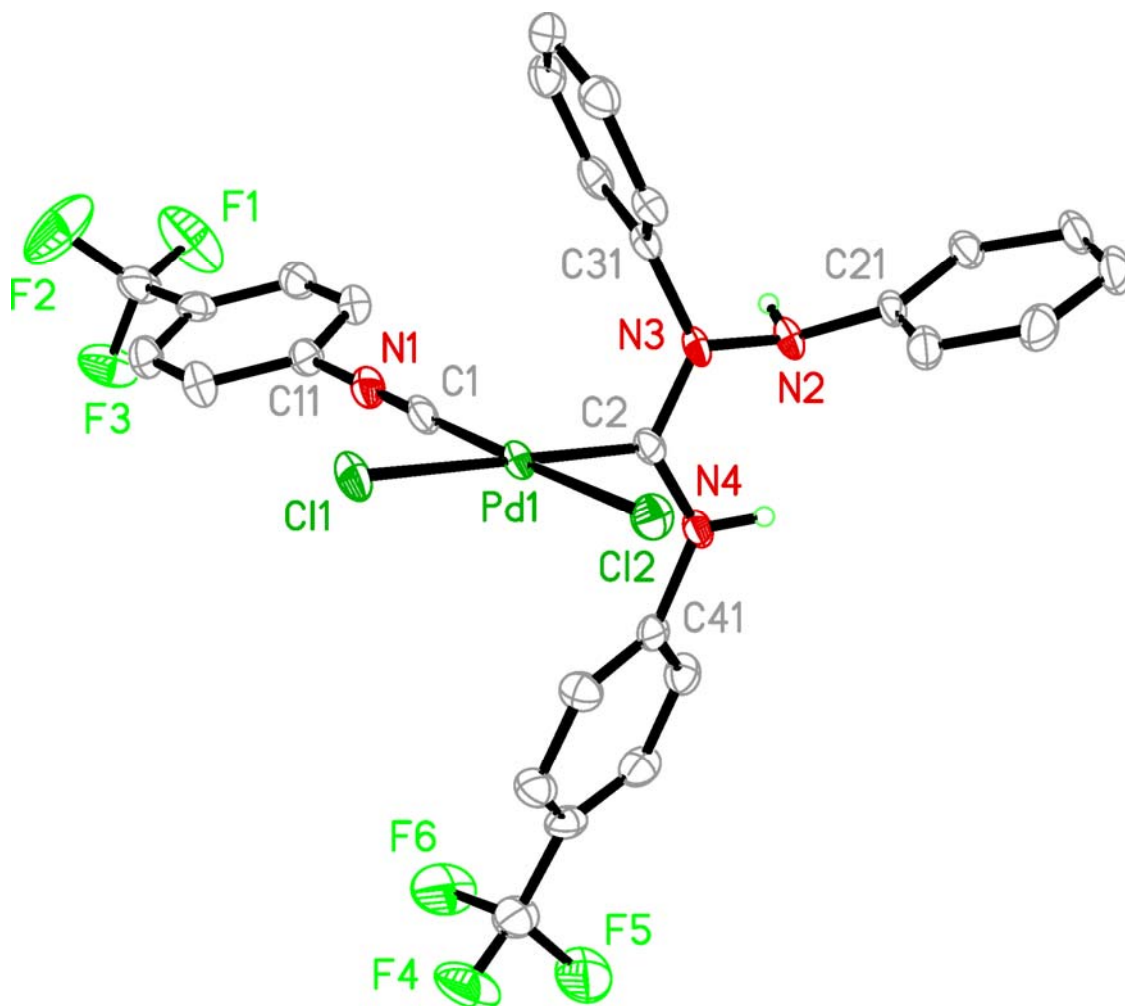


Figure 4.1. Molecular structure of complex **16** with 50% probability ellipsoids. Non-NH hydrogens are omitted for clarity.

The unreacted isocyanide group in complex **16** displayed a single IR stretching band at 2210 cm^{-1} . The ^1H NMR displayed two different NH signals at 11.46 ppm and 9.26 ppm and a set of aryl resonances displaying two different phenyl resonances and two different *p*-trifluoromethylphenyl groups. Two different fluorine signals were observed in the ^{19}F NMR at -61.1 and -62 ppm, indicating the presence of two different CF_3 groups in the molecule. The ^{13}C NMR signal at 184

ppm was characteristic of a coordinated carbene carbon.¹⁰ The X-ray crystallographic structure obtained for complex **16** confirmed the presence of a monodentate aminohydrazino carbene ligand and an unreacted *p*-trifluoromethylphenyl isocyanide group in the molecule (Figure 4.1). The Pd(1)-C(2) bond length is 1.973(3) Å, which is in the reported range for Pd-C_{carbene} distances^{11,12}. In addition, the bond lengths for C(2)-N(3) and C(2)-N(4) of 1.334(4) Å and 1.332(4) Å are very close to the values previously reported for Chugaev-type bis(ADC) complexes by our research group (Table 4.1).¹⁰ The C(1)-N(1) distance of 1.151(4) Å is near to the value expected for a free isocyanide C≡N, 1.14 Å,¹³ which further provides evidence of little or no weakening of the C≡N bond due to π -backbonding interactions.

Table 4.1. Selected bond lengths (Å) and bond angles (°) of complex **16**.

	Bond Lengths (Å)
Pd(1)-C(1)	1.926(3)
Pd(1)-C(2)	1.973(3)
Pd(1)-Cl(1)	2.3385(7)
Pd(1)-Cl(2)	2.3295(8)
N(1)-C(1)	1.151(4)
N(3)-C(2)	1.334(4)
N(4)-C(2)	1.332(4)
N(2)-N(3)	1.414(3)

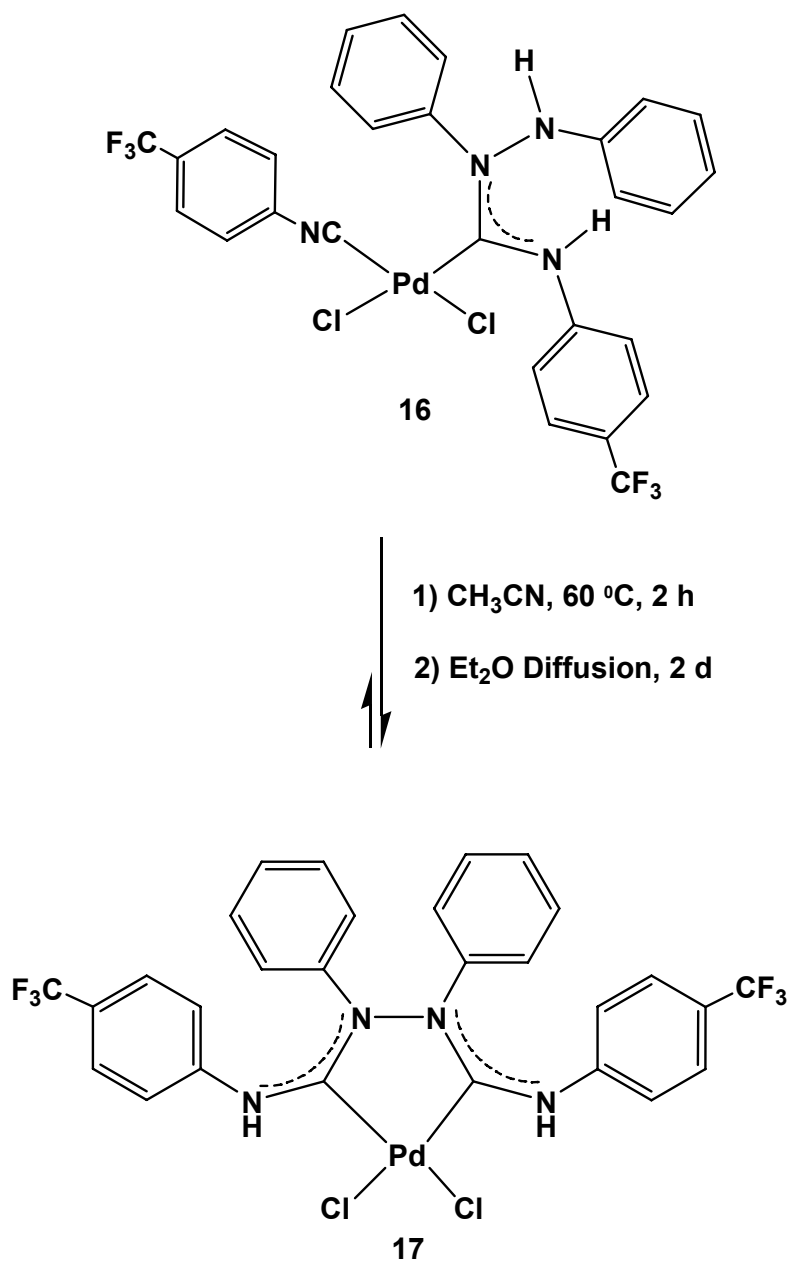
	Bond angles (°)
Pd(1)-C(1)-N(1)	178.6(3)
C(1)-N(1)-C(11)	178.2(3)
N(3)-C(2)-N(4)	116.1(2)
C(2)-N(3)-N(2)	119.2(2)
C(1)-Pd(1)-C(2)	90.41(12)
C(1)-Pd(1)-Cl(1)	90.44(9)
C(2)-Pd(1)-Cl(2)	86.68(8)
Cl(1)-Pd(1)-Cl(2)	92.46(3)

Table 4.2. Crystal data and structure refinement details for complex **16**.

Empirical formula	C ₂₈ H ₂₀ Cl ₂ N ₄ F ₆ Pd
Formula weight	703.78
Crystal system	Monoclinic
Space group	P21/c
Unit cell dimensions	$a = 10.4570(8) \text{ \AA}$ $\alpha = 90^\circ$ $b = 22.908(2) \text{ \AA}$ $\beta = 93.873(5)^\circ$ $c = 12.7945(11) \text{ \AA}$ $\gamma = 90^\circ$
Volume, z	3057.9(4) Å ³ , 4
Density (calculated)	1.529 Mg/m ³
Absorption coefficient	0.842 mm ⁻¹
Crystal size	0.21 x 0.14 x 0.02 mm ³
θ range for data collection	1.83 to 28.28°
Index ranges	$-13 \leq h \leq 13$, $-29 \leq k \leq 30$, $-16 \leq l \leq 17$
Temperature	100(2) K
Wavelength	0.71073 Å
Reflections collected	33056
Independent reflections	7575 ($R_{\text{int}} = 0.0690$)
Final R indices [$I > 2\sigma(I)$]	$R1 = 0.0432$ $wR2 = 0.0854$
R indices (all data)	$R1 = 0.0722$ $wR2 = 0.0926$
Goodness-of-fit on F^2	0.981

Complex **16** was synthesized on > 200 mg scale using this method with out significant modifications. This product is soluble in dimethyl sulfoxide, partially soluble in acetonitrile and relatively insoluble in tetrahydrofuran and methylene chloride. Samples of complex **16** dissolved in acetonitrile for crystal growing produced a molecular structure in the X-ray analysis which was different from the structure expected for the intermediary complex **16**. According to the X-ray analysis, the new compound was identified as the hydrazobenzene-derived bis(ADC) palladium dichloride complex **17** (Figure 4.2). This transformation of complex **16** to **17** in hot acetonitrile showed that Chugaev-type bis(ADC) formation was possible given sufficient activation energy. Further studies sought to maximize the yield of **17** obtained from **16**. When complex **16** was heated at 60°C for five hours, a ~60% conversion to complex **17** was observed by ¹H NMR. Heating of complex **16** at higher temperatures than 60°C for a long period of time resulted in slow decomposition of the complex with formation of Pd black. It was also noted that X-ray crystal samples of complex **16** which were set for slow diffusion of diethyl ether into an acetonitrile solution displayed relatively higher conversion to the bis(ADC) complex **17** possibly due to the change in solvent polarity. Thus, the synthesis procedure for complex **17** was devised considering both of the above observations. The improved method involved heating complex **16** at 60 °C for two hours in distilled acetonitrile under nitrogen in a thick walled sealed glass vessel to initiate the conversion. Then the reaction mixture was sent to the glove box, and distilled diethyl ether was diffused into the acetonitrile solution for two days in a glass vial to gradually decrease the polarity in the medium and thereby favor the formation of the

bis(ADC) complex **17** (Scheme 4.5). Solvent was removed under reduced pressure using a rotatory evaporator, and the residue was triturated three times with distilled methylene chloride to remove traces of acetonitrile from the reaction mixture. The crude product was redissolved in methylene chloride and filtered to remove unconverted complex **16**. The product was recrystallized and isolated as a white precipitate by layering hexanes onto a concentrated methylene chloride solution. Complex **17** displayed a higher solubility in solvents such as methylene chloride and THF than complex **16**.



Scheme 4.5. Synthesis of the bis(carbene) complex **17** from the intermediary monocarbene complex **16**.

The ^1H NMR and ^{13}C NMR spectra of complex **17** was indicative of a twofold symmetric molecule. ^1H NMR displayed only one resonance for the NH groups in the molecule. In, addition, the ^1H NMR and ^{13}C NMR displayed signals for only one type of phenyl and *p*-trifluoromethylphenyl groups in the molecule. The X-ray crystal structure of complex **17** confirmed the hydrazobenzene derived Chugaev-type bis(ADC) ligand (Figure 4.2). The five membered chelate ring which contained four aryl groups were arranged in a *syn* configuration where all the aryl groups were pointing to one side of the molecule. The aryl groups are rotated away from a perpendicular disposition compared to the bis(ADC) plane with torsion angles of 13-31° and the molecule displays a near- C_2 symmetry in the solid state. The average N- $\text{C}_{\text{carbene}}$ bond length of 1.337 Å indicates the presence of a delocalized double bond system in the bis(ADC) ligand. The geometry around the palladium center is distorted square planar, with the sum of bond angles around the palladium center equal to 360° (Table 4.3).

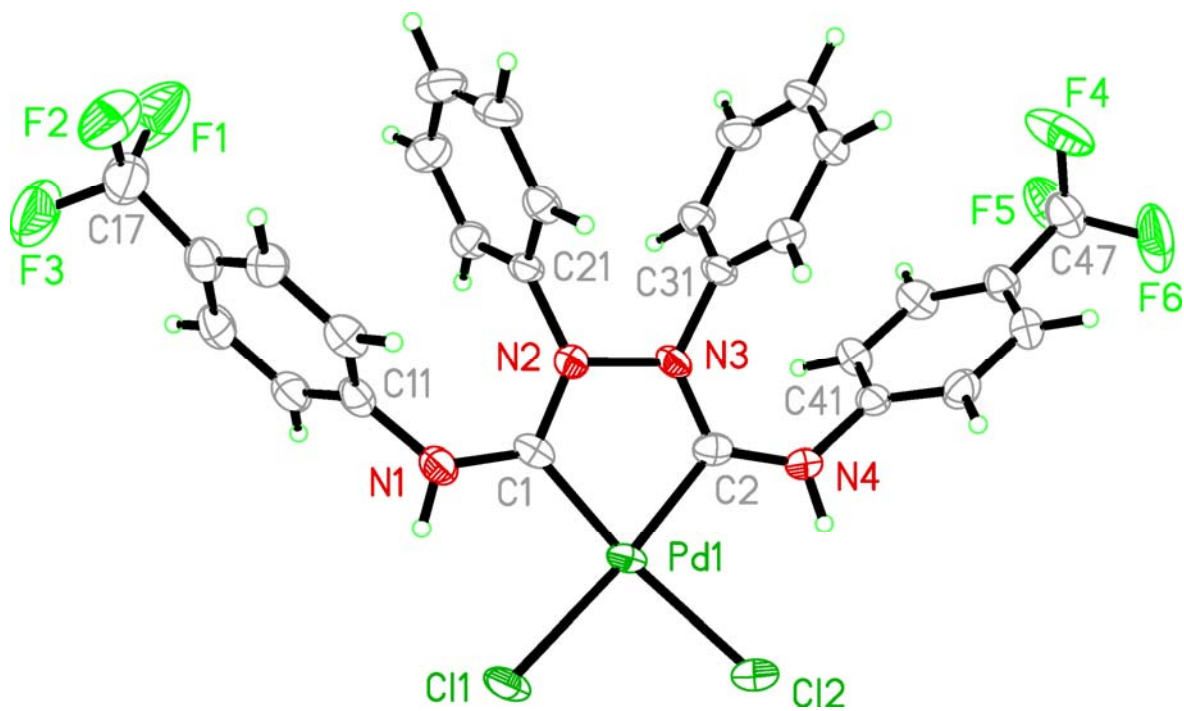


Figure 4.2. The molecular structure of complex (17) with 50% probability of ellipsoids. Non-NH hydrogens are omitted for clarity.

Table 4.3. Selected bond lengths (Å) and bond angles (°) of complex **17**.

	Bond Lengths (Å)
Pd(1)-C(1)	1.953(4)
Pd(1)-C(2)	1.962(4)
Pd(1)-Cl(1)	2.3654(9)
Pd(1)-Cl(2)	2.3669(11)
N(1)-C(1)	1.344(5)
N(2)-C(1)	1.340(5)
N(3)-C(2)	1.331(5)
N(4)-C(2)	1.334(5)
N(2)-N(3)	1.451(4)

	Bond angles (°)
N(3)-C(2)-N(4)	123.2(3)
N(2)-C(1)-N(1)	121.8(4)
C(1)-Pd(1)-C(2)	80.66(16)
C(1)-Pd(1)-Cl(1)	93.87(11)
C(2)-Pd(1)-Cl(2)	92.89(13)
Cl(1)-Pd(1)-Cl(2)	92.65(4)

Table 4.4. Crystal data and structure refinement details for complex **17**.

Empirical formula	C ₂₈ H ₂₀ Cl ₂ N ₄ F ₆ Pd
Formula weight	703.78
Crystal system	Triclinic
Space group	P-1
Unit cell dimensions	$a = 9.0014(5) \text{ \AA}$ $\alpha = 110.666(3)^\circ$ $b = 11.4002(6) \text{ \AA}$ $\beta = 93.013(3)^\circ$ $c = 14.6460(7) \text{ \AA}$ $\gamma = 100.034(3)^\circ$
Volume, z	1374.07(12) \AA^3 , 2
Density (calculated)	1.701 Mg/m ³
Absorption coefficient	0.937 mm ⁻¹
Crystal size	0.11x0.06x0.06 mm ³
θ range for data collection	1.95 to 26.37°
Index ranges	$-11 \leq h \leq 10$, $-11 \leq k \leq 14$, $-18 \leq l \leq 18$
Temperature	170(2) K
Wavelength	0.71073 \AA
Reflections collected	10778
Independent reflections	5572 ($R_{\text{int}} = 0.0630$)
Final R indices [$I > 2\sigma(I)$]	$R_1 = 0.0477$ $wR_2 = 0.1077$
R indices (all data)	$R_1 = 0.0630$ $wR_2 = 0.1175$
Goodness-of-fit on F^2	1.034

Equilibrium Between Bis(ADC) complex 17 and Mono(ADC) complex 16

The ^1H NMR in CD_3CN of purified samples of complex **17** showed small quantities of complex **16** which increased in concentration with time. However, when the same samples were checked for purity by ^1H NMR in CD_2Cl_2 , the only product observed was complex **17** with no indication of complex **16**. This observation suggested that the bis(ADC) complex **17** is in equilibrium with the monocarbene intermediate **16** in certain solvents. This equilibrium was attained rapidly in more polar solvents such as acetonitrile and was attained slowly in THF and methylene chloride. NMR tubes containing bis(ADC) complex **17** in CD_3CN and $\text{THF-}d_8$ were monitored over several days using ^{19}F NMR spectroscopy to measure the equilibrium with the monocarbene complex **16**. The monocarbene complex **16** showed two different fluorine signals in the ^{19}F NMR due to two different CF_3 groups in the molecule. In contrast, the more symmetric bis(ADC) complex **17** displayed one fluorine signal for the two CF_3 groups present in the molecule. The integration ratio between these different fluorine peaks in the ^{19}F NMR spectra was measured to calculate the equilibrium constant at that particular temperature (Figure 4.3). The equilibrium constant at $25\text{ }^\circ\text{C}$ was calculated to be 2.56(15) in CD_3CN and 10.0(5) in $\text{THF-}d_8$. These values suggest that the monocarbene intermediate **16** is slightly favored in more polar solvents. In addition, the equilibrium was reached faster in CD_3CN than in $\text{THF-}d_8$, the latter solvent needing more than five days to reach to the equilibrium. This may be due to the formation of a zwitterionic (Figure 4.4) which is stabilized by the polar solvent in the interconversion of complex **16** to **17**.

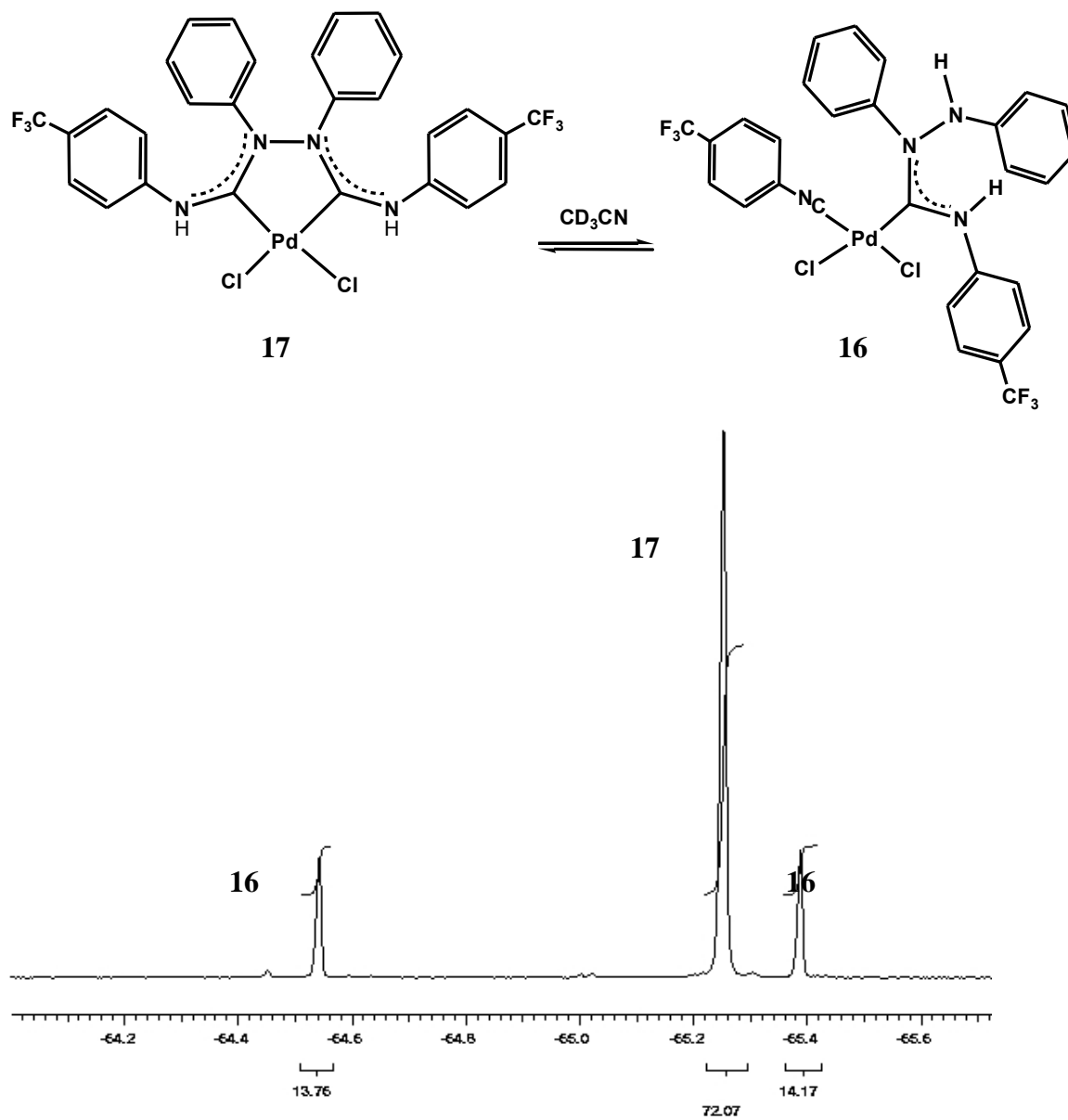


Figure 4.3. ^{19}F NMR spectrum showing the equilibrium between complexes **16** and **17** at 25 °C in CD_3CN .

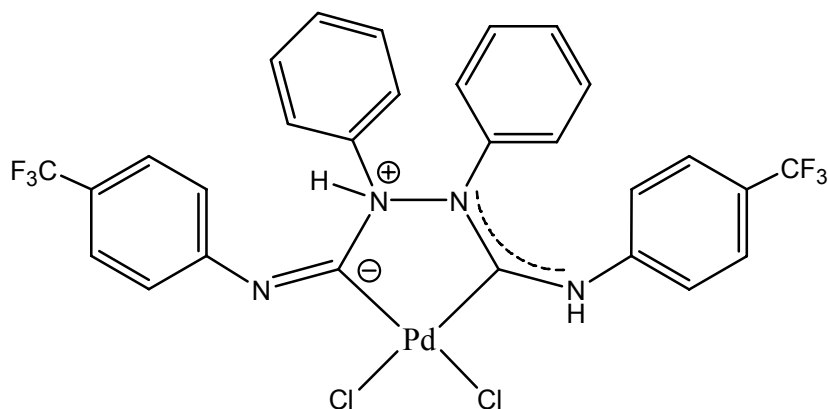


Figure 4.4. The possible zwitterionic intermediate in the interconversion of complex **16** and **17**.

In order to obtain thermodynamic information, changes in the equilibrium constant were studied over the temperature range of 25 °C to 55°C starting with complex **17** in CD₃CN (Table 4.5). Measured equilibrium constants (K_{eq}) decreased with increasing temperature as shown by the van't Hoff plot (Figure 4.5). The slope obtained from the van't Hoff plot was used to calculate the ΔH° of $-1.7(3)$ kcal mol⁻¹, and the intercept was used to calculate the ΔS° of $-3.7(9)$ eu for the conversion of monocarbene intermediate **16** to bis(ADC) complex **17**. The ΔH° for this conversion was calculated theoretically using DFT calculations (B3LYP(SBK(d) method) to obtain a ΔH° of -4 kcal mol⁻¹. This value was very close to the ΔH° obtained experimentally given the inherent error of ± 5 kcal mol⁻¹ for DFT methods. The experimental value obtained for ΔH° and ΔS° were used to calculate ΔG° which was $-0.6(4)$ kcal mol⁻¹ at 25°C for the equilibrium using the equation $\Delta G^\circ = \Delta H^\circ - T \Delta S^\circ$. The negative value of $-0.6(4)$ kcal mol⁻¹ obtained for ΔG° suggest that the small favorable enthalpic driving force (ΔH°) of $-1.7(3)$ kcal mol⁻¹ gained by ring-closing

attack of the free hydrazino group on the unreacted isocyanide group in complex **16** is sufficient to mitigate the unfavorable entropy effect (ΔS°) of - 3.7(9) eu which results from chelate formation.

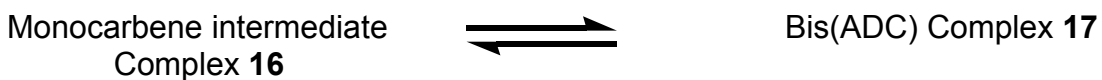


Table 4.5. Data for the van't Hoff Plot.

T (K)	Integration Ratio		K_{eq}	1/T	ln K_{eq}
	Complex 16	Complex 17			
298	28.44	71.36	2.509	0.0034	0.9199
308	29.96	69.63	2.324	0.0032	0.8433
318	31.58	67.88	2.150	0.0031	0.7652
328	33.72	65.21	1.934	0.0030	0.6595

Van't Hoff Analysis between complexes 16 and 17.

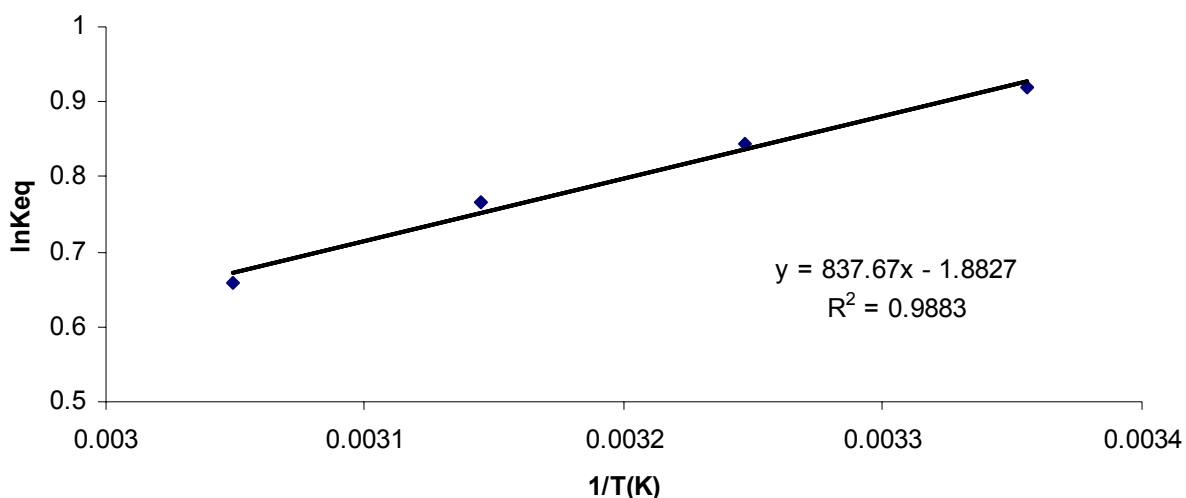


Figure 4.5. Van't Hoff plot for the equilibrium between monocarbene complex **16** and bis(ADC) complex **17**.

The instability of dicarbene complex **17** towards chelate ring opening may be due to the high steric strain imposed by the aryl groups on the ligand backbone. According to the X-ray structure of complex **17**, the distances between *ipso* carbons of the aryl groups are 2.941(5) Å for C(11)-C(21), 2.736(5) Å for C(21)-C(31) and 2.952(6) Å for C(31)-C(41). These values are lower than the C-C van der Waals contact of 3.4 Å, which indicates a significant amount of steric crowding between the aryl rings on the backbone. The NC_{carbene}N angles were expanded to 121.8(4)° and 123.2(3)° compared to the typical value for Chugaev-type carbenes of <120°. ¹⁰ Also, the aminohydrazino carbene ligand of intermediate complex **16** is rotated out of the palladium coordination plane to minimize the repulsion between the aryl groups, and it displays a NC_{carbene}N angle of 116.1(4)° which is typical for unstrained ADC ligands. ¹⁴

Complex **17** is unusual because it has a highly sterically crowded bis(ADC) ligand that shows a *syn, syn* arrangement of substituents, with the functional aryl groups pointing towards the same side as the phenyl groups on the hydrazobenzene derived backbone. The only other reported tetrasubstituted Chugaev carbene ligands were prepared by Villacampa and coworkers in 1984 ¹⁵ using *cis*-[Au(C₆F₆)₂(CNR)₂]ClO₄ as a precursor where R = Ph or *p*-tolyl, in reactions with NHPPhNHPPh. However, these gold(III) bis(ADC) complexes were not analyzed by X-ray crystallography to determine their molecular structure. These complexes probably adopt the less crowded *amphi* configuration ¹⁶ by analogy to trisubstituted Chugaev carbene complex derived from the reaction between phenyl hydrazine and *cis*-[Au(C₆F₆)₂(CN*p*-Tol)₂]ClO₄, in which the *p*-tolyl group on the isocyanide is

pointing out towards to the Au(III) coordination sphere in an *amphi* geometry.¹⁵ Similar bis(carbene) metal complexes prepared by nucleophilic addition of *N,N'*-dilithiohydrazobenzene to carbonyl groups of Cr(CO)₆ and W(CO)₆ followed by alkylation with [Et₃O][BF₄] displayed an *amphi, amphi* configuration on both carbene units.¹⁷ In complex **17** the *amphi* configuration is probably thermodynamically unstable since the outer aryl groups on the bis(carbene) ligand and the chloride ligands on the palladium coordination sphere may interact with each other in a sterically unfavorable manner. A similar *syn* configuration was observed in a trisubstituted palladium(II) Chugaev carbene complex which was derived from nucleophilic attack of methyl hydrazine on palladium bound methyl isocyanide ligands.¹⁰ The most important feature observed in the formation of bis(ADC) complex **17** is the thermodynamic favorability of the planar Chugaev-type chelate formation in spite of the steric strain caused by close proximity of aryl groups on the bis(ADC) backbone.

Summary and Conclusions

The first example of stepwise formation of an isocyanide-derived tetrasubstituted Chugaev-type bis(ADC) complex **17** through a monocarbene-isocyanide intermediate **16** has been described here. During this study, both complex **16** and complex **17** have been isolated and the molecular structures of both complexes have been determined using X-ray crystallography. This study provides the first example of a directly observed equilibrium between an isocyanide-derived bis(carbene) complex and its monocarbene-isocyanide intermediate. According to the molecular structure of bis(ADC) complex **17**, a significant amount of steric strain is imposed by the eclipsed arrangement of aryl rings on the ligand backbone. This may be the main reason for the instability observed in bis(carbene) complex **17** towards chelate ring opening to form the monocarbene intermediate complex **16** in some solvents such as acetonitrile and THF. The van't Hoff analysis of the temperature dependence of the equilibrium between bis(carbene) complex **17** and its monocarbene intermediate **16** revealed that the chelate ring closing that occurs in the formation of bis(carbene) complex **17** is enthalpically favorable with a ΔH° of $-1.7(3) \text{ kcal mol}^{-1}$, overriding the unfavorable entropic factor of $\Delta S^\circ = -3.7(9) \text{ eu}$. This net negative enthalpy change results in an overall ΔG° of $-0.6(4) \text{ kcal mol}^{-1}$ for the chelate ring closing reaction in the bis(carbene) formation. This suggests that nucleophilic addition of amines to palladium bound isocyanides is an efficient method to generate structurally diverse palladium bis(diaminocarbene) complexes given that a significant amount of steric strain in the ligand backbone can be tolerated.

Experimental

General Considerations

All manipulations were performed under vacuum or nitrogen in dry solvents unless otherwise noted. Anhydrous acetonitrile was purchased in septum-sealed bottles from Acros and used as received. Dichloromethane (Pharmco), diethyl ether (Acros), and hexanes (Pharmco) were dried according to the methods described previously in Chapter 2. NMR solvents were purchased from Cambridge Isotope Laboratories. CD_3CN and $\text{DMSO-}d_6$ were dried by stirring over activated 4Å molecular sieves followed by distillation under vacuum and were stored in an air-free glove box under nitrogen. CD_2Cl_2 was dried similarly and then stored over and distilled from P_2O_5 before use. THF- d_8 was dried and stored over sodium using benzophenone ketyl as an indicator and distilled on the vacuum line before use. Hydrazobenzene (Aldrich) was recrystallized from hot ethanol under argon using a swivel frit and stored in the glove box under nitrogen to prevent oxidation to azobenzene. Preparation of complex **8** was discussed in the previous Chapter 3. NMR spectra were recorded on Varian GEMINI 2000 (300 MHz) and Unity INOVA (400 MHz and 600 MHz) spectrometers. Reported chemical shifts are referenced to residual solvent peaks (^{13}C , ^1H) or to calibrated external standards (^{19}F). IR spectra were acquired from KBr pellets on a Nicolet Protégé 460 FT-IR spectrometer. Elemental analyses were performed by Desert Analytics, Tucson, Arizona. J Young NMR tubes were used for equilibrium measurements, and they were flame-dried under vacuum before use.

Synthesis of Hydrazobenzene-derived Monocarbene Palladium Complex 16

Complex **8** (0.200 g, 0.385 mmol) was dissolved in ~20mL of distilled methylene chloride in a sealable, thick walled vessel, and hydrazobenzene was added (0.078 g, 0.423 mmol) under N₂ in the glove box. The reaction mixture was stirred for 2 hours at room temperature. The product **16** formed as a white precipitate, which was separated by filtration using a fine frit and then washed with 5 mL of distilled methylene chloride. The product was dried under vacuum overnight. (0.218 g, 81%) ¹H NMR (300 MHz, DMSO-*d*₆): δ 11.46 (1H, s, NH), 9.26 (1H, s, NH), 8.04-8.00 (4H, m, Ar), 7.87 (4H, t, *J*=8.7, 8.4 Hz, Ar), 7.76 (2H, d, *J*=8.1 Hz, Ar), 7.51-7.39 (3H, m, Ar), 7.24 (2H, t, *J*=8.1, 7.8 Hz, Ar), 6.95 (2H, d, *J*=7.8 Hz, Ar), 6.87 (1H, t, *J*=6.9, 7.5 Hz, Ar). ¹³C NMR (75 MHz, DMSO-*d*₆): δ 184.01 (carbene), 144.16 (Ar *ortho*), 143.82 (Ar *ipso*), 143.36 (Ar *ipso*), 131.27 (Ar *ipso*), 131.10 (Ar *ipso*), 129.12 (Ar *ortho*), 128.65 (Ar *para*), 127.76 (Ar *ortho*), 127.36 (q, ³*J*_{CF}=3.6 Hz, Ar *meta*), 126.80 (Ar *meta*), 126.14 (Ar *ortho*), 125.88 (Ar *meta*), 121.22 (Ar *para*), 114.54 (Ar *meta*). Anal. Calcd for C₂₈H₂₀N₄F₆Cl₂Pd: C, 47.78, H, 2.86, N, 7.96. Found: C, 47.56, H, 2.73, N, 7.98. IR (KBr): ν_{max}/cm⁻¹ 3205 (NH), 3059 (NH), 2210 (CN). ¹⁹F NMR (282 MHz, DMSO-*d*₆): δ -61.7, -62.6.

Synthesis of Hydrazobenzene-derived bis(carbene)Palladium Complex 17

Complex **16** (0.200 g, 0.284 mmol) was dissolved in 5 mL of distilled acetonitrile in a sealable vessel under N₂ and stirred at 60 °C for 2 hours until the solution became clear. The reaction mixture was then sent into the glove box, and

anhydrous diethyl ether was diffused into the solution for 2 days. The product precipitated as crystals. After 2 days, the solvent was evaporated using a rotovap under reduced pressure, and the residue was triturated with 5 mL of distilled methylene chloride three times. The product was redissolved in ~5 mL of distilled methylene chloride and filtered through a fine frit to remove any unconverted starting complex **16** which was suspended in the methylene chloride solution. The frit was washed with an additional ~3 mL of methylene chloride. The clear, colorless filtrate was concentrated using the rotovap, and distilled hexanes was added to precipitate the product as a pale yellow powder. The product was dried under vacuum overnight. (0.1329 g, 67%) ^1H NMR (300MHz, CD_2Cl_2): δ 10.51 (2H, s, NH), 7.14 (4H, d, $J=8.4$ Hz, Ar), 7.04 (4H, d, $J=8.7$ Hz, Ar), 6.95-6.92 (2H, m, Ar), 6.83-6.76 (8H, m, Ar). ^{13}C NMR (150 MHz, CD_2Cl_2): δ 183 (carbene), 140.82 (Ar *ipso*), 136.87 (Ar *ipso*, 131.18 (Ar *ortho*), 130.63 (Ar *para*), 129.34 (q, $^2J_{\text{CF}}=32.8$ Hz, Ar *para*), 127.21 (Ar *meta*), 125.82 (q, $^3J_{\text{CF}}=3.76$ Hz, Ar *meta*), 123.8 (q, $^1J_{\text{CF}}=272.07$ Hz, CF_3). Anal. Calcd for $\text{C}_{28}\text{H}_{20}\text{N}_4\text{F}_6\text{Cl}_2\text{Pd}$: C, 47.78, H, 2.86, N, 7.96. Found: C, 48.11, H, 3.03, N, 7.84. ^{19}F NMR (282 MHz, CD_2Cl_2); δ -63.6.

Equilibrium Measurements

Palladium bis(carbene) complex **17** (1.6 mg, 2.3 μmol) was added to a flame-dried J Young NMR tube. The tube was evacuated and ~0.6 mL of CD_3CN or THF-d_8 was added by vacuum distillation through the vacuum line. The NMR tube was placed in a Fisher Isotemp 210 constant temperature water bath set at 25 $^\circ\text{C}$, and a Hg thermometer was placed in the water bath to calibrate the temperature. ^{19}F NMR

spectrum were acquired every 1-2 days until the equilibrium concentrations were reached as judged by constant integration ratios. After three days, the equilibrium constant at each temperature was calculated using integration ratios obtained for the respective CF₃ groups in complex **16** and complex **17** in the ¹⁹F NMR spectrum. In order to ensure accurate integrations of NMR signals, acquisition times (at) of 5 seconds and delay time (d1) of 3 seconds were used. The relaxation time for the CF₃ group in the ¹⁹F NMR was found to be in the range of 1.15 – 1.30 seconds by the inversion-recovery method. Uncertainties were reported at the 95% confidence level. These were determined from triplicate sample analysis at 3 days for CD₃CN. For the THF-d₈ equilibrium, uncertainties were determined from three spectra in a single sample starting at 15 days and taken at 2 day intervals.

Van't Hoff Analysis

Palladium bis(carbene) complex **17** (8 mg, 11 μmol) was placed in a vial under nitrogen, and ~0.6 mL of distilled CD₃CN was added. The solution was mixed thoroughly using a pipette to obtain a saturated solution. The solution was filtered through a frit to obtain a clear filtrate, which was transferred to a flame-dried J Young NMR tube. The tube was placed in the constant temperature water bath, and ¹⁹F NMR spectra was taken at 25°C, 35°C, 45°C and 55°C after sample incubation for 2 days at the respective temperature. The sample slowly degraded at 55°C, producing a yellow solution and a small amount of yellow precipitate. At 60°C, this decomposition was fast. Therefore further collection of NMR data was not possible at temperatures above 60°C. A similar temperature dependent equilibrium study

could not be performed starting with the intermediate complex **16**, as complex **16** degraded faster than complex **17** at elevated temperatures, accompanied by precipitation of a yellow solid. This may be due to the formation of a polymeric bis(carbene) palladium by product via intermolecular nucleophilic attack of the free amino group of the monocarbene palladium complex **16** on an unreacted *p*-trifluoromethylphenyl isocyanide ligand in another molecule of complex **16**. Uncertainties in thermodynamic quantities were derived from a least-squares regression analysis of the K_{eq} temperature dependence and were reported at the 95% confidence level.

X-ray Crystal Structure Determinations

Crystals of complex **16** and **17** were obtained by slow evaporation of concentrated acetonitrile solutions of the respective compounds. Crystals were immersed in Paratone N oil in a Nylon loop and placed in the cold stream of a Bruker SMART APEX II diffractometer at the appropriate temperature (100-170K). In the case of complex **16**, approximately half of the crystals screened were determined to be complex **17** by indexing. X-ray diffraction data were collected using graphite-monochromated Mo K α radiation ($\lambda=0.71073$ Å) via a series of φ and ω scans, with 0.5° scan widths and 30 seconds exposure times. Data integration employed the SAINT software package, and multi-scan absorption corrections were applied with SADABS.¹⁸ Structures were solved by direct methods and refined by full-matrix least-squares on F^2 using the SHELXTL software suite.¹⁹

References

1. Badley, E. M.; Chatt, J.; Richards, R. L.; Sim, G. A. *Journal of the Chemical Society D-Chemical Communications* **1969**, 1322.
2. Crociani, B.; Uguagliati, P.; Belluco, U. *J. Organomet. Chem.* **1976**, 117, 189.
3. Johnson, B. V.; Shade, J. E. *J. Organomet. Chem.* **1979**, 179, 357.
4. Steinmetz, A. L.; Johnson, B. V. *Organometallics* **1983**, 2, 705.
5. Wanniarachchi, Y. A.; Slaughter, L. M. *Chem. Commun.* **2007**, 3294.
6. Moncada, A. I.; Khan, M. A.; Slaughter, L. M. *Tetrahedron Lett.* **2005**, 46, 1399.
7. Burke, A.; Balch, A. L.; Enemark, J. H. *J. Am. Chem. Soc.* **1970**, 92, 2555.
8. Moncada, A. I.; Tanski, J. M.; Slaughter, L. G. M. *J. Organomet. Chem.* **2005**, 690, 6251.
9. Sawai, T.; Angelici, R. J. *J. Organomet. Chem.* **1974**, 80, 91-102.
10. Moncada, A. I.; Manne, S.; Tanski, J. M.; Slaughter, L. M. *Organometallics* **2006**, 25, 491.

11. Herrmann, W. A.; Elison, M.; Fischer, J.; Köcher, C.; Artus, G. R. J. *Angew. Chem. Int. Ed.* **1995**, *34*, 2371.
12. Ahrens, S.; Zeller, A.; Taige, M.; Strassner, T. *Organometallics* **2006**, *25*, 5409.
13. Smith, M. B.; March, J. *MARCH'S Advanced Organic Chemistry: Reactions, Mechanisms, and Structure*; John Wiley & Sons: New York, 2001.
14. Denk, K.; Sirsch, P.; Herrmann, W. A. *J. Organomet. Chem.* **2002**, *649*, 219.
15. Uson, R.; Laguna, A.; Villacampa, M. D.; Jones, P. G.; Sheldrick, G. M. *Journal of the Chemical Society-Dalton Transactions* **1984**, 2035.
16. Miller, J.; Balch, A. L.; Enemark, J. H. *J. Am. Chem. Soc.* **1971**, *93*, 4613.
17. Huy, N. H. T.; Pascard, C.; Dau, E. T. H.; Döötz, K. H. *Organometallics* **1988**, *7*, 590.
18. *APEX2 software suite (SAINT, SADABS)*, Version 2.0; Bruker AXS: Madison, WI, USA, 2006.
19. Sheldrick, G. M. *SHELXTL*, Version 6.14; Bruker AXS: Madison, WI, USA, 2000.

CHAPTER V

Catalytic Aza-Claisen Rearrangement with Chiral Palladium Bis(Acyclic Diaminocarbene) Complexes

“Portions were reproduced with permission from [Wanniarachchi, Y. A.; Slaughter, L. M. *Organometallics*, **2008**, 27, 1055-1062.] Copyright [2008] American Chemical Society.”

Introduction

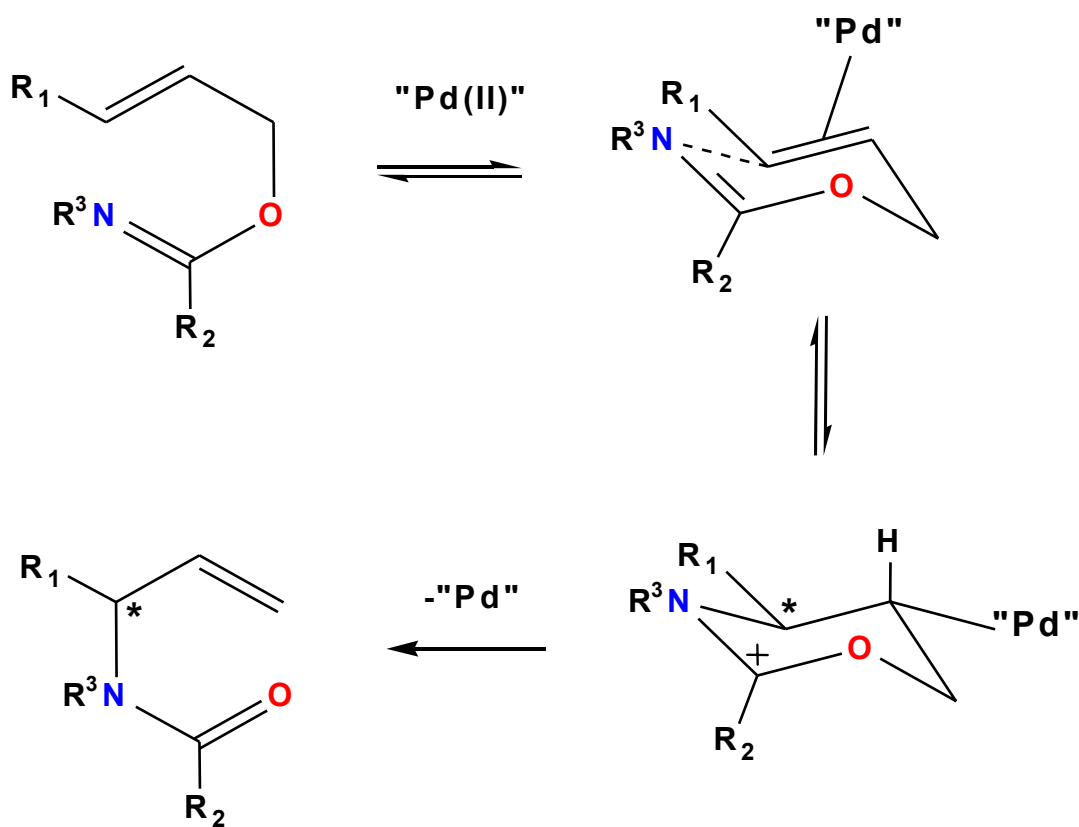
N-heterocyclic carbene (NHC) complexes have recently become some of the most widely used transition metal complexes in homogeneous catalysis. Favorable attributes such as high stability, easy synthetic access to NHC complexes, and strong σ -donation promote their diverse applications in catalysis.¹ The σ -donor abilities of NHC ligands have been compared with those of phosphine ligands by Nolan and others using thermochemical studies,² IR probes such as CO ligands,³ and theoretical pK_a values.⁴ IR probe studies using CO has most widely used. However, this approach has the disadvantage that σ -donor and π -acceptor effects cannot be separated. As a new approach to measure the ligand σ -donor ability of carbene ligands, methyl isocyanide has been used as an IR probe ligand in this study. Isocyanide ligands and their complexes are known to be similar in their electronic structure to carbon monoxide ligands and CO containing complexes. Importantly, isocyanides are considered been better σ -donors and poor π -acceptors than CO ligands.⁵ These features make isocyanide ligands more appropriate for ligand donor ability measurements than CO ligands when only an assessment of σ -donor ability is desired.

Stretching frequencies of methyl isocyanide ligands bound to a metal complex increase compared to the free isocyanide due to electron donation from the HOMO,

which is a weakly C≡N anti bonding orbital. A high change in frequency compared to the free isocyanide ($\Delta\nu$) indicates lower *trans* influence or lower σ -donation from the ligand bound *trans* to the isocyanide. Higher σ -donation from the *trans* ligand results in a lower stretching frequency difference ($\Delta\nu$) in metal bound isocyanide ligands. Therefore isocyanide ligands can be used as a convenient tool to measure the σ -donor strength or *trans* influence of the ligands bound *trans* to the isocyanide ligand.⁵ This study shows that new bis(ADC) ligands are surprisingly weak donors that can support electrophilic palladium centers.

Metal catalyzed reactions are regulated by the amount of σ -donation from the ligands attached around the metal center among other factors. Strong σ -donating ligands increase the electron density around the metal center, promoting reactions in which the metal becomes oxidized or acts as a nucleophile. Conversely, weakly σ -donating ligands facilitate electrophilic reactions at the metal center. Electrophilic reactions of palladium and platinum complexes in which the metal centers act as Lewis acids represents a growing area of homogeneous catalysis.⁶ Among electrophilic palladium-catalyzed reactions, the aza-Claisen rearrangement is among the most promising due to its potential usefulness in synthesis. Benefits associated with the aza-Claisen rearrangement are generation of a new chiral center in the product and the ability to convert the product easily to pharmaceutically and industrially important products.⁷ The palladium-catalyzed aza-Claisen rearrangement has been primarily studied by Overman using palladium complexes containing various imine and amine ligands.^{8,9,10,11} During the reaction, an imidate substrate undergoes [3,3] sigmatropic rearrangement to produce an allylic amide which

contains a new chiral center. The mechanism involves coordination of the olefin to the palladium center followed by nucleophilic attack by the imidate nitrogen atom to produce a metal bound six-membered cyclic intermediate. This intermediary metal bound six-membered ring rearranges rapidly to the allylic amide product (Scheme 5.1).^{8,12}



Scheme 5.1. Mechanism of palladium (II) catalyzed aza-Claisen rearrangement of allylic imidates.

This rearrangement demands a delicate balance of metal electrophilicity and steric crowding. Moderately electrophilic palladium centers efficiently catalyze the

reaction by binding the olefin to the metal and promoting nucleophilic attack of the imidate nitrogen at the olefin, rather than imidate binding to the palladium center. Direct binding of the imidate nitrogen to the palladium center may result in catalyst inactivation accompanied by formation of with various by-products. In addition, strict steric requirements must be met for high enantiomeric excess in the product. As an attempt to find efficient catalysts for enantioselective aza-Claisen rearrangements, the investigation of palladium (II) bis(ADC) complexes which contain electron withdrawing groups such as $-\text{CF}_3$ have been explored in this chapter.

Results and Discussion

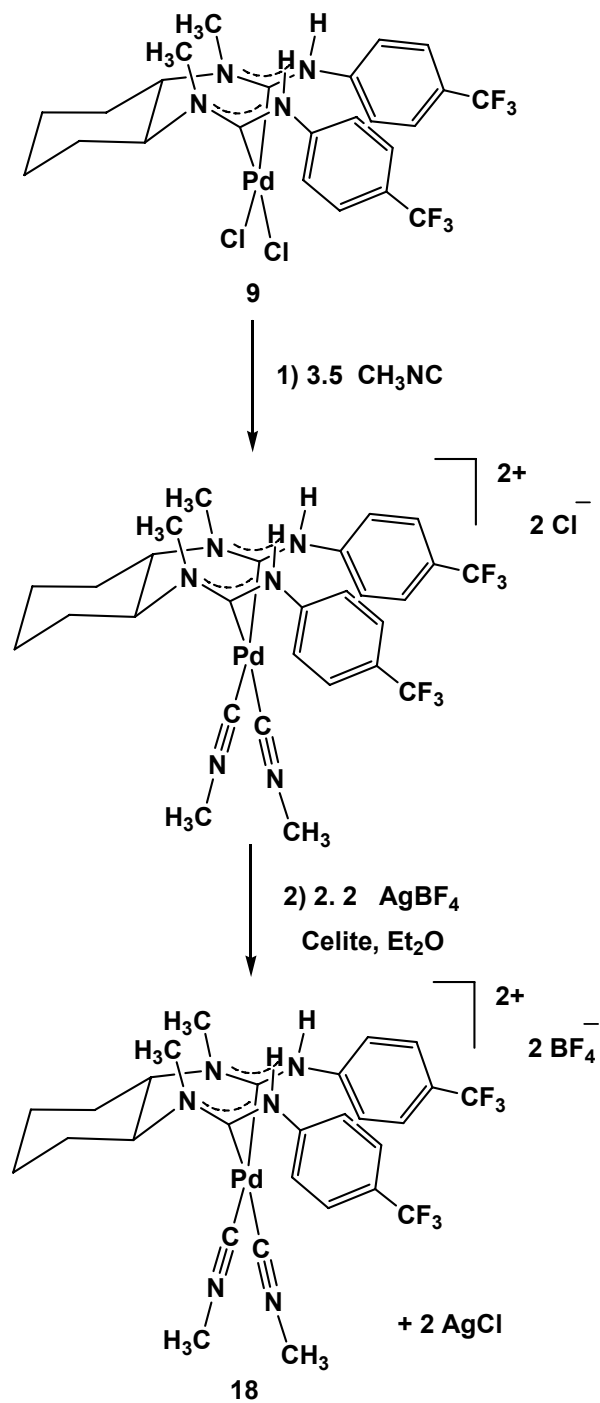
5.1 σ -donor abilities of bis(ADC) ligands

The σ -donor strengths of bis(ADC) ligands were evaluated using methyl isocyanide as an IR probe ligand in bis(ADC)Pd(CNCH₃)₂²⁺ derivatives. The weak π -backbonding and strong σ -donation of isocyanide ligands⁵ makes them useful probes for measuring σ -donor ability of ligands which are bound *trans* to isocyanides. As a result of weak π -backbonding, the changes in IR stretching frequencies ($\Delta\nu$) of methyl isocyanide ligands can be assumed to be almost entirely due to changes in the ligand σ -donor properties. Comparison of σ -donor ability of the new bis(ADC) ligands with other common bidentate ligands such as bis(N-heterocyclic carbene) (NHC) ligands and bis(phosphine) ligand was performed by synthesizing the respective methyl isocyanide palladium derivatives. 1,1'-dimesityl-3,3'-methylenediimidazol-2,2'-diylidene was selected as a typical bis(NHC) ligand,

while 1,2-bis(diphenylphosphino)ethane was selected as a typical bis(phosphine) ligand for the comparison.

Palladium bis(ADC) methyl isocyanide complex derived from (rac) N,N'-dimethyl-1,2-diaminocyclohexane (18)

The σ -donor ability of a new bis(acyclic diaminocarbene) ligand was initially evaluated using the palladium bis(ADC) methyl isocyanide complex **18**. The synthesis of complex **18** starts by treating dichloride complex **9** with excess methyl isocyanide in acetonitrile to replace the chloride ligands with methyl isocyanide ligands (Scheme 5.2). Chloride anions in the bis(ADC)Pd(CNCH₃)₂²⁺ adduct were then replaced with tetrafluoroborate anions by treatment with AgBF₄ in acetonitrile. The replacement of chloride anions from the outer coordination sphere of the molecule is fast; therefore, the reaction needed stirring for only 2 hours at room temperature. To replace coordinated halides from the palladium center, heat is usually needed.¹³ The reaction mixture was filtered through celite to remove the precipitated AgCl from the reaction mixture. Finally, the product was isolated by layering distilled diethyl ether onto the concentrated acetonitrile solution of complex **18**.



Scheme 5.2. Formation of bis(ADC) $\text{Pd}(\text{CNCH}_3)_2^{2+}$ derivative from complex **9**.

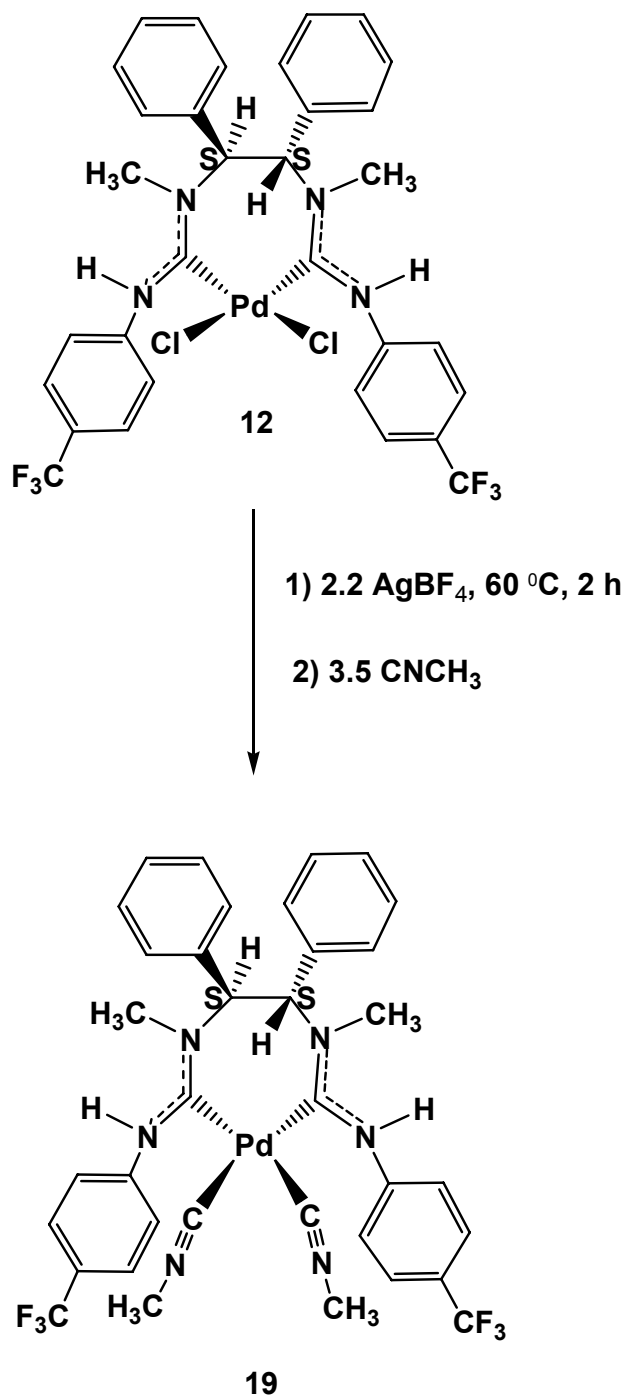
The ^1H NMR spectrum of complex **18** displayed two different NH and NCH_3 signals at 8.73 ppm, 8.43 ppm, 3.11 ppm, and 3.10 ppm respectively, indicating C_1

symmetry in the molecule similar to its starting complex **9**. In addition, four doublets at 7.86 ppm, 7.59 ppm, 7.27 ppm and 6.93 ppm were observed for aryl *ortho* and *meta* protons in complex **18**. The ^{13}C NMR spectrum of complex **18** displayed two different carbene carbon signals at 187.1 ppm, and 181.8 ppm providing more evidence for the C_1 symmetry in the molecule. Quartets at 130.0 ppm, 129.2 ppm, 128.1 ppm, and 127.0 ppm indicated aryl *para* and *meta* carbons respectively, and the C-F coupling constants of 32.8 Hz and 3.8 Hz were consistent with the expected values for two-bond and three-bond coupling with fluorine.¹⁴ Carbons in CF_3 groups appeared at 125.1 ppm and 125.0 ppm with their characteristic coupling constants¹⁴ of 272 Hz and 270 Hz. The ^{19}F NMR spectrum of complex **18** indicated two different fluorine signals at - 59.66 ppm and - 59.89 ppm further confirming the C_1 symmetry in the molecule. Methyl isocyanide stretching bands appeared in the IR spectrum as a singlet at 2271 cm^{-1} with a broad shoulder.

Palladium bis(ADC) methyl isocyanide complex derived from (1*S*,2*S*)-(-)-*N,N'*-dimethyl-1,2-diphenyl-1,2-ethanediamine (19**)**

The synthesis procedure was slightly different from the procedure used for palladium bis(ADC) methyl isocyanide complex **18**. This modification was necessary to generate recrystallizable product when using the (1*S*,2*S*)-(-)-*N,N'*-dimethyl-1,2-diphenyl-1,2-ethanediamine backbone. The modified procedure involved treating one molar equiv of palladium bis(carbene) complex **12** derived from (1*S*,2*S*)-(-)-*N,N'*-dimethyl-1,2-diphenyl-1,2-ethanediamine with 2.2 molar equiv of AgBF_4 prior to

addition of isocyanide (Scheme 5.3). The reaction mixture was heated at 60 °C for two hours in acetonitrile to replace the chloride ligands bound to the metal center with acetonitrile ligands. The reaction mixture was then filtered through celite to remove the precipitated AgCl, and the filtrate was mixed with excess methyl isocyanide to substitute the metal bound acetonitrile ligands with methyl isocyanide groups. The product was recrystallized by layering diethyl ether onto the reaction mixture and keeping it in ice to facilitate crystal formation. The yield obtained was 38% (47 mg).

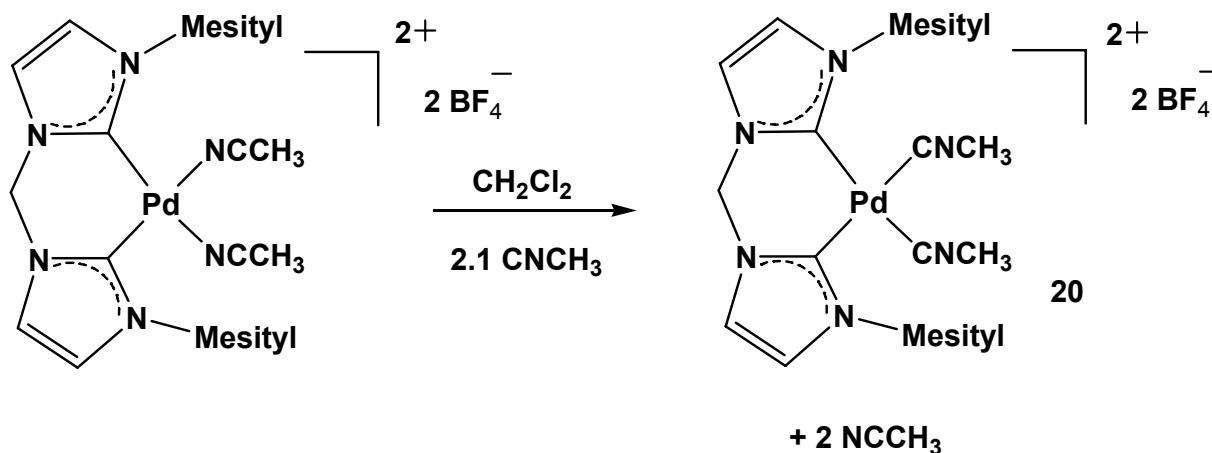


Scheme 5.3. Formation of bis(ADC)Pd(CNCH₃)₂²⁺ complex **19** derived from (1*S*,2*S*)-(-)-*N,N'*-dimethyl-1,2-diphenyl-1,2-ethanediamine.

The ^1H NMR spectrum of complex **19** displayed two broad peaks at 8.84 ppm and 8.66 ppm for the two different NH groups in the molecule. Three doublets were observed at 7.92 ppm, 7.69 ppm and 7.01 ppm due to *ortho* and *meta* protons in the N-aryl groups of the complex with coupling constants of 8.4 Hz, 8.1 Hz and 8.1 Hz, respectively. One of the CH_2 groups on the ethane backbone appeared at 5.63 ppm with a coupling constant of 12.0 Hz. Peaks at 3.59 ppm, 3.16 ppm, 3.23 ppm, and 3.00 ppm represented two different methyl isocyanide ligands and two different NCH_3 groups present in the molecule respectively, indicating C_1 symmetry. The IR spectrum displayed one signal at 2273 cm^{-1} as a single band with a shoulder, representing IR active symmetric and asymmetric stretching combinations of the isocyanide $\text{C}\equiv\text{N}$ bonds.

Palladium bis(NHC) methyl isocyanide complex (20)

Comparison of the σ -donor ability of the new bis(ADC) ligands with a typical bis(N-heterocyclic carbene) (NHC) ligand was performed by synthesizing a methyl isocyanide palladium complex containing 1,1'-Dimesityl-3,3'-methylenediimidazol-2,2'-diylidene.¹³ The synthesis of bis(NHC) palladium(CNCH_3)₂][BF_4]₂ **20** was accomplished by treating [(1,1'-dimesityl-3,3'-methylenediimidazol-2,2'-diylidene)palladium(II)-bis(acetonitrile)][BF_4]₂, synthesized according to Gardiner et al.,¹³ with 2.1 equiv of CH_3NC in methylene chloride.¹⁵ The product was isolated as a gray powder by adding hexanes to the reaction mixture (Scheme 5.4).



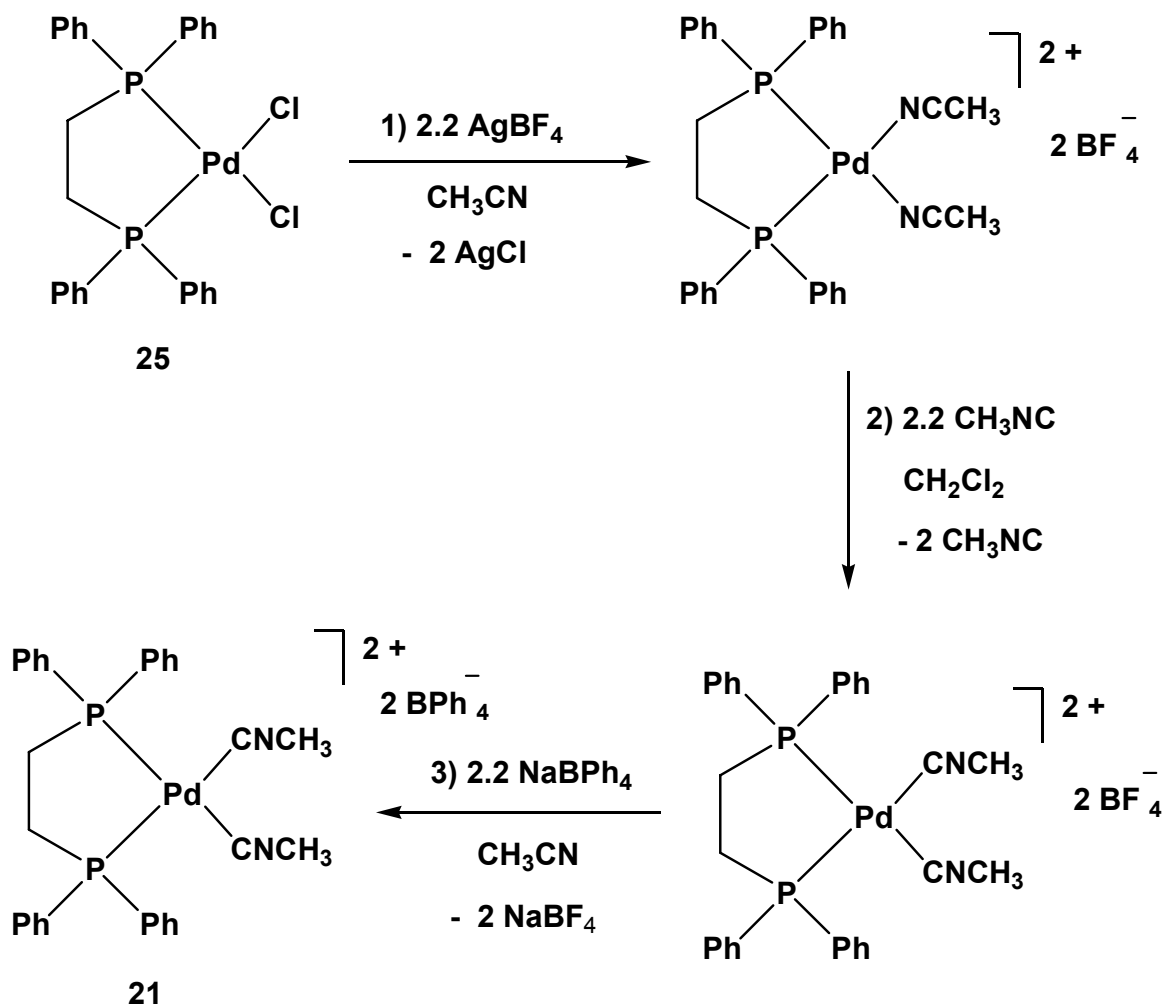
Scheme 5.4. Synthesis of $[\text{bis}(\text{NHC})\text{Pd}(\text{CNCH}_3)_2][\text{BF}_4]_2$ **20**.

The ^1H NMR spectrum of complex **20** displayed two doublets at 8.10 ppm and 7.77 ppm with a coupling constant of 1.8 Hz indicating the hydrogens on the imidazole ring. Four *meta* aryl hydrogens and methylene hydrogens were appeared at 7.18 ppm and 6.61 ppm as singlets. Methyl groups in the isocyanide ligands were visible at 3.21 ppm. The mesityl methyl groups were visible at 2.33 ppm and 1.95 ppm. The ^{13}C NMR spectrum displayed a peak at 155.8 ppm indicating the carbene carbons. Methyl isocyanide IR stretching frequency was at 2266 cm^{-1} .

Bis(diphenyl phosphino)ethane palladium methylisocyanide complex (21)

The σ -donor ability of the common bis(phosphine) ligand (1,2-bis(diphenylphosphino)ethane) was compared with the new bis(ADC) ligands and the bis(NHC) ligand by synthesizing $[1,2\text{-bis(diphenylphosphino)ethane Pd}(\text{CNCH}_3)_2][\text{BF}_4]_2$ **21**. The synthesis started by treating 1,2-bis(diphenylphosphino)ethanePdCl₂, or (DPPE)PdCl₂,¹⁶ with 2.2 equiv of AgBF₄ in

dry acetonitrile at 60 °C for one hour to substitute chloride ligands with acetonitrile (Scheme 5.5). The reaction was filtered through celite to remove the precipitated AgCl, and the filtrate was dried under vacuum for ~ 3 hours to remove acetonitrile from the reaction mixture. Traces of acetonitrile present in the solution tend to partially dissolve AgCl and may interfere with the binding of methyl isocyanide to palladium. To remove traces of AgCl present in the reaction, distilled methylene chloride was added to the reaction mixture, followed by filtration through celite to obtain a clear filtrate. The filtrate was treated with 2.2 equiv of methyl isocyanide and stirred at room temperature for 2 hours to complete the acetonitrile ligand exchange with methyl isocyanide (Scheme 5.5). After stirring, the methylene chloride was evaporated under reduced pressure (rotatory evaporator), and distilled acetonitrile was added as the solvent. NaBPh₄ (2.2 equiv) was introduced to the reaction mixture to replace the BF₄⁻ anions with BPh₄⁻ anions, since isolation of the product with BF₄⁻ anions proved difficult and generated an oily product instead of a crystalline solid. Distilled diethyl ether was added to the reaction mixture to precipitate NaBF₄ as a white crystalline solid, which was separated by filtration. The expected product [(DPPE)PdCl₂][BPh₄]₂ **21** was isolated as a pale yellow crystalline product by adding more diethyl ether to the filtrate.



Scheme 5.5. Synthesis of $[(\text{DPPE})\text{PdCl}_2][\text{BPh}_4]_2$ **21** from $(\text{DPPE})\text{PdCl}_2$.

The ^1H NMR spectrum contained four sets of multiplets in the region 7.76 ppm to 6.78 ppm, corresponding to all of the protons on the phenyl groups of complex **21** including the BPh_4^- anion. The singlet at 3.14 ppm corresponded to the CNCH_3 ligands in the molecule. The multiplet at 2.83 ppm corresponded to the ethylene ($-\text{CH}_2-\text{CH}_2-$) linkage in the ligand of **21**. In the ^{13}C NMR spectrum of complex **21** a doublet of doublets at 164.7 ppm was assigned to the isocyanide

carbons with P-C coupling constants of 98.4 Hz and 49.6 Hz. Aryl groups bound to phosphorus displayed three doublets corresponding to *meta*, *ipso* and *ortho* aryl carbons at 134.8 ppm, 134.2 ppm and 130.9 ppm with coupling constants of 3.1 Hz, 11.5 Hz and 12.3 Hz within the expected range for P-C coupling.¹⁴ The quartet at 126.6 ppm which displayed a 1:1:1:1 ratio of integration was assigned to the aryl *ipso* carbons in BPh₄⁻ anions due to apparent coupling with ¹¹B. Isocyanide CH₃ carbon signals were observed at 31.0 ppm, while -CH₂-CH₂- linkage carbons appeared as a doublet of doublets at 28.2 ppm due to P-C coupling with two phosphorous atoms in the molecule. The ³¹P NMR spectrum displayed one phosphorous signal at 69.5 ppm, indicating chemically equivalent phosphine groups in the molecule. A single IR band was detected at 2262 cm⁻¹ in the IR spectrum representing superposition of two expected isocyanide C≡N stretches.

X-ray quality crystals were developed by slow diffusion of diethyl ether into a concentrated solution of complex **21** in dichloromethane. The crystallizing solution was spiked with trace amounts of free methyl isocyanide, since complex **21** was not very stable in solution, as the methyl isocyanide ligands tend to slowly dissociate from the complex, leading to formation of (DPPE)₂Pd(BPh₄)₂ as a white crystalline solid. The X-ray crystal structure of **21** (Figure 5.1) confirms the presence of one DPPE ligand attached to the palladium center. This also confirms the *cis*-geometry of methyl isocyanide ligands attached to the palladium center. Bond lengths between Pd and phosphorus were 2.3024 Å and 2.2856 Å, close to the value reported for similar five-membered chelating palladium bis(phosphine) complexes.¹⁷ The P-Pd-P bite angle¹⁸ of 84.08 ° was similar to the reported value of 85.1°¹⁸ for a similar

bis(phosphine) complex. The Pd-C_{isocyanide} bond lengths were relatively similar (2.041 Å and 2.043 Å). Isocyanide C≡N bond lengths of 1.143 Å and 1.136 Å were within the expected range for a C≡N bond¹⁹ and confirm the presence of localized triple bonds in the molecule.

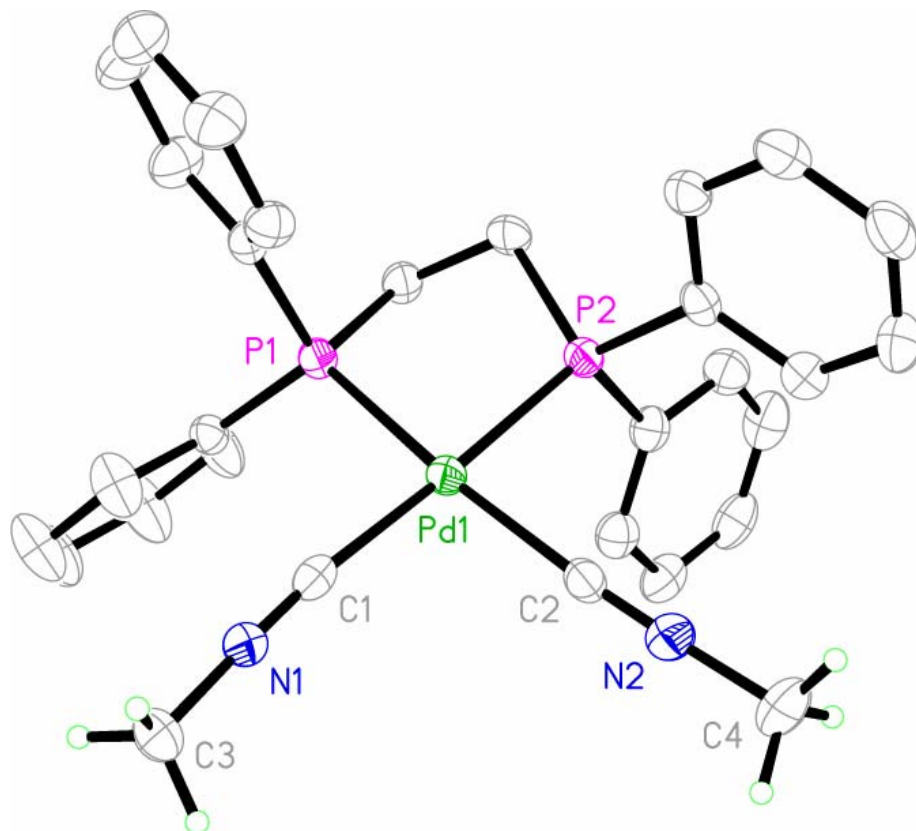


Figure 5.1. X-ray crystal structure of [(1,2-Bis(diphenylphosphino)ethane)Pd(CNCH₃)₂][BPh₄]₂ **21**.

Table 5.1. Selected bond lengths (Å) and bond angles (°) of complex **21**.

	Bond lengths (Å)
N(1)-C(1)	1.143(4)
N(2)-C(2)	1.136(4)
Pd(1)-C(1)	2.041(4)
Pd(1)-C(2)	2.043(4)
Pd(1)-P(1)	2.3024(9)
Pd(1)-P(2)	2.2856(9)

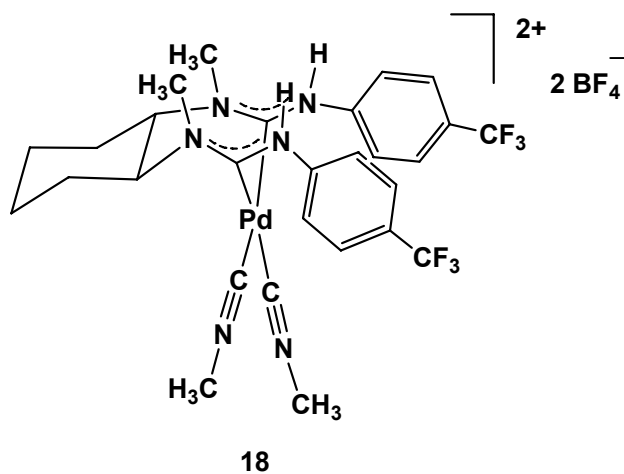
	Bond Angles (°)
Pd(1)-C(2)-N(2)	175.5(3)
Pd(1)-C(1)-N(1)	174.0(3)
C(2)-Pd(1)-C(1)	91.86(13)
C(1)-Pd(1)-P(1)	95.60(9)
C(2)-Pd(1)-P(2)	88.76(10)
P(2)-Pd(1)-P(1)	84.08(3)

Table 5.2. Crystal data and structure refinement details for complex **21** (includes two molecules of CH₂Cl₂).

Empirical formula	C ₈₀ H ₇₄ B ₂ Cl ₄ N ₂ P ₂ Pd
Formula weight	1395.17
Crystal system	Monoclinic
Space group	<i>P</i> 2 ₁ / <i>n</i>
Unit cell dimensions	<i>a</i> = 15.6015(14) Å α = 90 ° <i>b</i> = 21.5886(11) Å β = 107.574(5) ° <i>c</i> = 21.822(2) Å γ = 90 °
Volume, <i>z</i>	7007.0(11) Å ³ , 4
Density (calculated)	1.323 Mg/m ³
Absorption coefficient	0.509 mm ⁻¹
Crystal size	0.45x0.30x0.30 mm ³
θ range for data collection	1.66 to 25.00 °
Index ranges	-18 ≤ <i>h</i> ≤ 17 0 ≤ <i>k</i> ≤ 25 0 ≤ <i>l</i> ≤ 25
Temperature	115(2) K
Wavelength	0.71073 Å
Reflections collected	12263
Independent reflections	12263 (<i>R</i> _{int} = 0.0715)
Final <i>R</i> indices [<i>I</i> > 2σ(<i>I</i>)]	<i>R</i> 1 = 0.0474 <i>wR</i> 2 = 0.1200
<i>R</i> indices (all data)	<i>R</i> 1 = 0.0678 <i>wR</i> 2 = 0.1326

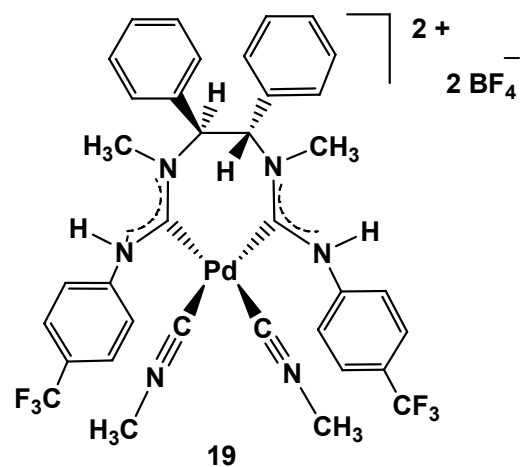
σ -Donor abilities of bis(ADC) ligands compared to bis(NHC) and bis(phosphine) ligands

Methyl isocyanide stretching frequencies (ν_{CN}) of complexes **18**, **19**, **20** and **21** are displayed in Figure 5.2. The differences in frequencies compared to the free methyl isocyanide stretching frequency (2160 cm^{-1}) are also displayed as $\Delta\nu$ values. Complexes **18** and **19** show the highest stretching frequencies at 2271 cm^{-1} and 2273 cm^{-1} as well as the highest $\Delta\nu$ values of 111 cm^{-1} and 113 cm^{-1} , (Figure 5.2) respectively. These high $\Delta\nu$ values indicate strong σ -donation from the methyl isocyanide σ^* orbital (HOMO) to empty metal d-orbitals with very weak or no π -backbonding from filled metal orbitals to empty anti-bonding orbitals of isocyanides.⁵ Therefore strong σ -donation of electrons from the isocyanide σ^* orbital makes the $\text{C}\equiv\text{N}$ bond stronger and cause a higher $\text{C}\equiv\text{N}$ stretching frequency observed in complexes **18** and **19** compared to complexes **20** and **21**. Strong σ -donation of methyl isocyanide groups in complex **18** and **19** is possible due to the weaker “*trans* influence” of the bis(ADC) ligands which are bound *trans* to the methyl isocyanide groups. Compared to the bis(ADC) ligand, the bis(NHC) ligand in complex **20** displayed stronger σ -donation to the palladium center. This is revealed by obtaining a lower $\Delta\nu$ value of 106 cm^{-1} for complex **20**. The bis(phosphine) ligand displayed higher σ -donation than both the bis(ADC) ligands and the bis(NHC) ligand judging by the lower $\Delta\nu$ value of 102 cm^{-1} (Figure 5.2).



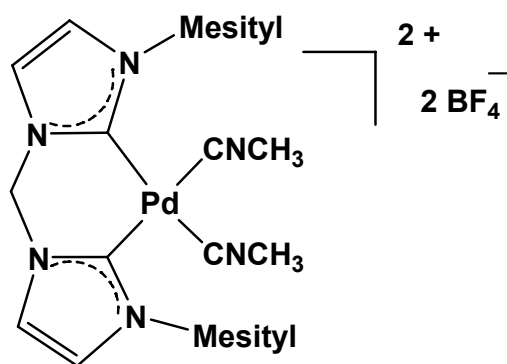
$$\nu(\text{CN}) = 2271 \text{ cm}^{-1}$$

$$\Delta\nu = 111 \text{ cm}^{-1}$$



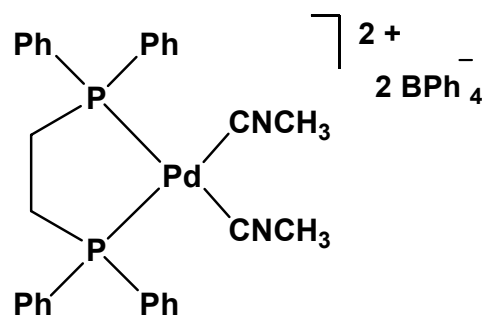
$$\nu(\text{CN}) = 2273 \text{ cm}^{-1}$$

$$\Delta\nu = 113 \text{ cm}^{-1}$$



$$\nu(\text{CN}) = 2266 \text{ cm}^{-1}$$

$$\Delta\nu = 106 \text{ cm}^{-1}$$



$$\nu(\text{CN}) = 2262 \text{ cm}^{-1}$$

$$\Delta\nu = 102 \text{ cm}^{-1}$$

Figure 5.2. Comparison of σ -donor ability of bis(ADC) ligands compared with bis(NHC) and bis(phosphine) ligands.

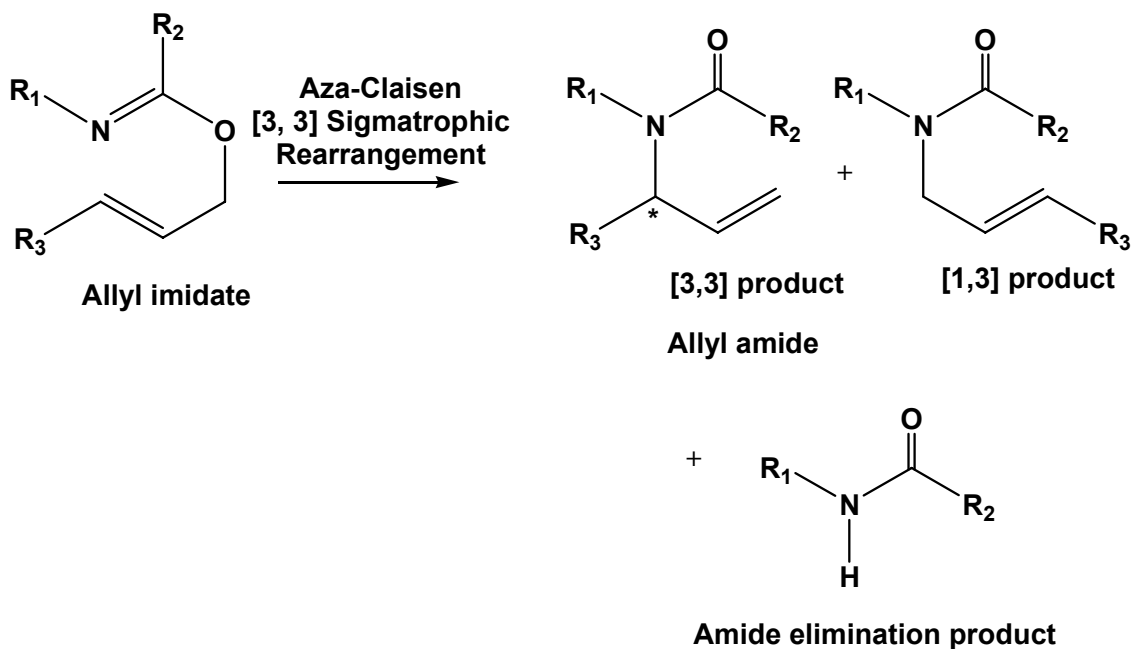
This observation of higher σ -donation from the bis(phosphine) ligand than bis(ADC) or bis(NHC) ligand contradicts with previous studies done on σ -donor

abilities of NHC ligands Vs phosphine ligands. According to calorimetric studies done by Nolan et al. NHC ligands are found to be strong σ -donors than phosphine ligands.² Therefore methyl isocyanide probes bound trans to the NHC ligand should show comparatively lower stretching frequency than phosphine ligands. However the intrinsic strong σ -donor ability of NHC ligands can be affected by other factors such as planarity of the molecule and the chelating ring size.

An important point to consider in this σ -donor ability comparison is their differences in chelating ring size. The complexes described here have different chelate ring sizes ranging from 7 membered for complex **18** and **19**, to 6 membered for complex **20**, to 5 membered for complex **21**. Chelating ring size plays an important role in governing σ -donation to the metal center. As the chelating ring size increases the bite angle increase to values larger than the optimal 90° ,^{18,17} causing poorer overlap of ligand donor orbitals with empty metal orbitals. This might continue to weaken σ -donation from the ligand to the metal. To avoid the changes in chelating ring size which affect the σ -donicity, ligands which have the same chelating ring size should be chosen for the comparison in future studies. However, only comparing the σ -donicity of ligands in complexes **18,19, 20** and **21** without considering their differences of variable chelating ring sizes, the bis(ADC) ligand shows the lowest σ -donation to palladium followed by bis(NHC) and bis(phosphine) ligands.

5.2 Aza-Claisen [3,3]-sigmatropic rearrangement

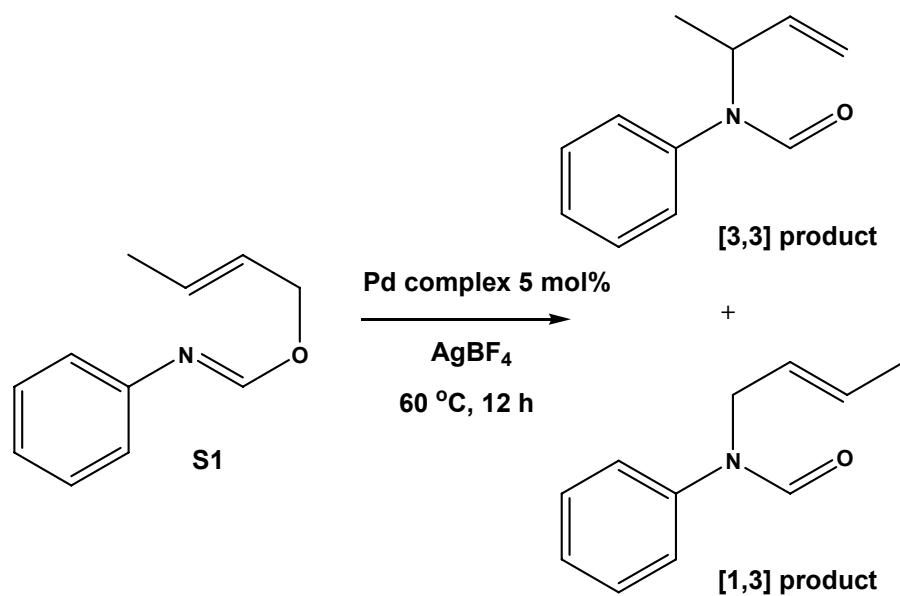
The relatively low σ -donor abilities of bis(ADC) ligands provide an opportunity to use palladium bis(ADC) complexes as pre-catalysts in reactions catalyzed by electrophilic metal centers. Among the chemical processes catalyzed by electrophilic metal centers, the aza-Claisen rearrangement of allylic imidates is considered synthetically important because it generates chiral allylic amides which can be converted to valuable chiral allylic amines (Scheme 5.6).²⁰ Enantioselective catalytic aza-Claisen rearrangements have been extensively studied by Overman and coworkers using palladium (II) complexes containing chiral diamine ligands⁸ and chiral palladacycles¹¹ and also by Jautze et al.²⁰ Possible by-products of this reaction include undesirable [1,3] product of the allyl imidate and an amide which is a decomposition product of the starting imidate (Scheme 5.6). Bis(ADC) ligand containing palladium(II) complexes have not been reported in catalytic aza-Claisen rearrangement. In the current study, palladium (II) bis(ADC) complexes were investigated as catalysts in the aza-Claisen rearrangement, with the goal of achieving improved substrate scope and/or enantioselectivity over existing catalysis.



Scheme 5.6. Aza-Claisen rearrangement of allyl imidate to allyl amide and possible by-products.

Preliminary aza-Claisen rearrangement of allyl *N*-phenylformimidates (**S1**, **S2**)

Preliminary catalytic studies were done using 3-methylallyl *N*-phenylformimidate or γ -methylallyl *N*-phenylformimidate as the first imidate substrate **S1** (Scheme 5.7). The synthesis of 3-methylallyl *N*-phenylformimidate was performed using a published procedure by Roberts and coworkers.²¹ The aza-Claisen rearrangement of 3-methylallyl *N*-phenylformimidate was examined with different pre-catalysts and AgBF_4 as the silver salt activator in different solvents. (Table 5.3).



Scheme 5.7. Catalytic aza-Claisen rearrangement of γ -methylallyl N-phenylformimidate **S1** to [3,3] product and [1,3] byproduct.

Table 5.3. Palladium catalyzed aza-Claisen rearrangement of γ -methylallyl N-phenylformimidate **S1**.

Entry	Precatalyst	AgBF ₄	Solvent	[3,3] product %*	[1,3] product %*
1	\pm 9	5 mol %	CD ₂ Cl ₂	9	21
2	\pm 9	11 mol%	CD ₂ Cl ₂	-	67
3	\pm 9	5 mol%	THF	15	6
4	\pm 18	-	CD ₂ Cl ₂	-	17
5	17	5 mol%	CD ₂ Cl ₂	11	36
6	17	5 mol%	C ₆ D ₆	8	22
7	17	5 mol%	THF	12	7

* Yields were recorded as % conversion from the starting substrate using the ¹H NMR spectrum of the crude reaction mixture.

\pm **9** Cyclohexane backbone bis(ADC)PdCl₂

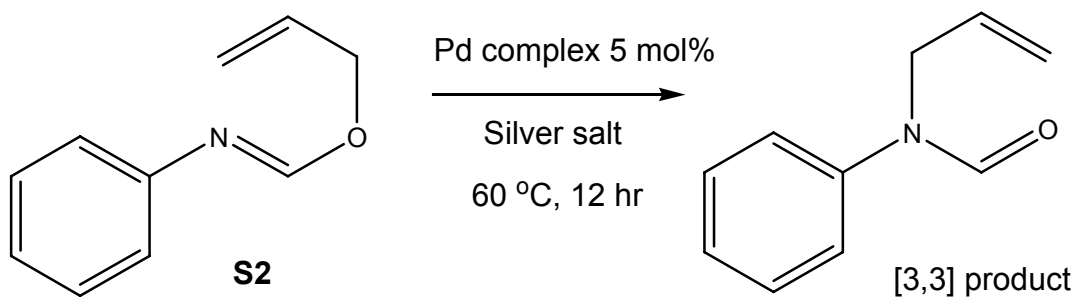
\pm **18** Cyclohexane backbone bis(ADC)Pd(CNCH₃)₂BAr^F₄

17 Hydrazobenzene back bone bis(ADC)PdCl₂

Catalytic reactions were done using AgBF₄ salt to generate the active catalyst in situ by removing the chloride ligands bound to the palladium center. Catalytic reactions were done in sealed J Young NMR tubes or in sealed glass ampoules set up under nitrogen. In both cases, the reaction mixtures were heated at 60 °C for 12 hours. NMR tube reactions were set up with dry CD₂Cl₂ or C₆D₆ as the solvent and analyzed by ¹H NMR spectroscopy to find the % conversion from the starting imidate. The reactions done in glass ampoules used dry THF as the solvent and

were analyzed by ^1H NMR by adding CDCl_3 to dissolve the products after evaporating THF under vacuum. Use of only one equiv of AgBF_4 gave the best result with catalyst **9** in CD_2Cl_2 leading to more of the desired [3,3] product as compared to reactions with 2 equiv of AgBF_4 (entry 1). This may be due to the increased positive charge on the palladium center when 2 equiv of AgBF_4 are used, which leads to more [1,3] product formation (entry 2) due to the higher electrophilicity of palladium. In moderately polar coordinating solvents such as THF, the reaction gave lower overall yields but more of the desired product compared to more polar, non-coordinating solvents such as CD_2Cl_2 (entry 3). Complex **18** displayed very poor catalyst activities towards aza-Claisen rearrangement compared to complex **9** (entry 4), likely because the affinity of methyl isocyanide groups for the metal were higher than the affinity of the substrate to the palladium center. Complex **17** displayed comparatively higher activity in a polar, non-coordinating solvent such as CD_2Cl_2 than in less polar solvents such as C_6D_6 and THF (entry 5,6 and 7), but byproduct formation was significant. Overall, aza-Claisen rearrangements using γ -methylallyl N-phenylformimidate **S1** as a substrate gave poor yields with bis(ADC) palladium complexes **9**, **18** and **17**.

Allyl N-phenylformimidate **S2** (Scheme 5.8) was used as another imidate substrate to explore the activity of complexes **9** and **17**. Allyl N-phenylformimidate **S2** when compared to γ -methylallyl N-phenylformimidate **S1** is less sterically crowded on the allyl side of the imidate, making it an easier substrate to bind to the palladium center. Catalytic reactions using allyl N-phenylformimidate **S2** are tabulated in Table 5.4.



Scheme 5.8. Product formation in catalytic aza-Claisen rearrangement of allyl N-phenylformimidate **S2**.

Table 5.4. Palladium catalyzed aza-Claisen rearrangement of allyl N-phenylformimidate **S2**.

Entry	Catalyst	Silver salt	Solvent	[3,3] product %*
1	\pm 9	AgBF ₄ 5 mol %	THF	11
2	\pm 9	AgSbF ₆ 5 mol%	THF	21
3	\pm 9	AgBAR ^F ₄ ** 4 mol%	THF	71
4	17	AgBF ₄ 5 mol %	THF	56

* Yields were recorded as % conversion from the starting substrate using the ¹H NMR of the crude reaction mixture.

** silver tetrakis[3,5-bis(trifluoromethyl)phenyl]borate (AgBAR^F₄)

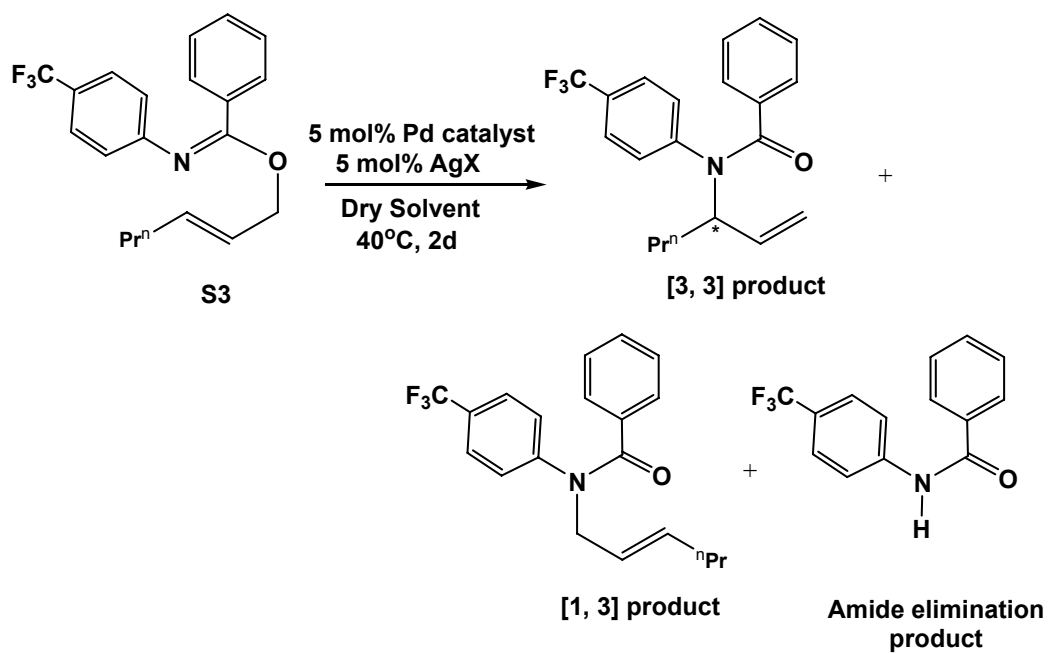
\pm **9** Cyclohexane backbone bis(ADC)PdCl₂

17 Hydrazobenzene back bone bis(ADC)PdCl₂

Reactions with allyl N-phenylformimidate **S2** displayed relatively higher yields of the expected [3,3] product than observed in reactions of γ -methylallyl N-phenylformimidate **S1**. The reaction of complex **9** with non-coordinating silver salt $\text{AgBAR}_4^{\text{F}}$ produced a substantially higher yield (entry 3) compared to silver salts of weakly coordinating anions such as AgBF_4 and AgSbF_6 in THF. The non-coordinating nature of the $\text{BAR}_4^{\text{F}-}$ anion may be the reason for obtaining higher yield than with BF_4^- or SbF_6^- counter ions.

Aza-Claisen rearrangement of (*E*)-2-hexenyl-*N*-[4-(trifluoromethyl)phenyl]benzimidate (S3**)**

Based on the preliminary aza-Claisen rearrangement studies described above, $\text{AgBAR}_4^{\text{F}}$ was selected as the best silver salt activator to be used with bis(ADC) palladium precatalysts. This catalyst-silver salt combination was used to catalyze rearrangements of other imidate substrates. Aza-Claisen rearrangement results obtained with (*E*)-2-hexenyl-*N*-[4-(trifluoromethyl)phenyl]benzimidate (Scheme 5.9) **S3** are tabulated in Table 5.5.



Scheme 5.9. Possible products in aza-Claisen rearrangement of (*E*)-2-Hexenyl *N*-[4-(trifluoromethyl) phenyl]benzimidate **S3**.

Table 5.5. Aza-Claisen rearrangement of (*E*)-2-Hexenyl *N*-[4-(trifluoromethyl) phenyl]benzimidate **S3** catalyzed by palladium complexes containing bis(ADC) and bis(NHC) ligands.

Entry	Catalyst	Silver salt	Solvent	Yield %		
				[3,3]	[1,3]	Amide
1	\pm 9	5 mol% AgBF ₄	CD ₂ Cl ₂	2	11	12
2	\pm 9	5 mol% AgOTf	CD ₂ Cl ₂	0	0	0
3	\pm 9	5 mol% AgBAR ^F ₄	CD ₂ Cl ₂	70(54) ^a	17	12
4	\pm 9	5 mol% AgBAR ^F ₄	THF	0	0	0
5	\pm 9	10 mol% AgBAR ^F ₄	CD ₂ Cl ₂	6	51	9
6	24	5 mol% AgBAR ^F ₄	CD ₂ Cl ₂	6	28	2
7	(R,R)-14	5 mol% AgBAR ^F ₄	CD ₂ Cl ₂	34	9	15
8	15	5 mol% AgBAR ^F ₄	CD ₂ Cl ₂	24	7	14

^a Isolated yield in parentheses was obtained by column chromatography.

\pm **9** Cyclohexane backbone bis(ADC)PdCl₂

24 (1,1'-dimesityl-3,3'-methylenediimidazol-2,2'-diylidene)palladium dibromide ¹³

14 (R,R) N, N'-bis(benzylmethyl)-1,3-diaminopropanebiscarbene palladium dichloride

15 N, N'-bis(1-naphthylethyl)-1,3-diaminopropanebiscarbene palladium dichloride

Reactions using (*E*)-2-hexenyl-*N*-[4-(trifluoromethyl) phenyl]benzimidate **S3** were done in sealable J Young NMR tubes which were setup under vacuum and

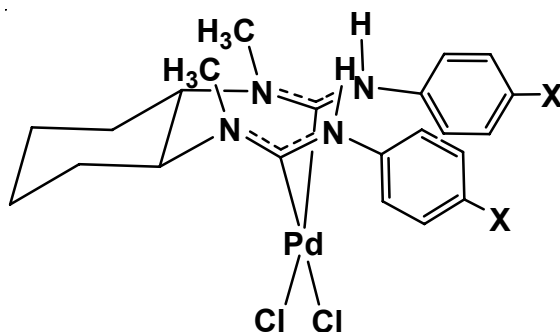
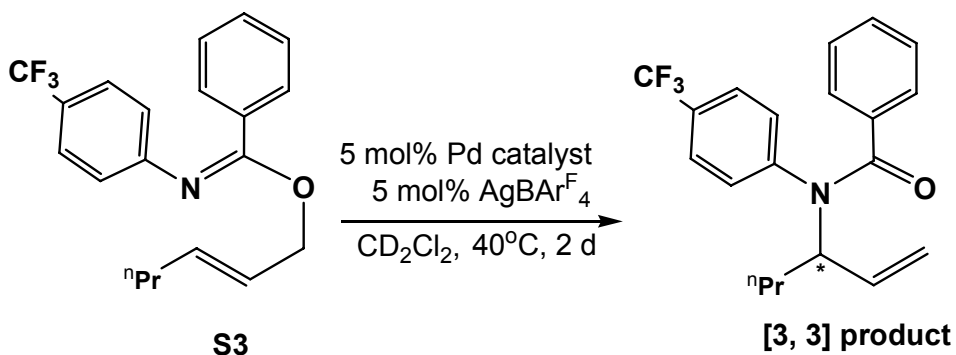
inert atmosphere. NMR tube reaction mixtures were heated at 40 °C for 2 days using a constant temperature water bath. Product yields were calculated by integration of product peaks in the ^{19}F NMR spectrum of the crude reaction mixture after adding a known volume (usually 30 μL) of *p*-fluoro nitrobenzene as an internal standard. For isolation of products, the reactions were done in sealed glass ampoules set up under vacuum and inert atmosphere, and reactions were heated in a constant temperature oil bath at 40 °C for 2 days. Activation of the catalyst was accomplished by adding one equiv of silver salt to the reaction mixture. Salts of weakly coordinating anions such as AgBF_4 and AgOTf produced comparatively poor yields of [3,3] product compared with $\text{AgBAR}^{\text{F}}_4$ (entries 1 & 2). Addition of one equiv of $\text{AgBAR}^{\text{F}}_4$ (entry 3) led to a more efficient catalyst, which produced a 70% yield of the expected [3,3] product, in contrast to the reaction with two equiv of $\text{AgBAR}^{\text{F}}_4$ added (entry 3 vs. entry 5) which produced more of the [1,3] byproduct than the desired [3,3] product. This is likely due to the replacement of both chloride ligands when two equiv of $\text{AgBAR}^{\text{F}}_4$ are added. The replacement of two chloride ligands generates a palladium complex which has an overall +2 charge, thereby becoming more electrophilic and leading to more byproduct formation such as N-phenyl benzamide elimination product as mentioned by Calter et al.⁸ Coordinating solvents such as THF inhibited formation of any product (entry 4), likely because the active catalyst is binding with THF. Palladium complex **24** containing a bis(NHC) ligand was a much poor catalyst than the bis(ADC) ligand containing catalyst **9** (entry 6). This is proposed to be due to the higher electrophilicity of the palladium center in complex **9** relative to **24** due to poorer σ -donation of the bis(ADC) ligand than the bis(NHC) ligand. This indicates

that a fine balance of the catalyst electrophilicity is needed for this reaction. Catalysts which are dicationic are too electrophilic, but neutral bis(NHC) complexes are not electrophilic enough for this reaction. Bis(ADC) palladium complexes **14** (entry 7) and **15** (entry 8) containing eight-membered chelate rings gave comparatively poor yields for aza-Claisen rearrangement. This may be due to low solubility of the catalysts in CD₂Cl₂, or to unfavorable donor properties of the larger chelate ligands.

Effect of bis(ADC) ligand electronic properties on palladium-catalyzed aza-Claisen rearrangement.

Bis(ADC) palladium complexes with tunable electronic properties were used to study the effect of changes in ligand donor ability on catalyst activity²² (Table 5.6). Catalytic reactions were done in J Young NMR tubes and analyzed similarly to the previously described reactions with (*E*)-2-Hexenyl *N*-[4-(trifluoromethyl)phenyl] benzimidate **S3**. Palladium bis(ADC) complex **±9** containing electron withdrawing –CF₃ groups on the *N*-aryl substituents displayed the highest [3,3] product yield in contrast to catalysts containing relatively electron donating groups or no electron donating groups. Quantitative analysis of the electron withdrawing property of the aryl substituents could be done using the Hammett σ parameter. The highest Hammett σ parameter obtained for –CF₃ group display the highest electron withdrawing property and hence highest activity in the catalytic rearrangement. This indicates the highly specific nature of the catalyst electrophilicity needed for this

reaction. A change from $-\text{CF}_3$ ($\sigma=0.53$) to $-\text{F}$ ($\sigma=0.15$) on the catalyst, made the catalyst inefficient. Lower σ -donation to the metal in $-\text{CF}_3$ containing bis(ADC) ligand compared to other groups may be the cause for this increase in [3,3] product yield. However the ^{13}C NMR values obtained for carbene carbons did not represent the expected pattern when studying electron withdrawing properties of aryl substituents of the above catalysts. The pattern expected was high down-field ^{13}C NMR shifts for carbene carbons with electron withdrawing groups and relatively up-field shifts for electron donating groups.



- 9 (X=CF₃)
- 9a (X=F)
- 9b (X=H)
- 9c (X=CH₃)
- 9d (X=OCH₃)

Structures correspond to Table 5.6

Table 5.6. Aza-Claisen rearrangement of (*E*)-2-hexenyl-*N*-[4-(trifluoromethyl)phenyl]benzimidate **S3** by palladium bis(ADC) complexes with different electronic properties.

Entry	X	¹³ C shifts of C _{carbene} (δ ppm)	Hammett σ parameter for X groups **	[3,3] product yield
1	- CF ₃	190.3, 184.4	0.53	70 %
2	- F*	184.4, 189.8	0.15	29 %
3	- H*	190.1, 183.7	0	22 %
4	- CH ₃ *	189.7, 183.6	- 0.14	24%
5	- OCH ₃ *	189.8, 183.7	- 0.12	27 %

* Anthea J. Miranda unpublished work

** Hammett free-energy relationship ³⁴

$$\text{Log } K / K_0 = \sigma\rho$$

$$\sigma = \text{pKa (benzoic acid)} - \text{pKa (substituted benzoic acid)} \text{ when } \rho=1$$

K = Acid dissociation constant of substituted benzoic acid

K₀= Acid dissociation constant of benzoic acid

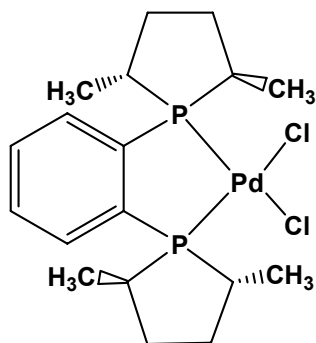
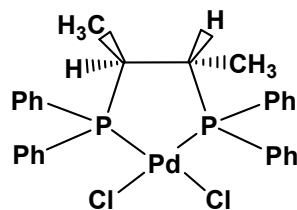
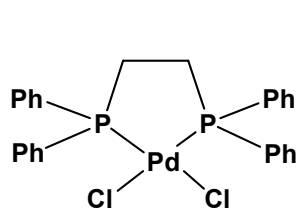
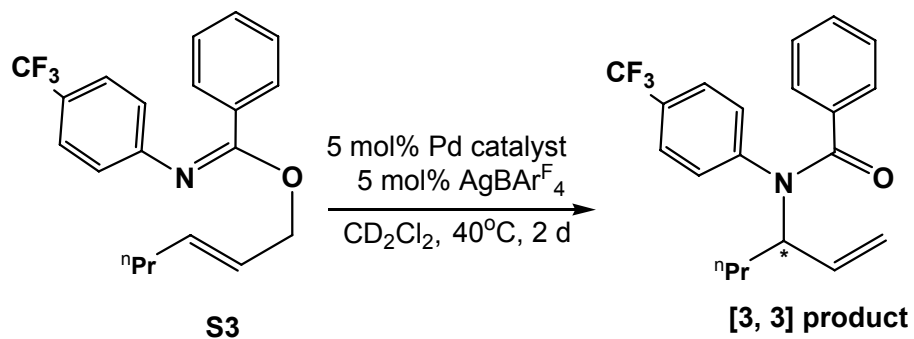
σ= Substituent constant

ρ= Sensitivity of the reaction to substituents effect

Aza-Claisen rearrangement of (*E*)-2-hexenyl-*N*-[4-(trifluoromethyl)phenyl]benzimidate **S3** with bis(phosphine) complexes

Aza-Claisen rearrangement of (*E*)-2-hexenyl-*N*-[4-(trifluoromethyl)phenyl]benzimidate **S3** using various bis(phosphine) palladium complexes as pre-catalysts were studied in order to compare their activities with those of bis(ADC) complexes. One equiv of AgBAR^F₄ was used with one equiv of the pre-catalyst to generate the active catalyst in-situ. Yields of products are tabulated in Table 5.7. Reactions were done similarly to previous reactions with (*E*)-2-hexenyl-*N*-[4-(trifluoromethyl)phenyl]benzimidate **S3**, in J Young NMR tubes with CD₂Cl₂ as the solvent. The crude reaction mixtures were analyzed by ¹⁹F NMR for reactions catalyzed by complex **25** using *p*-fluoro nitrobenzene as the internal standard. Bis(phosphine) palladium complex **25** displayed the highest yield for [3,3] product even though it was previously reported to be an inactive catalysts for aza-Claisen rearrangement.⁸ When compared with palladium complex **9**, the bis(phosphine) ligand of complex **25** is a stronger σ -donating ligand to the metal center. Thus, the high yield obtained contradicts the hypothesis that low metal electrophilicity is important. Complex **26**, containing a Chiraphos ligand displayed higher activity and higher [3,3] product yield than complex **27**, which contains a Duphos ligand (entry 2 vs. 3). Thus it is possible that the greater steric crowding and freedom of rotation of substituents around the phosphorus atom in complex **26** is more favorable for catalysis. Reactions catalyzed by complex **26** and **27** were analyzed by ¹H NMR using diethylene glycol dibutyl ether (6 μ L) as the internal standard. Also during the

reaction [1,3] by-product formation was not observed may be due to less electrophilicity of the metal in bis(phosphine) complexes.



Structures correspond to Table 5.7

Table 5.7. Aza-Claisen rearrangement with bis(phosphine) palladium complexes.

Entry	Catalyst	[3,3] product	Unreacted imidate
1	25	75 %	8 %
2	(2S,3S) 26	57 %	32 %
3	(2R,5R) 27	26 %	72 %

Enantioselective aza-Claisen rearrangement of (*E*)-2-hexenyl-*N*-[4-(trifluoromethyl)phenyl]benzimidate using palladium bis(ADC) complexes.

The relatively high [3,3] product yield obtained when using palladium bis(ADC) complex $\pm\mathbf{9}$ with (*E*)-2-hexenyl-*N*-[4-(trifluoromethyl) phenyl] benzimidate, inspired an investigation of whether enantioselective catalysis is possible with this palladium complex. To study enantioselective catalysis using complex **9**, enantiomerically pure (1*R*,2*R*)-(-) and (1*S*,2*S*)-(+)-*N,N'*-dimethyl-1,2-diaminocyclohexane-derived palladium bis(ADC) complexes (1*R*,2*R*)-**9** and (1*S*,2*S*)-**9** were synthesized according to the method described in Chapter 3 for the racemic complex $\pm\mathbf{9}$. Catalytic aza-Claisen reactions were done in J Young NMR tubes for calculating NMR yields and then repeated in glass vessels for isolation of the products. All of the reactions were performed under vacuum in distilled CH₂Cl₂ with 5 mol% AgBAR₄^F added. Isolated [3,3] products from catalytic reactions were analyzed by chiral HPLC using *n*-hexane : ethanol (95:5) as the mobile phase. The enantiomeric excesses (%ee) were calculated from the ratios of areas of HPLC signals obtained for the two enantiomers of the aza-Claisen products. Before running the samples obtained from the

enantiomerically pure catalyst, a racemic [3,3] product sample was run in order to assign the peak retention times from the two different enantiomers and to ensure that baseline resolution was obtained. The absolute configuration of the product was identified using the optical rotation of the chromatographically purified [3,3] product and comparing the optical rotation reported⁸ for the enantiomerically pure compound. When using palladium bis(ADC) complex **12** derived from (1*S*,2*S*)-(-)-*N,N'*-dimethyl-1,2-diphenyl-1,2-ethanediamine as a catalyst, an optical rotation of $[\alpha]_{\text{D}}^{25} + 34.4$ (c 0.5, CH₂Cl₂) was observed for the [3,3] product enantiomer which had a lower retention time (6.17 min). Overman et al. reported optical rotation of $[\alpha]_{\text{D}}^{25} - 37.2$ (c 0.5, CH₂Cl₂) for the (*R*)-(-) enantiomer.⁸ On this basis, (*S*)-(+) configuration was assigned to the [3,3] product major enantiomer with a lower retention time obtained when using catalyst **12**. The remaining enantiomer with the higher retention time was assigned as the (*R*)-(-) configuration. The enantioselective catalytic results obtained are tabulated in Table 5.8.

Table 5.8. Enantioselective catalytic results for (*E*)-2-hexenyl-*N*-[4-(trifluoromethyl)phenyl]benzimidate.

Entry	Catalyst	Yield		
		[3,3] Product %	[1,3] Product %	Amide %
1	(1 <i>R</i> ,2 <i>R</i>)- 9	50 (41) ^a , 30% ee (<i>S</i>)-(+)	14(12) ^a	20
2	(1 <i>S</i> ,2 <i>S</i>)- 9	36 (24) ^a , 32% ee (<i>R</i>)-(-)	14	13
3	(1 <i>S</i> ,2 <i>S</i>)- 12	34 (33) ^a , 59% ee (<i>S</i>)-(+)	11	15

^a yield was determined using ¹⁹F NMR spectrum of the catalytic reaction.

The (1*R*,2*R*) enantiomer of complex **9** provided a moderate yield of 50 % for the [3,3] product, with a 30 % enantiomeric excess of the (*S*)-(+ enantiomer (entry 1). The (1*S*,2*S*) enantiomer of complex **9** produced a yield of 36 % of [3,3] product with a 32 % enantiomeric excess of the (*R*)-(-) enantiomer (entry 2). The observation of similar but opposite % ee with two different enantiomers of the same catalyst suggests that the bis(ADC) ligand chirality on the palladium complex plays the dominant role in determining enantioselectivity. This also suggests that the ligand is strongly bound to the palladium center and does not dissociate from the catalyst during catalytic reactions. The 59 % ee obtained using complex **12** was twice as high as the % ee obtained with enantiomerically pure complex **9** (Table 5.8). This

higher % ee is proposed to result from the improved asymmetric environment around the palladium center of complex **12**. The improved asymmetric environment around the palladium center is created by having one phenyl group in the amine back-bone pointing towards the palladium center (Figure 3.6, Chapter 3) when compared with complex **9** which has a poorer asymmetric environment due to the presence of hydrogens instead of phenyl substituents.

The yields of [3,3] products obtained using enantiomerically pure catalysts ((1*R*,2*R*)-**9** and (1*S*,2*S*)-**9**) were considerably lower (36%-50%) than the yield of 70% obtained with racemic complex \pm **9** (entry 3, Table 5.5). A plausible explanation for this change is that different types of palladium dimers are formed in the catalytic system. The racemic catalyst can form either (*R,R*)-(*R,R*), (*S,S*)-(*S,S*) or (*R,R*)-(*S,S*) dimeric isomers that can have different rates in binding to the substrate due to differences in the monomer-dimer equilibria. In contrast, the enantiomerically pure catalyst can produce only (*R,R*)-(*R,R*) or (*S,S*)-(*S,S*) dimeric isomers which may not be efficient as (*R,R*)-(*S,S*) dimers in binding to the substrate as a consequence of monomer-dimer equilibria. Alternatively, racemic catalyst \pm **9** has a greater ability to act efficiently in substrate binding compared with the enantiomerically pure catalysts, which suggests that the (*R,R*)-(*S,S*) dimer more easily dissociates to a monomer compared to the single enantiomer dimers.

The bis(ADC) palladium dimer formation was further studied by synthesizing and isolating the palladium dimer complexes **22** (diastereomeric mixture of [bis(ADC)PdCl]₂ [BAr^F₄]₂) and **23** ((1*R*,2*R*)-[bis(ADC)PdCl]₂ [BAr^F₄]₂) from the racemic complex \pm **9** and enantiopure complex (1*R*,2*R*)-**9** respectively. The synthesis

was done by treating complex **9** with one equiv of $\text{AgBAR}^{\text{F}}_4$ in dry methylene chloride followed by filtration and then precipitation from the reaction mixture by layering hexanes over the filtrate to obtain dimeric complexes as white crystalline solids. Interestingly, the ^1H NMR spectrum of complex **22** displayed four major methyl peaks, indicating four different NCH_3 groups at 3.22, 3.16, 3.10 and 3.04 ppm with an approximately 1:1:1:1 integration ratio, while the ^1H NMR spectrum of complex **23** displayed only two major peaks at 3.16 and 3.20 ppm, indicating only two different NCH_3 groups with a 1:1 integration ratio. This observation suggests that the dimeric palladium complex **22** contains a mixture of diastereomers of (1R, 2R)-(1S, 2S), (1R, 2R)-(1R, 2R) and (1S, 2S)-(1S, 2S) in a 2:1:1 statistical mixture. (1S, 2S)-(1S, 2S) and (1R, 2R)-(1R, 2R) diastereomers have identical spectral data as they are enantiomers. However (1R, 2R)-(1S, 2S) diastereomer spectral data can be different from the others. The presence of four different fluorine signals at -63.56, -63.58, -63.60 and -63.63 ppm with integration ratio of 1:1:1:1 in the ^{19}F NMR spectrum of complex **22** and the presence of only two different fluorine signals at -63.60 and -63.65 ppm in 1:1 integration ratio in complex **23** can also be explained using the previous hypothesis.

X-ray quality crystals from complex **23** were developed using slow evaporation of 1,2-dichloroethane solution under atmospheric conditions (Figure 5.3). According to the molecular structure, complex **23** contains a C_2 symmetry axis through the chloride atoms. Pd- $\text{C}_{\text{carbene}}$ bond lengths were 2.008(5) and 1.966(5) Å which were comparatively longer than reported values for monomeric bis(ADC) palladium complexes.²³ The sum of bond angles around the palladium center is

close to 360° indicating a square planer geometry around the palladium center. The N-C-N bond angles of $117.7(5)^\circ$ and $115.8(5)^\circ$ were comparable with the values reported by Moncada et al. for bis(ADC) palladium complexes (Table 5.9).²³

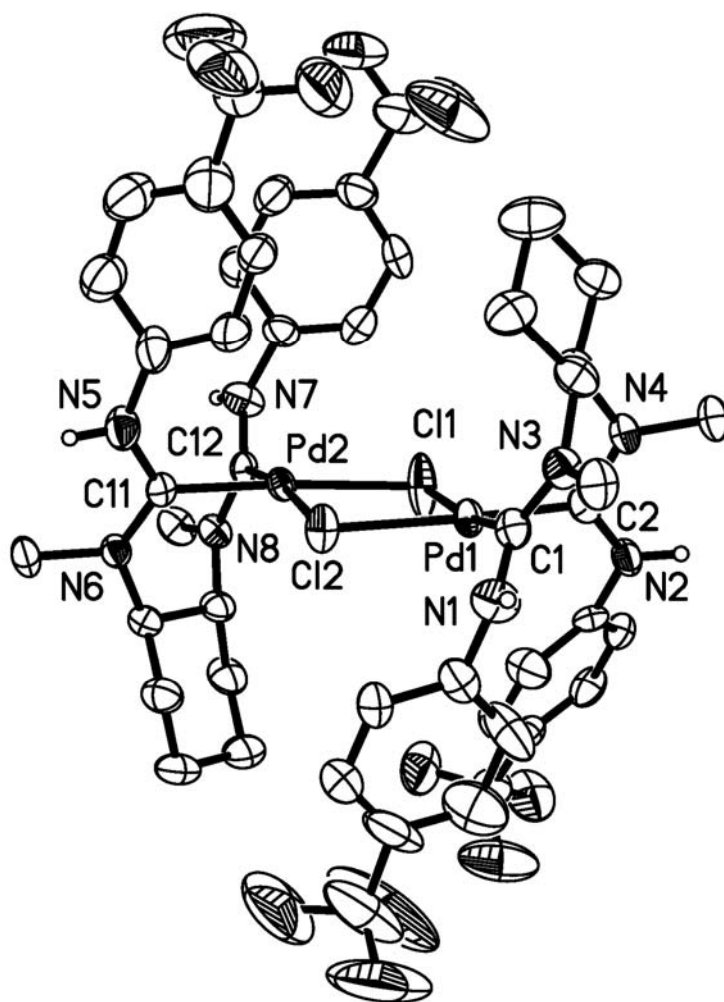


Figure 5.3. Molecular structure of complex **23** with 50% probability ellipsoids.

Table 5.9. Selected bond lengths (Å) and bond angles (°) of complex **23**.

	Bond lengths (Å)
N(1)-C(1)	1.320(7)
N(2)-C(2)	1.318(6)
Pd(1)-C(1)	2.008(5)
Pd(1)-C(2)	1.966(5)
Pd(1)-Cl(1)	2.3861(14)
Pd(1)-Cl(2)	2.3817(13)

	Bond Angles (°)
C(2)-Pd(1)-C(1)	87.9(2)
C(1)-Pd(1)-Cl(2)	94.72(15)
C(2)-Pd(1)-Cl(1)	90.67(15)
Cl(2)-Pd(1)-Cl(1)	86.43(4)
N(2)-C(2)-N(4)	117.7(5)
N(3)-C(1)-N(1)	115.8(5)

Table 5.10. Crystal data and structure refinement details for complex **23** (includes a molecule of 1,2-dichloroethane).

Empirical formula	$C_{114}H_{80}B_2Cl_4N_8F_{60}Pd_2$
Formula weight	3078.08
Crystal system	Triclinic
Space group	$P1$
Unit cell dimensions	$a = 13.4347(2) \text{ \AA}$ $\alpha = 96.4850(10)^\circ$ $b = 13.5208(2) \text{ \AA}$ $\beta = 97.5280(10)^\circ$ $c = 17.4634(2) \text{ \AA}$ $\gamma = 90.5680(10)^\circ$
Volume, z	$3123.74(7) \text{ \AA}^3$, 1
Density (calculated)	1.636 Mg/m^3
Absorption coefficient	0.514 mm^{-1}
Crystal size	$0.35 \times 0.20 \times 0.11 \text{ mm}^3$
θ range for data collection	1.18 to 26.28°
Limiting indices	$-16 \leq h \leq 16$ $-16 \leq k \leq 16$ $-21 \leq l \leq 21$
Temperature	$170(2) \text{ K}$
Wavelength	0.71073 \AA
Reflections collected	93251
Independent reflections	24822 ($R_{\text{int}} = 0.0474$)
Final R indices [$I > 2\sigma(I)$]	$R1 = 0.0407$ $wR2 = 0.1070$
R indices (all data)	$R1 = 0.0456$ $wR2 = 0.1113$

Aza-Claisen rearrangement of different N-substituted phenyl benzimidates

Aza-Claisen rearrangements using different N-substituted phenyl benzimidates other than (*E*)-2-hexenyl-*N*-[4-(trifluoromethyl)phenyl]benzimidate **S3** were studied in order to understand the effect of having different functional groups on the substrate and to possibly expand the substrate scope of this reaction. The substrates (*E*)-2-hexenyl-*N*-phenyl benzimidate **S4**,⁸ (*E*)-2-hexenyl-*N*-[4-methoxyphenyl]benzimidate **S5**⁹ and (*E*)-2-hexenyl-*N*-methyl benzimidate **S10** (Figure 5.4) were used to study the effect of increased nucleophilicity of the imidate N for the reaction. Nucleophilicity of the imidate N is assumed to be increased when going from **S3**, **S4**, **S5** and **S10**. Substrates **S4** and **S5** have been widely studied by Overman's group and reported good yields with cyclopalladated catalysts.^{11,10} (*E*)-2-butenyl-*N*-[4-(trifluoromethyl)phenyl]benzimidate **S8**, (*E*)-2-cinnamyl-*N*-(4-trifluoromethyl)phenyl benzimidate **S9**¹¹ (Figure 5.4) were synthesized to measure the effect of having bulky olefinic substituents in the substrate on the catalytic reaction. Catalysts used were *N,N'*-dimethyl-1,2-diaminocyclohexane and *p*-trifluoromethylphenyl isocyanide derived palladium complex **±9**, *N,N'*-dimethyl-1,2-diaminocyclohexane and phenyl isocyanide derived palladium complex **9b** and (DPPE)PdCl₂ **25**. All of the reactions were done in sealed J Young NMR tubes under vacuum. Yields were calculated using ¹⁹F NMR for fluorine-containing imidates such as **S8**, with *p*-fluoronitrobenzene (30 μL) added as the internal standard. For imidate substrates that did not contain fluorinated functional groups, ¹H NMR spectra were used to calculate the yields of products using diethyleneglycol dibutyl ether (6 μL) as the internal standard. 5 mol % of the palladium catalyst and 5 mol% of AgBAR^F₄ were

used for the catalytic reactions. Product yields obtained for the catalytic reactions are tabulated in Table 5.11.

Table 5.11. Aza-Claisen rearrangement with different N-substituted phenyl benzimidates.

Entry #	Substrate	Catalyst	[3,3] product	[1,3] product
1	S4	\pm 9	26% ^a	52% ^a
2	S4	\pm 9b	22% ^a	10% ^a
3	S4	25	80% ^a	-
4	S5	\pm 9	15% ^a	51% ^a
5	S5	\pm 9b	0% ^a	14% ^a
6	S5	25	57% ^a	-
7	S8	\pm 9	70% ^b	6% ^b
8	S9	\pm 9	No Reaction	
9	S10	\pm 9	No Reaction	
10	S10	\pm 9b	No Reaction	
11	S10	25	No Reaction	

^a Yields were calculated by ¹H NMR spectroscopy

^b Yields were calculated by ¹⁹F NMR spectroscopy

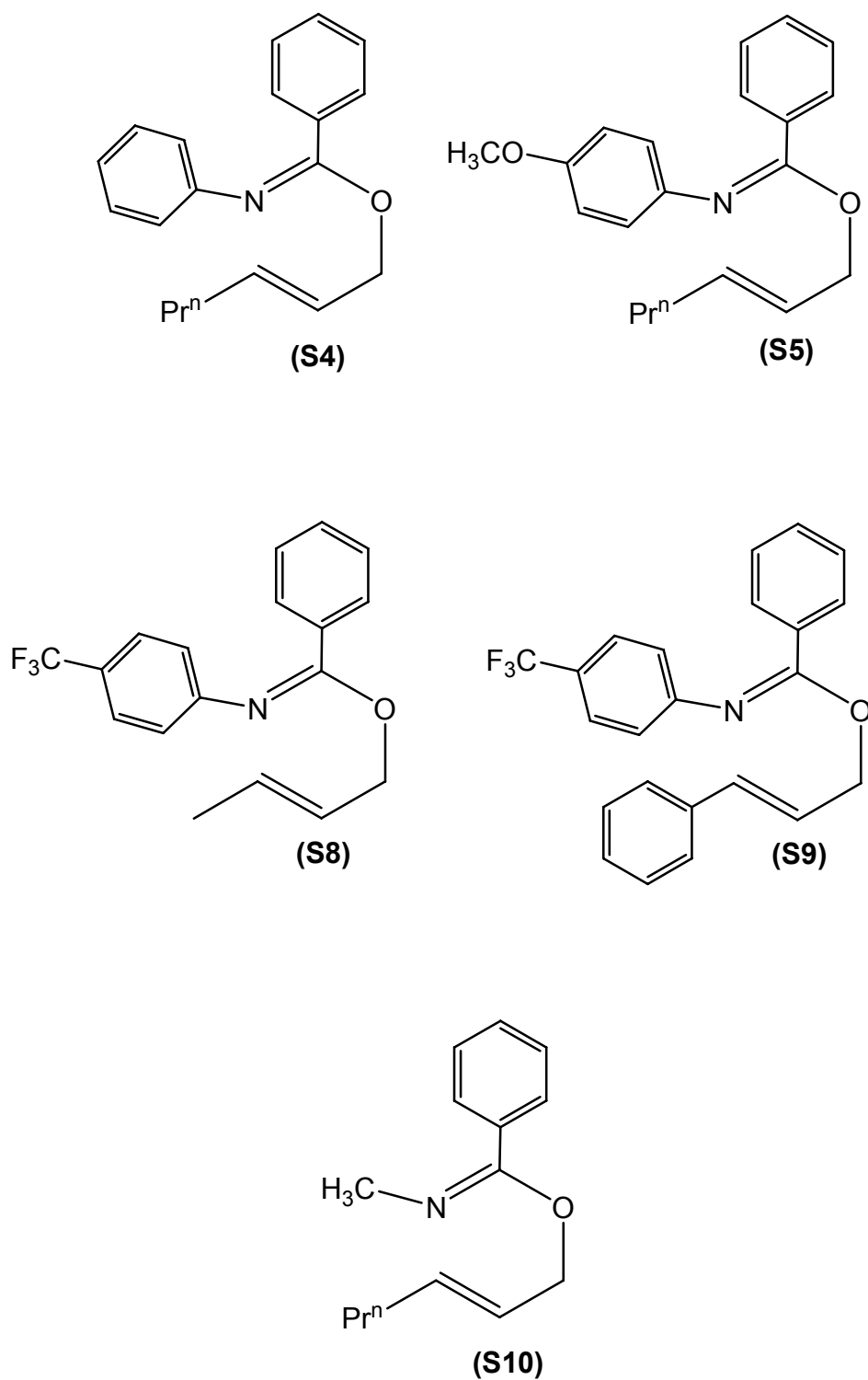


Figure 5.4. N-substituted phenyl benzimidates used in palladium-catalyzed aza-Clasien rearrangements.

In comparison, to (*E*)-2-hexenyl *N*-[4-(trifluoromethyl)phenyl]benzimidate **S3**, aza-Claisen rearrangements of (*E*)-2-hexenyl phenyl benzimidate **S4** with complex **±9** as precatalyst displayed a lower yield of 26% for [3,3] product and a higher yield of 52% for the [1,3] byproduct (entry 1 in Table 5.11 vs. entry 3 in Table 5.5). The main reason for this observation may be the higher nucleophilicity of the imidate nitrogen atom in **S4** compared with **S3** due to the absence of a -CF₃ substituent on the *N*-aryl group. Higher nucleophilicity of the imidate N atom may allow this site to compete with the olefin group in the imidate in binding to the palladium center, which has been proposed to facilitate more byproduct formation including [1,3] product, during the catalytic reaction.²⁴ The [1,3] byproduct formation was low when using comparatively less electrophilic palladium complex **±9b** (10%, entry 2) than complex **±9** (52%, entry 1) which displays tuning of the catalyst to obtain low amounts of byproducts. The proposed explanation for this observation is the low affinity of imidate N-binding to the palladium center when using less electrophilic complex **±9b**. Consistent with reactions of substrate **S3** (Table 5.7) (DPPE)PdCl₂ **25** displayed a higher yield of the expected [3,3] product (80%) in reactions of **S4** with no [1,3] byproduct formation (entry 3). Although, **25** has a less electrophilic palladium center, favorable steric crowding, or other stereoelectronic effects may be the reason for the observed higher yield of [3,3] product and lack of [1,3] byproduct. Entries 4, 5 and 6 involving reactions of substrate **S5** having a more nucleophilic N atom, displayed a similar behavior to reactions of **S4**. Lower amounts of [1,3] product were obtained with less electrophilic metal centers. However, yields of the desired [3,3] product were low to moderate, with the best yield obtained with bis(phosphine) catalyst **25**.

(*E*)-2-butenyl-*N*-[4-(trifluoromethyl)phenyl] benzimidate **S8** displayed similar yield for [3,3] product (70%, entry 7) in comparison with (*E*)-2-hexenyl *N*-[4-(trifluoromethyl)phenyl]benzimidate **S3**, even though the steric crowding on the olefin was less due to a –CH₃ group replacing the –ⁿPr group on imidate **S3**. (*E*)-2-cinnamyl *N*-(4-trifluoromethyl)phenyl benzimidate **S9** displayed no aza-Claisen rearrangement with palladium precatalyst **±9** (entry 8). This may be due to the steric hindrance created by the allylic phenyl group which inhibits the olefin from binding to the palladium center. In addition, the presence of a mildly electron-withdrawing phenyl group might be lowering the σ -donor ability of the olefin, further inhibiting its binding to palladium. None of the reactions with (*E*)-2-hexenyl-*N*-methyl benzimidate **S10** resulted in any aza-Claisen rearrangement product formation with palladium complexes **±9**, **±9b** or **25** (entry 9, 10 and 11). This may be due to the presence of a –CH₃ group on imidate N atom which makes it more nucleophilic as well as sterically unhindered, allowing strong binding to the palladium center and inhibiting the olefin binding needed for catalysis.

Aza-Claisen rearrangement of (*E*)/(*Z*)-2-Hexenyl trichloroacetimidate (S6**) and (*E*)/(*Z*)-2-Hexenyl-*N*-(4-methoxyphenyl) trifluoroacetimidate (**S7**).**

(*E*)/(*Z*)-2-Hexenyltrichloroacetimidates²⁵ **S6** and (*E*)/(*Z*)-2-hexenyl-*N*-(4-methoxyphenyl)trifluoroacetimidates²⁶ **S7** were synthesized according to literature procedures. These substrates have been chosen since their aza-Claisen [3,3] product can be easily transformed to allyl amines which are used in unnatural amino acid synthesis.²⁰ Among (*E*) and (*Z*) configurations of these substrates, the (*Z*)

imidates are considered challenging and Jautze et al. has obtained a high product ee % for (*Z*)-2-hexenyl-*N*-(4-methoxyphenyl)trifluoroacetimidate.²⁰ Aza-Claisen rearrangement of these substrates were performed using 5 mol% of precatalyst **9** and 5 mol% of AgBAR^F₄ in CD₂Cl₂ under vacuum in J Young NMR tubes. All of the catalytic results are tabulated below in Table 5.12.

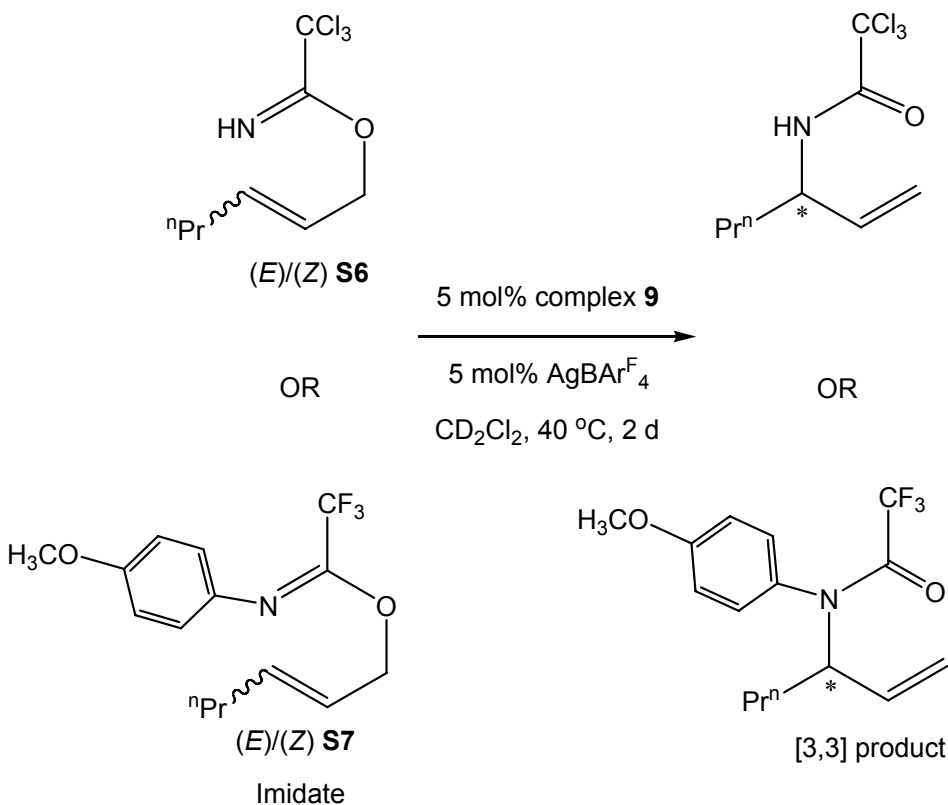


Figure 5.5. Aza-Claisen rearrangements of (*E*)/(*Z*)-2-hexenyltrichloroacetimidate **S6** and (*E*)/(*Z*)-2-Hexenyl-*N*-(4-methoxyphenyl) trifluoroacetimidate **S7**.

Table 5.12. Aza-Claisen rearrangement [3,3] product of (*E*)/(*Z*)-2-hexenyl trichloroacetimidate **S6** and (*E*)/(*Z*)-2-Hexenyl-*N*-(4-methoxyphenyl) trifluoroacetimidate **S7** using precatalyst ± 9 .

Imidate substrate	[3,3] product %
(<i>E</i>)-S6	20 ^a
(<i>Z</i>)-S6	20 ^a
(<i>E</i>)-S7	28 ^a
(<i>Z</i>)-S7	26 ^a

^a Yields were determined by ¹H NMR using % conversion with respect to the starting imidate.

Compared with (*E*)-2-hexenyl-*N*-[4-(trifluoromethyl)phenyl]benzimidate **S3**, 2-hexenyl trichloroacetimidates **S6** and 2-hexenyl-*N*-(4-methoxyphenyl) trifluoroacetimidates **S7** displayed poor yields in the aza-Claisen rearrangement with palladium complex ± 9 . This is most likely due to the presence of $-CCl_3$ and $-CF_3$ groups near to the nitrogen atom in imidates **S6** and **S7** respectively. Electron withdrawing groups such as $-CCl_3$ and $-CF_3$ on imidates tend to reduce the nucleophilicity of the neighboring nitrogen atom. That makes it less active towards nucleophilic attack on an olefin bound to the palladium center, causing less [3,3] product formation. However, a small amount of electron-withdrawing ability as in **S3** can have positive effects, as it prevents [1,3] byproduct formation. A fine balance of

imidate nucleophilicity and metal electrophilicity must be found for high aza-Claisen activity.

Summary and Conclusions

Ligand σ -donor abilities of palladium-bound bis(ADC) ligands derived from N-methylated diamines and palladium bis(isocyanide) precursor complex **8** (Chapter 3) were evaluated using the palladium bis(methyl isocyanide) derivatives. Changes in the stretching frequencies of methyl isocyanide ligands in the palladium complexes reflect differences in the σ -donor abilities of the ligand bound *trans* to the methyl isocyanides. According to methyl isocyanide stretching frequencies, a bis(ADC) ligand displayed the lowest σ -donation to the metal when compared with a bis(NHC) ligand and a bis(phosphine) ligand. The relatively low σ -donation from the bis(ADC) ligand makes the palladium center suitable for electrophilic catalytic reactions, including aza-Claisen rearrangements. Preliminary study of aza-Claisen rearrangement was done using γ -methylallyl-N-phenylformimidate **S1** and allyl-N-phenylformimidate **S2** to obtain poor to moderate yields of desired [3,3] product. From these preliminary studies, AgBAR^F₄ was selected as the best silver salt activator to be used in the catalysis. Aza-Claisen rearrangements of (*E*)-2-hexenyl-N-[4-(trifluoromethyl)phenyl]benzimidate **S3** using palladium bis(ADC) complexes displayed low to moderate yields of the desired [3,3] product, along with some [1,3] product and amide elimination product as byproducts. Complex **±9** displayed the highest yield of 70% for the [3,3] product with **S3**. Bis(ADC) palladium complexes were activated by adding one molar equiv of AgBAR^F₄ to generate the active catalyst

in situ from the reaction mixture. This active catalyst is proposed to be a dimeric bis(ADC) palladium complex with an overall +2 charge and two BAR^{F}_4 non-coordinating anions. Two equivalents of $\text{AgBAR}^{\text{F}}_4$ per palladium produced more of the [1,3] byproduct. Most of the aza-Claisen rearrangements were more successful in non-coordinating, polar solvents such as CH_2Cl_2 than in less-polar, coordinating solvents such as THF. Bis(ADC) palladium complexes with tunable different electronic properties, achieved by substituting the N-aryl group with either electron withdrawing groups such as $-\text{CF}_3$ or electron donating groups such as $-\text{OCH}_3$, were used in aza-Claisen rearrangement, leading to an observation of optimal activity with electron withdrawing group ($-\text{CF}_3$) on the palladium bis(ADC) complex **9**. Palladium bis(phosphine) complexes, which were previously reported to be inactive catalysts for aza-Claisen rearrangements⁸ produced comparable yields to (\pm)-**9** when treated with one molar equivalent of $\text{AgBAR}^{\text{F}}_4$. Asymmetric aza-Claisen rearrangements were done using enantiomerically pure palladium bis(ADC) complexes (*1R,2R*)-**9**, (*1S,2S*)-**9** and **12** to obtain enantiomeric excesses of 30%, 32% and 59% ee respectively. Complex **12** displayed the highest % ee due to the improved asymmetric environment created by phenyl groups on the amine backbone. The equal but opposite enantiomeric excesses of [3,3] product obtained using complexes (*1R,2R*)-**9** and (*1S,2S*)-**9** indicate that the ligand remains bound to palladium during catalysis. Together, these results are the first examples of enantioselective catalysis using bis(ADC) palladium complexes. These studies focused on the most commonly used imidate substrate for aza-Claisen rearrangement, (*E*)-2-hexenyl-*N*-[4-(trifluoromethyl)phenyl]benzimidate **S3**. In hopes of expanding the substrate scope,

different N-substituted phenyl benzimidates were examined to study the effect of different functional groups on the aza-Claisen rearrangement. Among them, substrates which contain electron-neutral or -donating groups such as –H **S4** and –OCH₃ **S5** displayed higher amounts of [1,3] byproducts. The amount of [1,3] byproduct was reduced by tuning the catalyst to have a less electrophilic palladium center. (*E*)-2-cinnamyl-*N*-(4-trifluoromethyl)phenyl benzimidate **S9** was a difficult substrate for aza-Claisen rearrangements, because the allyl phenyl group created steric hindrance and low donicity that inhibited attachment of the substrate to the palladium center. (*E*)-2-hexenyl-*N*-methyl benzimidate **S10** was completely inactive toward aza-Claisen rearrangement, most likely due to the nucleophilic imidate N atom which could easily bind to the palladium center, making the metal center inactive for catalysis. Finally, aza-Claisen rearrangements of (*E/Z*)-2-Hexenyl trichloroacetimidates **S6** and (*E/Z*)-2-Hexenyl-*N*-(4-methoxyphenyl) trifluoroacetimidates **S7** were studied, but unfortunately both of the imidates produced low yields of [3,3] product with palladium bis(ADC) complexes. The major advantage of using chiral bis(ADC) palladium complexes described here in aza-Claisen rearrangement is their easy synthesis and isolation compared with reported chiral catalytic systems such as ferrocenyl oxazoline palladacycles¹⁰ and ferrocenyl imidazoline palladacycles.²⁰ But unfortunately bis(ADC) palladium complexes lack the ability to catalyze a broad spectrum of substrates when compared with other reported catalysts.

Experimental

General Considerations

All manipulations were performed under air unless otherwise noted. Acetonitrile (Pharmco) was pre-dried over anhydrous CaCl_2 for 2-3 hours and refluxed over CaH_2 overnight under nitrogen. Dichloromethane (Pharmco), hexanes (Pharmco), and diethyl ether (Acros) were dried according to methods described in Chapter 2. 1,2-Dichloroethane was purified and dried using the same method described for dichloromethane in Chapter 2. NMR solvents were purchased from Cambridge Isotopes Laboratories. CD_3CN and $\text{DMSO-}d_6$ were dried by stirring over activated 4Å molecular sieves followed by vacuum distillation at room temperature. CD_2Cl_2 and 1,2-dichloroethane- d_4 were dried over activated 4Å molecular sieves and then stored over fresh P_2O_5 before use. Resolved (1R,2R)-(-) and (1S,2S)-(+)-1,2-diaminocyclohexane (98% purity) were purchased from Acros. (2S,3S)-(-)-bis(diphenylphosphino)butane [(S,S)-CHIRAPHOS] and (-)-1,2-bis((2R,5R)-2,5-dimethylphospholano)benzene [(R,R)-Me-DUPHOS] were purchased from Strem Chemicals and used without further purification. All other reagents were purchased from Aldrich or Acros and used as received. Methylisocyanide,²⁷ (1,1'-dimesityl-3,3'-methylenediimidazol-2,2'-diylidene)palladium dibromide **24**,¹³ (DPPE) PdCl_2 **25**,¹⁶ (2S,3S)-(-)-bis(diphenylphosphino)butane PdCl_2 **26**,²⁸ (-)-1,2-bis((2R,5R)-2,5-dimethylphospholano)benzene PdCl_2 **27**²⁸ and silver tetrakis[3,5-bis(trifluoromethyl)phenyl]borate ($\text{AgBAR}^{\text{F}4}$),²⁹ were prepared following previously published procedures. (\pm)-**9** and bis(*p*-trifluoromethylphenylisocyanide) PdCl_2 **5** were prepared as previously reported.³⁰ NMR spectra were recorded on Varian GEMINI

2000 (300 MHz) and Unity INOVA (400 MHz) spectrometers. Reported chemical shifts are referenced to residual solvent peaks (^{13}C , ^1H) or to calibrated external standards (^{19}F , ^{31}P). IR spectra were acquired from Nujol mulls on a Nicolet Protégé 460 FT-IR spectrometer. Optical rotations were measured from freshly prepared solutions on an Autopol V polarimeter (Rudolph Research Analytical, Hackettstown, NJ) using a 100 mm cell. Elemental analyses were performed by Desert Analytics (Tucson, Arizona) and Midwest Microlab (Indianapolis, Indiana).

Resolved (1R,2R)-(-) and (1S,2S)-(+)-N,N'-dimethyl-1,2-diaminocyclohexane

Methylations of diamines were done according to the reported procedure for (racemic) *trans*-1,2-diaminocyclohexane described by Buchwald et al.³¹ (1R,2R)-(-)-1,2-diaminocyclohexane (1.0 g, 8.75 mmol) was treated with excess ethyl formate (4.25 mL, 52.5 mmol) to obtain the bis(amide) product as a white crystalline solid (0.797 g, 54% yield). The bis(amide) (0.797 g, 4.68 mmol) was treated with LiAlH_4 (0.48 g, 12.6 mmol) to obtain (1R,2R)-(-)-N,N'-dimethyl-1,2-diaminocyclohexane as a colorless oil (0.458 g, 69% yield). $[\alpha]_{\text{D}}^{20}$ -132.4° ($c = 0.5$, MeOH). Similarly, (1S,2S)-(+)-1,2-diaminocyclohexane (0.5 g, 4.38 mmol) was treated with ethyl formate (2.12 mL, 26.2 mmol) to obtain the bis(amide) product (0.551 g, 74% yield). Then bis(amide) (0.551 g, 3.24 mmol) was treated with LiAlH_4 (0.33 g, 8.74 mmol) to obtain (1S,2S)-(+)-N,N'-dimethyl-1,2-diaminocyclohexane (0.444 g, 97% yield). $[\alpha]_{\text{D}}^{20}$ $+133^\circ$ ($c = 0.5$, MeOH). The ^1H NMR spectra of both amines were similar to values reported by Betschart et al.³²

Bis(ADC)palladium dichloride complexes derived from (1*R*,2*R*)-(-) and (1*S*,2*S*)-(+)-*N,N'*-dimethyl-1,2-diaminocyclohexane

(1*R*,2*R*)-**9** and (1*S*,2*S*)-**9** were synthesized following the same procedure described for (±)-**9**³⁰ in Chapter 3. Yields obtained were 70% for (1*R*,2*R*)-**9** and 52% for (1*S*,2*S*)-**9**. All analytical data of (1*R*,2*R*)-**9** and (1*S*,2*S*)-**9** matched the racemic compound (±)-**9**.³⁰

(rac)-Bis(ADC)palladium(II)-bis(methylisocyanide) complex derived from *N,N'*-dimethyl-1,2-diaminocyclohexane (18)

Methylisocyanide (12 μL, 0.21 mmol) was added to a solution of (±)-**9** (40 mg, 0.060 mmol)³⁰ in 5 mL of acetonitrile. The solution was stirred at room temperature for 1 hour, followed by addition of AgBF₄ (26 mg, 0.13 mmol) and stirring for an additional 2 hours at room temperature. The reaction mixture was filtered through celite, and the volume of the filtrate was reduced by one half under vacuum. Diethyl ether was layered onto the solution to precipitate complex **18** as white needles. The product was filtered and dried under vacuum. Yield: 38 mg, 73%. ¹H NMR (300 MHz, CD₃CN): δ 8.73 (br s, 1H, NH), 8.43 (br s, 1H, NH), 7.86 (d, 2H, *J*=9.0 Hz, Ar), 7.59 (d, 2H, *J*=8.4 Hz, Ar), 7.27 (d, 2H, *J*=9.0 Hz, Ar), 6.93 (d, 2H, *J*=8.4 Hz, Ar) 5.50 (m, 1H, ^oHex *ipso* CH), 3.68 (m, 1H, ^oHex *ipso* CH), 3.49 (s, 3H, CNCH₃), 3.26 (s, 3H, CNCH₃), 3.11 (s, 3H, NCH₃), 3.10 (s, 3H, NCH₃), 2.43-2.33 (m, 1H, ^oHex), 2.27-2.15 (m, 1H, ^oHex), 1.96-1.80 (m, 2H, ^oHex), 1.66-1.27 (m, 4H, ^oHex). ¹³C NMR (101 MHz, CD₃CN): δ 187.1 (carbene), 181.8 (carbene), 145.1 (Ar *ipso*), 143.2 (Ar *ipso*), 130.0 (q, ²*J*_{CF}=32.8 Hz, Ar *para*), 129.2 (q, ²*J*_{CF} =32.8 Hz, Ar *para*), 128.1 (q, ³*J*_{CF}

=3.8 Hz, Ar *meta*), 127.3 (s, Ar *ortho*), 127.0 (q, $J=3.8$ Hz, Ar *meta*), 125.1 (q, $^1J_{CF}$ =272 Hz, CF_3), 125.0 (s, Ar *ortho*), 124.9 (q, $^1J_{CF}$ =270 Hz, CF_3), 69.1 (NCH₃), 68.4 (NCH₃), 41.9 (^cHex), 33.8 (^cHex), 32.5 (^cHex), 31.2 (CNCH₃), 30.6 (^cHex), 30.4 (CNCH₃), 25.5 (^cHex), 25.4 (^cHex), CNMe not detected. ¹⁹F NMR (282 MHz, CD₃CN): δ -59.66 (s), -59.89 (s). IR (Nujol, cm⁻¹): ν 2271 (m w/shoulder). Anal. Calcd for C₂₈H₃₂B₂F₁₄N₆Pd: C, 39.72; H, 3.81; N, 9.93 %. Found: C, 38.30; H, 3.49; N, 9.64 %.

Bis(ADC)palladium(II)-bis(methyl isocyanide) complex derived from (1S,2S)-(-)-N,N'-dimethyl-1,2-diphenyl-1,2-ethanediamine (19)

Complex **12** (0.1 g, 0.132 mmol) described in Chapter 3 was treated with AgBF₄ (0.0566 g, 0.291 mmol) in distilled acetonitrile at 60 °C for 40 min followed by filtration through celite. The filtrate was mixed with methyl isocyanide (26 μ L, 0.465 mmol) and stirred for another 40 min at room temperature. After the reaction volume was reduced by rotovap, distilled diethyl ether was layered over the ice cold reaction mixture to precipitate the product as a white crystalline solid. The product was filtered and dried under vacuum overnight. Yield 38%, 47 mg. ¹H NMR (300 MHz, CD₃CN): δ 8.84 (br s, 1H, NH), 8.66 (br s, 1H, NH), 7.92 (d, 2H, $J=8.4$ Hz, Ar), 7.69 (d, 2H, $J=8.1$ Hz, Ar), 7.60-7.53 (m, 4H, Ar), 7.41-7.30 (m, 9H, Ar) 7.01 (d, 2H, $J=8.1$ Hz, Ar), 5.63 (d, 1H, $J=12$ Hz, CH), 3.59 (s, 3H, CNCH₃), 3.23 (s, 3H, NCH₃), 3.16 (s, 3H, CNCH₃), 3.00 (s, 3H, NCH₃). IR (Nujol, cm⁻¹): ν 2273 (m w/shoulder). Anal. Calcd for C₃₆H₃₄B₂F₁₄N₆Pd: C, 45.77; H, 3.63; N, 8.89 %. Found: C, 45.40; H, 3.62; N, 8.78 %.

[(1,1'-Dimesityl-3,3'-methylenediimidazol-2,2'-diylidene)palladium(II)-bis(methylisocyanide)][BF₄]₂ (20)

1,1'-dimesityl-3,3'-methylenediimidazolium dibromide was synthesized according to Gardiner et al.¹³ and was used to synthesize [(1,1'-dimesityl-3,3'-methylenediimidazol-2,2'-diylidene)palladium(II)-bis(acetonitrile)][BF₄]₂ as reported by Gardiner et al.¹³ for the *N*-methyl analogue, [(1,1'-dimethyl-3,3'-methylenediimidazol-2,2'-diylidene)palladium(II)-bis(acetonitrile)][BF₄]₂. A dichloromethane solution (1 mL) of [(1,1'-dimesityl-3,3'-methylenediimidazol-2,2'-diylidene)palladium(II)-bis(acetonitrile)][BF₄]₂ (70 mg, 0.094 mmol) and methylisocyanide (10 μL, 0.20 mmol, 2.1 equiv) was stirred for 2 hours at room temperature. Addition of hexanes to the suspension led to precipitation of a grayish-white powder. The product was filtered, washed with hexane, and dried under vacuum. Yield: 54 mg, 77%. ¹H NMR (300 MHz, DMSO-*d*₆): δ 8.10 (d, 2H, *J*=1.8 Hz, imidazole), 7.77 (d, 2H, *J*=1.8 Hz, imidazole), 7.18 (s, 4H, *m*-H), 6.61 (s, 2H, CH₂), 3.21 (s, 6H, CNCH₃), 2.33 (s, 6H, *p*-CH₃), 1.95 (s, 12H, *o*-CH₃). ¹³C NMR (101 MHz, DMSO-*d*₆): δ 155.8 (carbene), 139.9 (Mes), 134.9 (Mes), 134.0 (Mes), 129.1 (Mes), 124.6 (im), 123.8 (im), 122.0 (CNMe), 62.6 (CH₂), 30.2 (CNCH₃), 20.5 (*p*-CH₃), 17.4 (*o*-CH₃). IR (Nujol, cm⁻¹): ν 2266 (m). Anal. Calcd for C₂₉H₃₄B₂F₈N₆Pd: C, 46.65; H, 4.59; N, 11.26 %. Found: C, 46.37; H, 4.31; N, 11.05 %.

[(1,2-Bis(diphenylphosphino)ethane)Pd(CNCH₃)₂][BPh₄]₂ (21)

A mixture of (DPPE)PdCl₂¹⁶ (100 mg, 0.174 mmol), AgBF₄ (74 mg, 0.38 mmol), and anhydrous acetonitrile (10 mL) was placed in a sealable flask under

nitrogen. The reaction mixture was heated at 60 °C for 1 hour with stirring. The mixture was then filtered through celite to remove the precipitated AgCl. The filtrate was dried under vacuum to remove the solvent, and the residue was dried in vacuum for a further 3 hours. Dichloromethane (10 mL) was added, and the mixture was again filtered through celite. The filtrate was treated with methylisocyanide (21 μ L, 0.38 mmol) and stirred at room temperature for 2 hours. The solvent was evaporated under reduced pressure, 10 mL of anhydrous acetonitrile was added, and solid NaBPh₄ (131 mg, 0.383 mmol) was introduced. The reaction mixture was stirred for 2 hours at room temperature, and diethyl ether was added to the solution to precipitate NaBF₄ as a white crystalline solid. The mixture was filtered through celite to remove NaBF₄, and diethyl ether was added to the filtrate to obtain complex **21** as pale yellow crystals. The product was isolated by filtration, washed with deionized water to remove any unreacted NaBPh₄ (4 mL), then washed with diethyl ether (10 mL) and dried under vacuum for 12 hours. Yield: 81 mg, 38%. ¹H NMR (300 MHz, CD₃CN): δ 7.76-7.56 (m, 20H, Ph), 7.31-7.22 (m, 16H, Ph), 7.02-6.93 (m, 16H, Ph), 6.86-6.78 (m, 8H, Ph), 3.14 (s, 6H, CNCH₃), 2.83 (m, 4H, CH₂). ¹³C NMR (101 MHz, CD₃CN): δ 164.7 (dd, ²J_{PC}=98.4, 49.6 Hz, PdCNMe), 136.7 (s, Ph), 134.8 (d, ³J_{PC}=3.1 Hz, PPh₂ *meta*), 134.2 (d, ¹J_{PC}=11.5 Hz, PPh₂ *ipso*), 130.9 (d, ²J_{PC}=12.3 Hz, PPh₂ *ortho*), 126.9 (s, Ph), 126.6 (q, ¹J_{BC}=2.8 Hz, BPh₄ *ipso*), 126.3 (s, Ph), 122.8 (s, Ph), 31.0 (s, CNCH₃), 28.2 (dd, J_{PC}=35.1, 10.7 Hz, CH₂). ³¹P NMR (162 MHz, CD₃CN): δ 69.5 (s). IR (Nujol, cm⁻¹): ν 2262 (m). Anal. Calcd for C₇₈H₇₀B₂N₂P₂Pd: C, 76.45; H, 5.75; N, 2.29 %. Found: C, 76.14; H, 5.68; N, 2.24 %.

Dimeric chiral [bis(ADC)PdCl₂][BAr^F₄]₂ complexes (**22**), (**23**)

Complex (\pm)-**9** (0.06g, 0.091mmol), AgBAr^F₄ (0.088 g, 0.091mmol) and 10 mL of distilled methylene chloride were mixed in a thick walled glass vessel and stirred at room temperature under nitrogen for 2 hours. The Initially cloudy solution turned clearer with time, but some cloudy precipitate remained after 2 hours of the reaction due to AgCl formation. The vessel was opened to air, and the solution was filtered through a fine frit to remove precipitated AgCl from the reaction mixture. The solid on the frit was washed with 10 mL of fresh distilled methylene chloride. The volume of the clear filtrate was reduced using a rotovap to about half and distilled hexanes were added to maximize the precipitation of complex **22** as a white crystalline solid. The product was collected on a frit and dried under vacuum overnight (0.1065 g, 79% yield) ¹H NMR (400 MHz, CD₂Cl₂): δ 7.77-7.68 (m, 21H, BAr^F₄ *ortho* and Ar), 7.54 (s, 8H, BAr^F₄ *para*), 7.50 (s, 2H, NH), 7.44 (s, 2H, NH), 7.32-7.13 (m, 11H, Ar), 7.01 (m, 2H, ^cHex *ipso* CH), 3.44 (m, 2H, ^cHex *ipso* CH), 3.22 (s, 3H, NCH₃), 3.16 (s, 3H, NCH₃), 3.10 (s, 3H, NCH₃), 3.04 (s, 3H, NCH₃), 2.54-1.32 (m, 16H, ^cHex). ¹⁹F NMR (376 MHz, CD₂Cl₂): δ -63.24 (s, 48F, BAr^F₄⁻), -63.56 (s, 3F, CF₃C₆H₄), -63.58 (s, 3F, CF₃C₆H₄), -63.60 (s, 3F, CF₃C₆H₄), -63.63 (s, 3F, CF₃C₆H₄). Anal. Calcd for C₁₁₂H₇₆B₂N₈F₆₀Cl₂Pd₂: C, 45.15; H, 2.57; N, 3.76 %. Found: C, 45.02; H, 2.55; N, 3.99 %. Similarly, enantiomerically pure (1R, 2R) complex **9** (0.06g, 0.091mmol) and AgBAr^F₄ (0.088g, 0.091mmol) were allowed to react according to the procedure described above to obtain the dimeric (**1R,2R**) [bis(ADC)PdCl₂][BAr^F₄]₂ complex **23** in 92% yield (0.1236 g). ¹H NMR (400 MHz, CD₂Cl₂): δ 7.72 (m, 16H, BAr^F₄ *ortho*), 7.59-7.57 (m, 4H, NH), 7.55 (s, 8H, BAr^F₄ *para*), 7.27-7.15 (m, 16H, Ar *ortho*, *meta*),

7.06 (m, 2H, ^oHex *ipso* CH), 3.41 (m, 2H, ^oHex *ipso* CH), 3.16 (s, 6H, NCH₃), 3.10 (s, 6H, NCH₃), 2.46-1.36 (m, 16H, ^oHex). ¹⁹F NMR (376 MHz, CD₂Cl₂): δ -63.23 (s, 48F, BAr^F₄⁻), -63.60 (s, 6F, CF₃C₆H₄), -63.65 (s, 6F, CF₃C₆H₄). Anal. Calcd for C₁₁₂H₇₆B₂N₈F₆₀Cl₂Pd₂: C, 45.15; H, 2.57; N, 3.76 %. Found: C, 44.90; H, 2.44; N, 3.68 %.

γ-Methylallyl-N-phenylformimidate (S1)

The method described by Roberts et al.²¹ was followed using ethyl *N*-phenyl formimidate (10 g, 0.067 mol) and 2-buten-1-ol (11.4 mL, 0.134 mol) to obtain γ-methylallyl *N*-phenylformimidate **S1** in 71% yield (8.3 g). ¹H NMR (300 MHz, CD₂Cl₂): δ 7.73 (m, 1H, NCH), 7.33-7.26 (m, 2H, Ph), 7.14-7.08 (m, 1H, Ph), 6.97-6.92 (m, 2H, Ph), 5.93-5.68 (m, 2H, allyl CH), 4.70-4.69 (m, 2H, CH₂), 1.77-1.73 (m, 3H, CH₃).

Allyl-N-phenylformimidate (S2)

The same method was followed²¹ as for substrate **S1** using ethyl *N*-phenyl formimidate (8 g, 0.0536 mol) and allyl alcohol (7.3 mL, 0.107 mol) to obtain allyl *N*-phenylacetimidate **S2** in 23% yield (2.0 g). ¹H NMR (300 MHz, CDCl₃): δ 7.73 (m, 1H, NCH), 7.32-7.24 (m, 2H, Ph), 7.14-7.08 (m, 1H, Ph), 6.96-6.93 (m, 2H, Ph), 6.11-5.98 (m, 1H, allyl CH), 5.43-5.25 (m, 2H, allyl CH₂), 4.77-4.75 (m, 2H, allyl CH₂).

(E)-2-Hexenyl-N-[4-(trifluoromethyl)phenyl]benzimidate (S3)

Procedure published by Calter et al. was followed, and the ^1H NMR data obtained were in agreement with the published values.⁸

(E)-2-Hexenyl-N-phenylbenzimidate (S4)

The same procedure published by Calter et al.⁸ was followed. ^1H NMR (300 MHz, CDCl_3): δ 7.31-7.12 (m, 7H, Ar), 6.92 (m, 1H, Ar *para*), 6.71-6.68 (m, 2H, Ar *meta*), 5.81 (m, 2H, allyl CH), 4.79 (d, 2H, $J=5.7$ Hz, allyl CH_2), 2.07 (m, 2H, ^nPr CH_2), 1.46 (sextet, 2H, $J=7.5$ Hz, ^nPr CH_2), 0.91 (t, 3H, $J=7.2$ Hz, CH_3).

(E)-2-Hexenyl-N-(4-methoxyphenyl) benzimidate (S5)

The same procedure published by Calter et al.⁸ was followed. ^1H NMR (300 MHz, CDCl_3): δ 7.31-7.12 (m, 5H, Ar), 6.73-6.62 (m, 4H, Ar), 5.82 (d, 2H, $J=5.7$ Hz, allyl CH), 3.74 (s, 3H, OCH_3), 2.08 (q, 2H, $J=7.2$ Hz, ^nPr CH_2), 1.45 (sextet, 2H, $J=7.5$ Hz, ^nPr CH_2), 0.93 (t, 3H, $J=7.2$ Hz, CH_3).

(E)/(Z)-2-Hexenyl trichloroacetimidate (S6)

The procedure published by Anderson et al. was followed for the synthesis.²⁵

(E)-S6: ^1H NMR (400 MHz, CDCl_3): δ 8.25 (s, 1H, NH), 5.88-5.63 (m, 2H, allyl CH), 4.72 (d, 2H, $J=6.4$ Hz, allyl CH_2), 2.04 (q, 2H, $J=7.2$ Hz, ^nPr CH_2), 1.41 (sextet, 2H, $J=7.6$ Hz, ^nPr CH_2), 0.89 (t, 3H, $J=7.2$ Hz, CH_3). **(Z)-S6:** ^1H NMR (300 MHz, CDCl_3): δ 8.26 (s, 1H, NH), 5.71-5.65 (m, 2H, allyl CH), 4.83 (d, 2H, $J=4.2$ Hz, allyl CH_2),

2.11 (q, 2H, $J=7.2$ Hz, $^n\text{Pr CH}_2$), 1.41 (sextet, 2H, $J=5.4$ Hz, $^n\text{Pr CH}_2$), 0.90 (t, 3H, $J=5.7$ Hz, CH_3).

(E)/(Z)-2-Hexenyl-N-(4-methoxyphenyl) trifluoroacetimidate (S7)

The procedure published by Overman et al. was followed for the synthesis.²⁶

(E)-S7: $^1\text{H NMR}$ (300 MHz, CDCl_3): δ 6.84-6.73 (m, 4H, Aryl), 5.75 (m, 2H, allyl CH), 4.68 (m, 2H, allyl CH_2), 3.77 (s, 3H, OCH_3), 2.06 (q, 2H, $J=7.2$ Hz, $^n\text{Pr CH}_2$), 1.43 (sextet, 2H, $J=7.2$ Hz, $^n\text{Pr CH}_2$), 0.91 (t, 3H, $J=7.5$ Hz, CH_3). **(Z)-S7:** $^1\text{H NMR}$ (400 MHz, CDCl_3): δ 6.83-6.73 (m, 4H, Aryl), 5.68 (m, 2H, allyl CH), 4.79 (m, 2H, allyl CH_2), 3.77 (s, 3H, OCH_3), 2.10 (m, 2H, $^n\text{Pr CH}_2$), 1.40 (sextet, 2H, $J=7.2$ Hz, $^n\text{Pr CH}_2$), 0.90 (t, 3H, $J=7.6$ Hz, CH_3).

(E)-2-Butenyl N-[4-(trifluoromethyl)phenyl] benzimidate (S8)

The procedure published for (E)-2-hexenyl-N-[4-(trifluoromethyl) phenyl] benzimidate **S3** by Calter et al.⁸ was followed using 2-butene-1-ol (0.59 mL, 6.96 mmol) and *p*-trifluoromethylphenylbenzimidoyl chloride (1.98 g, 6.99 mmol)⁸ to obtain **S8** as a colorless oil in 91% yield (2.02g). $^1\text{H NMR}$ (400 MHz, CD_2Cl_2): δ 7.43 (d, 2H, $J=8.0$ Hz, Ar), 7.36-7.23 (m, 5H, Ar), 6.80 (d, 2H, $J=8.0$ Hz, Ar), 5.96-5.78 (m, 2H, allyl CH), 4.80-4.78 (m, 2H, allyl CH_2), 1.78 (m, 3H, CH_3). $^{19}\text{F NMR}$ (376 MHz, CD_2Cl_2): δ -61.99 (ArCF_3).

(E)-2-Cinnamyl N-(4-trifluoromethyl)phenyl benzimidate (S9)

The procedure published by Calter et al.⁸ was followed using *trans*-cinnamyl alcohol (0.82 mL, 6.33 mmol) and *p*-trifluoromethylphenylbenzimidoyl chloride (1.80

g, 6.35 mmol)⁸ to obtain **S9** as a white crystalline solid in 78% yield (1.87 g). ¹H NMR (400 MHz, CDCl₃): δ 7.42-7.40 (m, 4H, Ar), 7.33-7.20 (m, 8H, Ar), 6.80-6.73 (m, 3H, Ar and allyl CH), 6.48 (dt, 1H, *J*=6.4 Hz, 6.0 Hz, allyl CH), 5.01 (d, 2H, *J*=6.4 Hz, allyl CH₂). ¹⁹F NMR (376 MHz, CD₂Cl₂): δ -61.97 (ArCF₃).

(E)-2-Hexenyl N-methyl benzimidate (S10)

N-Methyl benzamide (1.00 g, 7.4 mmol) was refluxed with thionyl chloride (7.3 mL, 99.9 mmol) under nitrogen using a CaCl₂ drying tube at the end of the condenser to afford *N*-methylbenzimidoyl chloride as a colorless oil (0.734 g, 65%) after drying in vacuum. The compound was stored under nitrogen to prevent conversion back to the amide. ¹H NMR (400 MHz, C₆D₆): δ 8.07-8.05 (m, 2H, Ph), 7.03-7.01 (m, 3H, Ph), 3.20 (s, 3H, CH₃). *N*-methylbenzimidoyl chloride (0.3 mL, 2.2 mmol) was dissolved in 10 mL of dry THF and cannula transferred under nitrogen onto a solution of sodium hydride (0.088 g, 2.2 mmol) and (*E*)-2-hexene-1-ol (0.26 mL, 2.2 mmol) in dry THF (10 mL). The mixture was kept at 0 °C for 30 min, then at room temperature for 30 min. The solution was then stirred for one day at room temperature. After the reaction, the solution was filtered through a fine frit to remove the unreacted sodium hydride, and the solvent was evaporated to obtain the expected product as a pale yellow oil. (0.26 g, 83%). ¹H NMR (400 MHz, CD₂Cl₂): δ 7.44-7.34 (m, 5H, Ar), 5.82-5.65 (m, 2H, allyl CH), 4.58 (d, 2H, *J*=6.4 Hz, allyl CH₂), 3.03 (s, 3H, CH₃), 2.05 (q, 2H, *J*=7.2 Hz, ⁿPr CH₂), 1.42 (sextet, 2H, *J*=7.2 Hz, ⁿPr CH₂), 0.91 (m, 3H, CH₃).

General procedure for catalytic aza-Claisen rearrangement

Palladium precatalyst (7.5 μmol), silver salt (7.5 μmol), and (*E*)-2-hexenyl-*N*-[4-(trifluoromethyl)phenyl]benzimidate (**S3**) (52 mg, 0.15 mmol)⁸ were added to a sealable J Young NMR tube under nitrogen. The tube was evacuated on a vacuum line, and 0.6 mL of dry CD_2Cl_2 (or $\text{THF-}d_8$) was added by vacuum distillation. The NMR tube was kept in a constant temperature water bath for 2 days at 40 °C. To determine yields, 30 μL of *p*-fluronitrobenzene was added to the tube as an internal standard, and the mixture was analyzed by ^1H and ^{19}F NMR spectroscopy. Product identities were assigned based on previously reported ^1H NMR data for aza-Claisen rearrangements of **S3**.⁸ NMR yields were determined from integrations of ^{19}F NMR signals of the products and the internal standard. The products and side products appeared with the following chemical shifts: desired [3,3] product -62.82 ppm; undesired [1,3] product -62.75 ppm and the by-product amide -62.36 ppm. These values were determined from samples of each product purified by flash chromatography. For allyl imidate substrates which did not contain fluorine atoms, yields were calculated using ^1H NMR by adding 6 μL of diethylene glycol dibutyl ether as the internal standard.

Larger scale aza-Claisen rearrangements for isolated yield % ee determinations

The same reagent concentrations and molar ratios were used as for NMR experiments, but reactions were performed in glass vessels that could be sealed with a PTFE stopcock. Pd precatalyst (22 μmol), $\text{AgBAR}_4^{\text{F}}$ (21 mg, 22 μmol),

benzimidate **S3** (152 mg, 440 μmol), and distilled CH_2Cl_2 (1.9 mL) were added to the vessel under N_2 . The mixture was degassed under vacuum via three freeze-pump-thaw cycles. The vessel was then sealed and heated at 40 $^\circ\text{C}$ for 2 days in a constant temperature oil bath. The solvent was removed under vacuum, and the vessel was opened to the air. The residue was taken up in 5 mL of diethyl ether and filtered to remove insoluble materials. The ether was removed under reduced pressure, and the crude product was purified by flash chromatography³³ on silica gel using a 10:90 mixture of ethyl acetate and hexanes. Fractions of 3 mL each were collected up to 30 fractions. Fractions containing only the desired product as identified by TLC were placed in a tared flask, and solvent was removed under vacuum to yield the product. The [3,3] product (allylic amide) was obtained as a colorless oil that was further dried for 2 hours before determining yield. Samples of the [3,3] product typically contained 5-8% of [1,3] product as estimated by ^1H NMR spectrum due to the difficulty of resolving the two compounds from the column.

Determination of enantiomeric excess of [3,3] product

A 2 mg sample of purified [3,3] product (allylic amide) was dissolved in 2 mL of 95:5 *n*-hexane/EtOH to make a solution of roughly 1000 ppm concentration. An aliquot of this solution was diluted to 30-50 ppm to be used for HPLC analysis. Enantiomeric excesses were determined using a Beckman System Gold HPLC equipped with a 25 cm Chiralpak AD-H column (Chiral Technologies, Inc.) and UV detector (254 nm). Sample injections were 20 μL , and a Shimadzu CR501 Chromatopac integrator was used to determine enantiomeric ratios. Test runs of

racemic mixtures were performed before each % ee measurement. In all cases, baseline resolution of the two enantiomers of the [3,3] product was achieved with peak separations of 1.0-1.5 min. Absolute configurations were determined by comparing the optical rotations for enantiomerically enriched samples of [3,3] product with literature values.⁸ For an example [3,3] product obtained with complex **12** (Chapter 3) displayed an optical rotation of $[\alpha]_D^{25} + 34.4$ (c 0.5, CH₂Cl₂).

References

1. Herrmann, W. A. *Angewandte Chemie-International Edition* **2002**, *41*, 1290.
2. Huang, J. K.; Schanz, H. J.; Stevens, E. D.; Nolan, S. P. *Organometallics* **1999**, *18*, 2370.
3. Dorta, R.; Stevens, E. D.; Scott, N. M.; Costabile, C.; Cavallo, L.; Hoff, C. D.; Nolan, S. P. *J. Am. Chem. Soc.* **2005**, *127*, 2485.
4. Magill, A. M.; Cavell, K. J.; Yates, B. F. *J. Am. Chem. Soc.* **2004**, *126*, 8717.
5. Treichel, P. M. *Adv. Organomet. Chem.* **1973**, *11*, 21.
6. Strukul, G. *Topics in Catalysis* **2002**, *19*, 33.
7. Swift, M. D.; Sutherland, A. *Tetrahedron Lett.* **2007**, *48*, 3771.
8. Calter, M.; Hollis, T. K.; Overman, L. E.; Ziller, J.; Zipp, G. G. *J. Org. Chem.* **1997**, *62*, 1449.
9. Hollis, T. K.; Overman, L. E. *Tetrahedron Lett.* **1997**, *38*, 8837.
10. Donde, Y.; Overman, L. E. *J. Am. Chem. Soc.* **1999**, *121*, 2933.

11. Anderson, C. E.; Donde, Y.; Douglas, C. J.; Overman, L. E. *J. Org. Chem.* **2005**, *70*, 648.
12. Schenck, T. G.; Bosnich, B. *J. Am. Chem. Soc.* **1985**, *107*, 2058.
13. Gardiner, M. G.; Herrmann, W. A.; Reisinger, C. P.; Schwarz, J.; Spiegler, M. *J. Organomet. Chem.* **1999**, *572*, 239.
14. Wehrli, F. W.; Marchand, A. P.; Wehrli, S. *Interpretation of Carbon-13 NMR Spectra*; John Wiley & Sons: New York, 1988; pp.92.
15. Wanniarachchi, Y. A.; Kogiso, Y.; Slaughter, L. M. *Organometallics* **2008**, *27*, 21.
16. Sanger, A. R. *Journal of the Chemical Society-Dalton Transactions* **1977**, 1971.
17. Palenik, G. J.; Mathew, M.; Steffen, W. L.; Beran, G. *J. Am. Chem. Soc.* **1975**, *97*, 1059.
18. Tolman, C. A. *Chem. Rev.* **1977**, *77*, 313.
19. Smith, M. B.; March, J. *MARCH'S Advanced Organic Chemistry: Reactions, Mechanisms, and Structure*; John Wiley & Sons: New York, 2001; pp.20.

20. Jautze, S.; Seiler, P.; Peters, R. *Angewandte Chemie-International Edition* **2007**, *46*, 1260.
21. Roberts, R. M.; Hussein, F. A. *J. Am. Chem. Soc.* **1960**, *82*, 1950.
22. Miranda, A. J. Unpublished work. 2008.
23. Moncada, A. I.; Manne, S.; Tanski, J. M.; Slaughter, L. M. *Organometallics* **2006**, *25*, 491.
24. Hollis, T. K.; Overman, L. E. *J. Organomet. Chem.* **1999**, *576*, 290.
25. Anderson, C. E.; Overman, L. E. *J. Am. Chem. Soc.* **2003**, *125*, 12412.
26. Overman, L. E.; Owen, C. E.; Pavan, M. M.; Richards, C. J. *Organic Letters* **2003**, *5*, 1809.
27. Schuster, R. E.; Scott, J. E.; Casanova, J. *Org. Synth.* **1966**, *46*, 75.
28. Moncarz, J. R.; Brunker, T. J.; Jewett, J. C.; Orchowski, M.; Glueck, D. S.; Sommer, R. D.; Lam, K. C.; Incarvito, C. D.; Concolino, T. E.; Ceccarelli, C.; Zakharov, L. N.; Rheingold, A. L. *Organometallics* **2003**, *22*, 3205.
29. Miller, K. J.; Kitagawa, T. T.; bu-Omar, M. M. *Organometallics* **2001**, *20*, 4403.

30. Wanniarachchi, Y. A.; Slaughter, L. M. *Chemical Communications* **2007**, 3294.
31. Antilla, J. C.; Klapars, A.; Buchwald, S. L. *J. Am. Chem. Soc.* **2002**, *124*, 11684.
32. Betschart, C.; Schmidt, B.; Seebach, D. *Helv. Chim. Acta* **1988**, *71*, 1999.
33. Still, W. C.; Kahn, M.; Mitra, A. *J. Org. Chem.* **1978**, *43*, 2923.
34. Carey F. A., Sundberg R. J. *Advanced Organic Chemistry*; Kluwer Academic / Plenum Publishers: New York, 2000.

VITA

Yoshitha Anju Wanniarachchi

Candidate for the Degree of

Doctor of Philosophy

Thesis: SYNTHESIS, REACTIVITY, AND CATALYTIC STUDIES OF
TRANSITION METAL COMPLEXES OF CHELATING CYCLIC AND
ACYCLIC DIAMINOCARBENE LIGANDS

Major Field: Inorganic Chemistry

Biographical:

Education:

2003–2008 Completed the requirements for the Doctor of Philosophy in Inorganic Chemistry at Oklahoma State University, Stillwater, Oklahoma in December, 2008.

1998 – 2003 B.Sc. Special Degree in Chemistry with first class honors, University of Kelaniya (Sri Lanka)

Professional Memberships:

American Chemical Society

Name: Yoshitha Anju Wanniarachchi

Date of Degree: December, 2008

Institution: Oklahoma State University

Location: Stillwater, Oklahoma

Title of Study: SYNTHESIS, REACTIVITY, AND CATALYTIC STUDIES OF
TRANSITION METAL COMPLEXES OF CHELATING CYCLIC AND
ACYCLIC DIAMINOCARBENE LIGANDS

Pages in Study: 234

Candidate for the Degree of Doctor of Philosophy

Major Field: Inorganic Chemistry

Scope and Method of Study:

Findings and Conclusions:

Since the first report of a stable diaminocarbene by Arduengo in 1991, carbene ligands have been widely explored in organometallic chemistry due to their favorable features in catalysis. In order to find broad applications of carbenes in catalysis, the preparation of electronically and sterically tunable carbene transition metal complexes are needed. Two major approaches used in synthesizing chelating bis(carbene) complexes of catalytically important transition metals will be discussed. The first approach involves the synthesis of a sterically bulky silver bis(N-heterocyclic carbene) complex which is effective for transferring the bis(carbene) ligand to other transition metals. The second approach is based on nucleophilic attack of secondary diamines or hydrazines on palladium-bound arylisocyanide precursors to generate bis(acyclic diaminocarbene) (ADC) palladium(II) complexes. This reaction shows similarities to a self-assembly process in that it is highly selective and produces no by-products. This route has been utilized to synthesize bis(ADC) palladium complexes with different chelating ring sizes and chiral backbones. Bis(ADC) palladium complexes have been successfully used as electrophilic catalysts for enantioselective aza-Claisen rearrangements of allylic imidates.

ADVISER'S APPROVAL: Dr. LeGrande M. Slaughter